THE RE-ENGINEERING OF VHF MOBILE RADIO SERVICES IN THE UK

Roger Edward Fudge

Submitted for the degree

Doctor of Philosophy

THE CITY UNIVERSITY

Department of Electrical and Electronic Engineering

April 1984

Volume II

TABLE OF CONTENTS

TABLE OF CONTENTS

TABLE OF CONTENTS

TABLE OF CONTENTS

TABLE OF CONTENTS

TABLE OF CONTENTS

TABLE OF CONTENTS

TABLE OF CONTENTS

TABLE OF CONTENTS

TABLE OF CONTENTS

TABLE OF CONTENTS

TABLE OF CONTENTS

List of Figures

Page Numbering as Bound

List of Figures

List of Figures

List of Figures

List of Figures

List of Figures

List of Figures

List of Figures

List of Figures

List of Figures

APPENDIX A

Signal strength vs. Distance - A Propagation Law

A.1. Introduction

Figures 4.2.1 to 4.2.7 of chapter 4 show the variation of signal level measured in a mobile as a function of range of that mobile from the tranmitter. Each has an inverse fourth power curve drawn on it to show the degree of correspondence to that predicted by simple theory and confirmed by the workers cited in chapter four. The placing of each inverse fourth power curve was done by eye and the fit can be seen to be good. The aim of this appendix is to discuss these results and obtain a 'universal propagation law' (at least as far as the Directorate is concerned) in order to determine transmitter powers to be used at base stations. To do the latter task will entail using information from several chapters which are subsequent to chapter 4 so the construction is given here to minimise the discontinuous flow of information in the main body of the report.

Initial interest is directed to the validity/usability of the results obtained and the place of the 90% curves in the overall determination.

A.2. Validity of Results

Chapter 4 provides a brief description of the way in which the curves were obtained. A pertinent point is that the measuring system was not designed for this task. It was intended to measure signal strengths and plot 'characteristic values' on a map to show the degree and extent of coverage. To do this the levels were measured at fixed intervals of distance travelled and the average of 62 successive readings, representing 10 metres distance, was recorded on tape in the vehicle as the characteristic value for that section. Each individual reading was obtained by electronically adjusting an attenuator on the input to the measuring receiver until a threshold was crossed; this threshold was near the noise level.

The attenuator of course stepped in dB increments and so the averaging process was an average of the dB values - ie an average of the log of the signal strengths. This is obviously different from the arithmatic mean of the levels and although the results for the initial purpose are best presented in dB form there will be a difference between the mean of the log of the values and the log of the mean of the values. This difference was judged to be not important for the original purpose since only a relatively crude indication of overall signal strength was desired and this was further quantised into one of four categories so that maps of signal strength could be plotted of the roads traversed showing the four categories as different colours. This was deemed of merit in showing the overall situation to the customers (police and fire services) for their comments on acceptability of coverage.

For the analysis used in deriving the chapter four figures, each 10m average was converted into a power equivalent by taking the square of the antilog, and these were averaged for each 0.5km of range from the transmitter. The question arises as to how much information has been lost in the 'dB averaging' process for the 10m intervals.

A.3 Computer Simulation

Detail will almost certainly have been lost here since the fine structure of any Rayleigh fading (see chapter 6 and appendix D) will have been lost by averaging - let alone the dB averaging.

No analytic formulae could be derived for this so recourse was made computer simulation. Attention was directed at this stage to the 50% (ie median) curves.

A microcomputer was set to produce a signal with Rayleigh probability distribution statistics. Firstly a Gaussian distribution was produced by summing four successive values of a computer generated (pseudo) random variable, and the statistics of this process were checked. The square root of the sum of the squares of two Gaussian variables was then taken as the Rayleigh variable (see Clarke 1968) and the statistics of the process checked. Having checked the validity of producing such a variable, the log of the mean of 10,000 values was compared to the mean of the log of the same values. The difference was found to be 2.4dB. This agreed with the value found by another method based on numerical integration of the Rayleigh characteristics (Pearce 1983).

This value of 2.4dB inaccuracy was judged to be acceptable in view of the inherent variability of the situation. Thus the 50% curves could be taken as giving a good indication of the expected levels as a function of distance.

A.4 Median Curves

Thus the inverse fourth power curve fits to the results could be taken as the basis for the 'universal' propagation law at the median level. Such curves are shown on the figures of chapter 4.

Many such results for a number of transmitting sites were analysed and the average best fit curve was found to be within 10dB of any trace and significantly better than this for most, particularly over the larger ranges.

This then was taken as the 'universal' median law

Loss between dipoles $L_{50} = 84.2 + 40 \log d$ (dB)

where d is the range in km.

A.5 The 90% case

At first sight a similar treatment could have been given to the 90% curves - those which represent the levels exceeded for 90% of the locations, and the figure used for providing acceptable communications.

Two main factors argued against this however. Firstly an initial assessment of the 10m averging process showed that the likely discrepancy was large, showing that fine detail had been lost. Secondly the surveys had been conducted with only 10 watts of radiated power. This coupled with the fact that the measuring equipment threshold was near the noise level meant that the lack of sensitivity would be most marked for the weaker signals. Thus the 90% results were rather suspect in accuracy. An additional factor was that only 'major' roads had been included in the surveys and there was some question as to how representative this was for the overall situation which had to be considered.

For these reasons recommendations were made that future surveys would be best conducted with a higher transmitter power if use was to be made of this form of analysis. To obtain a propagation law for this 90% case use was made of CCIR predictions of the variations of signal levels (CCIR report 567-1) which gives (presumably as the result of many careful measurements) a confirmation that the gross locations are log normally distributed (see chapter 6) with standard deviation of 8dB. From this the difference between the 90% case and 50% (median) case was calculated as 10dB.

Thus the 'universal' law to be used for the Directorates purpose was in part derived from measurements of representative locations and a correction from CCIR work applied. The law is then:

$$\text{Path loss for 90\% locations } L_{90} = 94.2 + 40 \log d \quad \text{(dB)}$$

where d is the range in km.

A.6 Transmitter Power

The base station transmitter powers are dependant on the range it is desired to achieve, the modulation used, and the grade of service to be provided. Chapter 7 discussed the requirement for QSAM operation and the recommended level (section 7.8) for this was 10 μVemf in areas of equal signal overlap, this corresponds to - 124dBW. Now a typical spacing between base stations is 30km. So, for a range of 15km the path loss becomes 141.2dB, and the transmitter radiated power is 17.2dBW. With this figure the ranges of signal levels of 4 μVemf (-131dBW) and 2 μVemf (-137dBW), which have been taken as the minimum desirable and absolute minimum usable signal levels, are respectivly 22km (13.8 miles) and 31.2km (19.5 miles). These latter figures were in resonable agreement with expectations but it was recognised that they had to be treated with some caution due to the increasing effect of shadowing here. Overall however it confirmed the intuitive feeling that the situation at 150MHz would be very similar to 100MHz where 50 watt (+17dBw) tansmitters are used.

The return path merits some discussion. The path loss will, by reciprocity, be the same. The lower transmitter power available on the mobile, some 20W (+13dBW) is compensated for by the fact that not only

will the receiver not be subject to quasi synchronous reception but it will also be in a low noise environment. Therefore overall operation on the return paths is, as happens in the present bands, expected to match that of the outgoing one.

APPENDIX B

Multibase Station Area Coverage

Protection ratio as a function of Clustering

The case of a single base station per coverage area was discussed in the main text at 5.6.4 and a formula given for relating re-use distance u to the number of cells or channels n which form a tessellating pattern. For a cell to cell spacing of D the re-use distance u was given by

$$u = D(i^2 + ij + j^2)^{\frac{1}{2}}$$

and the number of channels $n = i^2 + ij + j^2$

When considering a system where several base stations are used to provide coverage of an area, then it is necessary to limit the numbers to those which form repeating multi-hexagonal patterns. This provides the repeating patterns necessary for hexagonal geometry. Thus only clusters of 3, 4, 7, 9 etc base stations can be considered, and for each of these there may be several choices of numbers of clusters (ie. of number of channels) which then form tessellating patterns. Following the terminology of section 5.6.4, a group of base stations on one channel will be a cluster and a grouping of clusters to tessellate the plane will be termed a conglomerate.

The basis for comparison of performance between the single and multi base station clusters should be that of protection ratio afforded to the service area against co-channel interference.

For the case of four base stations examined in section 5.6.3, it will be seen that the re-use distance for the single station case is given by i = 2, j = 1 ie. $u = D\sqrt{7}$. Now the worst case for protection occurs at the corner of the wanted cell since this is nearest to the unwanted transmitter and furthest from the wanted. Whilst the exact protection ratio for this point could be calculated using the inverse fourth power law, it will be reasonable to approximate the coverage to a circle of diameter D, the cell to cell distance. This is even more appropriate for some of the particular patterns to be considered later. Once again

this can be justified on the grounds of demonstrating the nature of the effects.

When this is done then the range r = D/2 and the formulae given in section 5.6.2 apply.

So from $u_1 = r\ (\Gamma^{\frac{1}{4}} + 1)$ we can derive

$$\Gamma = \left(\frac{2u_1}{D} - 1\right)^4 \text{ as the general case}$$

Thus for the four base station case the protection ratio is 25.3 dB.

From the diagrams 5.6.7 (a) and (b) it will be seen that this protection ratio applies to a 4 cell cluster - 4 cluster conglomerate, also.

The protection ratios for single cell clusters can be derived from the above formula and the factors are tabulated in Table B1 overleaf.

TABLE B1

i	j	$u_{1/D}$	No. of Channels	Protection Ratio dB
1	0	1	1	0
1	1	1.73	3	15.7
2	0	2	4	19.1
2	1	2.65	7	25.3
2	2	3.46	12	30.9
3	0	3	9	28.0
3	1	3.61	13	31.7
3	2	4.36	19	35.5
3	3	5.2	27	38.9
4	0	4	16	33.8
4	1	4.58	21	36.5
4	2	5.29	28	39.3
4	3	6.08	37	41.9
5	0	5	25	38.1

Figures B1 (a) and (b) show 3 cell clusters in 3 and 4 cluster conglomerates respectively, and it will be seen that the protection ratios can be derived from the previous formula on the basis of closest co-channel cells. Thus $u_{3,3} = \sqrt{3}$ and $u_{3,4} = 4$ yielding $\Gamma_{3,3} = 15.7$ and $\Gamma_{3,4} = 19.1$ dB respectively. The suffixes here are in turn cells per cluster and clusters per conglomerate.

It is necessary that, not only should the cluster be a tessellating shape, but also should the conglomerate be. Therefore the admissible structures are restricted to those which have the number of cells per cluster as given by the number of channels in Table B1 and those which have the number of cells per conglomerate restricted to that sequence as well. On that basis a 3,5 structure is not viable since the number 15 does not appear in the number of channels [ie. no integer values of i and j exist to satisfy $i^2 + ij + j^2 = 15$].

The 4,4 case has been considered in section 5.6.3, other possibilities for a 4 cell cluster are 4,3 and 4,7. These are shown in figures B2 and B3.

The seven cell cluster has solutions of 7,3 and 7,4 which are shown in Figures B4 and B5.

The table of protection ratios, Tabe B2, given below shows the protection ratios as a function of cells per cluster and clusters per conglomerate - the latter being the number of channels required.

TABLE B2

Channels (clusters per conglomerate)	3			4			7
Cells per cluster	3	4	7	3	4	7	4
Protection ratio dB	15.7	15.7	25.3	19.1	25.3	31.7	31.7
Number of channels for single cell case for same protection ratio	3	3	7	4	7	13	13

This table is used to plot the points for multibase station operation in Figure 5.6.8 and Table B1 figures are used to plot the single cell case on the same figure.

APPENDIX C

Multi-Base Station Area Coverage

Effect of many cells per cluster

The protection ratio for a particular arrangement of clusters of cells will be dependent on the number of cells within the cluster. It would be indicative of the assymptotic value for large numbers if the case of an infinite number, a continuum, of very low power transmitters, could be calculated. Given the value of signal power at a distance from the edge of the cluster then the power for the various clusters could be summed for representative locations on the edge of an interfered with cluster.

Figure C1 shows the requirement for a point distance d from the edge of a circular cluster (circles seem a good starting point) the contribution from an elemental area are summed for the whole cluster area. A first attempt was made using the configuration shown in Figure C2. This summed all areas in a strip width δx wide and occupying an angle of $\delta\theta$ subtended at the point. This made all the contributions within the arc have the same contribution. But the treatment is not viable since the elemental areas need to be equal, in order to simulate a true continuum, and the areas here increase with x.

A simplifying calculation can be made by taking a square shaped cluster and dividing it into m^2 smaller ones as shown in Figure C3. Using the symbols defined in that figure:

The range to the corner from the centre is $q\sqrt{2}$ so that a transmitter power of $P_1 = 4\ q^4$ watts is required to just give a reference level at the corner (assuming inverse fourth power law and normalising).

Now the power received at a distance d from the edge of cover is

$$\frac{4q^4}{(D+q)^4}$$

and compared to the unity value at the corner, a protection ratio

$$\Gamma = \frac{(D+q)^4}{4q^4}$$

would be obtained.

If the square were divided to contain m cells on a side, a total of m^2 cells, then the transmitter power at the centre of each to give the reference level at the corner of a small cell is deduced from the new range of $\frac{q\sqrt{2}}{m}$ as

$$P_m = \frac{4q^4}{m^4}$$

At point R the power received from the cell shown is

$$\frac{P_m}{[(d+x)^2+y^2]^2}$$

The question now arises of how the powers of the tranmissions from other small cells will add. If all transmissions were synchronous, then they will add on a voltage basis and the exact distance in terms of wavelength will be critical. In this case a small movement of R axially or laterally would redistribute the phasing and hence receiver level. In pratice the transmitters are unlikely to be synchronous and the receiver may well be in motion so that addition on a power basis is then meaningful.

When performing the summation x and y will take on discrete values. x will be given by

$$x = \tfrac{1}{2}\left(\tfrac{2q}{m}\right) + I\left(\tfrac{2q}{m}\right) = \tfrac{2q}{m}[I+0.5]$$

where I is an integer from 0 to m-1

or $$x = \tfrac{2q}{m}[J-0.5]$$

where J is an integer from 1 to m

similarly $y = -q + \frac{2q}{m}[J-0.5]$

where J is an integer from 1 to m

So that total power at R a distance d from cluster

$$P_m = \frac{4q^4}{m^4}\left\{\sum_{I=1}^{m}\sum_{J=1}^{m}\frac{1}{\left\{\left[d+\frac{2q}{m}(I-0.5)\right]^2+\left[-q+\frac{2q}{m}(J-0.5)\right]^2\right\}^2}\right\} \quad \text{---(C1)}$$

This could be plotted as a protection ratio against d for various values of m^2 as a parameter. But it would still leave the question of summing the contributions from other co-channel clusters. It should be viewed as a step on the way to solving the continuum situation. Figure C4 sets out the geometry for this taking the conceptually better circular case.

For a single transmitter at the centre, a power of

$P_1 = \frac{1}{r^4}$ is required for the same reference as before.

The transmitter power required for the elemental area $\delta x.\delta y$ can be deduced from scalling considerations. Assuming the same shape of coverage (which is not strictly true here but the errors will be small) then the range changes as the square root of area ratio and the transmitter power as the square of area ratio (fourth power law).

Therefore elemental transmit power $P_\delta = \frac{\delta_x^2 \delta_y^2}{\pi^2 r^4} \frac{1}{r^4}$

Power received at point R from one elemental area

$$= \frac{\rho_\delta}{[(d+x)^2 + y^2]^2}$$

and power received at R from whole vertical strip

$$P_x = \int_{y=0}^{y=\sqrt{r^2-(r-x)^2}} \frac{\rho_\delta}{[(d+x)^2+y^2]^2}$$

and power received at R from whole cluster

$$\rho = \int_{x=0}^{x=2r} P_x$$

Thus

$$\rho = \frac{2}{\pi^2 r^8} \int_{x=0}^{x=2r} \int_{y=0}^{y=\sqrt{r^2+(r-x)^2}} \frac{\delta_x^2 . \delta_y^2}{[(d+x)^2+y^2]^2} \quad --- \quad (C2)$$

This is a strange integral since it involves the square of the δ portion for each step of the integration.

Equation C1 points the way here - consider increasing values of m. Then, providing d is not zero, the I and J terms become vanishingly small compared to d and q. So that received power becomes:

$$\frac{4\varepsilon^4}{m^4} \sum_{1}^{m} \sum_{1}^{m} \frac{1}{(d^2+\varepsilon^2)^2}$$

$$= \frac{4\varepsilon}{m^2} \frac{1}{(d^2+\varepsilon^2)^2}$$

which given $m \to \infty$, is zero.

A similar interpretation can be given to equation C2; where, taking the δ's to tend to zero, then the fact that they occur in square form makes the integral zero, providing d is not zero.

Thus in the limit as the number of cells in a cluster increase towards infinity the power outside the cluster will fall to zero. This will not depend on the shape of the cluster.

APPENDIX D

Some Notes on the Rayleigh Probability Distribution

The mobile radio receiver is often said to be operating in a 'Rayleigh fading environment', and the form, nature, and parameters of this type of distribution merit discussion.

The quantity which is Rayleigh distributed is the envelope of the electric field. Since there is a direct linear relationship between this and the voltage delivered from the aerial to the receiver then the latter will be used for convenience and is of most direct use.

The instantaneous voltage of the envelope from the aerial will be taken as v, and the Rayleigh probability density distribution has the form:-

$$p(v) = \frac{v}{\sigma} \exp\left(-\frac{v^2}{2\sigma}\right) \qquad \ldots\ldots (31)$$

p(v) is the probability of v lying between v and δv as $\delta v \to 0$, and σ is a distribution parameter. The cummulative probability distribution is given by $P(V) = \int_0^V p(v) = 1 - \exp\left(-\frac{v^2}{2\sigma}\right)$

where P(V) is the probability of v lying between zero and V. It will be seen that the probability of finding the voltage anywhere is $P(\infty)$ (ie the assumption that the voltage exists is 1.

The questions of prime interest are what is the mean value, the median value and the rms value in terms of the parameter σ; and how close are they to each other.

The mean is given by v_1 where

$$v_1 = \int_0^\infty v\, p(v)\, dv$$

$$= \int_0^\infty \frac{v^2}{\sigma} \exp\left(-\frac{v^2}{2\sigma}\right) dv$$

$$= \frac{1}{\sigma}\left[\frac{\Gamma(1.5)}{2} \cdot (2\sigma)^{\frac{3}{2}}\right]$$

[Γ( ) is the Gamma function]

Therefore $v_1 = 0.886\sqrt{2\sigma}$

The rms value is v_2 where

$$v_2^2 = \int_0^\infty v^2 \, p(v) \, dv = \int_0^\infty \frac{v^3}{\sigma} \exp\left(\frac{-v^2}{2\sigma}\right) dv$$

$$= \frac{1}{\sigma}\left[\frac{(2\sigma)^2}{2}\right] = 2\sigma$$

Therefore $v_2 = \sqrt{2\sigma}$

And the median v_3 is derived from

$$0.5 = \int_0^{v_3} p(v) \, dv = 1 - \exp\left(\frac{-v_3^2}{2\sigma}\right)$$

from which $v_3 = \sqrt{2\sigma \log_e 2}$

these relationships can be shown in Table D1.

TABLE D1

	Symbolic	relative	dB relation
rms value	$\sqrt{2\sigma}$	1	0
mean value	$0.886\sqrt{2\sigma}$	0.886	-1.05
median value	$\sqrt{\log_e 2}\sqrt{2\sigma}$	0.832	-1.60

The plots of the basic Rayleigh distribution and the cumulative one of figures 6.1.1 and 6.1.2, are repeated here for completeness as figures D1 and D2.

APPENDIX E

The Effects of Pre- and De-Emphasis on Quoted FM Performance

E.1 The Concept of Pre and De-Emphasis

The chapter (7) on modulation has pointed out that although the term frequency modulation (FM) is in general use throughout the mobile radio industry, what is actually used is generally thought to be phase modulation. This appendix will show that in fact the modulation used is at best a hybrid of the two and it is somewhat difficult to even place it under the heading angle modulation.

If pure FM were used then it would suffer from the well known effect of having a noise spectrum at the output of the receiver which was not flat (ie independant of baseband frequency). Theory predicts, and practice confirms, that the noise voltage level in any one small baseband bandwidth is proportional to the centre frequency of that bandwidth, and that for a given total audio noise power that the upper audio frequencies will be greatest and dominate the output. The noise power will be proportional to the square of the audio frequency.

[It is worth noting in passing that the noise spectrum from the demodulator extends to half the IF bandwidth - this can of course be much greater than the highest (audio) modulating frequency for systems with high deviation ratios. Only the deliberate inclusion of low pass filter characteristics in the receiver's audio stages will restrict the audio noise to that of the highest audio signal frequency].

The predominance of high frequency noise makes the impact of this on a listener more disturbing than would flat noise of the same total power. There is therefore advantage to be gained in subjective performance by making the audio response of the receiver have a (voltage) characteristic which falls with increasing audio frequency. In fact this is equivalent to including an integrator in the audio stages or a network with a response inversely proportioned to frequency. This is the de-emphasis network - to be covered by the expression DE.

To ensure that the overall audio response between transmitter and receiver is flat, it is necessary to ensure that the transmitter has a complementary stage in its audio circuits before frequency modulation. Thus this has to have a differentiating characteristic, ie one which is equivalent to a filter with a voltage characteristic which is proportioned to the audio frequency. This is the pre-emphasis network or PE.

If the networks were just as described then the PE - FM - FM - DE chain would be equivalent to a PM - PM chain ie phase modulation and demodulation. This of course has an inherently flat noise output characteristic. [The equivalence is not strictly true since a phase demodulator requires a phase reference].

The PE and DE characteristics are shown in Figure E1. The dotted line of the characteristic is that which is found in practice since the response at low frequencies is not considered important and is in any case it is difficult to define here since the region is not transmitted. The break point to the dotted line is not defined.

E.2 The Effect of PE and DE on Deviation

The simple block diagram of the chain described in the previous section can be drawn as in Figure E2. This is frequently realised in the form shown in Figure E3, since it is often easier to realise this with the centre frequency accuracy and stability necessary in mobile radio.

So although the modulation seems at this stage to be PM it is called FM and its performance is derived - certainly as far as manufacturers quoted figures are concerned - as if it were an FM system.

The performance of general interest is the input carrier level required to give a certain audio signal to noise ratio at the output of the receiver - say 20 dB. For operation above the FM threshold, as this would be, then it is equivalent to setting the carrier level at some value and then measuring the output signal to noise ratio. Obviously this will depend on the deviation allowed.

The practice is to choose a modulating frequency of about, or equal to, 1 kHz as a test tone, and to set the deviation of a signal genertor so

that this test tone reaches the peak allowable deviation (2.5 kHz for a 12.5 kHz channelled system). This allows the performance to be measured. But this level of deviation cannot be used to plot the frequency response for if it were kept at constant deviation then the respone would be that of the DE - ie a falling one. So for this either a true phase modulator is used or a FM one with PE.

But now the full system deviation can only be reached at the highest modulating frequency - say 3 kHz - and the deviation at 1 kHz will only be a fraction of this (one third in this case). Thus the system should not be allowed to reach 2.5 kHz deviation at a 1 kHz modulating frequency.

On strict scientific grounds therefore there should be a choice. Either the system performance in signal to noise terms is measured at a modulating frequency of 3 kHz (and 2.5 kHz deviation) - in which case the effects of the overdeviation at this frequency cited in chapter 7 would be apparent as at least a drop in signal or more probably as a poor figure on a SINAD measurement. Or the deviation should be made proportional to frequency such that the signal to noise ratio, if measured with a 1 kHz tone, should have a deviation of 2.5/3 kHz - this will reduce the signal and hence the signal to noise ratio by some 10 dB!

FM advocates, and manufacturers, reply to these points with comments about peak of speech response being around 1 kHz and therefore it is acceptable to have system enhancements in this region, but this hardly counters the arguments.

E.3 Further Complications

The previous section stated that certain deviations should not be allowed and in fact there is a regulatory requirement (and test) that ensures that overdeviation cannot happen. The method of so doing is not specified. Presumably this would ideally be implemented by very tight filtering of the modulated signal, but this would certainly introduce distortions to non limited signals and would be impossible to realise at the carrier frequencies and bandwidths in use. So instead a voltage clipper or limiter is used prior to the modulator. The transmission chain therefore takes the form shown in Figure E.4. Or

for the practical case where a phase modulator is used Figure E.5 applies. This has been presented by a manufacturer in the form shown in E.6 and, although at first sight an apparant unnecessary complication of E.4, is used to explain its operation. The action is said to be as follows. If the input audio signals to the transmitter are of a very low level then the limiter does not act so that the first two emphasis networks (PE and DE) cancel each other. Thus the net result is of PE FM or phase modulation PM as desired and is compatible with the receiver's DE circuit. If the input audio is however at a high level then the limiter will act and thus cancel the effect of the first PE circuit, in addition the next two emphasis circuits, DE and PE, can be considered to cancel each other, so that the result is FM and the receiver's output will have a falling characteristic due to its DE network.

Interest lies in intermediate audio levels. In this case up to some frequency the output of the first PE will be below limiting level and overall frequency response up to the point is correct. Above this frequency then the response will not be correct but it does enable an intermediate frequency to be given full system deviation. It will not come as a surprise therefore to find that this break point is set just above 1 kHz.

This does not destroy the previous argument about changing drive level for the two tests - this still has to be done, but it does ensure that over deviation will not in fact occur when test tone level is applied at high frequencies. Furthermore it might be possible to achieve a good signal to noise ratio figure when using a high level - high frequency test tone since the effective wave form will be near squrae. What the spectral spread of this will be is unknown!

Thus practical systems are said to change from a PM characteristic at low audio frequencies to a FM one at high frequencies. In reality the whole situation is clouded by the relationship between peak speech and peak test tone and more particularly the inability to measure it in the field. The net result is that even if the chain is set up on an accurate instrumental test tone basis, when speech is applied the deviation is set at that which gives best overall results.

For instance the UK cellular radio phase system will be deliberately allowed to overdeviate and corrupt the adjacent channel. But a trade-off has been made of the degredation due to noise from an adjacent channel due to this cause and the increased signal level due to the increased deviation of the wanted channel. Such action is perhaps admissable when one authority has overall responsibility for all the adjacent channels and can plan on a forward looking and national basis (although some of the reasoning could be considered simplistic for a real situation). But for normal mobile radio operation by a number of different users in a developing situation such action must be considered questionable.

APPENDIX F

The Derivation of Quasi-Synchronous Amplitude, Phase, and Frequency Relations

F.1 Amplitude

This appendix dervies the formulae from which Figures 7.5.3, 7.5.5 and 7.5.6 were drawn. They all stem from Figure 7.5.2 which is reproduced here as Figure F1 for ease of reference. It will be recalled that the phasors shown as P and Q represent the stronger and weaker carrier voltages received in a mobile receiver. P is taken as the reference for phase purposes. In general the angle α will be steadily increasing due to the difference in angular frequency ω between the two transmitters. The resultant carrier as seen by the mobile will be the vector sum of P and Q and is shown as R.

The magnitude of R is readily dervied from the cosine formula as

$$R = (P^2 + Q^2 + 2PQ \cos\alpha)^{\frac{1}{2}}$$

This is used for Figure 7.5.3.

F.2 Phase

The phase angle θ of the resultant is derived from the sine formula. The reference angle of the stronger carrier P is taken since this will be the mean value

$$\frac{\sin\theta}{Q} = \frac{\sin\alpha}{R} \qquad \ldots\ldots(F1)$$

$$\text{Thus} \qquad \theta = \sin^{-}\left[\frac{Q\sin\alpha}{(P^2+Q^2+2PQ\cos\alpha)^{\frac{1}{2}}}\right]$$

This is used to plot the curves of figure 7.5.5

F.3 Frequency

The effective instantaneous frequency of the resultant carrier with respect to that of the stronger component P is given by $\Omega = \frac{d\theta}{dt}$

This is most easily determined by differentiating both sides of equation F(1) with respect to time.

$$\frac{d\left(\frac{\sin\theta}{Q}\right)}{dt} = \frac{d\left(\frac{\sin\alpha}{r}\right)}{dt}$$

Hence $$\frac{d\theta}{dt} \cdot \frac{d\left(\frac{\sin\theta}{Q}\right)}{d\theta} = \frac{d\alpha}{dt} \cdot \frac{d\left(\frac{\sin\alpha}{r}\right)}{d\alpha}$$

Therefore $$\frac{\Omega}{Q}\cos\theta = \omega\left[\frac{\cos\alpha}{r} + \frac{dR}{d\alpha}\cdot\frac{d\left(\frac{\sin\alpha}{r}\right)}{dr}\right]$$

$$= \omega\left[\frac{\cos\alpha}{R} - \frac{\sin\alpha}{R^2}\frac{dR}{d\alpha}\right]$$

Now:- $R^2 = P^2 + Q^2 + 2PQ\cos\alpha$

So $$2R\,dR = -2PQ\sin\alpha\,d\alpha$$

$$\therefore \quad \frac{dR}{d\alpha} = -\frac{PQ\sin\alpha}{R}$$

Thus $$\frac{\Omega}{Q}\cos\theta = \frac{\omega}{R}\left[\cos\alpha + \frac{PQ\sin^2\alpha}{R^2}\right]$$

or $$\Omega = \frac{\omega Q}{R\cos\theta}\left[\cos\alpha + \frac{PQ\sin^2\alpha}{R^2}\right]$$

but $R\cos\theta = P + Q\cos\alpha$

So $$\Omega = \omega\left\{\left[\frac{Q}{P+Q\cos\alpha}\right]\cdot\left[\cos\alpha + \frac{PQ\sin^2\alpha}{P^2+Q^2+2PQ\cos\alpha}\right]\right\}$$

which reduces to $$\Omega = \omega\left[\frac{Q(Q+\cos\alpha)}{P^2+Q^2+2PQ\cos\alpha}\right] \quad \ldots (F2)$$

The right hand side of the equation F2 is a multiplier or magnification factor which is applied to the angular beat frequency ω. If both the frequencies Ω and ω are converted to cyclic frequencies by dividing each by 2π then the magnifier remains unaltered.

Thus the magnifier

$$\frac{Q(Q+\cos\alpha)}{\rho^2+Q^2+2\rho Q\cos\alpha}$$

was used to plot the curve in Figure 7.5.6

APPENDIX G

The Analysis of Fraction of Time Below a Threshold

G.1 Portion of time spent below a threshold for two carriers

The phasor diagram representing the two carriers P and Q is shown in Figure G1 with the larger of the two designated P and taken as the reference for angle purposes. The locus of a threshold, which could be that of the mute setting, is a circle of radius equal to the threshold voltage H. Since Q is rotating with respect to P at a rate given by the carrier offset frequency, the fraction of time for which the resultant is below threshold is the fraction of the circumference of the resultant locus which lies inside the locus of H.

This is $\tau_2 = \frac{2\alpha}{2\pi} = \frac{\alpha}{\pi}$

from simple geometry $H^2 = P^2 + Q^2 - 2PQ\cos\alpha$

It is convenient to use the ratios of the quantities concerned, so setting:- the threshold to major carrier ratio $\frac{H}{P} = h$,

and minor to major carrier ratio (the carrier ratio) $\frac{Q}{P} = q$

$$\text{gives} \quad \tau_2 = \frac{1}{\pi}\cos^{-1}\left[\frac{1+q^2-h^2}{2q}\right] \qquad \text{- - - (G1)}$$

the curves of Figures 7.5.19 and 7.5.20 were plotted from this relation.

G.2 Portion of time spent below threshold for three carriers

The phasor diagram for the three carrier case is depicted in Figure G2 where S is the amplitude of the third carrier. The ratio of $\frac{S}{P}$ is taken as s and S is assumed to be smaller than Q.

Since the frequency offset of Q from P will be different to that of S from Q then in the phasor diagram both Q and S will be rotating but at different rates. Therefore the locus of the resultant R will not be a

simple one. Since the rotation rates are independent then the fractional probability of R lying within H can be calculated as the product of the fractional probability (τ_β) of R lying within H for a fixed position of Q, and the probability (τ_α) of Q having this position, then summing over all positions of Q.

Referring to Figure G3 it will be seen that the first probability

$$\tau_\beta = \frac{2\beta}{2\pi} = \frac{\beta}{\pi}$$

and β can be derived as

$$\beta = \cos^{-1}\left[\frac{1+q^2+s^2-h^2-2q\cos\alpha}{2s\,(1+q^2-2q\cos\alpha)^{\frac{1}{2}}}\right] \qquad \ldots (G2)$$

The region of α over which the tip of S lies within the threshold can be deduced from Figure G4 a, b. The minimum value of α is given by

$$\alpha_{min} \left| \begin{array}{ll} = \cos^{-1}\left[\frac{1+q^2-(s-h)^2}{2q}\right] & q+s>h \\ = 0 & \text{otherwise} \end{array} \right| \ldots (G3)$$

and the maximum value of α is given by

$$\alpha_{max} \left| \begin{array}{ll} = \cos^{-1}\left[\frac{1+q^2-(s+h)^2}{2q}\right] & q+s>1-h \\ = 0 & \text{otherwise} \end{array} \right| \ldots G4$$

The probability of finding Q at any position is the probability of the corresponding value of α. This is independent of α, and the probability τ_α of α lying between α and $\alpha+\delta\alpha$ is $\frac{\delta\alpha}{2\pi}$. Taking account of the symetry about the vertical in Figure G3, the probability of the resultant of the three carriers lying within the threshold circle is

$$\tau_3 = 2\int_{\alpha_{min}}^{\alpha_{max}} \tau_\alpha\,\tau_\beta\,d\alpha$$

which on expansion and taking the limiting value of $\delta\alpha \to d\alpha$ becomes

$$\tau_3 = \frac{1}{\pi^2}\int_{\alpha_{min}}^{\alpha_{max}} \cos^{-1}\left[\frac{1+q^2+s^2-h^2-2q\cos\alpha}{2s\,(1+q^2-2q\cos\alpha)^{\frac{1}{2}}}\right] d\alpha$$

This was evaluated numerically and the results are shown in Figures 7.5.22 to 7.5.25. The limiting condition for which the threshold is never crossed is, from equn G4 $q + s < 1-h$.

APPENDIX H

The Coupling Harness

H.1 Device Characteristics

This device is a 3 port junction widely used to connect, to a common feeder, two aerials of the same type, which are either stacked vertically of bayed horizontally in the form of an aerial array. Such a junction is often regarded as a perfectly matched power splitter or combiner, but simple scattering matrix theory (Colin 1966) shows that a matched, reciprocal, lossless 3 port is not realizable. For this reason alone it is worthy of some examination, therefore, but the real interest here stems from its use as both a combiner (chapter 10) and as coupler (chapter 11).

Its most frequent physical form provides the starting point for analysis, this is shown diagramatically in figure H1 as a Y junction of three cables. Its analytic form is shown in figure H2 as a junction of three quarter-wavelength coaxial cables with different characteristic impedances. Due to its symmetry two ports (P_1 and P_2) are identical in performance and their associated cable characteristic impedances are likewise identical as Z_1. The third port P_3 has a cable of characteristic impedance Z_2 connected between it and the common junction A.

The characteristics of the device will be determined on the assumption that each port is terminated in a load impedance Z_o therefore the impedance of branch 1 seen at juction A is:

$$\frac{Z_1^2}{Z_o}$$

and this will be paralleled by the same value for port 2 so that their combined impedance is:

$$\frac{Z_1^2}{2Z_o}$$

This appears at port 3 as: $$\frac{2Z_oZ_2^2}{Z_1^2}$$

For this to appear matched to Zo then: $Z_1^2 = 2Z_2^2$

$$\text{or } Z_1 = Z_2\sqrt{2} \qquad \text{.. .. H.1.}$$

This is achieved by the manufacturers, often $Z_2 = 50\Omega$ in 50Ω systems in which case $Z_1 = 70.71\Omega$ which is close to the readily available 75Ω standard. Given that equation H1 is satisfied then the match for port 3, and the symmetry, show that any power incident on port 3 will be equally split between the other two ports as shown in figure H3. But the conditions for power incident on port 2 also need examination.

The impedance of branch 1 and branch 3 of the junction A are respectively:

$$\frac{Z_1^2}{Z_0} \quad \text{and} \quad \frac{Z_2^2}{Z_0}$$

These will be in parallel, and, on tranformation by the quarter wavelength cable to port 2, will appear there as an impedance of:

$$Z_1^2\left(\frac{Z_0}{Z_1^2} + \frac{Z_0}{Z_2^2}\right) = Z_0\left(1 + \frac{Z_1^2}{Z_2^2}\right)$$

which for the conditions of equation H1 give the input impedance as $3Z_0$.

This is a significant mismatch and any incident power on this port will be partially reflected. The reflected portion is given by:

$$\left(\frac{3Z_0 - Z_0}{3Z_0 + Z_0}\right)^2 = \frac{1}{4}$$

So that one quarter of the power incident on port 2 is reflected, and, by reciprocity, one half is transmitted to port 3. Since the device is lossless the remainder appears at port 1. The power transfer diagram for this situation is shown as H4. By symmetry it also applies of course to port 1.

H.2 Use with Aerials

As stated earlier the coupling harness is most usually used with aerials as shown in figure H5 where it is shown connected to two Yagi aerials. If power is incident on port 3, as would be the case for

transmitting then the operation is simply described by the power split to ports 1 and 3 and the array polar diagram can apparantly be determined from simple array considerations assuming equal, in phase, driving power to the elements.

If considered for the receiving situation then at first sight there will be some power reflected at say port 2 due to the impedance mismatch. But there will be an equal amplitude signal from port 1 tansmitted to port 3 and this will be in antiphase due to the total half wavelength path between them. This cross-coupled signal will therefore cancel the reflected one, and the device will behave as is usually considered to be a perfect combiner. There have however been several important and not necessarily true assumptions made in this analysis.

Firstly the two signals were assumed to be of the same frequency. Since any receiver connected to the harness output will deal only with one frequency then there is no limitation here. Secondly the amplitudes were assumed to be the same which would be true only for the case where the signal source is distant, the aerials equal in performance, and algined parallel. In a number of situations, such as a circular array, these conditions are not met. The third assumption was that the signals were in phase and this will be the case, even for parallel alignment of aerials, if the source is in the direction of alignment. If the source lies in a different direction then there will be a path length difference to the two aerials which will be manifest as a phase difference at ports 1 and 2.

The effect of such inequalities will cause the output to port 3 to be determined by the phasor addition of the input quantities as would be expected. But there is an additional effect if the aerials themselves are not perfectly matched under these circumstances. For then the power which is either reflected from the incident port or cross coupled to the other one, is returned to the aerials and further reflected from them. Thus a (lossy) filter is formed by the feeder cables and the overall response is indeterminate. This can then be manifest in the true polar diagram of the array with coupling harness and feeders.

For this reason the four port 'hybrid' as shown in figure H5 is a more tractable device. It is generally, but incorrectly, assumed to be

inferior in performance due to the incorporation of the resistive load where 'half the power goes'. In fact the power loss is the same as for the coupling harness but much greater isolation between ports 1 and 2 can be achieved.

Philosophically since only 3 ports are used it is again a 3 port, but this time with the important addition of being lossy.

H.3 Use for Intermod Measurements

Chapter 11 (section 11.3) discusses intermodulation measurements on towers using the intermodulation test set. To prove the performance of this set it was necessary to simulate the coupling of the various ports of the set in the form which would be found to exist between the aerials in use on the tower but without involving aerials or the tower, both of which were suspect. It was necessary therefore to simulate the three port network of the aerial feeders. This was characterised by 20dB loss between tranmitter ports and 30dB loss between receiver port and any other. This is shown in figure H7, again the scattering matrix requirements of match etc. can be met for this 3 port since it inherently has loss.

The required network could obviously be realised as either a star or delta resistive network. But the resistors would have to dissipate virtually all the incident power (100W) and have to perform at 100 MHz. So a star combination of attenuators was conceived, the tricky point being the three way junction of these.

The conventional hybrid was tried but those used were found to be susceptible to the production of intermodulation products within themselves, they were also susceptable to ageing in this respect. So recourse was made to the coupling harness which it was found was made with good joints and performed well from an intermod point of view.

Similarly the attenuators which were evaluated also generated intermods at the power levels used. They were therefore replaced by lengths of reasonable quality, but not low loss, coaxial cable. The length being chosen to give the desired attenuation.

The network was therfore realised in the form shown in figure H8, where the I's are coaxial cable attenuators, H is the coupling harnes, and

the numerals indicate the coupling/attenuation of the devices between the ports shown.

This then simulated the aerial couplings and successfully proved the intermod performance of the test set. The match of the overall coupling device can easily be shown to be adequate for the purpose desired.

APPENDIX J

Intermodulation Tutorial

J.1 General Representation of a Nonlinearity

One method of representing a nonlinear device is by means of a polynomial transfer characteristic

$$y = A_o + A_1 x + A_2 x^2 + A_3 x^3 + \ldots\ldots A_n x^n \qquad J1$$

where the exciting or input quantity is x, the response or output is y and $A_o A_1$ etc. are constant coefficients. For a truly linear system all coefficients except A_1 are zero, and for practical systems which aim to be linear it is usual to find $A_o = 0$, $A_1 > A_2 > A_3 > A_4$ etc. For the systems under consideration here there is evidence that this does not always hold and one or more higher order terms can exceed the magnitude of lower order ones.

Equation 1 can be written more generally as:-

$$y = \sum_{n=o}^{d} y_n = \sum_{n=o}^{d} A_n x^n \qquad J2$$

where d is the degree of the polynomial (the highest value of n it is considered necessary to include) and n is the order of the constituent component.

J.2 Two Carrier Excitation

If the excitation x is composed of two components such that $x = r + s$ then the n^{th} order response is

$$y_n = A_n(r + s)^n \qquad J3$$

The form of the expansion of this for the first four orders is given in Table J1. The coefficients for this table are most easily derived from Pascal's triangle.

Table J.1

Order n	Expansion of $\frac{y_n}{A_n}$
1	$r + s$
2	$r^2 + 2rs + s^2$
3	$r^3 + 3r^2s + 3rs^2 + s^3$
4	$r^4 + 4r3s + 6r^2s^2 + 4rs^3 + s^4$
5	$r^5 + 5r^4s + 10r3s^2 + 10r^2s3 + 5rs^4 + s^5$

If the two exciters are of sinusoidal form then the polynomial representation of a nonlinearity can be used to predict the intermodulation frequencies. To this end we let

$$r = a \cos(\omega_1 t + \alpha) \ , \ s = b \cos(\omega_2 t + \beta)$$

these can be inserted in the expanded form of y_n and the amplitudes and locations of the intermodulation products derived. Neglecting for the moment the problem of amplitude prediction, to just predict locations the A_n, a, b, α, β terms can be ignored, this then leaves the expansion in the form

$$Y_n = \sum_{q=1}^{n} \cos^{(q-n)}(\omega_1 t).\cos^{q}(\omega_2 t)$$

where Y_n represents the frequency components of y_n this can be simply, but tediously, expanded by the use of trigonometrical relationships. If this is performed, and at the same time amplitudes are again discarded together with a change to non-angular frequencies

$$f_z = \frac{\omega_z}{2\pi}$$

then the relationship can be stated succinctly as

$$F_n = \sum_{m=1}^{n} g_m \ f_m$$

where F_n is understood to mean the intermodulation frequencies of order n, g_m has the value ± 1 and f_m is either f_1 or f_2. Thus F_n consists of all possible combinations of $\pm f_1$, $\pm f_2$ taken n at a time.

By way of example consider n = 2 (the square law mixer case) then, taking f_2 as being higher than f_1 and listing only the positive frequency results gives

$$F_n = (f_1+f_1) + (f_1-f_1) + (f_1+f_2) + (f_2-f_1) + (f_2+f_2) + (f_2-f_2)$$
$$= 0 + (f_2-f_1) + 2f_1 + (f_2+f_1) + 2f_2$$

also for n = 5

$$F_n = 5f_1 + 5f_2 + 3f_1 + 3f_2 + f_1 + f_2$$
$$+ (4f_1-f_2) + (4f_1+f_2) + (4f_2-f_1) + (4f_2+f_1)$$
$$+ (3f_1-2f_2) + (3f_1+2f_2) + (3f_2-2f_1) + (3f_2+2f_1)$$
$$+ (2f_1-f_2) + (2f_1+f_2) + (2f_2-f_1) + (2f_2+f_1)$$

It should be noted from this that the coefficients do not always add to n, they may sum to n, n-2, n-4 etc. This arises when a frequency has associated with it both positive and negative signs deriving from different values of g_m. Thus

$f_1 + f_1 - f_1 - f_2 - f_2$ gives $2f_2 - f_1$.

It should be noted therefore that the intermod frequencies of order n include all those of order n-2. It follows that an intermod found at freqency F which can be calculated as an n^{th} order may in fact be a $n+2N^{th}$ product (N is an integer).

J.3 Multiple Carrier Excitations

When there are more than two exciters then the treatment can follow that given above with the outcome that the n^{th} order products are derived by taking all possible combinations of the exciting frequencies n at a time!

Some examples for the 5th order case are therefore:

$f_1 + f_2 + f_3 + f_4 + f_5$

$f_1 + f_2 + f_4 - 2f_3$

$3f_5 - (f_2 + f_3)$

$f_2 + f_5 - f_1$

The spectral range covered by the intermods extends from, at its lower end, zero frequency in the case of even orders or the smallest difference between two carriers in the odd order case, to n times the highest source frequency at the upper end.

J.4 Carrier Modulation

A modulated carrier can be considered as a cluster of exciting sinusoids covering the range $f-\Delta$ to $f+\Delta$ (where Δ is the half bandwidth required by the modulation, for AM it is the highest modulating frequency). The effect of this is to broaden the intermod spectral line of the unmodulated carried by an amount which is dependent on the bandwidth occupied by the modulations of the contributing carriers and the multiplication factor of that contribution. A simple example for n=3 is shown in figure J1, and another example can be taken for one of the cases considered in the previous section of a 5th order product: $3f_5 - (f_2+f_3)$. This will be broadened by $\pm (3\Delta_5 + \Delta_2 + \Delta_3)$ where Δ_j is the bandwidth occupied by the modulated carried of frequency f_j. If all the modulations occupy the same bandwidth then the maximum spread of an nth order product will be $\pm n\Delta$ about the product frequency.

J.5 Narrow Band Systems

The narrow band of the title is not in the sense of the modulation spectrum but the spread of carrier frequencies likely to be encountered. Figure J2 shows the spectral distribution of intermod products for orders 2 and 3 for the case of two unmodulated carriers f_1 and f_2. The amplitudes are shown diagramatically as decreasing with order number as an aid to clarity rather than indicating their actual magnitude, and the order number of the product is also shown. It will be seen that the order 2 products are thrown well clear of the exciting frequency whereas the order 3 ones can be reflected back to lie close to the originators. This behaviour difference can be generalised to show that, where the exciters are close together in frequency (i.e. narrow band), then only the odd order products will produce intermods close to them (in band).

These in-band products are of particular interest in most systems and particularly so in the case of land mobile radio where base station tranmitter products can affect either the mobile receiver or the return path base receiver.

J.6 Mobile Receiver Influence

The front end of the mobile receiver is to a degree nonlinear and this nonlinearity will generate intermodulation products. Such a product, generated in the mobile by receiving two or more base station carriers, can fall on a frequency assigned for reception by that mobile, and if strong enough can open the mute in the absence of the desired signal, causing severe annoyance to the user. For any given degree of receiver nonlinearity the carriers will be strong enough to do this if the mobile is close enough to the base station (remember the working dynamic range of the mobile is of the order of 100 dB which is greater than the carrier to intermod level for high level carriers) thus there will be a region round the base station in which the mobile could not operate if it decided to avoid this effect. Since the region could well be part, and possibly an important part, of its desired coverage it is usual to choose base station frequency assignments such that no two or three channels form a 3rd order product on another channel, or even that no 2, 3, 4 or 5 channels form a 5th order product on another channel.

Tables or suitable spacings have been produced for up to 8 channel 3rd order by Edwards, Durkin and Green (1969). These are closest spacing (i.e. minimum bandspread) solutions, subsequent (as yet unpublished) work as part of a frequency allocation exercise by PE Consultants (Quarrel 1983) for the Directorate has shown that it is not difficult to generate up to 13 channel 3rd order free sequences but these are not necessarily minimum bandwidth solutions. This work shows that to allocate 13 channels free of 3rd order intermods requires a frequency span equal to 127 channels. If a frequency span greater than this is available then more sequences are possible, for instance 66 sequences of 13 channels were found in a spread of 150 channels. Table J2 shows channel allocations for 3-8 and 13 channel sequences.

Table J2 3rd Order Free Assignments

No of Channels	Channel Assignment
3	1, 3, 6
4	1, 3, 6, 10
5	1, 3, 7, 10, 15
6	1, 4, 8, 13, 19, 21
7	1, 3, 11, 17, 22, 26, 29
8	1, 4, 9, 15, 19, 31, 38, 40
13	1, 3, 6, 10, 23, 31, 42, 54, 69, 87, 111, 121, 127

J7 Base Station Receiver Assignments

The base station receiver is also vulnerable to intermods. Those which are generated in the transmitter equipment, and those which would be generated in the receiver, are in principle amenable to treatment with suitably located and designed filters. Neither transmitter nor receiver filtering can affect however the intermods generated by site nonlinearities. The treatments here are either to quench the intermod at source (a subject in its own right) or to take account of them when allocating transmitter and receiver bands of operation.

The spread of odd order intermod products is shown in Fig J3. This assumes an allocated band B Hz wide for the base transmitter and assumes that the actual assignments at any one site can be anywhere within this band. On this basis the bands shown are blighted by the intermod band and have a spread of nB Hz. For any blanket planning considerations therefore, the associated receiver band at the same site should be clear of the intermod spread up to the order which gives troublesome product levels. For 50W transmitters, measurements have shown that this should be at least the 11th order.

It is possible in principle to seek receiver assignments within the blighted bands on the assumption that the intermods will be discrete rather than continuous. This becomes difficult for moderate numbers of channels due to the number of products (see the next section), the

chore of calculating and assessing them (even with processor help), and the impact of modulation. For these reasons the simplest approach is to cluster the actually assigned transmit frequencies as closely as possible to form a sub band B' Hz wide such that B' is smaller than B and the subsequent intermod spread is correspondingly reduced. Thus a localised assignment band B' is formed which can be located anywhere within B.

The arguments used in this section have assumed that the designer has only two bands of frequencies to contend with (one transmit, one receive) and that he has full control of the site. It is not uncommon, however, to find that there are other users, or site sharers, present. Just one other user transmitting outside the band B can cause the product distribution to be as shown in Fig.J4. The extra bands which are blighted are shown shaded. Thus just one extra radiated signal can significantly exacerbate the frequency assignment problems where intermods have to be taken into account.

J8 Number of in-band products

It is instructive to gain an idea of the rate at which the number of intermod products increase as extra numbers of channels are considered and/or higher order numbers. The in-band (i.e. odd order numbers with a difference of 1 in the number of positive to negative contributions) case is considered since it gives an idea of the difficulty of finding intermod free locations for the situation considered in the previous sections. These are shown in Table J3.

Table J3 Number of in-band Intermodulation Products

Non linearity order / Number of channels	3rd	5th	7th	9th
2	2	2	2	2
3	9	15	21	27
4	24	64	124	204
5	50	200	525	1095
6	90	510	1770	4625
7	147	1127		

APPENDIX W

High Order Intermodulation : Location Diagrams

W.1 Discrete Transmissions

There is a need to be able to predict, in perhaps fairly broad terms, those frequencies which will be affected by high order intermodulation products from various combinations of transmitter frequencies. This has been done in chapters 12 and 13 for the cases where all the transmissions can be considered as part of a virtualy continuous comb or spectrum of emissions. This Appendix applies the same sort of reasoning to the situation where the transmissions occur in two distinct spectral regions or bands, and specifically for the bands 152-153 MHz and 154-156 MHz.

Consider first the case of just two discrete transmissions at frequencies A and B. Now current interest lies in the region immediately below these bands. The frequencies of the intermodulation product are then given by

$$\frac{A(N+1)}{2} - \frac{B(N-1)}{2}$$

where N is the order of the product in question.

Figure W.1 shows the intermodulation spectrum resulting from two transmissions as the frequency of one, B, is altered. It is obvious that this can be presented in a semi-graphical form as in figure W.2. This shows the location of the various odd order (in band) intermod products as a function of location of the upper transmission, with the lower one fixed. Other similar diagrams could be drawn for different locations of the lower transmit frequency A.

W.2 Bands of Transmissions

In the case considered above there will be only one intermod product for each order. [This applies in the specially restricted sense under consideration, but not in general].

If there is more than one transmission associated with what is now frequency band A and also for band B, then there wil be, correspondingly, a number of intermodulation products. For each order they can be considered to group around the discrete ones, discussed in W.1, and form intermodulation bands.

Appendix X discusses the number of products in the bands, but here interest is directed to the width of the band. This can be determined by calculating the highest and lowest frequency for that product.

Take now the lower transmit band to be defined as of width a and the middle frequency to be A as before, and similarly for b and B the intermod band will be given by

$$\left(A \pm \frac{a}{2}\right) \frac{(N+1)}{2} - \left(B \pm \frac{b}{2}\right) \frac{(N-1)}{2}$$

thus the lowest intermod frequency will be determined by taking the lowest part of band A, $(A - \frac{a}{2})$, and the highest frequency of band B, $(B + \frac{b}{2})$. The highest intermod frequency for a given order will be a function of the highest frequency of band A, $(A + \frac{a}{2})$ and the lowest of band B, $(B - \frac{b}{2})$. Therefore the intermod band extends from

$$\left(A - \frac{a}{2}\right)\left(\frac{N+1}{2}\right) - \left(B + \frac{b}{2}\right)\left(\frac{N-1}{2}\right) \quad \text{to} \quad \left(A + \frac{a}{2}\right)\left(\frac{N+1}{2}\right) - \left(B - \frac{b}{2}\right)\left(\frac{N-1}{2}\right)$$

It is therefore has a width of

$$a \frac{(N+1)}{2} + b \frac{(N-1)}{2}$$

[Note if a = b then width of intermod bands = aN].

The location of the intermod bands is still a function of the location of the middle frequencies of the two transmissions A and B. An example is shown in figure W.3 for a = b = 100 kHz. This shows how different parts of the prospective receive bands will be blighted by intermod products emanating from the multiple transmissions in the bands at A and B, as a function of the location of the upper of these 100 kHz bands. As the width of the bands A and/or B is increased so the intermodulation band increases in width for each order. Even a modest increase will cause the 9th and 11th order bands to overlap at the bottom of figure W.3. In chapters 12 and 13 the overlap can be considerable.

APPENDIX X

High Order Intermodulation: Calculation and Results

X.1 Introduction

Appendix W gives the means of predicting the locations of either discrete intermodulation products from two transmitters or the overall band of intermods from two transmit bands. This Appendix calculates the actual intermodulation frequencies (channels) for any number, or combination, of transmissions in the two transmit bands (152-153 MHz and 154-156 MHz). Like Appendix W it treats only the specific case of odd order intermods falling just below the transmit band. This covers the region of immediate interest - the receive bands - and the restriction is necessry in order to admit the large number of potential transmissions and high order products. In particular it does not cover the intermodulation products falling above the transmit band and, more importantly, it excludes those products which result from considerations of either transmit band on its own (this will in any case not reach the receive bands if neither band is wider than 1 MHz). Therefore it takes one or more transmissions from the lower transmit band and considers them interacting with one or more transmissions from the upper band.

X.2 Aims and Conditions

The object of this exercise is, for a given distribution of transmitter frequencies, to calculate those specific receive frequencies which are hit by the intermodulationn products (up to 11th order). Thus to assess the degree to which intermod free gaps might be found in those bands which Appendix W indicated would be blighted. It was thought to be of additional interest to record the number of intermodulation products on each channel.

This analysis ignores any modulation, treating only carriers, and assumes that each is at the centre of its channel. This admits the technique of dealing only with 'channel numbers' - rather than frequencies. This is highly beneficial for the computation necessary since it means that instead of having to deal with frequencies such as 152.6250, 152.6125, 155.3375 etc the corresponding channel numbers 50,

59, 267 ... can be used. The computer then needs to handle integers and can work correspondingly faster.

The channel numbering scheme used was as follows:-

142-144 MHz, channels 1-160 .... Receive band
146-148 MHz, channels 321-480 .... Receive band

thus the receive bands had a common reference, at 142 MHz, for the two bands.

For the transmit channels each band was treated separately and started channel numbering at its lowest frequency:-

152-153 MHz, channels 1-80 ... Lower Transmit band
154-156 MHz, channels 1-160 .... Upper Transmit band

X.3 Computation

Following the reasoning given in Appendix W the Nth order intermodulation products under consideration are determined by X = $\frac{1}{2}(N+1)$ components (transmissions) from the lower transmit band and Y = $\frac{1}{2}(N-1)$ components from the upper band. More precisely each is the sum of X of the L lower band components minus the sum of Y of the U components of the upper band. Thus the intermod frequencies or channel numbers are given by:-

$$I = \sum_{j=1}^{j=X} l_j - \sum_{k=1}^{k=Y} u_k \qquad - X1$$

where l_j takes any of the values of the lower band channels and u_k takes any of the values of the upper band channels. The qualification to this is that the same sequence of l_j's and u_k's is to be considered only once, irrespective of the arrangement within this sequence. The same channel number can however appear up to X or Y times respectively in any sequence.

A computer program was written in BASIC to run on a microcomputer (BBC model B) to calculate all the relevant products. It kept track of the

number of times an intermod fell on each receive channel, and it used integer arithmetic to improve its speed. Even so the calculations for 7 low band and 6 upper band channels for all odd orders from 5th to 11th took some 50 minutes to compute and another 6 to print. A listing of the program is shown in figure X.1.

X.4 Results

The program output was in the form of a printed list of receive channel numbers in sequence, with the number of intermod products of each order which fell in any one channel indicated. For ease of scanning the results, every channel which was completely free of intermod was marked by an asterisk.

Various combinatiions of transmit channel allocations were tried and are shown in the following figures for the conditions indicated.

- Figure X2(a-d): 13 channels; 7 lower transmit band, 6 upper. Full 3rd order intermod free sequence (Quarrell 1983) with a split into 2 bands. Approximately 0.5 MHz occupancy of lower band and 1 MHz occupancy of upper band. Similar to figures 12.3.4 and 12.3.5.

- Figure X3(a-d): 13 channels; 7 lower transmit band, 6 upper. Lower band channels contiguous, upper on 3rd order spacing for 5 channels (Edwards et al 1969) with each spacing increased by 6, as discussed in section 12.4.2. and shown in figure 12.4.5.

- Figure X4(a-d): 13 channels; 7 lower transmit band, 6 upper. Both bands on contiguous assignments. As discussed in section 12.5.3 and shown in figure 12.5.3 (@ 0.825 MHz).

X.5 Discussion

The first point of note concerning the results is that there is agreement between these and the corresponding figures of section 12.5 (derived from Appendix W) as to the general location of the intermodulation products. It might have been thought that there would

be some intermod free channels in the receive band for the 3rd order free transmitting sequence as shown in figure X.2. In fact there were none! This therefore confirms the view taken in Chapter 12 that the gaps in intermods would be at best few and that they could not be relied on [Note carriers only are considered here - no modulation, which could only spread the intermods.]

The major factor of note in figure X.2 is the unexpectedly high number of products which fall on virtually all receive channels. Thus not only are there no free channels but all channels are heavily blighted. The implications of this will be dealt with in section X7.

Figure X3, one contiguous band and one 3rd order free distribution, did show free receive channels in the regions indicated by the broad brush approach of section 12.5 and Appendix W. Again, however, there were no channels free of intermods in the regions of intermod predictions.

Figure X4 shows the effect of bunching the transmissions - the extreme case of contiguous channels. The intermod locations are again as expected, and there are no free channels in the intermod band, but the remarkable feature is the extremely high numbr of products on the blighted channels: 11,526 for the worst of the 11th order. It was to be expected that the bunching of the transmit channels would lead to bunching of the intermods and therefore there would be many more products per receive channel, in this case, compared to that of figure X.2 - both with 13 transmit channels.

The accuracy of the computer predictions was checked (again) for simple test conditions whose outcome could be easily predicted. This was satisfactory, so the theory was examined to see if it could easily predict or confirm the numbers.

X.6 Prediction of Numbers

Equation X1 (in section X.3) gives the generating equation, and the program listing shows the details of the calculation, but it is desirable to have an analytic expression for the number of intermodulation products.

The number of intermods can be deduced from equation X1. Since every combination of the low band transmissions (the first term of X1) is considered with every arrangement of the uper band transmissions (the second term of X1), then the total number of intermodulation products is the product of these two factors.

The question then reduces to one of determining the number of ways in which W items can be arranged Z at a time. This is not the normal 'combination' situation since each of the W items can appear more than once (up to Z times) and yet the order of the arrangement is not important. So that duplication of the form $W_1\ W_1\ W_2$, $W_1\ W_2\ W_1$ are the same.

This is given by $$\Sigma_{w,z} = \frac{(w-1+z)!}{z!\,(w-1)!}$$

So that the total number of products for order N (falling just below the transmit band) is:-

$$\sum_{I(L,U)} = \frac{(L - 1 + \frac{1}{2}(N+1))!}{\frac{1}{2}(N+1)!\ (L-1)!} \cdot \frac{(U - 1 + \frac{1}{2}(N-1))!}{\frac{1}{2}(N-1)!\ (U-1)!}$$

It can be noted that if it were desired to calculate all the products of the transmissions, L plus U, for the Nth order then this can be derived as:-

$$\sum_{I(L+U)} = \frac{(L + U - 1 + N)!}{N!\ (L + U - 1)!}$$

Values of $\sum_{I(L,U)}$ and $\sum_{I(L+U)}$ are given in Table X.1.

TABLE X.1

NUMBER OF INTERMODULATION PRODUCTS FOR VARIOUS CONDITIONS

Condition	Intermod Order No. N			
	5	7	9	11
4 Low Band Transmissions 5 Upper Band Transmissions	300	1,225	3,970	10,584
Total Nth Order Intermods for 9 Transmissions	1,287	6,435	24,310	75,582
7 Low Band Transmissions 6 Upper Band Transmissions	1,764	11,760	58,212	232,848
Total Nth Order Intermods for 13 Transmissions	6,188	50,388	293,930	1,352,078
8 Low Band Transmissions 8 Upper Band Transmissions	4,320	39,600	261,360	1,359,072
Total Nth Order Intermods for 18 Transmissions	26,334	346,104	3,124,550	21,474,180

X.7 Implications

The very large number of products falling on a receive channel raises the question of how they will add or combine. If the transmissions are each derived from a separate frequency source then the products will not be identical in frequency since there will be (a small) offset of each transmission from its true centre channel frequency. On this basis the products will add on a power basis. Therefore the effect of the 11,526 products in the worst 11th order channel discussed in the last section will be in effect quivalent to one product 40.6 dB greater than that of an individual 11th order one.

This is very significant increase in expected intermod level and is in part due to the bunching of transmissions. It raises interesting questions about the source of the intermod power when very large numbers of transmissions are present and the consequential numbers of products extremely large, but this cannot be dealt with here.

The situation where the transmissions have a common frequency reference must be considered, since there are attractions for operating base stations in this manner. For this situation the products will all be of exactly the same frequency and phase coherent! This then is covered by Rayleigh probability statistics, see Appendix A, with the rms value given by power addition. Under this situation, even more than in the straight power addition case, the variability about the mean can be considerable.

Two factors argue against the Rayleigh situation obtaining in practice even if a common frequency source is used. These are: (i). noise on the frequency reference lines and in the individual transmitter synthesisers causing a randomising effect, and (ii). the site intermods which are thought to come from a number of locations so that small movements of the tower etc will change the magnitude and phase relationships. Thus even if a common frequency reference is used then it is reasonable to add the intermodulation contributions on a power basis.

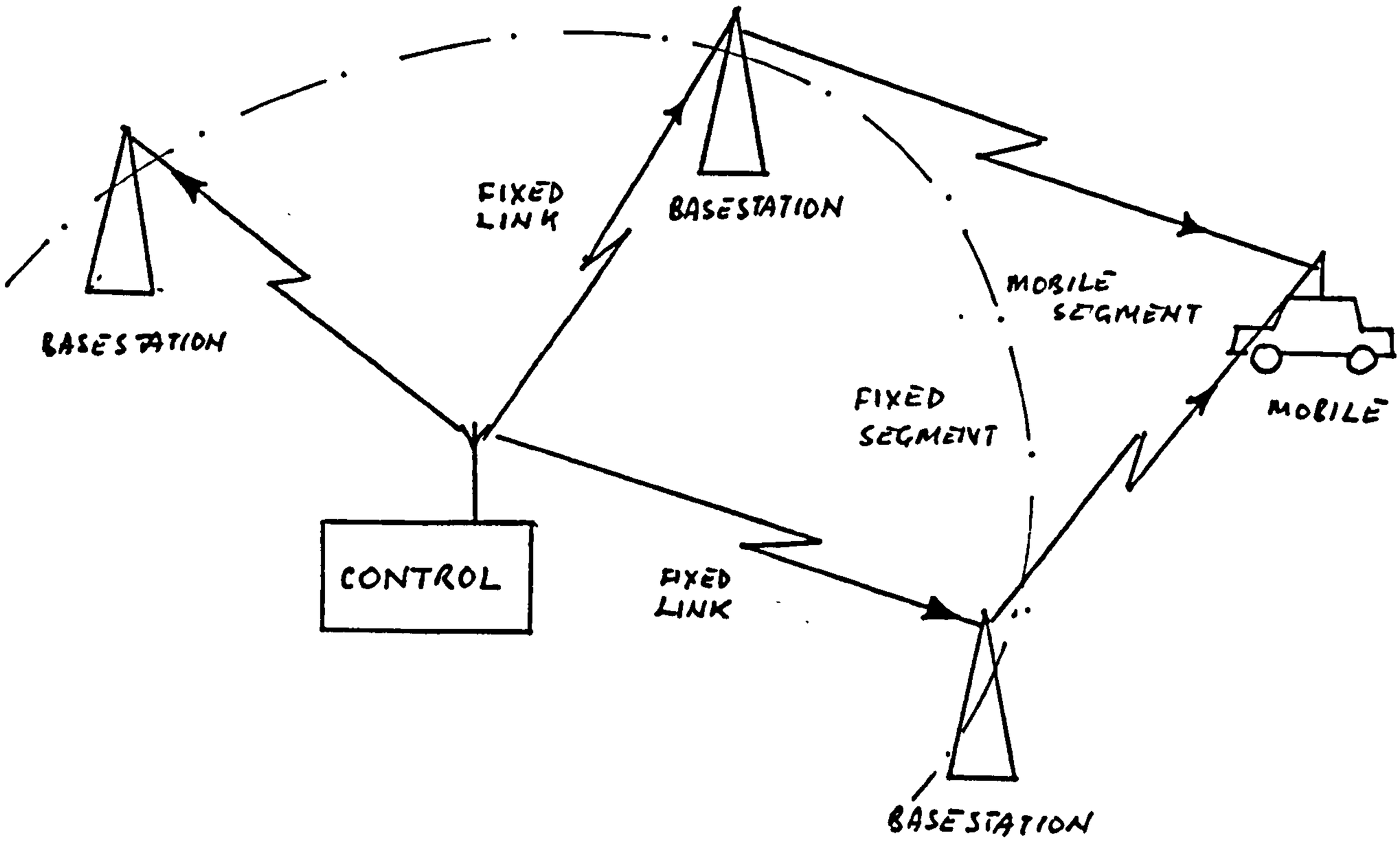

Fig. 2.1.1 Basic System - Pictorial

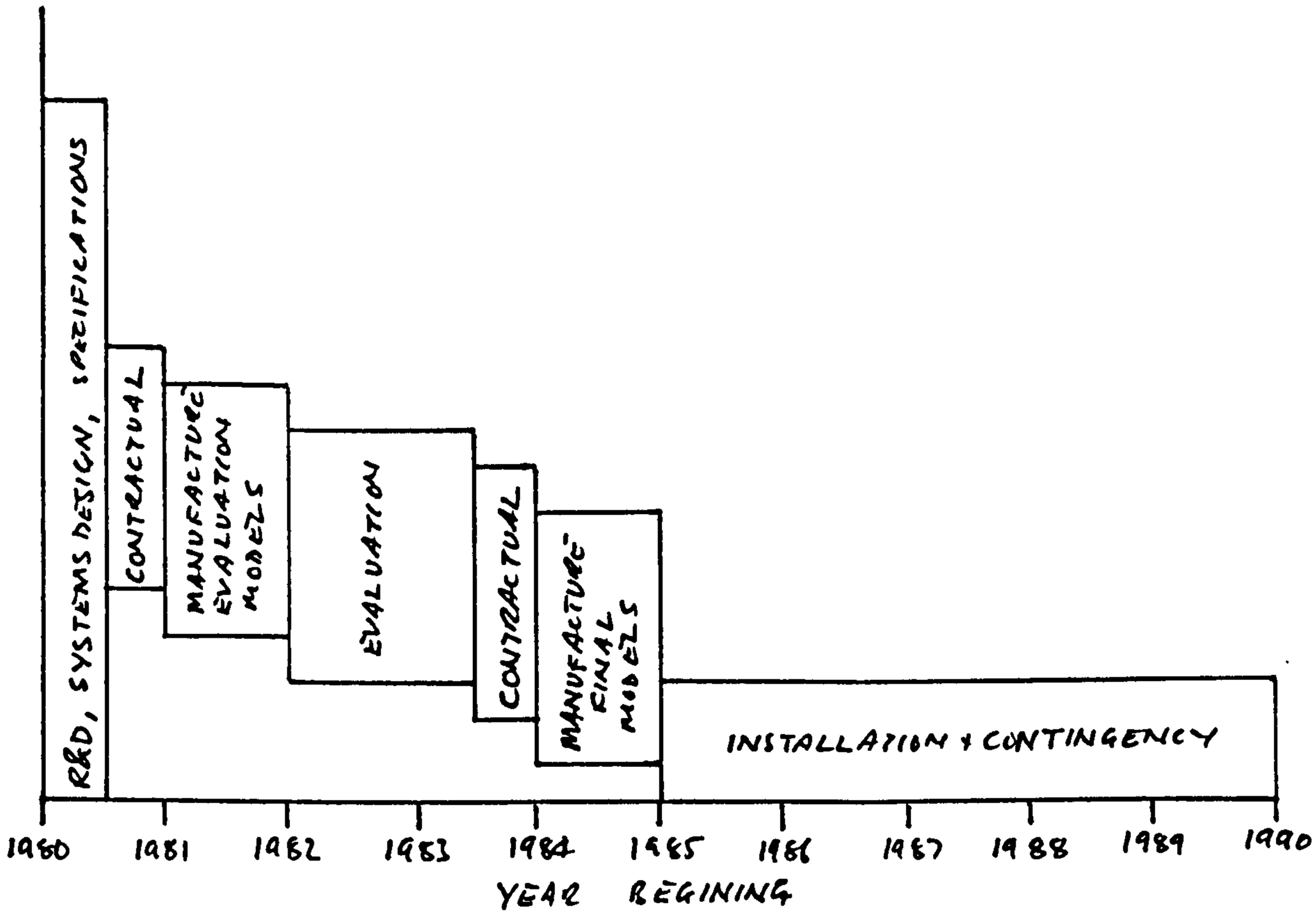

Fig. 2.3.1 Timescales - Bar-chart of Major Activities

INTERACTION DIAGRAM FOR MOBILE RADIO OUTGOING PATH DESIGN

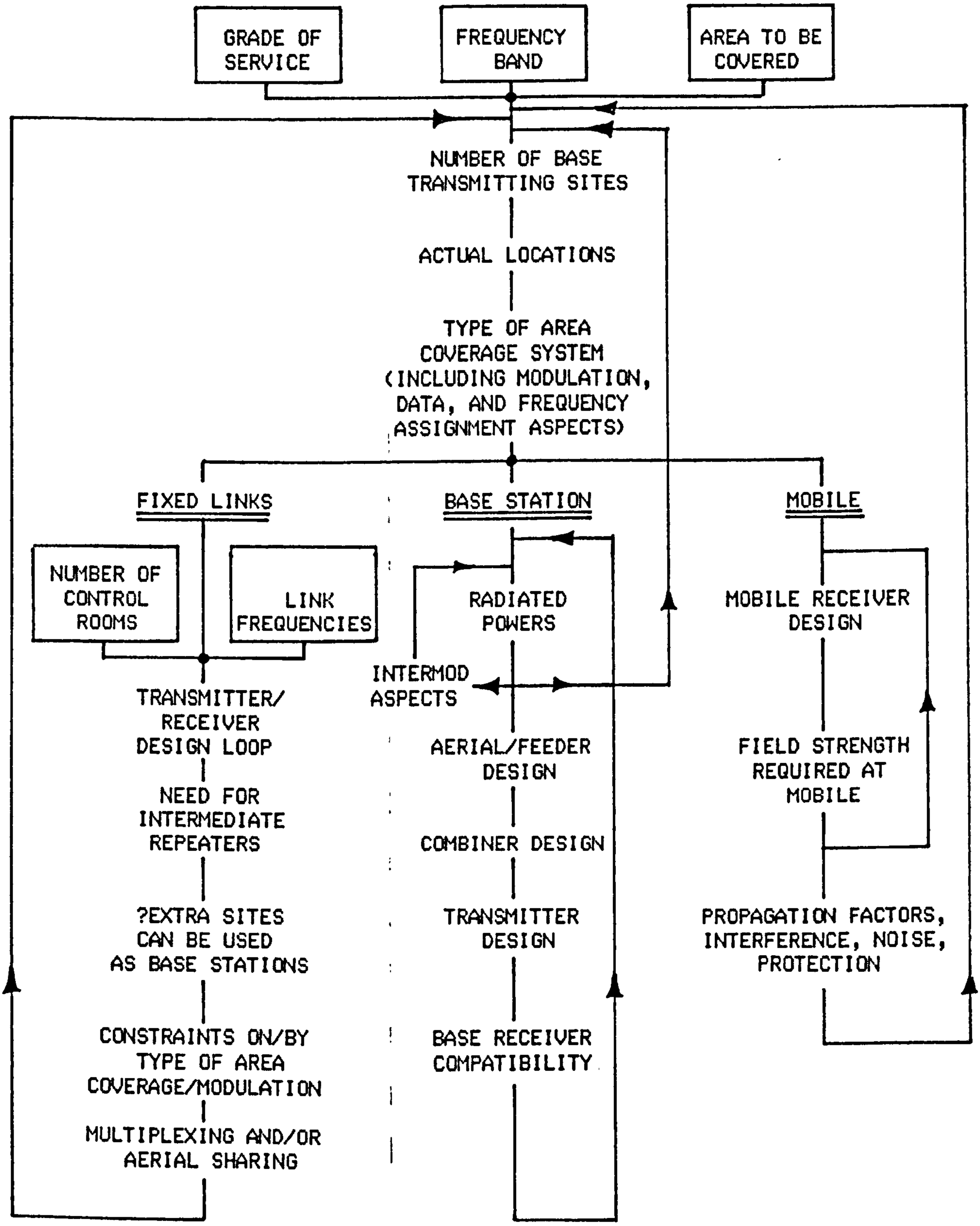

Fig. 3.2.1 The Interaction Diagram

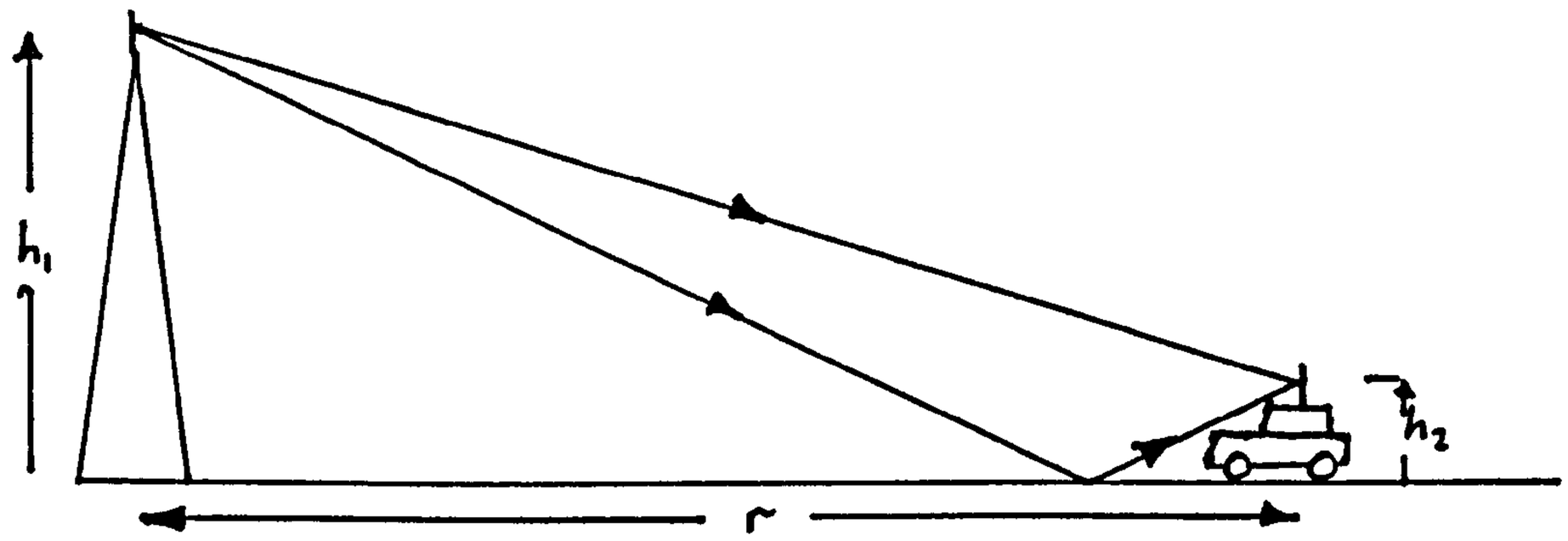

Fig. 4.1.1 Basic View of Propagation

Fig. 4.2.1 Measurement of Signal Levels vs. Range I

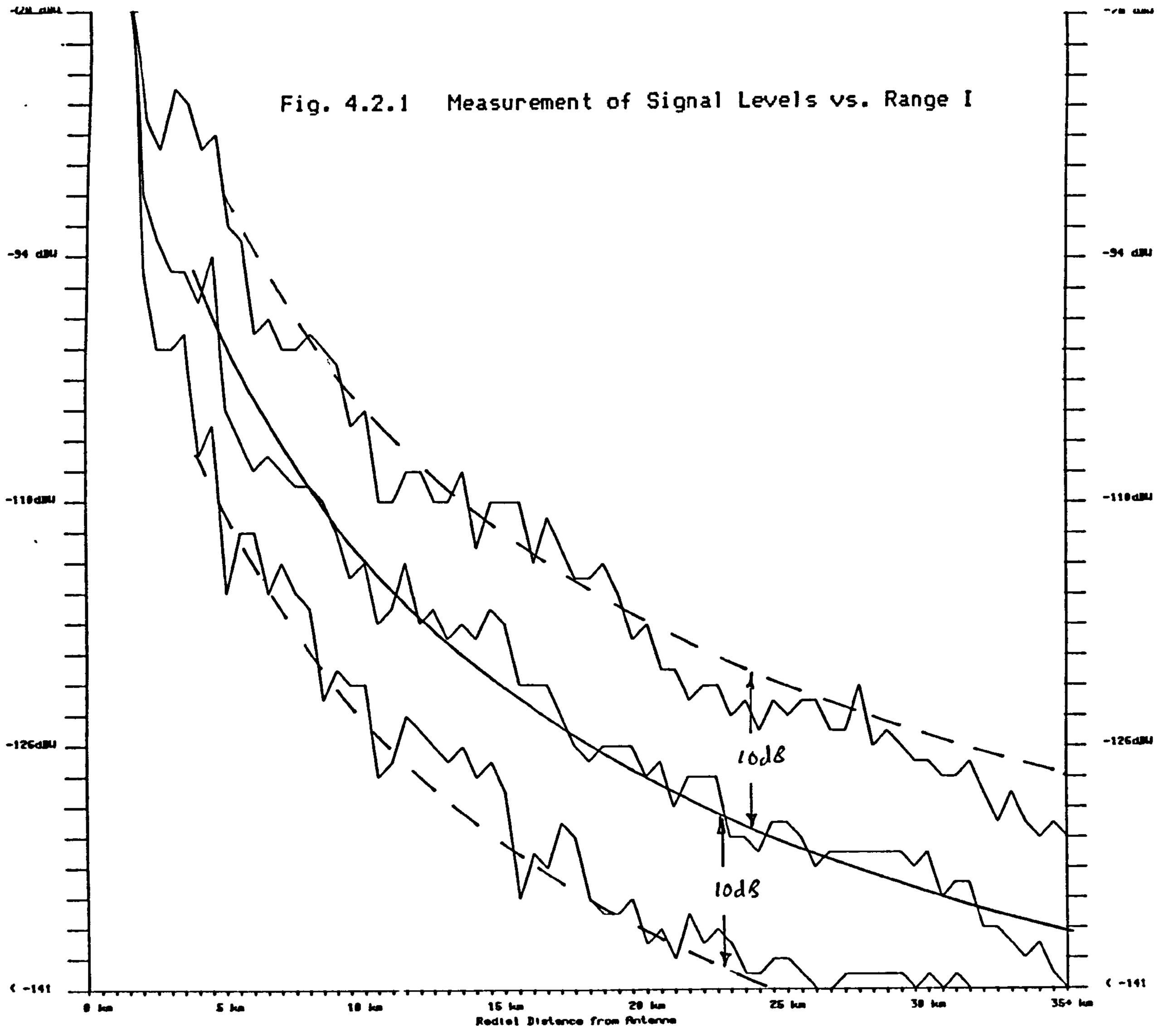

Strength vs Distance ↑ 10% level — 50% level ↓ 90% level
••••••••••• Statistical Abstraction •••••

Fig. 4.2.2 Measurement of Signal Levels vs. Range II

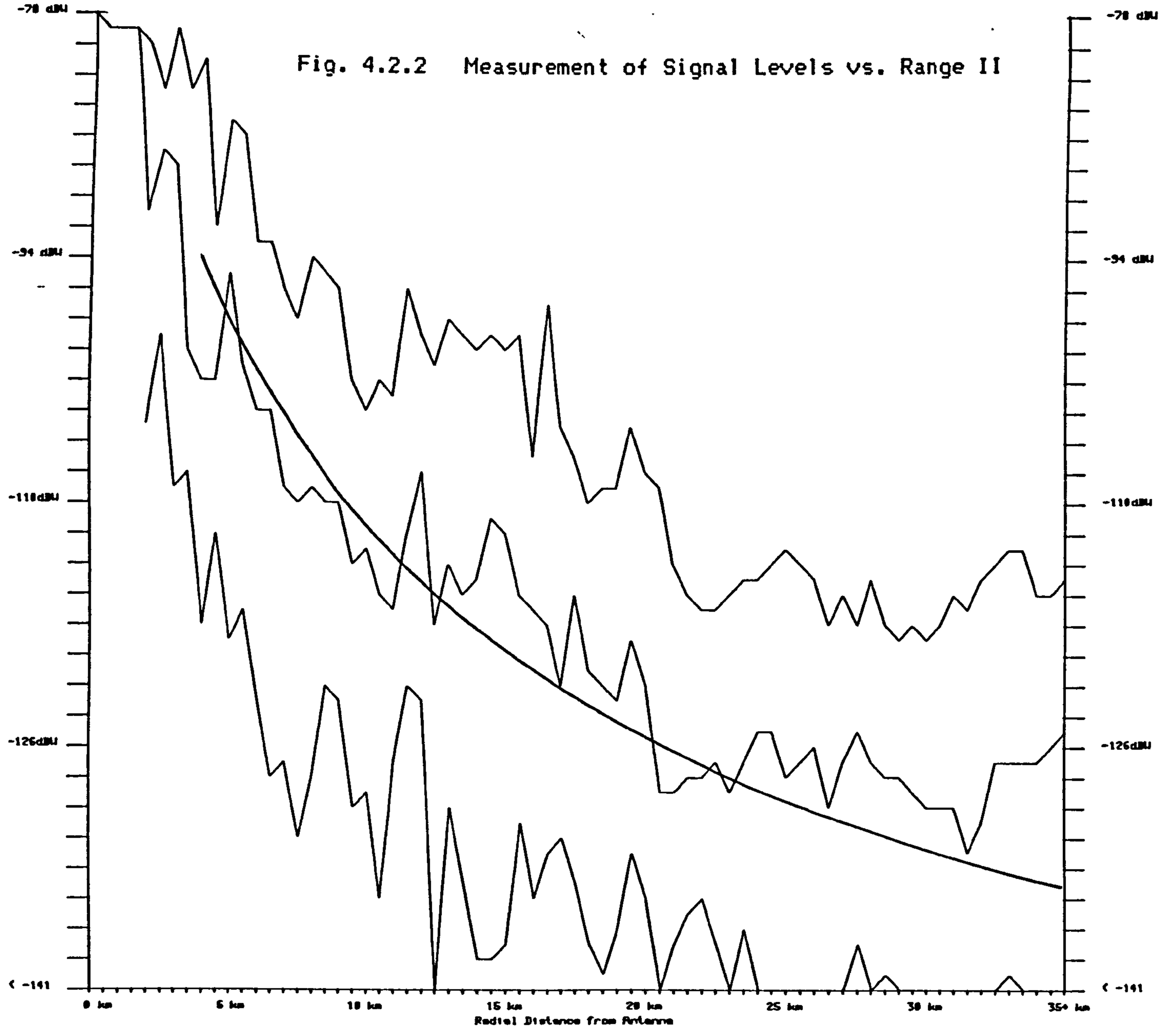

Strength vs Distance ↑ 10% level — 50% level ↓ 90% level
••••••••••• Statistical Abstraction ••••• ••••• •••••••••••

Fig. 4.2.3 Measurement of Signal Levels vs. Range III

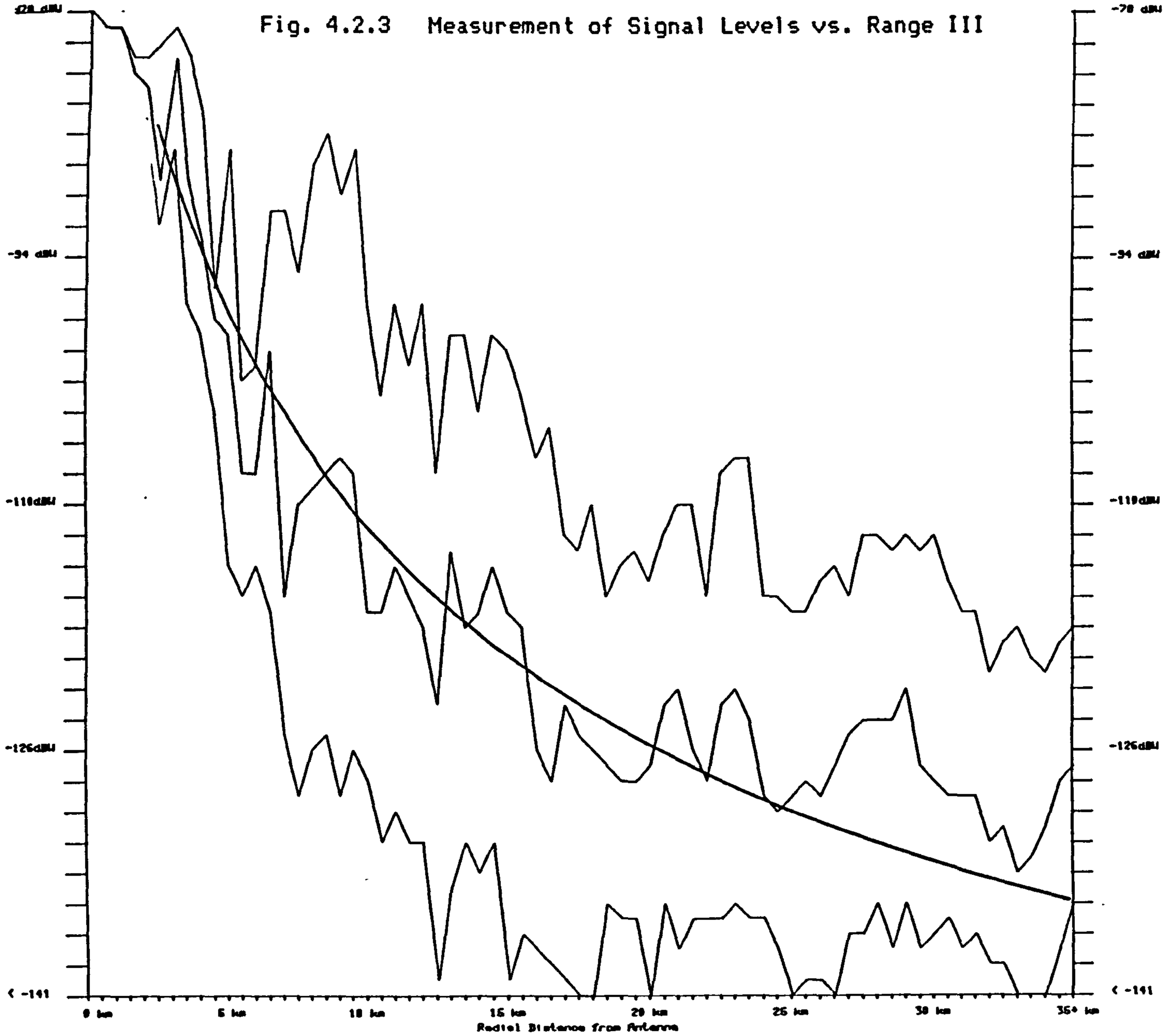

Strength vs Distance ↑ 10% level — 50% level ↓ 90% level

Fig. 4.2.4 Measurement of Signal Levels vs. Range IV

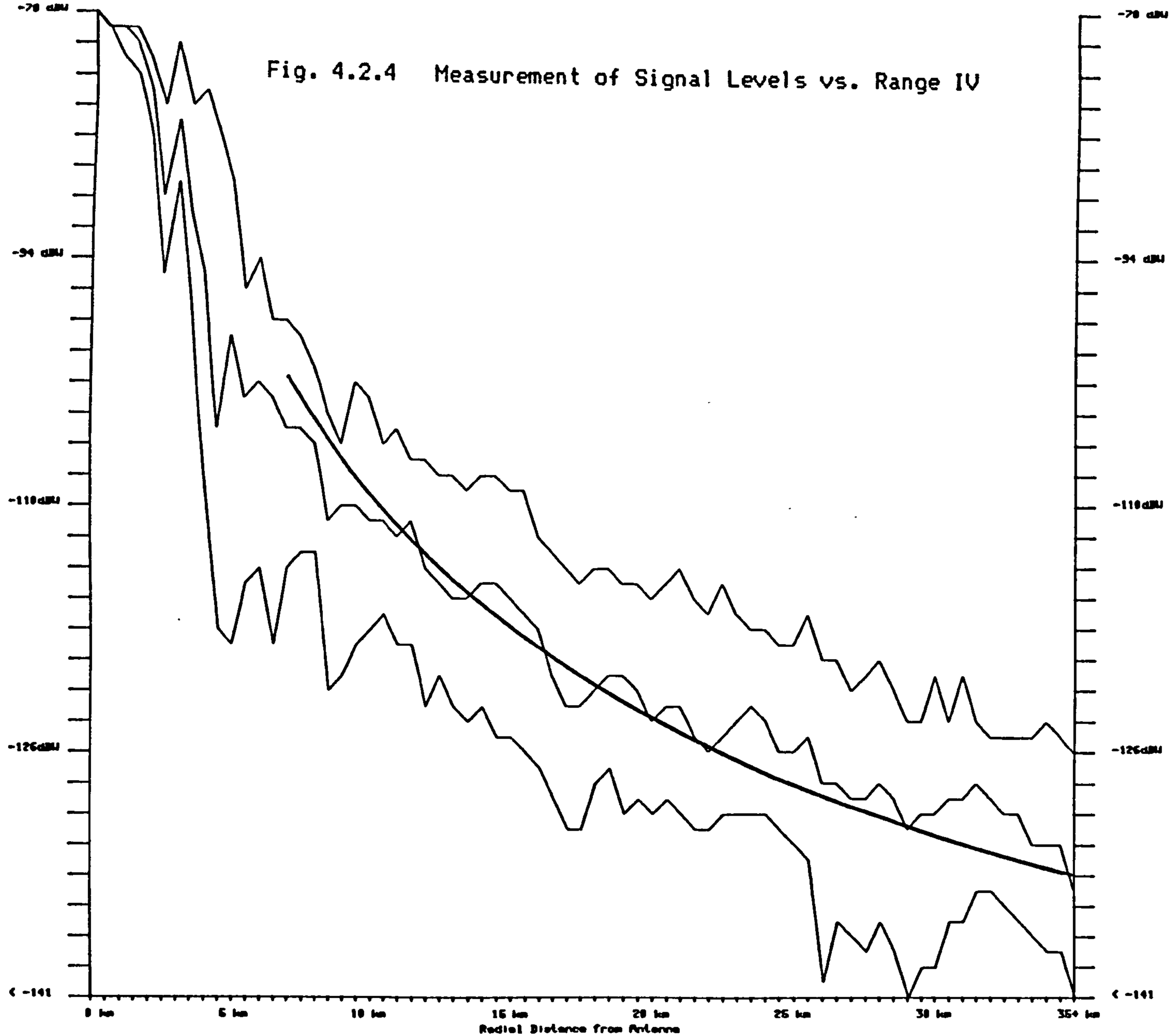

Fig. 4.2.5 Measurement of Signal Levels vs. Range V

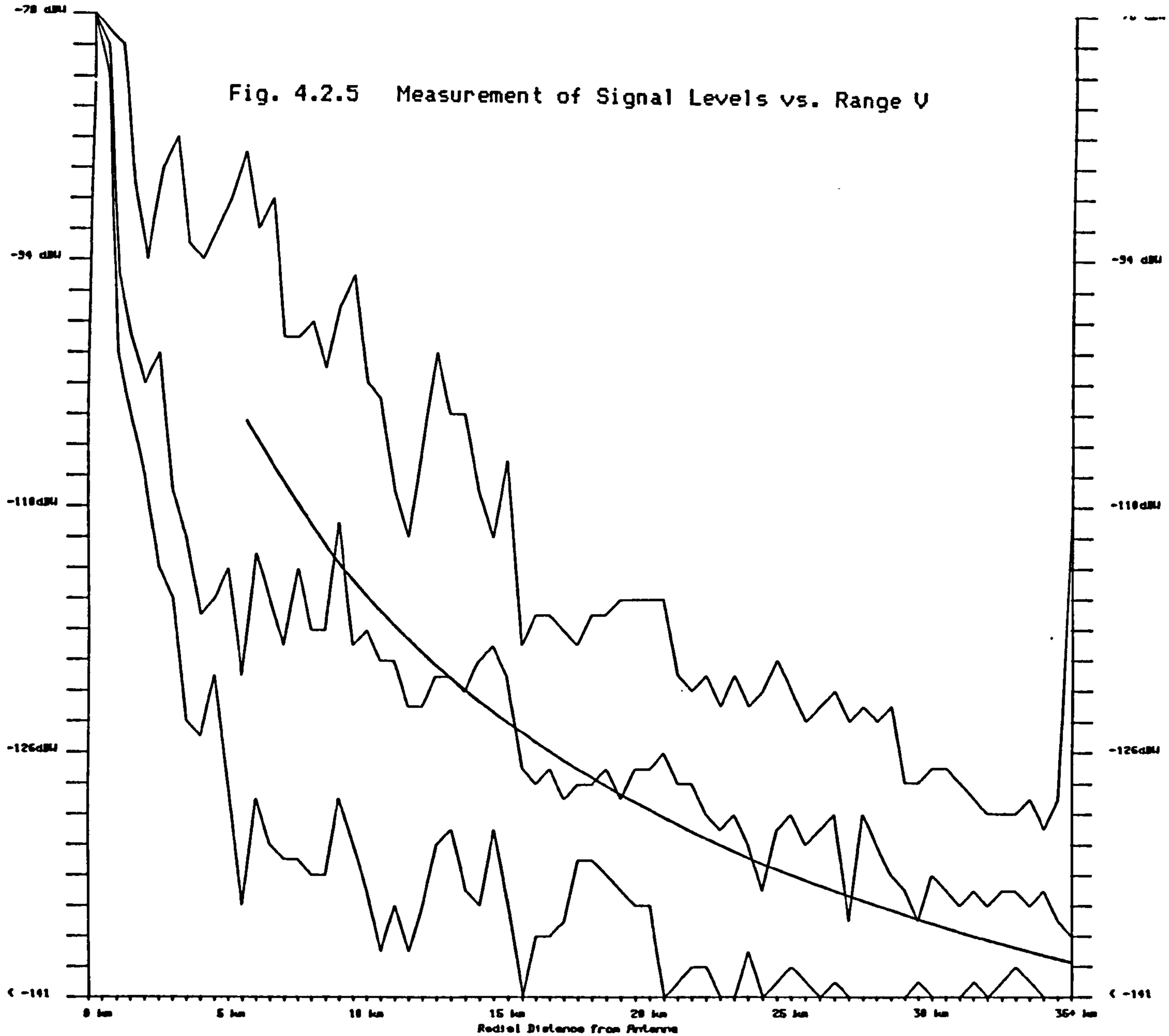

Strength vs Distance ↑ 10% level — 50% level ↓ 90% level
Statistical Abstraction

Fig. 4.2.6 Measurement of Signal Levels vs. Range VI

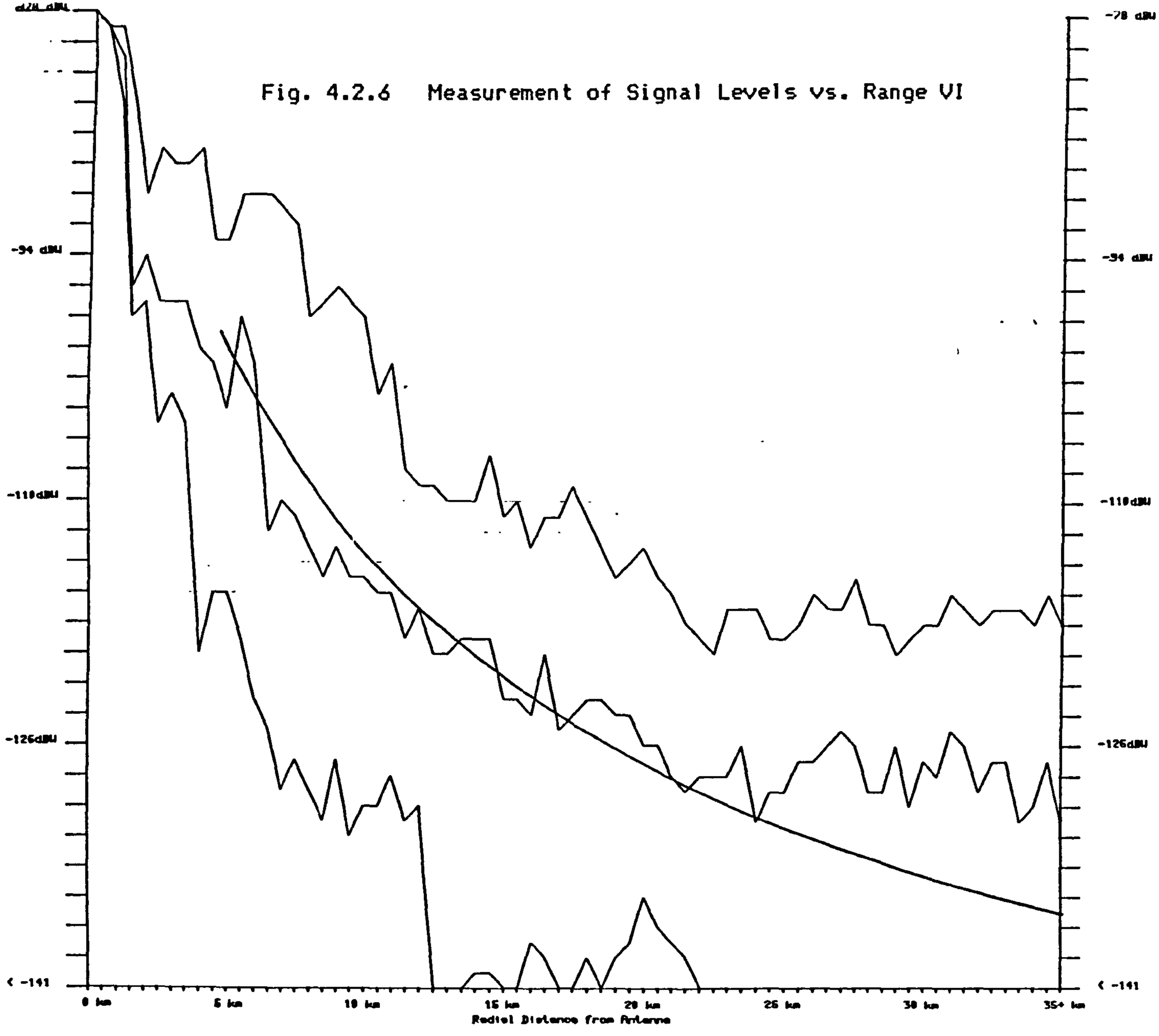

Strength vs Distance ↑ 10% level — 50% level ↓ 90% level
•••••••••• Statistical Abstraction •••••

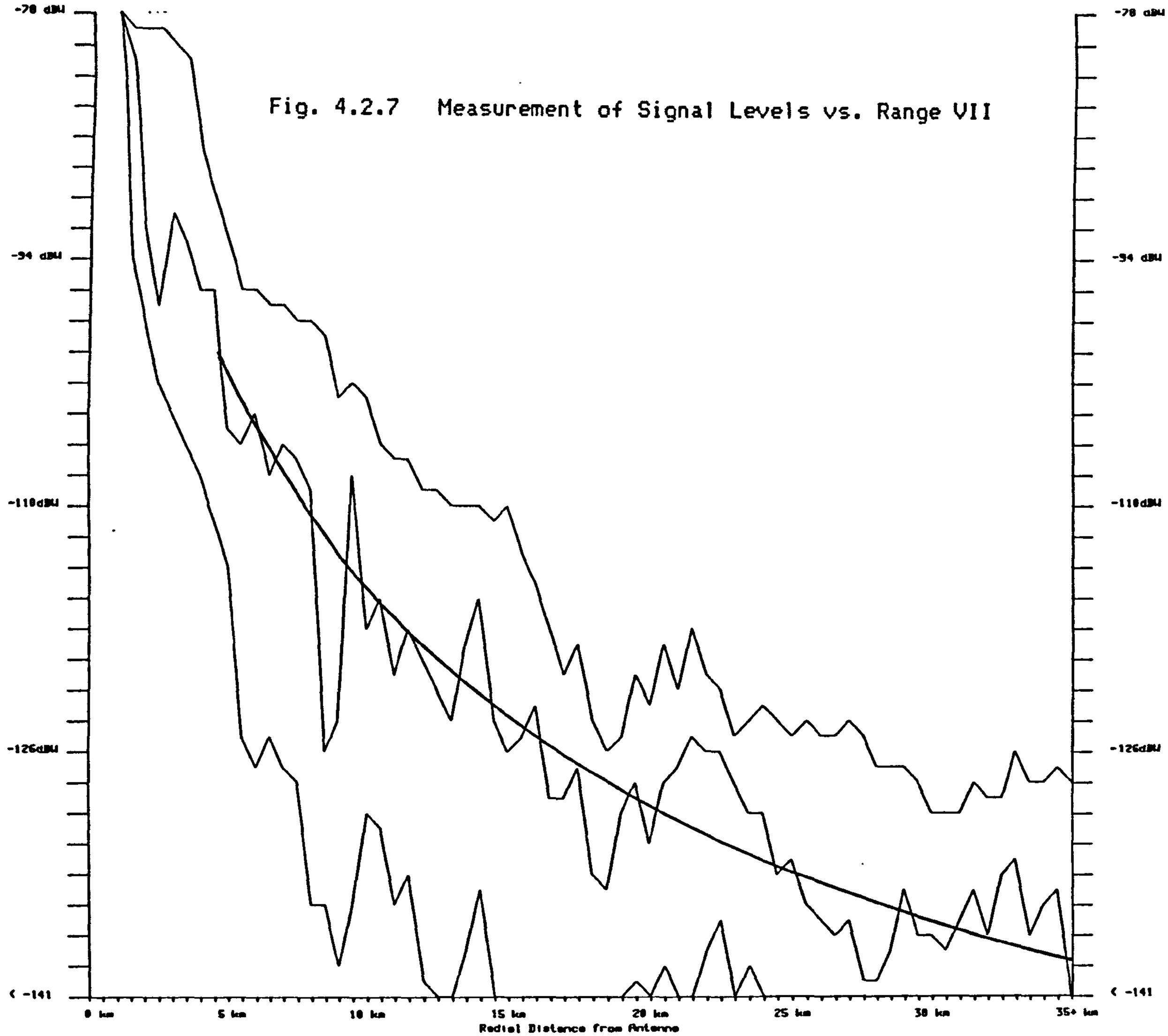

Fig. 4.2.7 Measurement of Signal Levels vs. Range VII

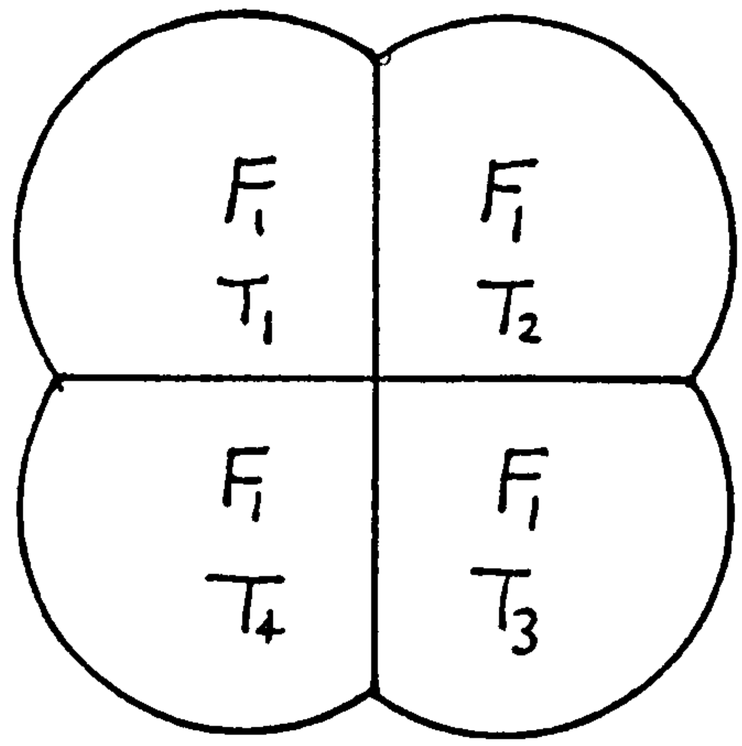

Fig. 5.2.1 Time Division Operation - Frequencies and Times

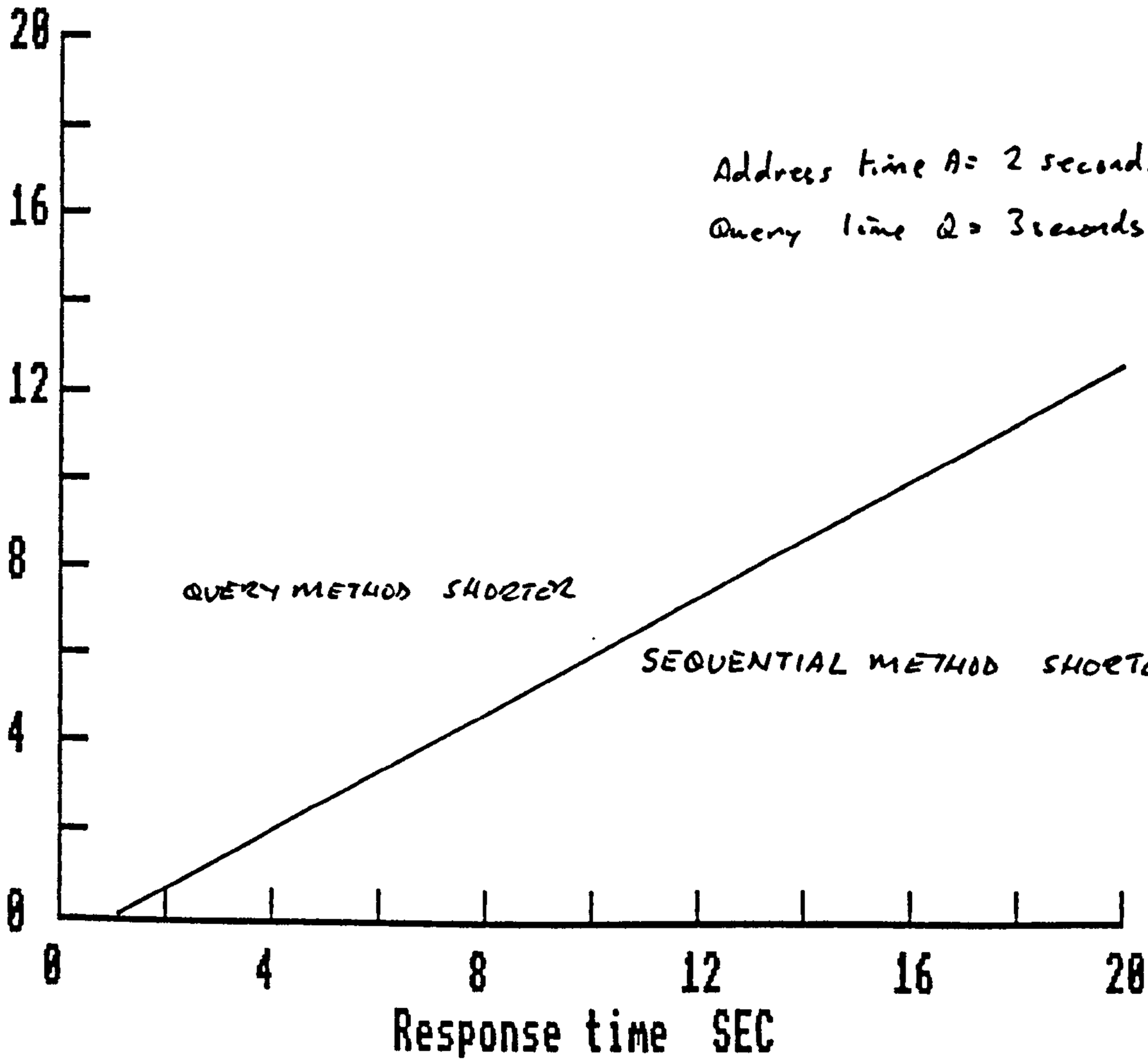

Fig. 5.2.2 Time Division Operation - Polling Mode

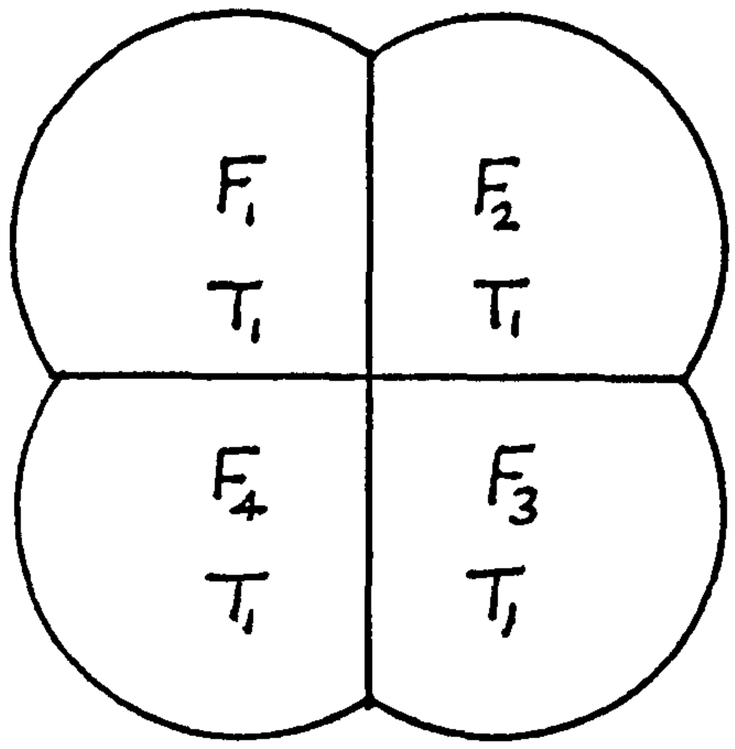

Fig. 5.3.1 Frequency Operation - Frequencies and Times

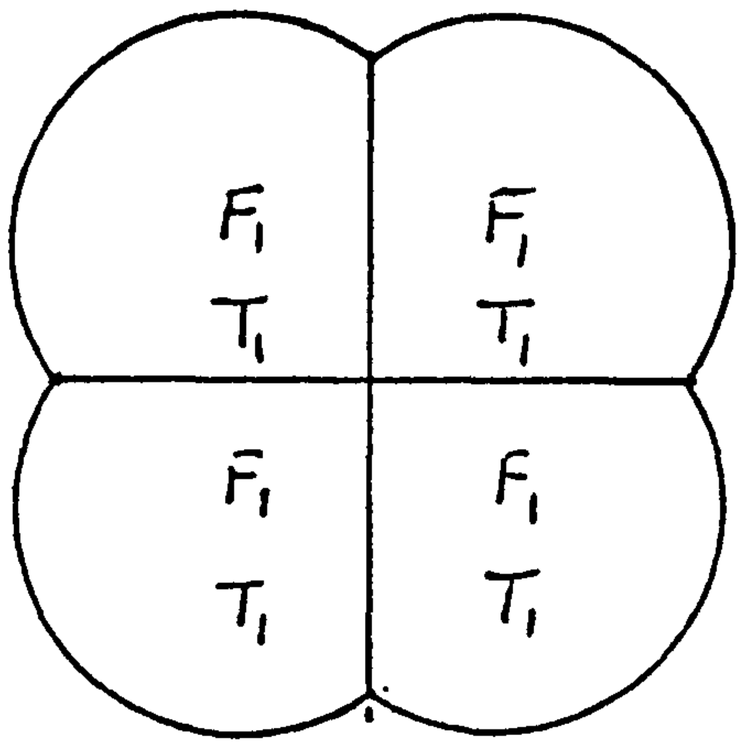

Fig. 5.4.1 Common Channel Operation - Frequencies and Times

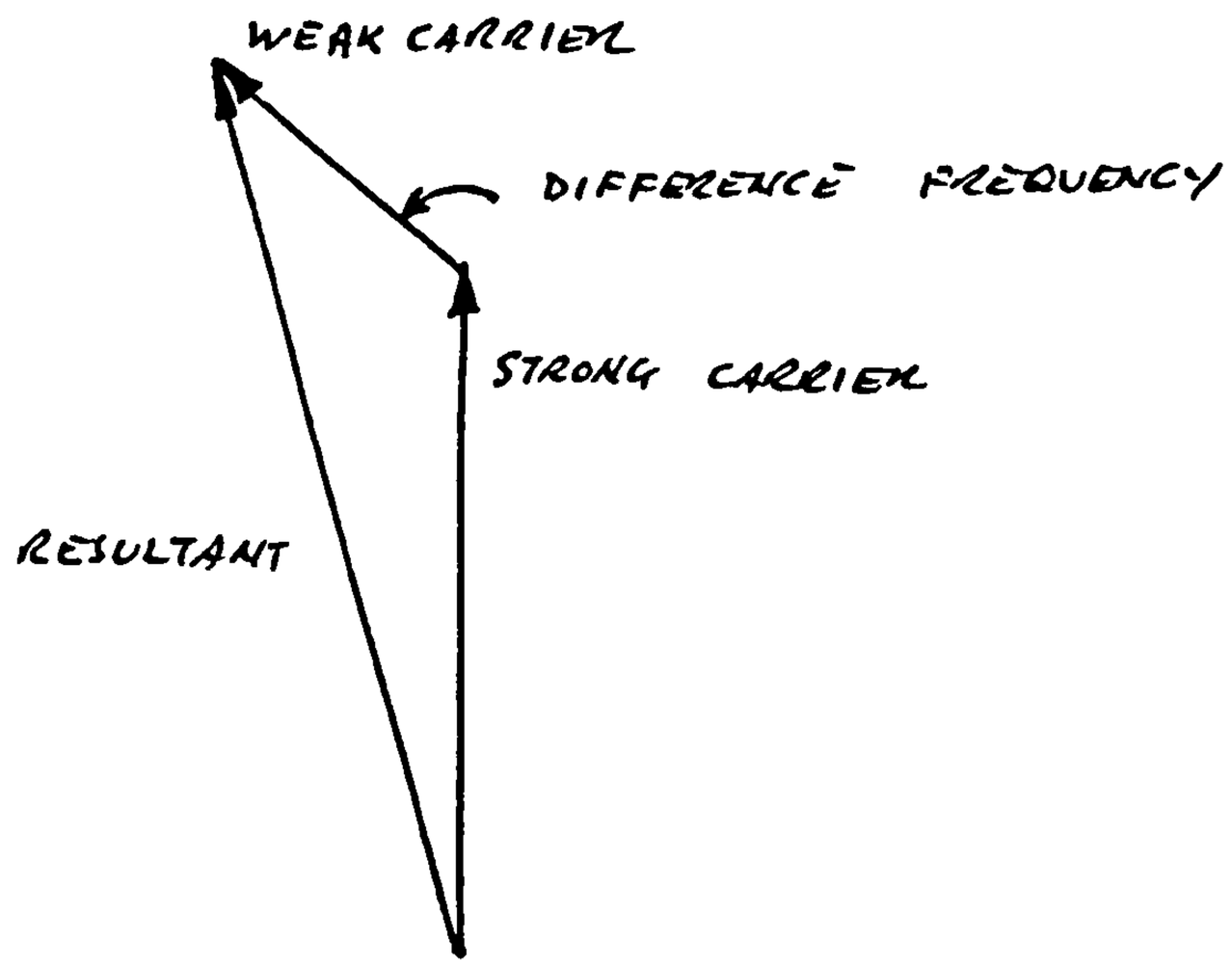

Fig. 5.4.2 Common Channel Operation - Two Carriers

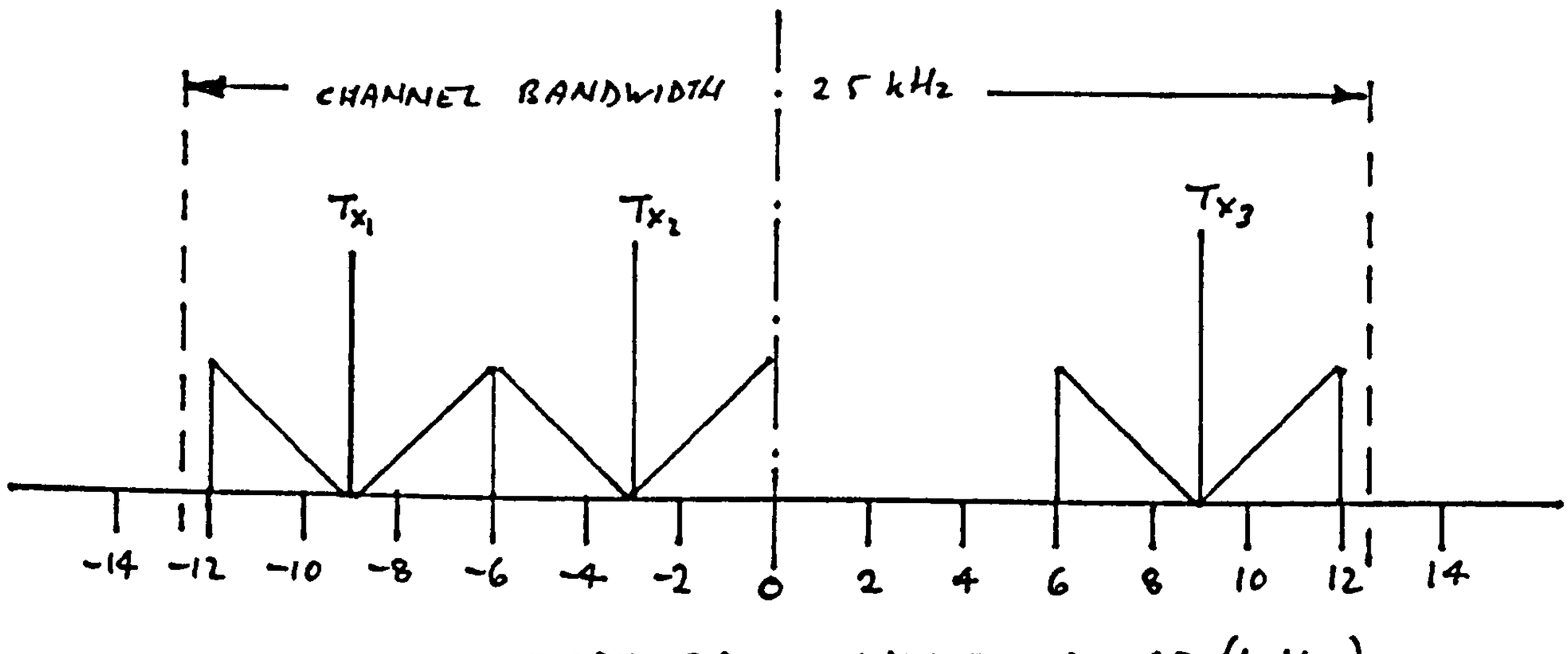

Fig. 5.4.3 Common Channel Operation - Spaced Carrier Mode, 3 Carriers

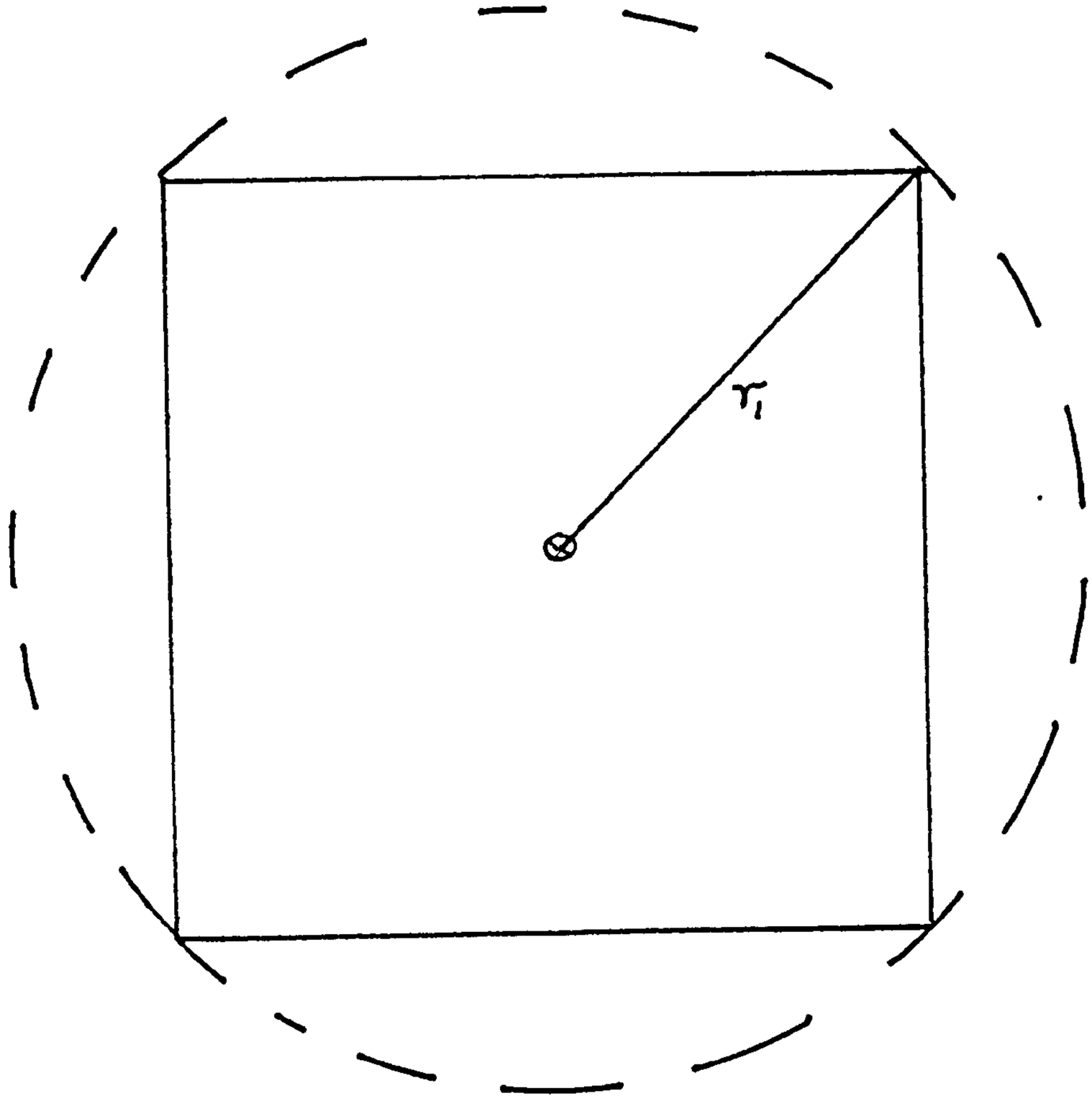

Fig. 5.5.3 Single Base Station Coverage

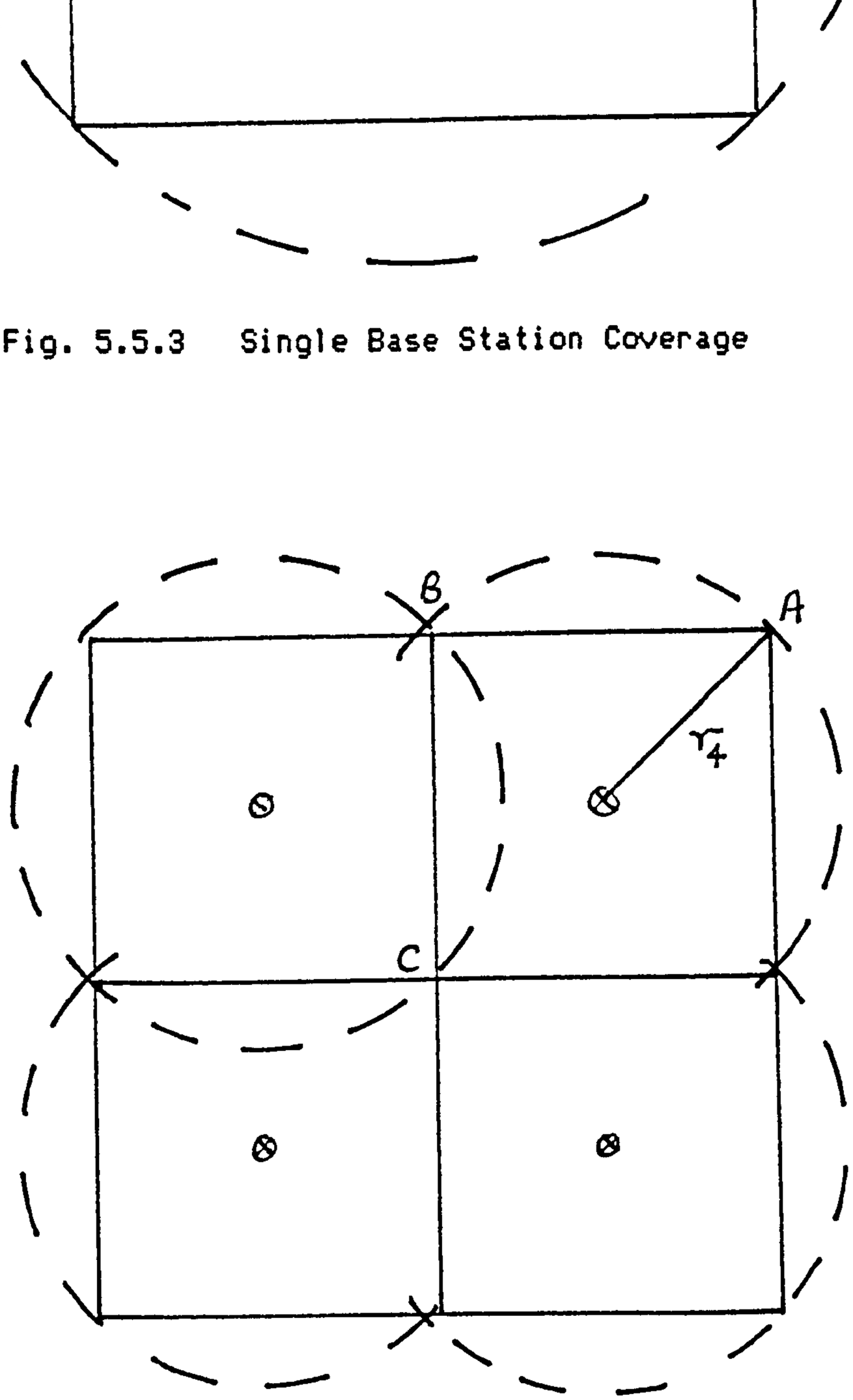

Fig. 5.5.2 Four Base Station Case

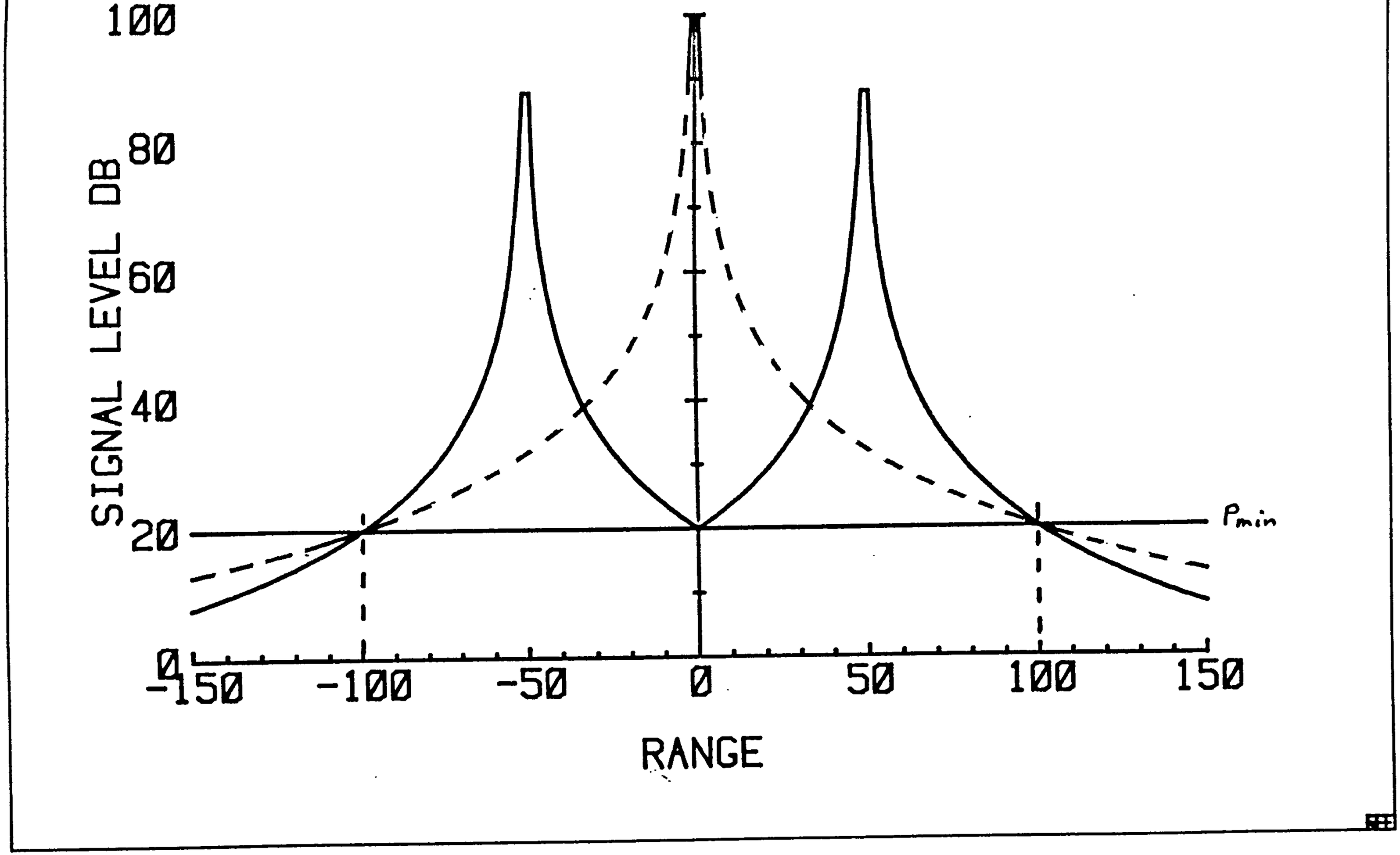

Fig. 5.5.3 Cross-section of Power Intensity

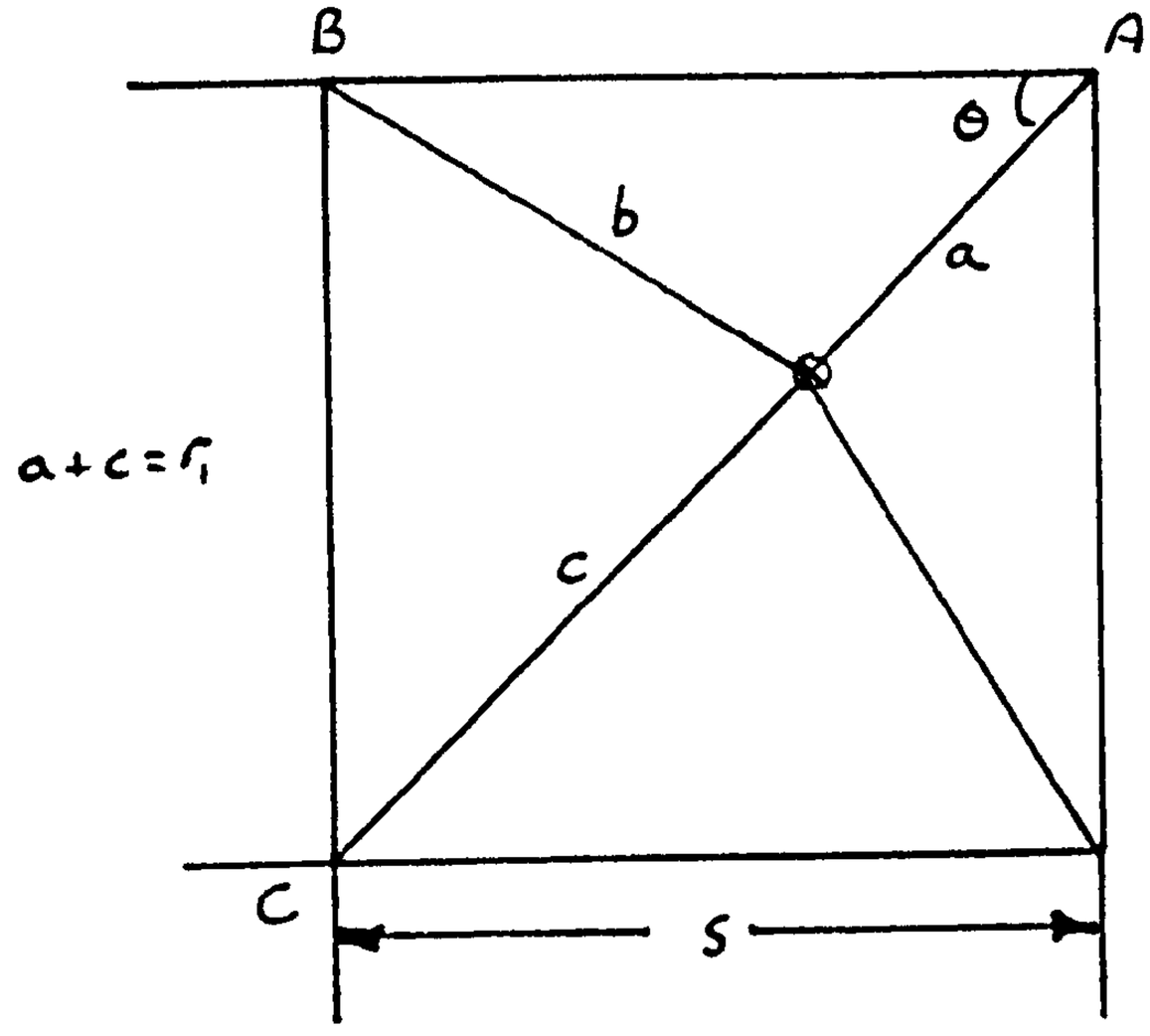

Fig. 5.5.4 Relocation of Base Station Positions

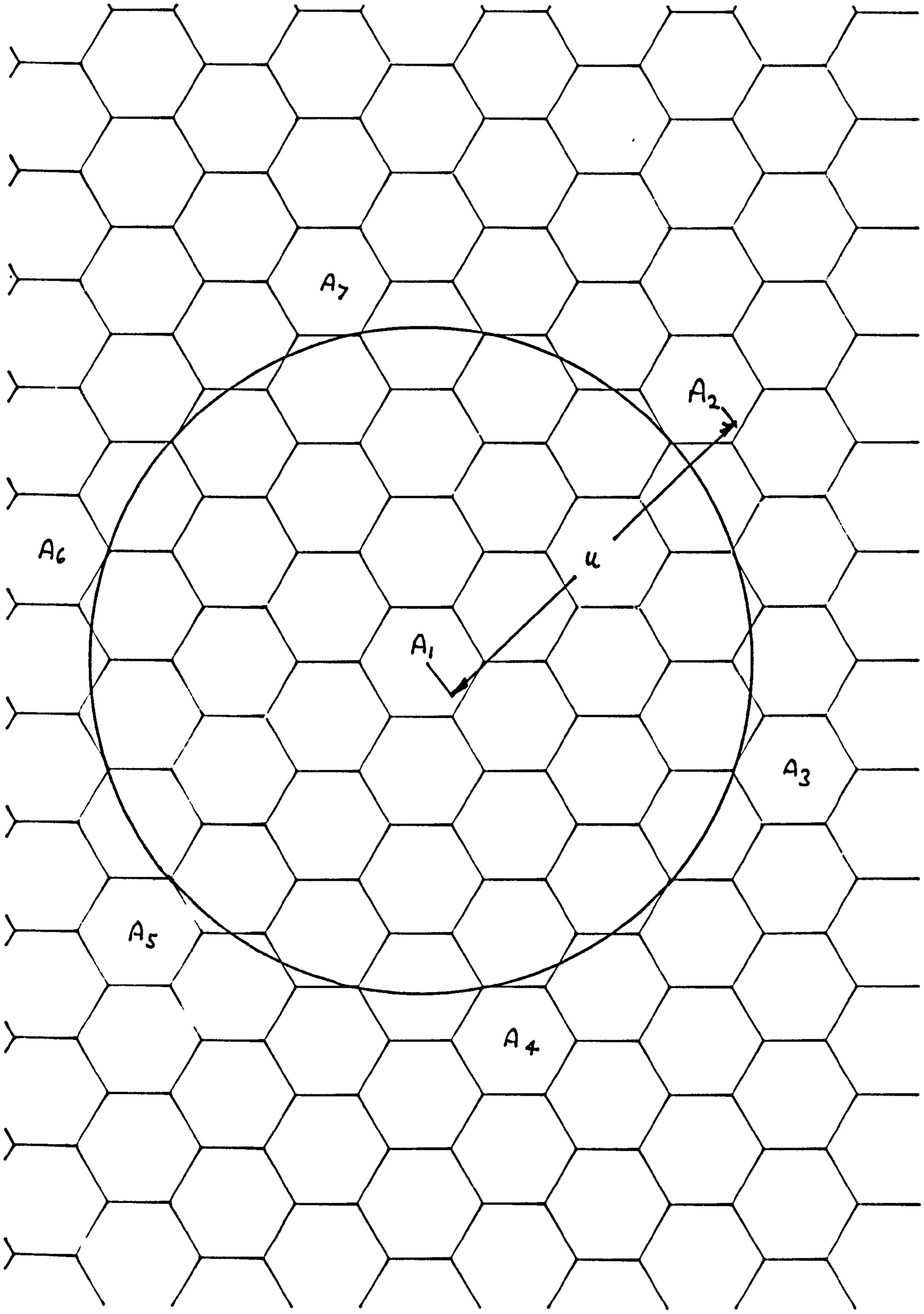

Fig. 5.6.1 Reuse Distances

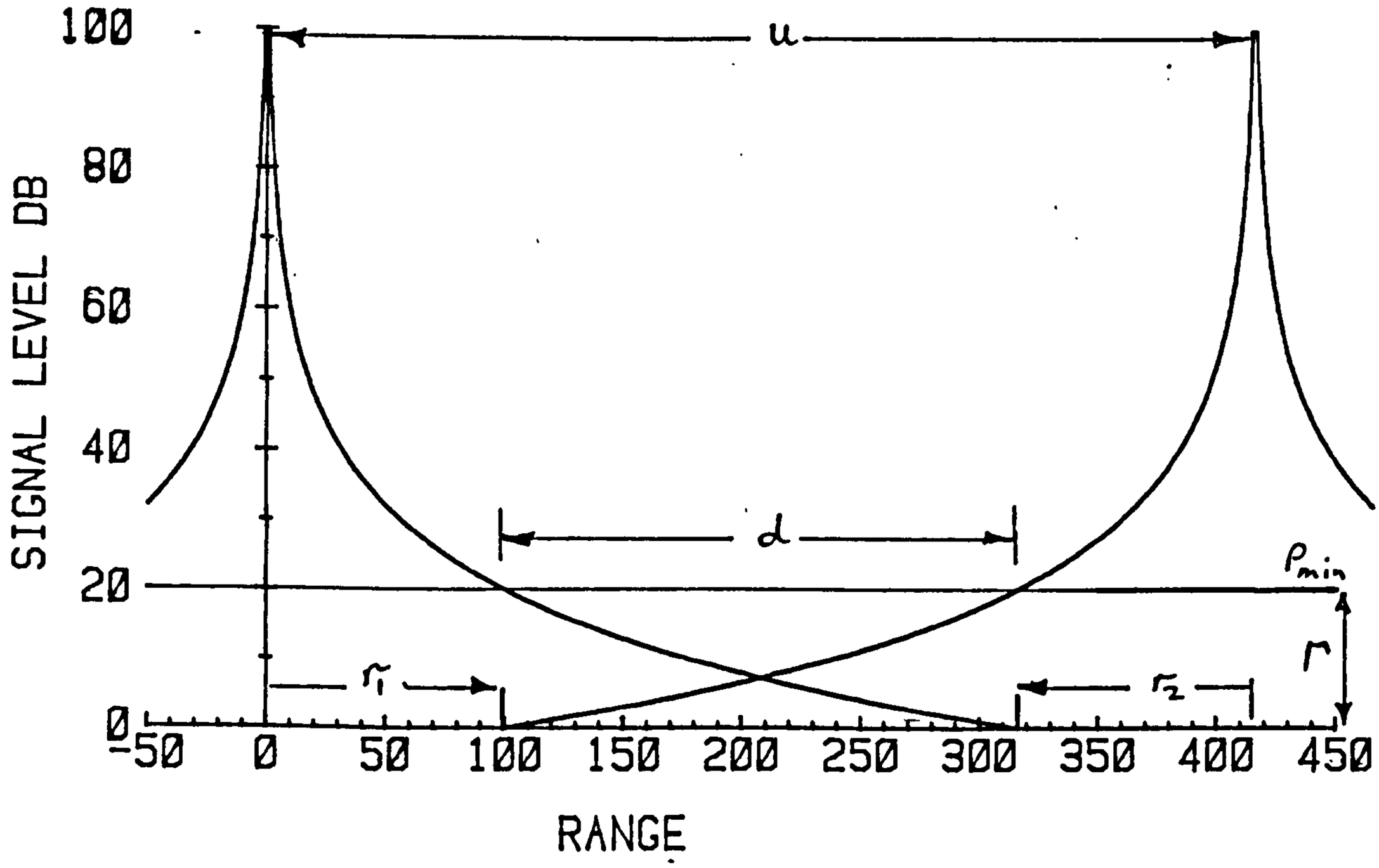

Fig. 5.6.2 Single Base Station Reuse

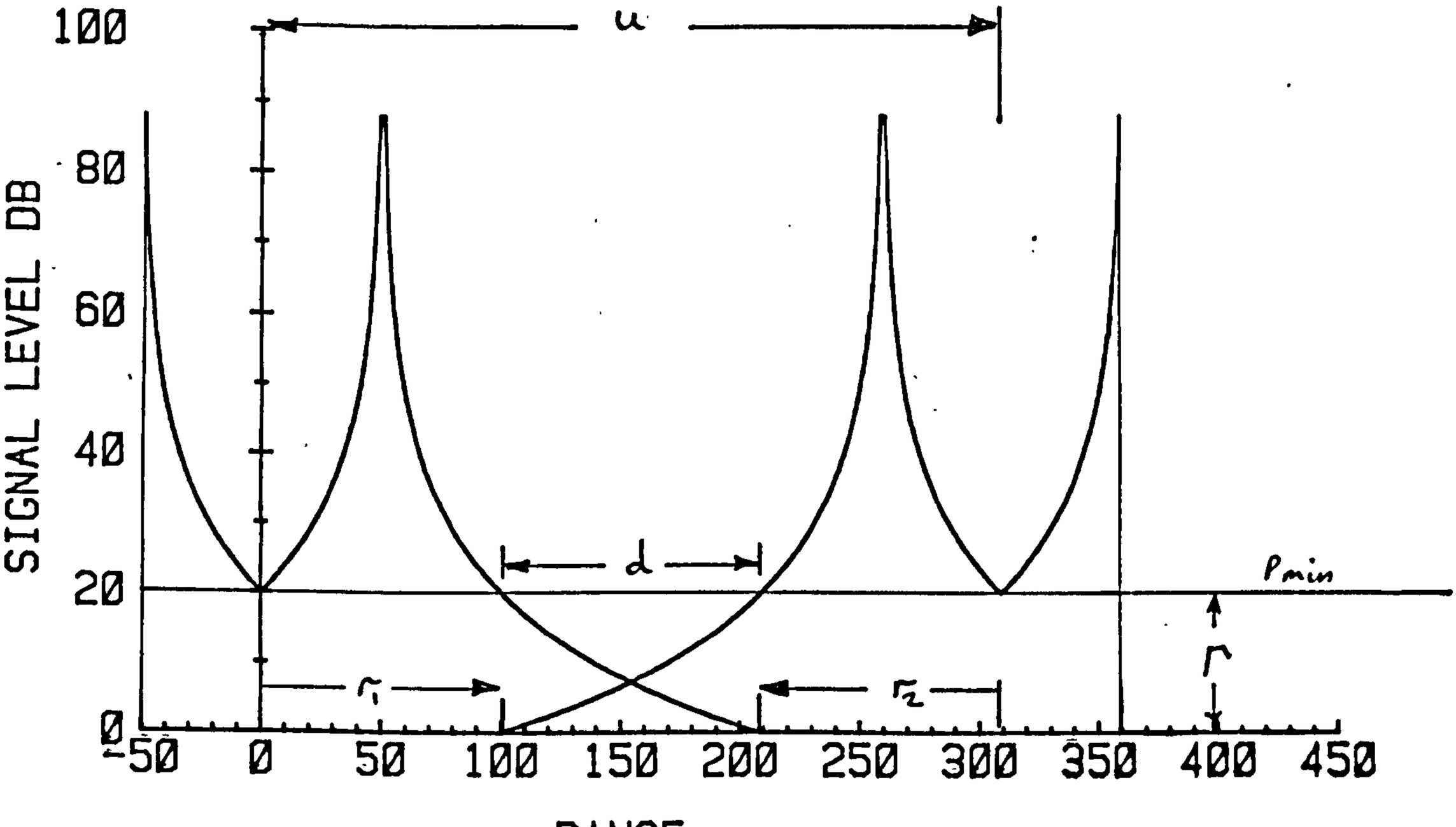

Fig. 5.6.3 Four Base Station Reuse

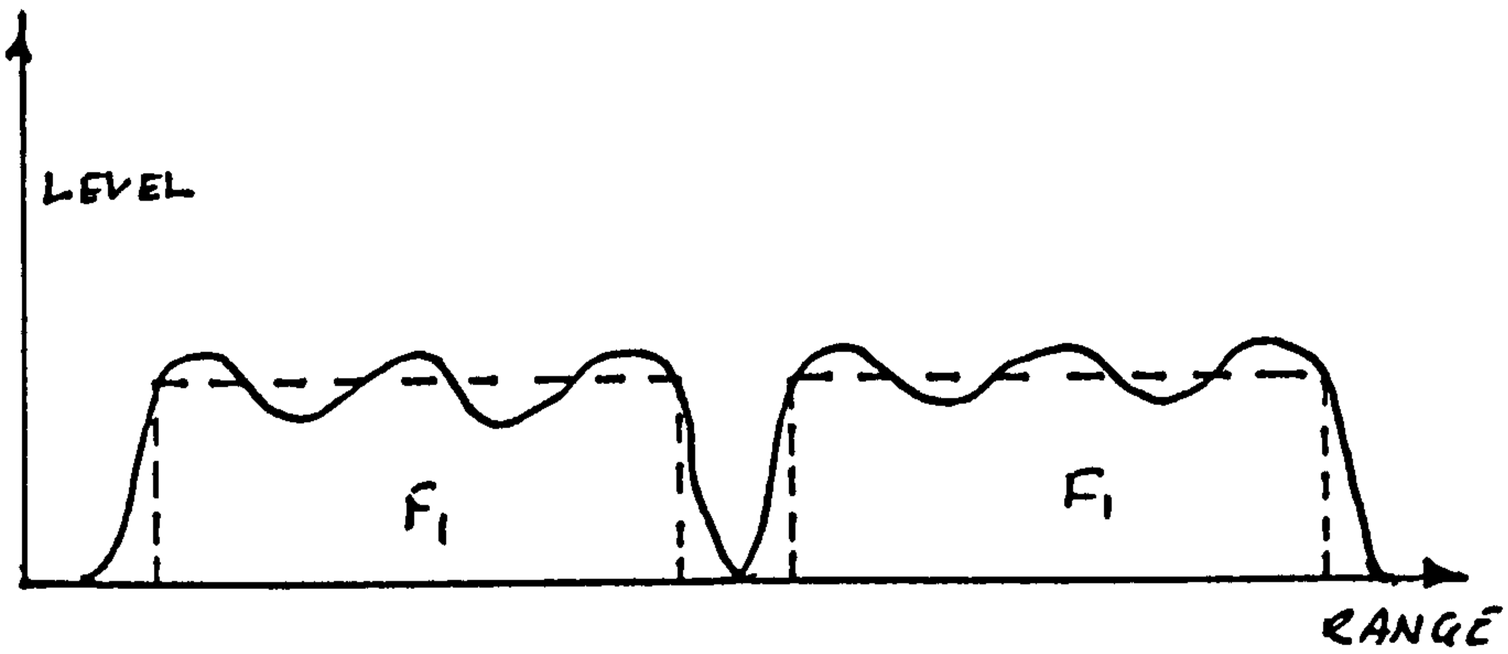

Fig. 5.6.4 Levels vs. Range for Many Transmitters per Cell

Fig. 5.6.5a Reuse Patterns I Single Base Station

Fig. 5.6.5b Reuse Patterns I Four Base Stations

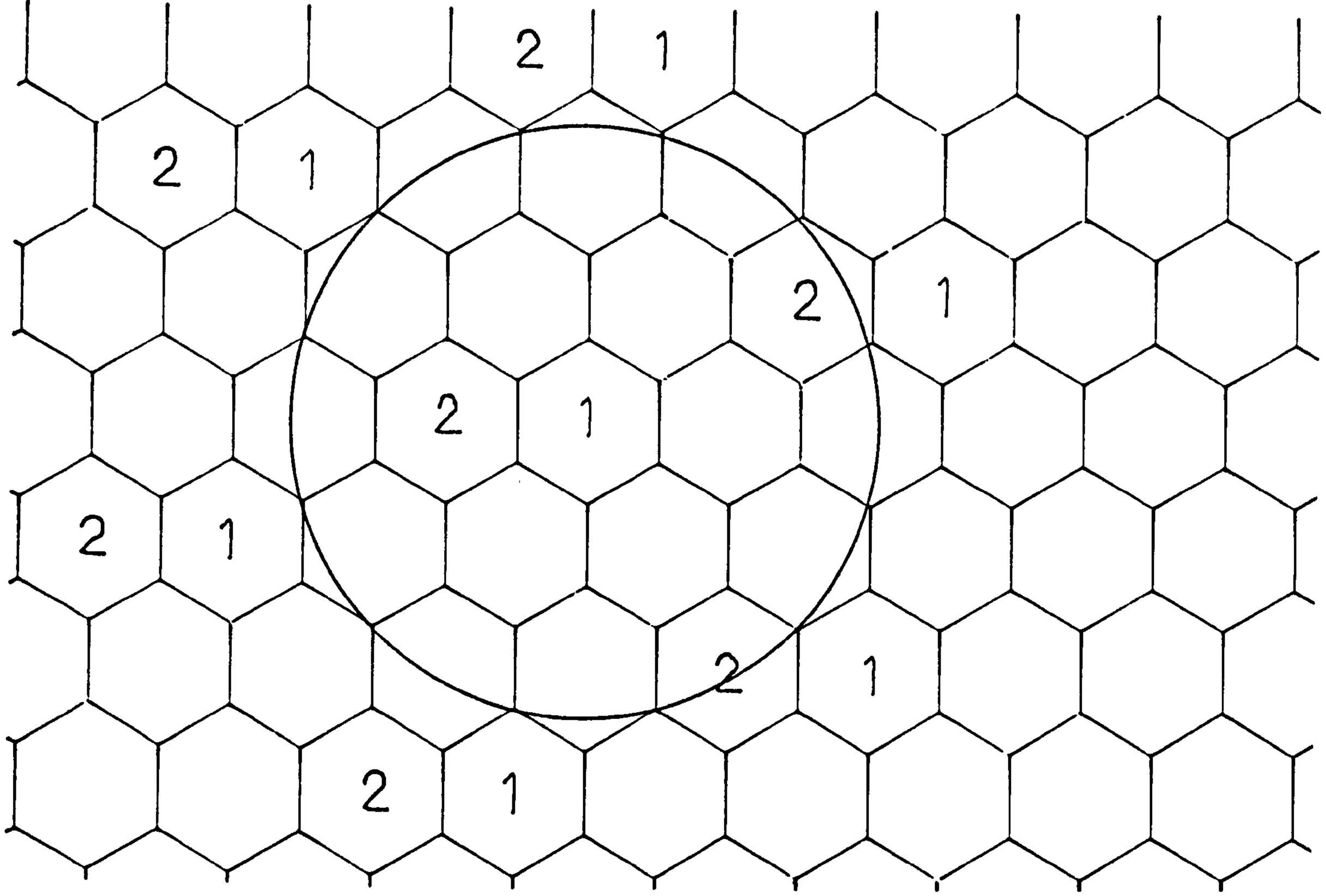

Fig. 5.6.6a Reuse Patterns II Single Base Station

Fig. 5.6.6b Reuse Patterns II Four Base Stations

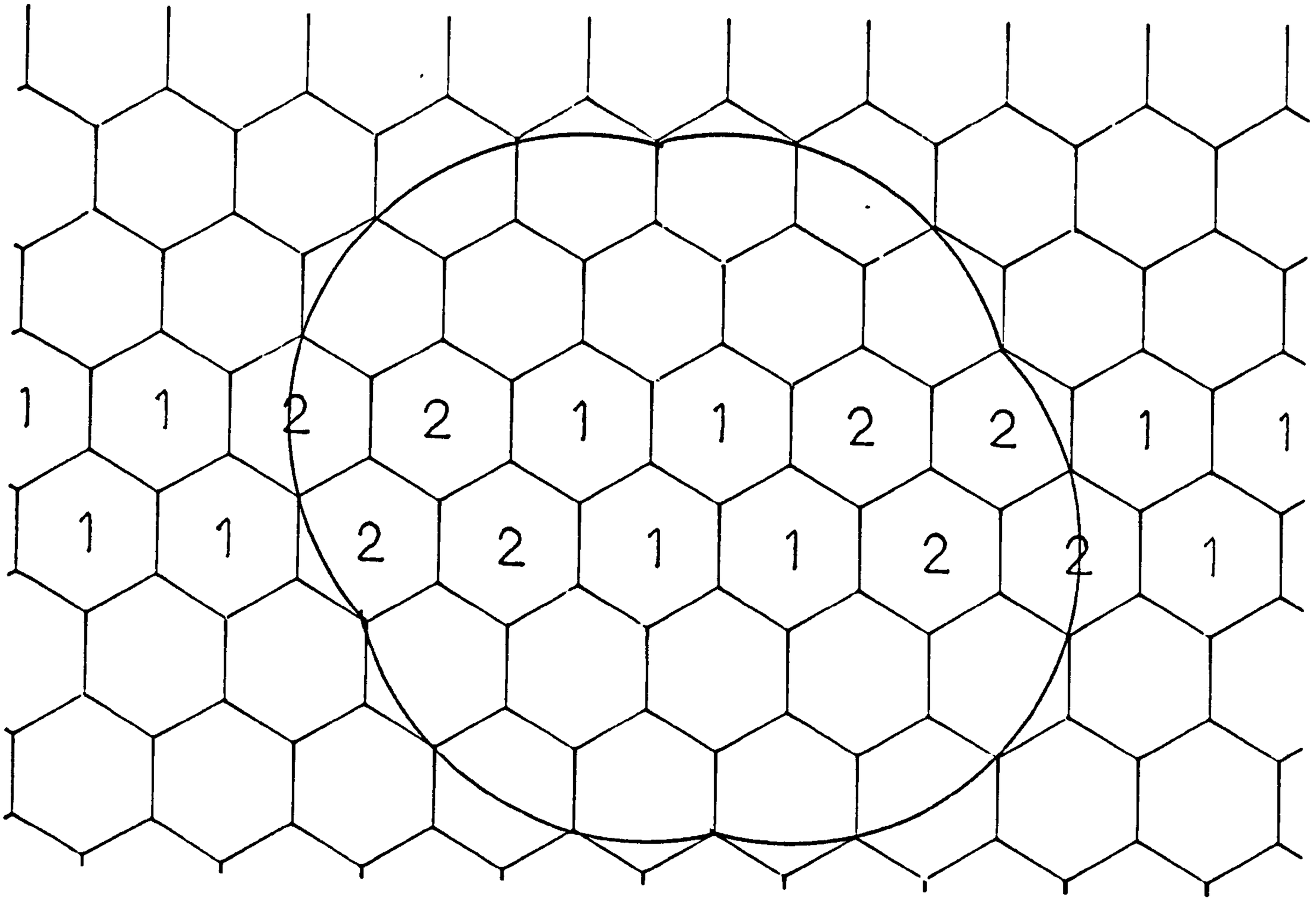

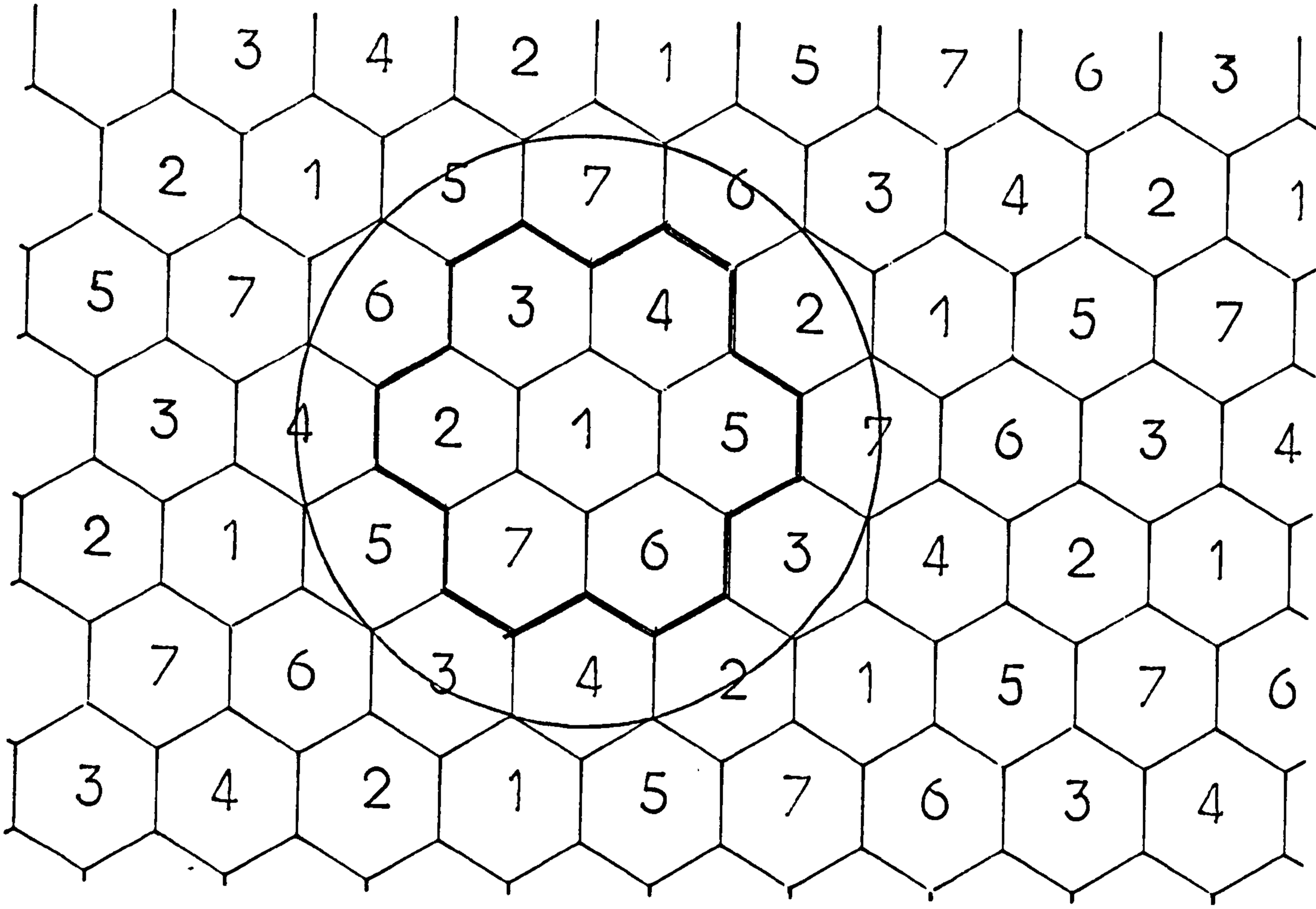

Fig. 5.6.7a Reuse Patterns III Single Base Station

Fig. 5.6.7b Reuse Patterns III Four Base Stations

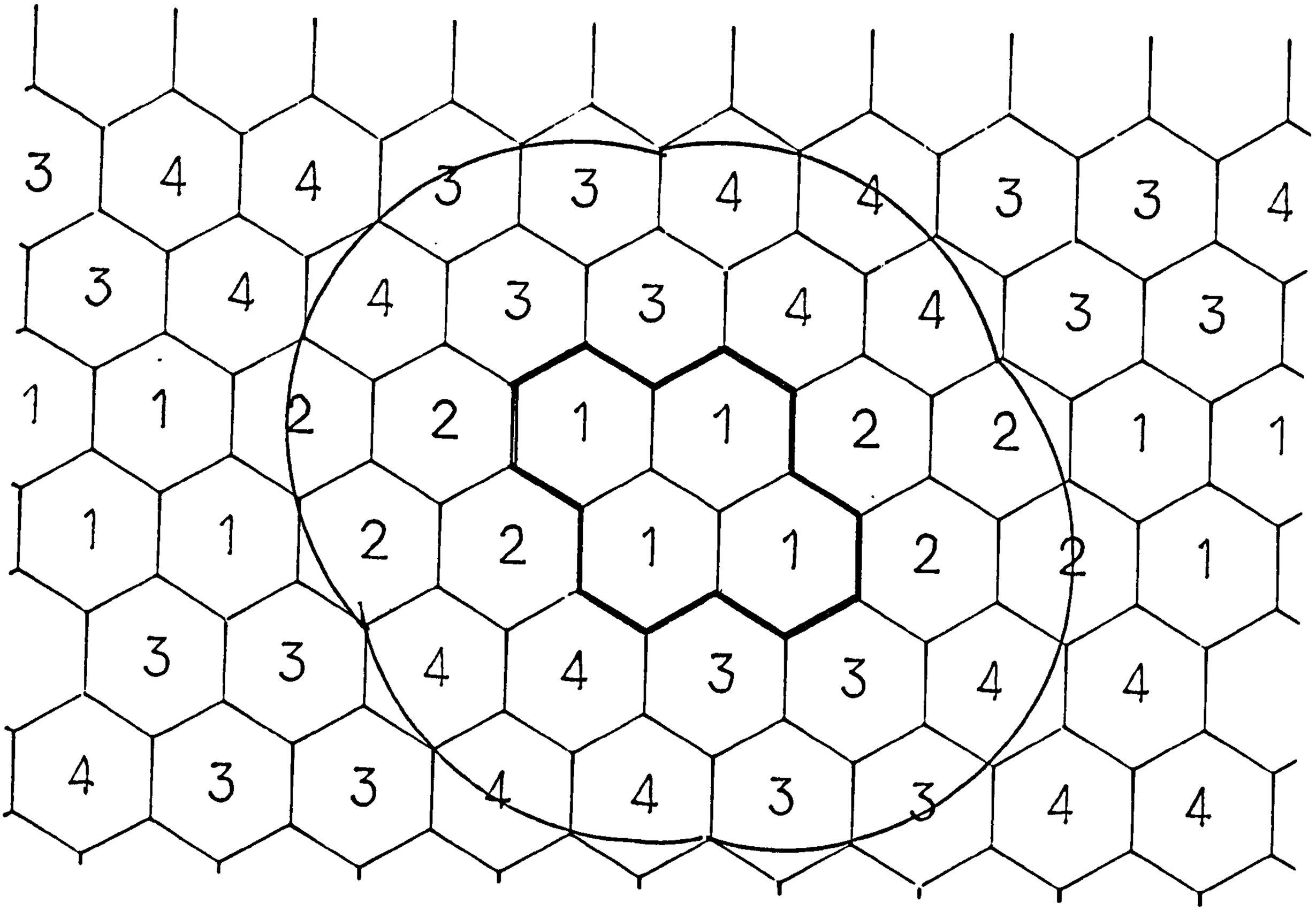

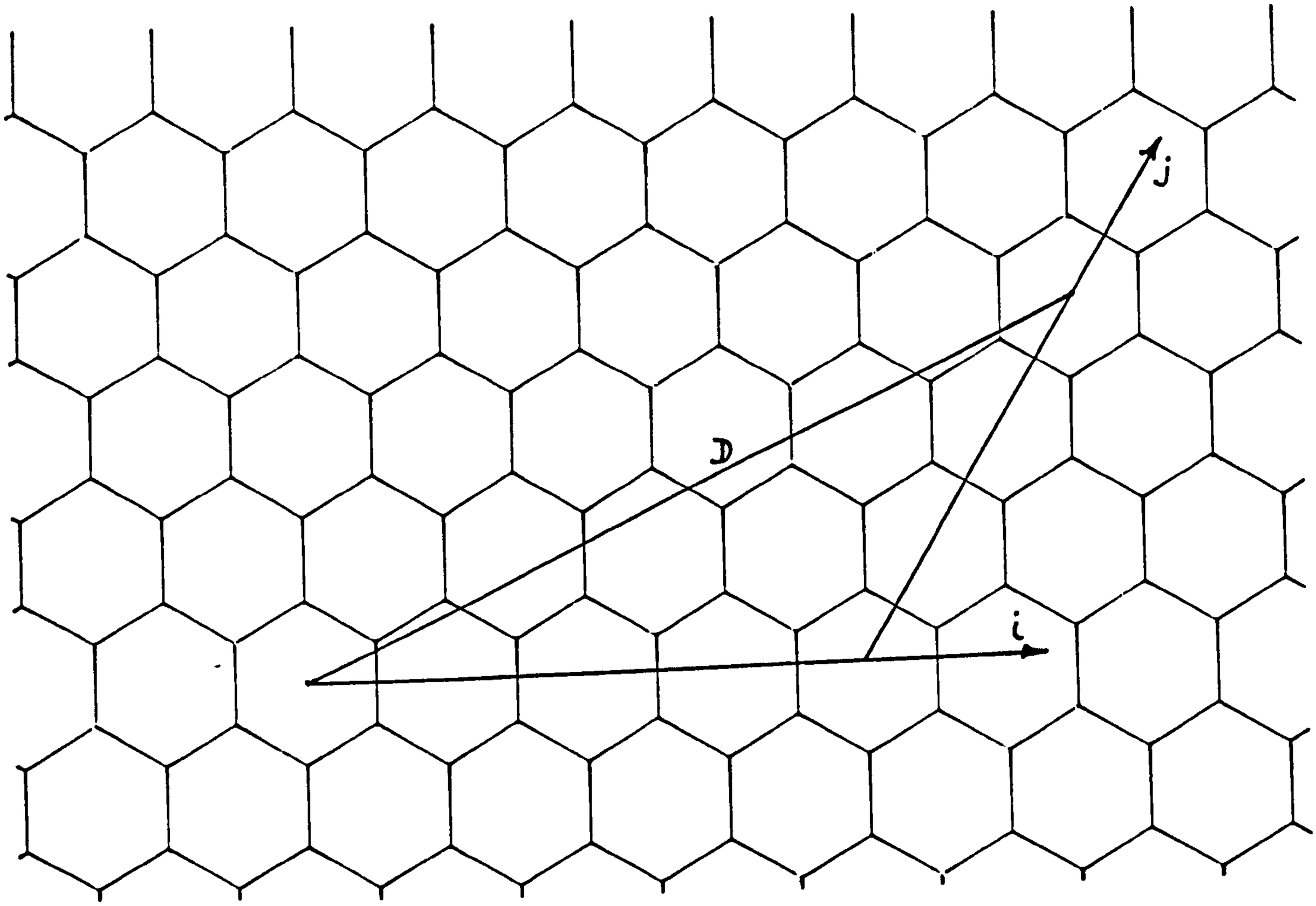

Fig. 5.6.8 Hexagonal Geometry

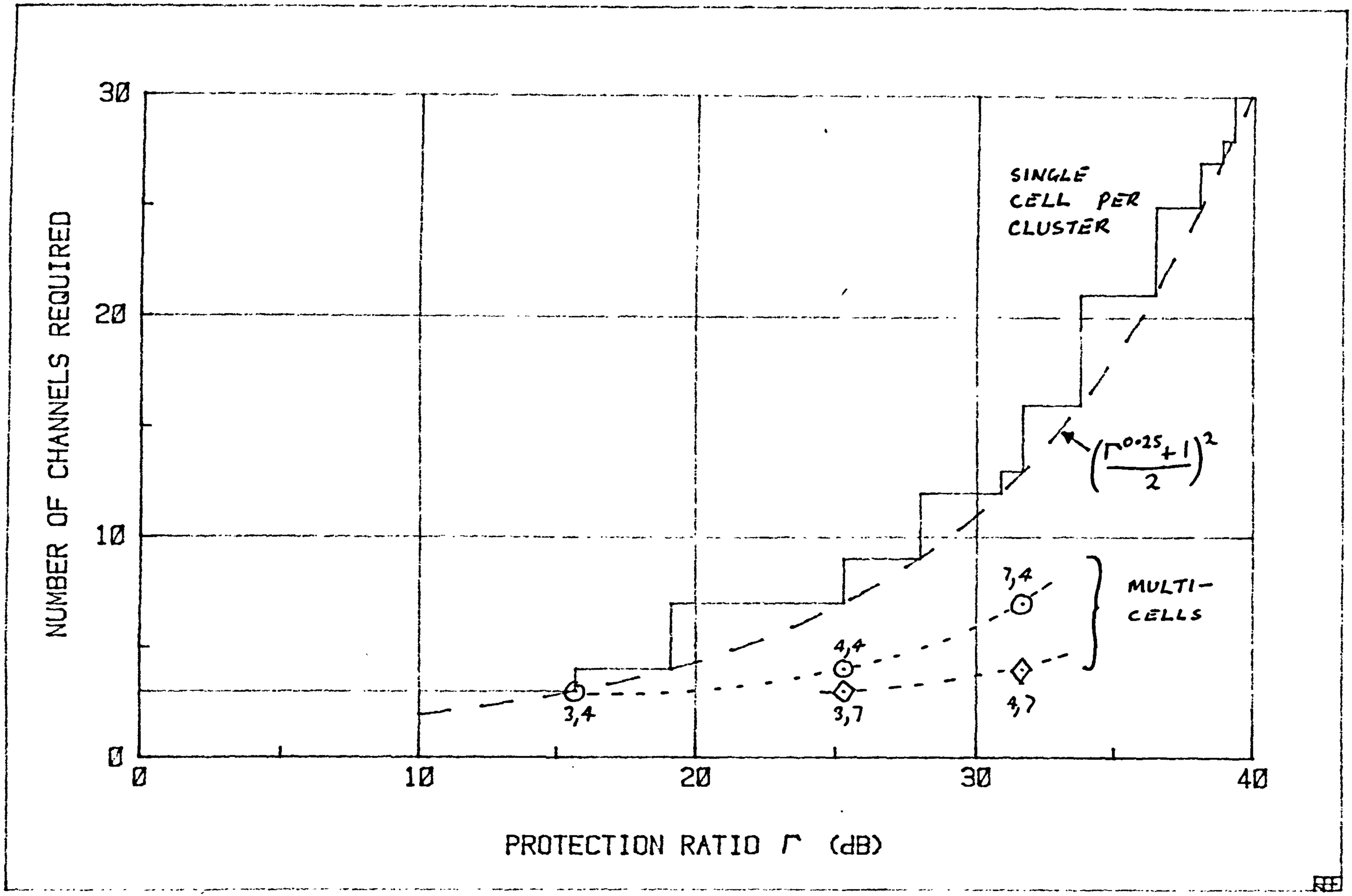

Fig. 5.6.9 Channel Requirements vs. Protection Ratio

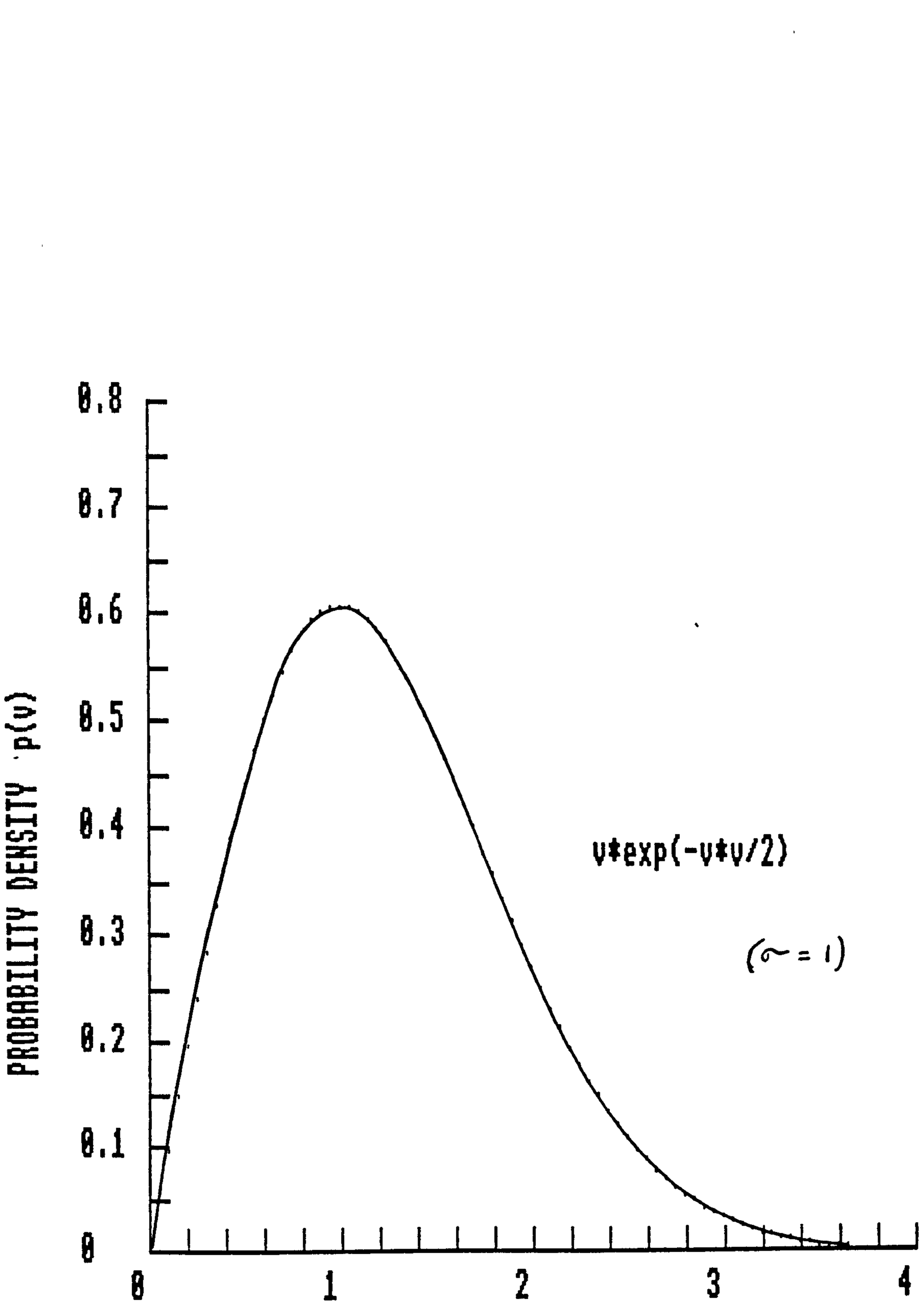

Fig. 6.1.1 Rayleigh Probability Distribution Function

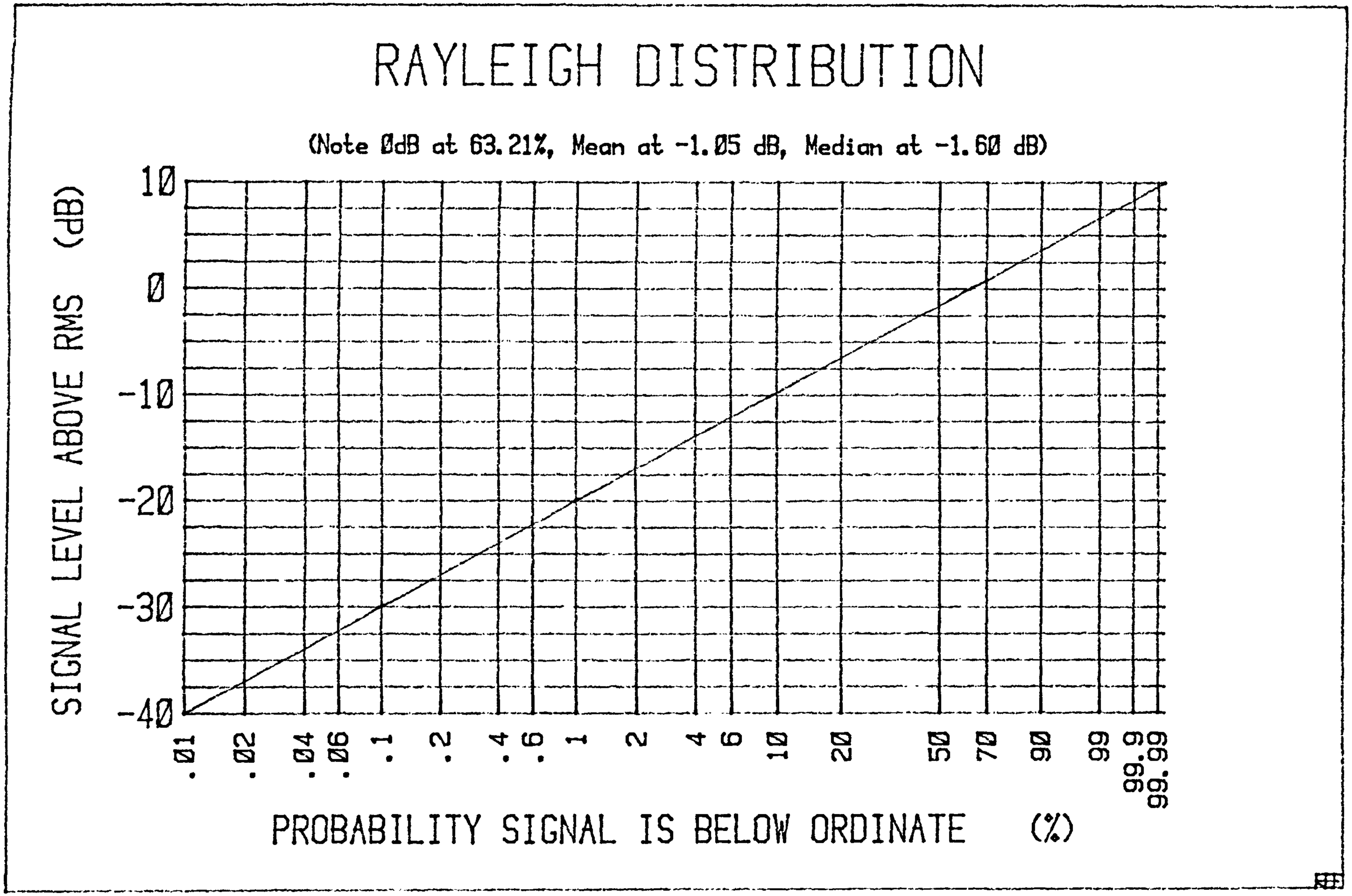

Fig. 6.1.2 Rayleigh Cumulative Distribution Function

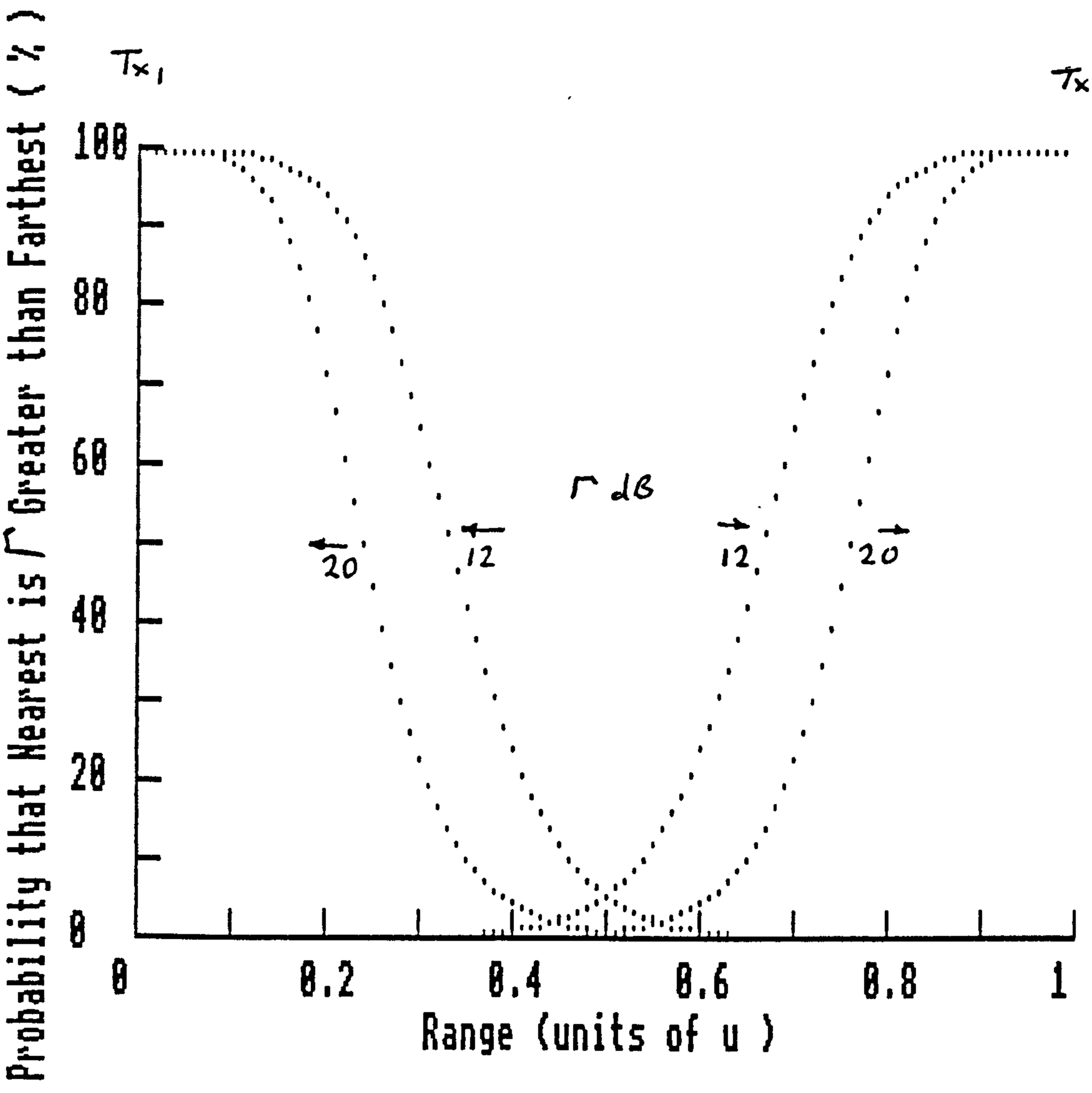

Fig. 6.2.1 Probability of Receiving Wanted Signal Γ above Unwanted

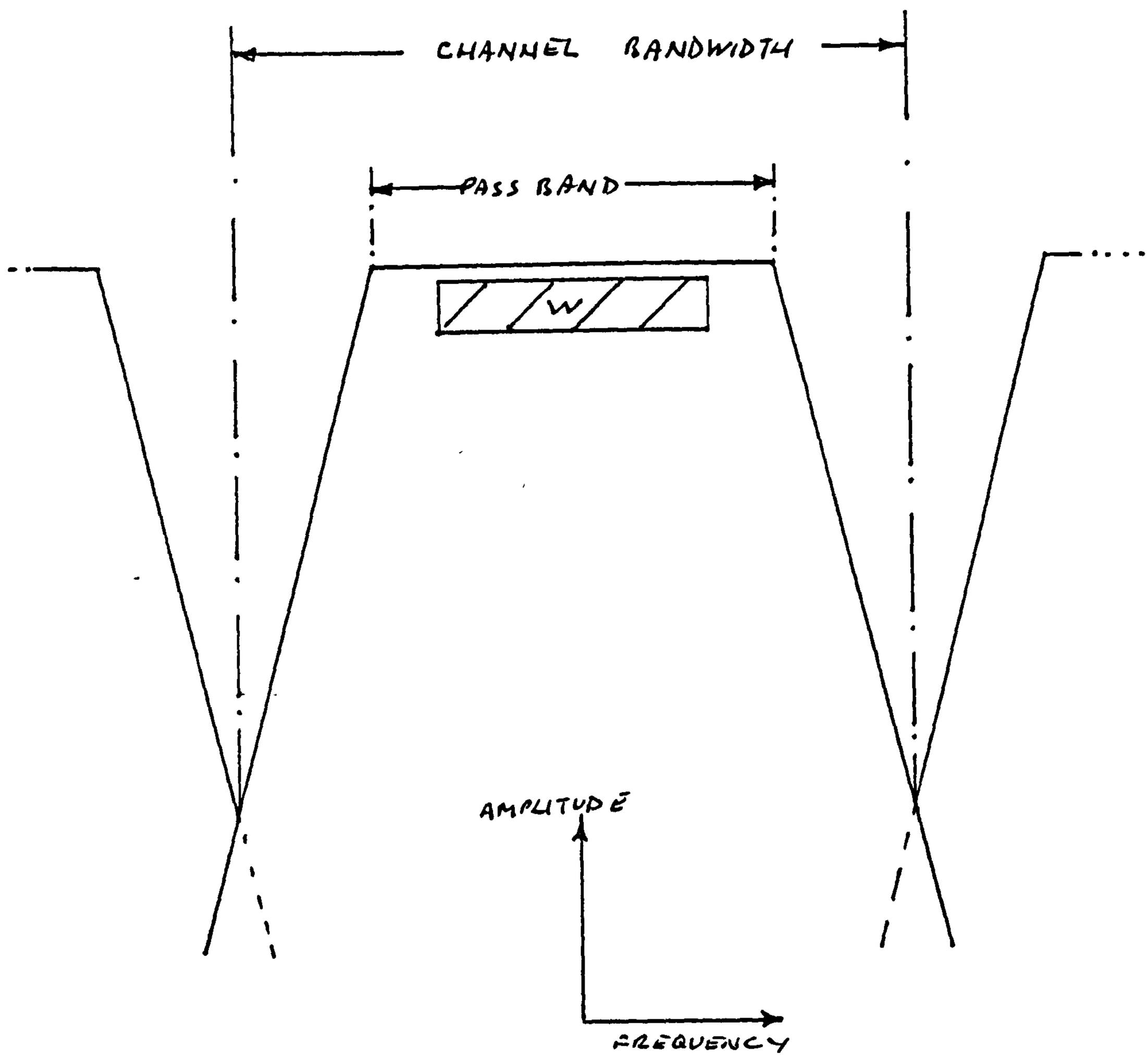

Fig. 7.3.1 Bandwidth Relationships

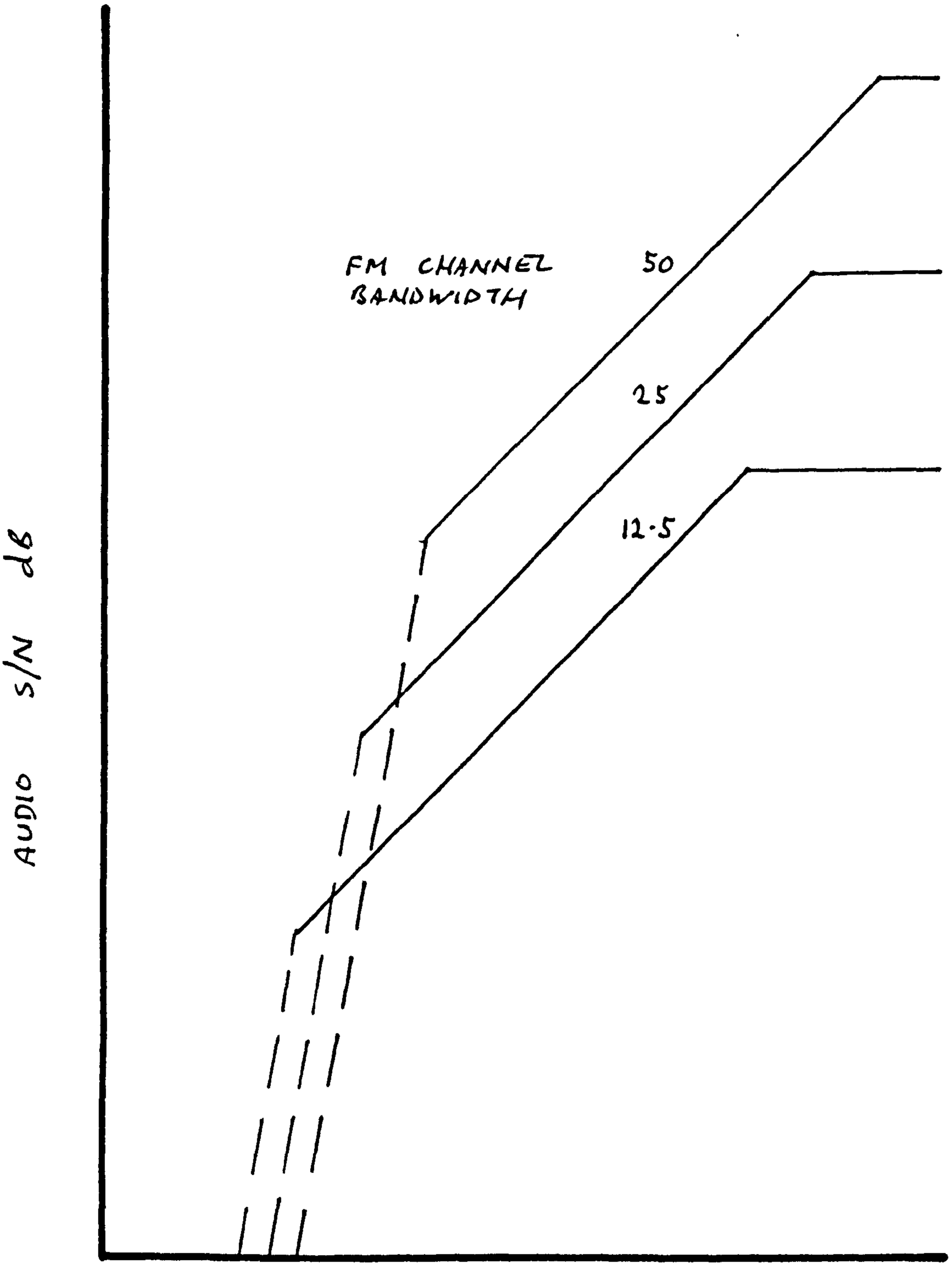

Fig. 7.4.1 FM Noise Performance

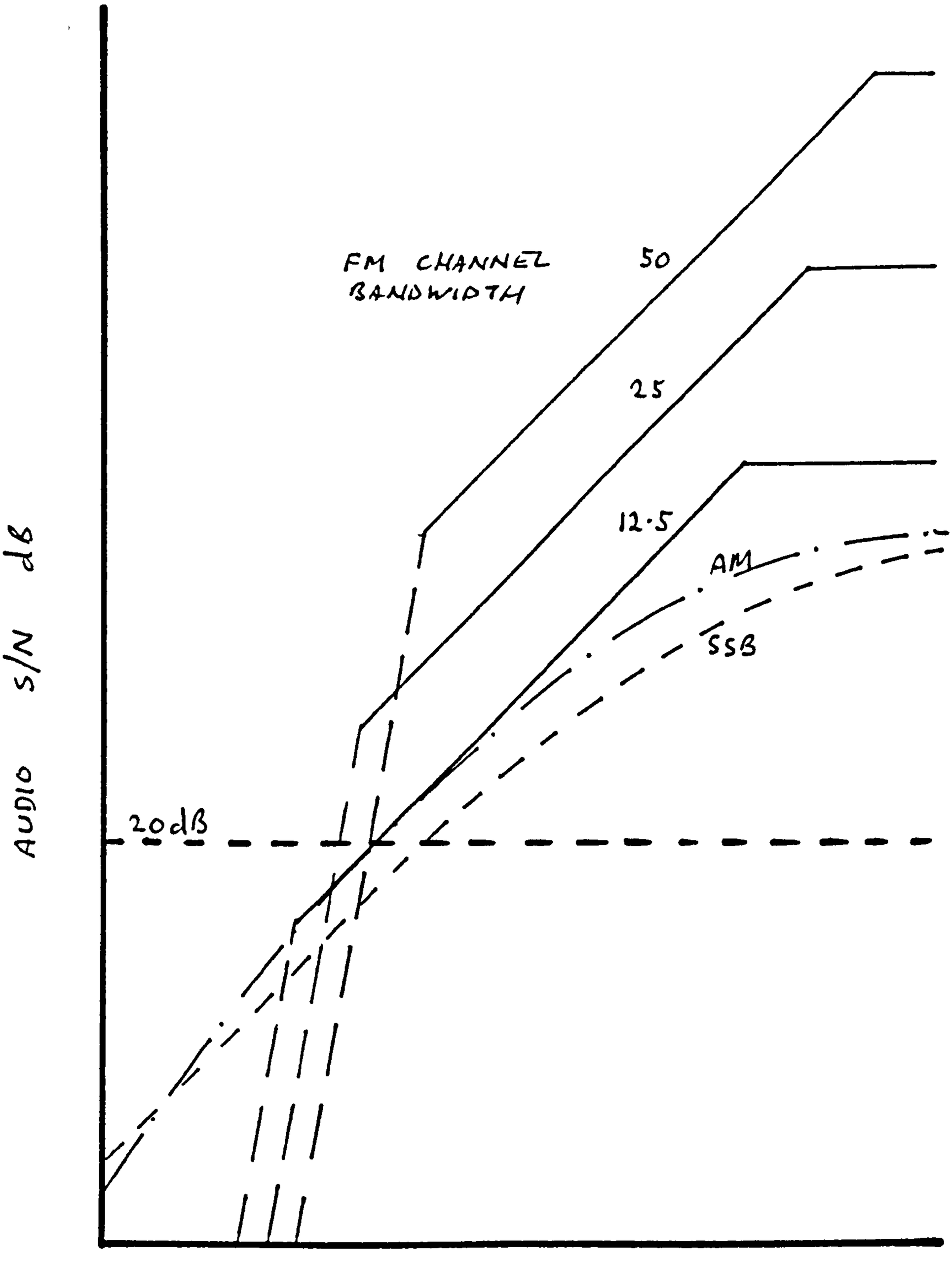

Fig. 7.4.2 FM, AM, and SSB Noise Performances

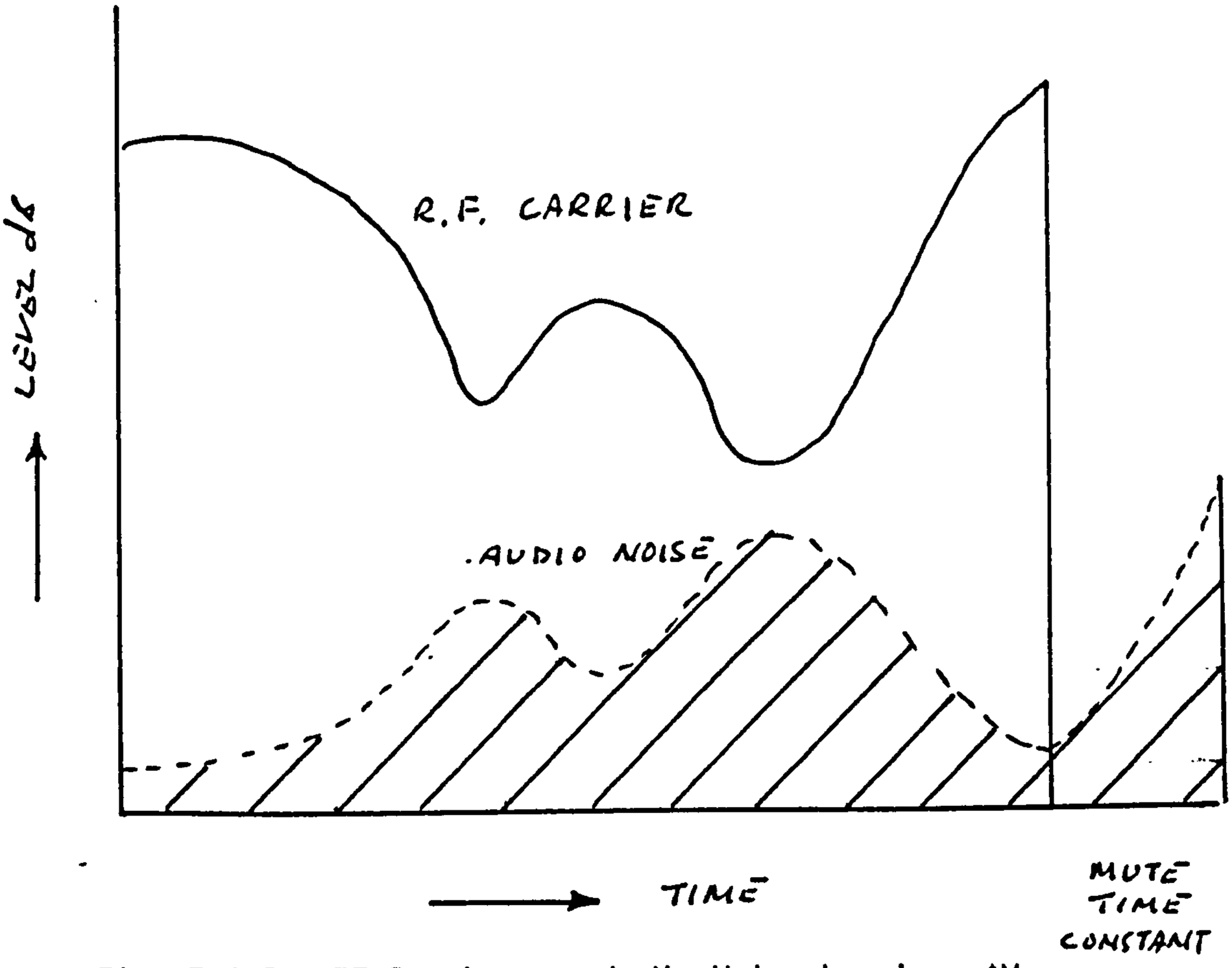

Fig. 7.4.3 RF Carrier vs. Audio Noise Levels - AM

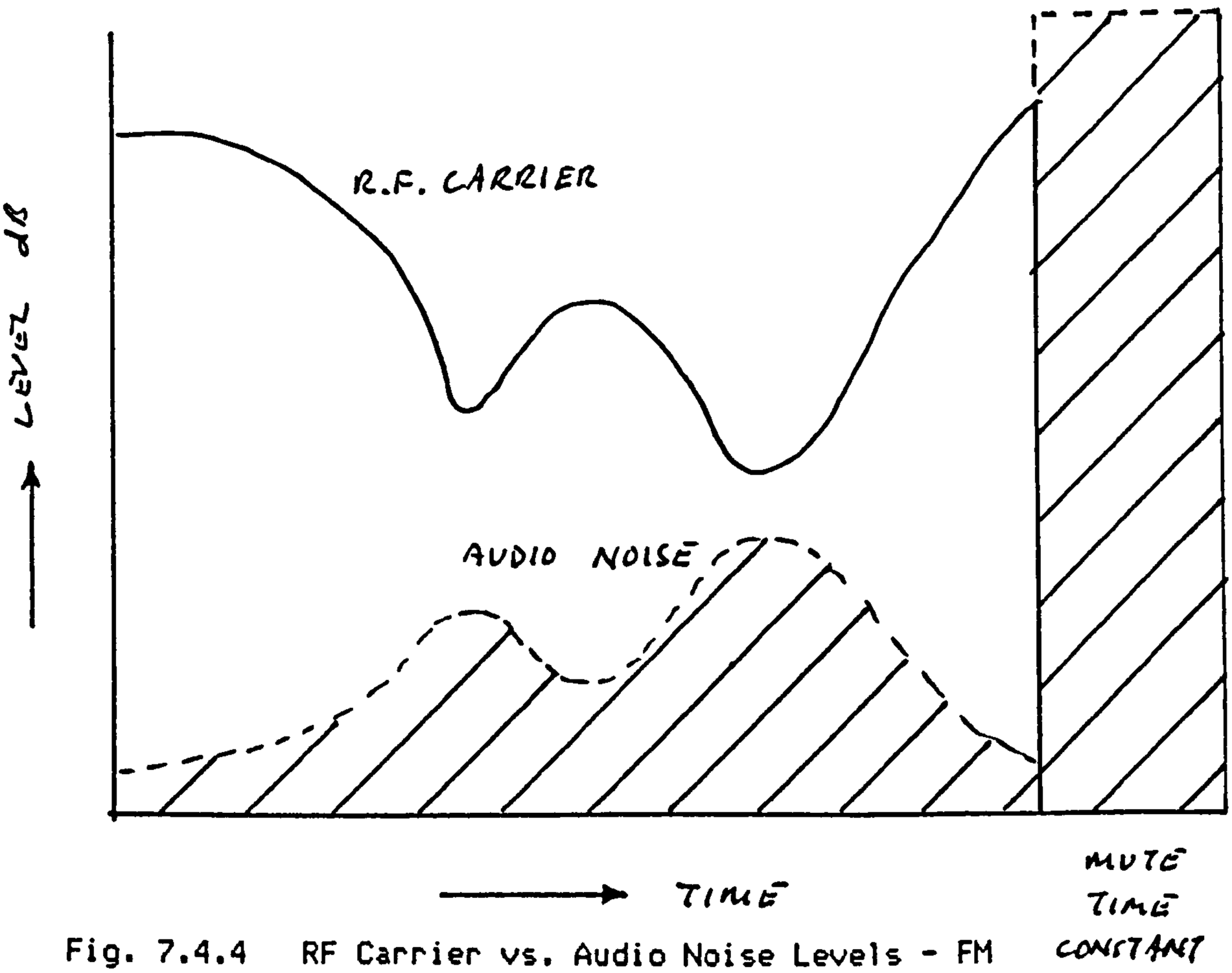

Fig. 7.4.4 RF Carrier vs. Audio Noise Levels - FM

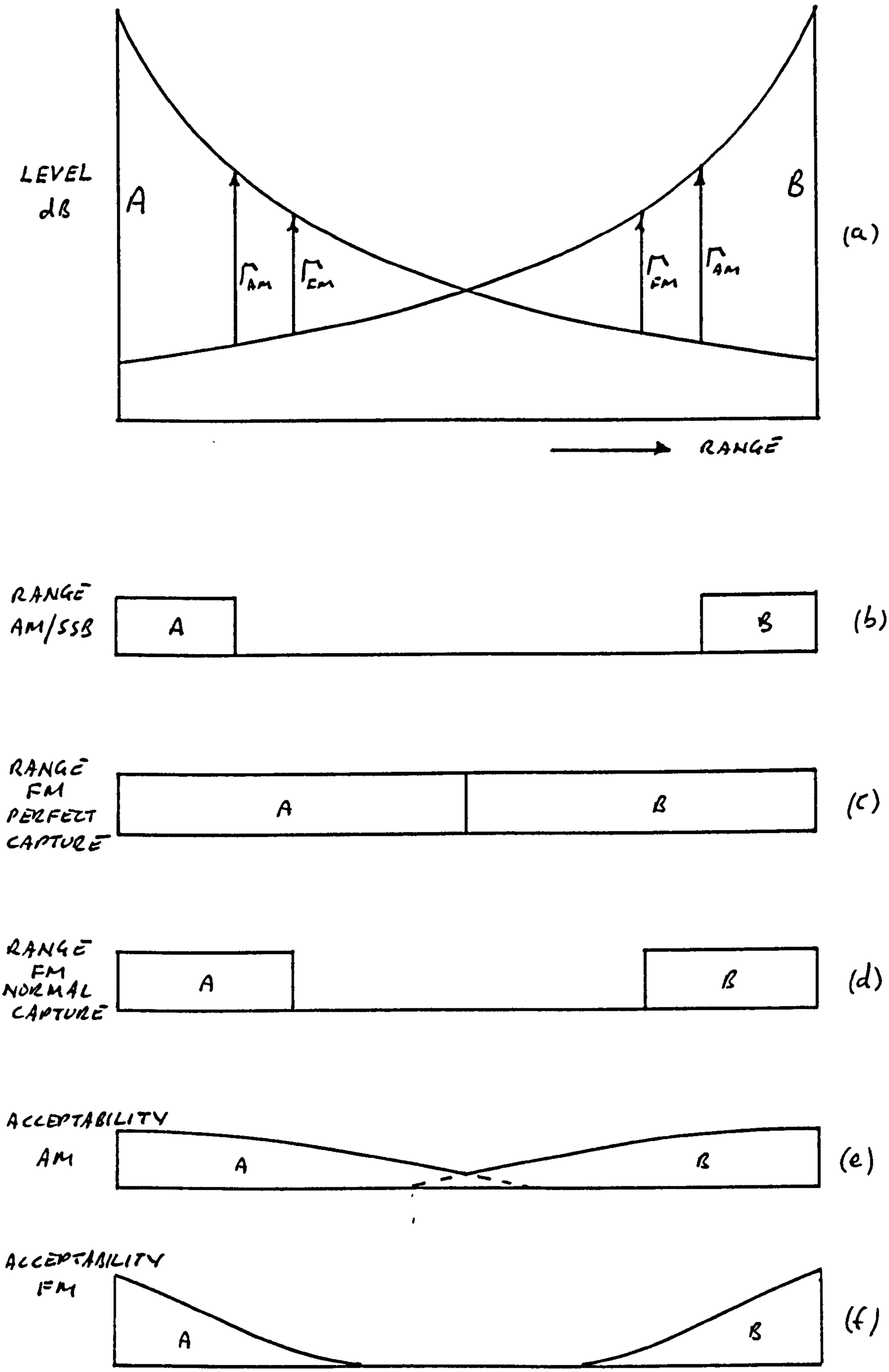

Fig. 7.4.5 Various Views of Capture and Range for AM and FM

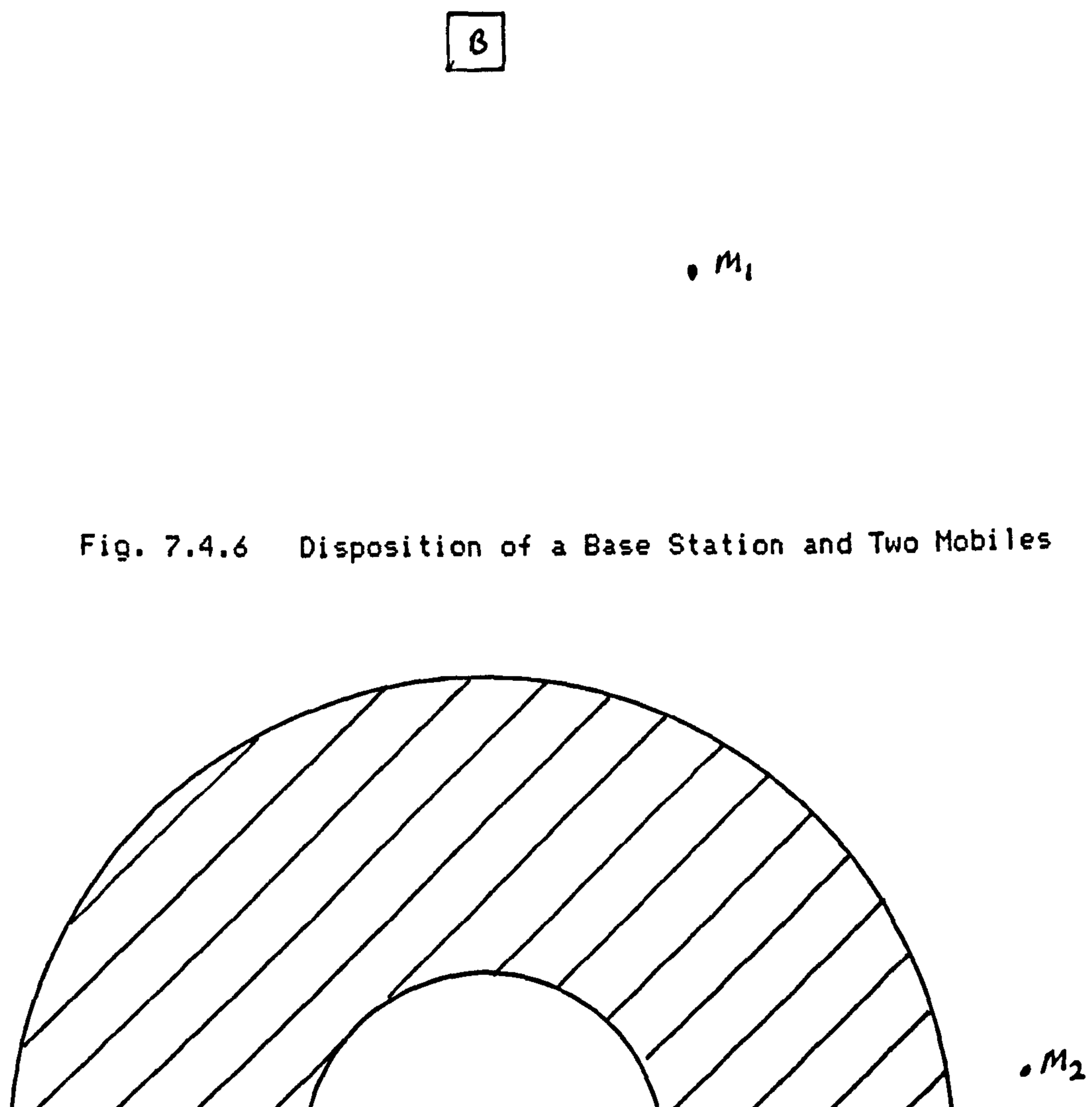

Fig. 7.4.6 Disposition of a Base Station and Two Mobiles

Fig. 7.4.7 Blighted Zone for FM Operation

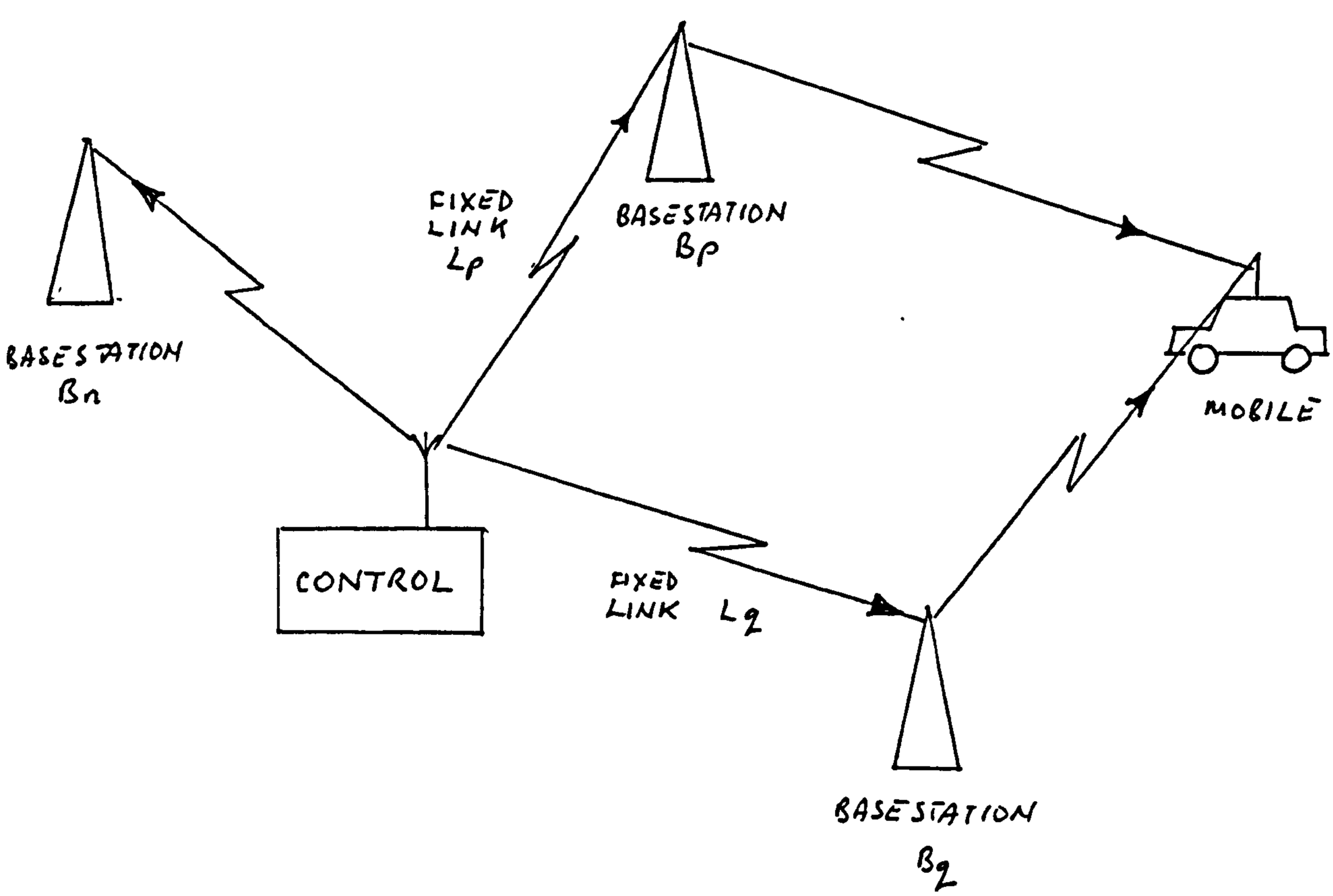

Fig. 7.5.1 Elements of a QS Radio System

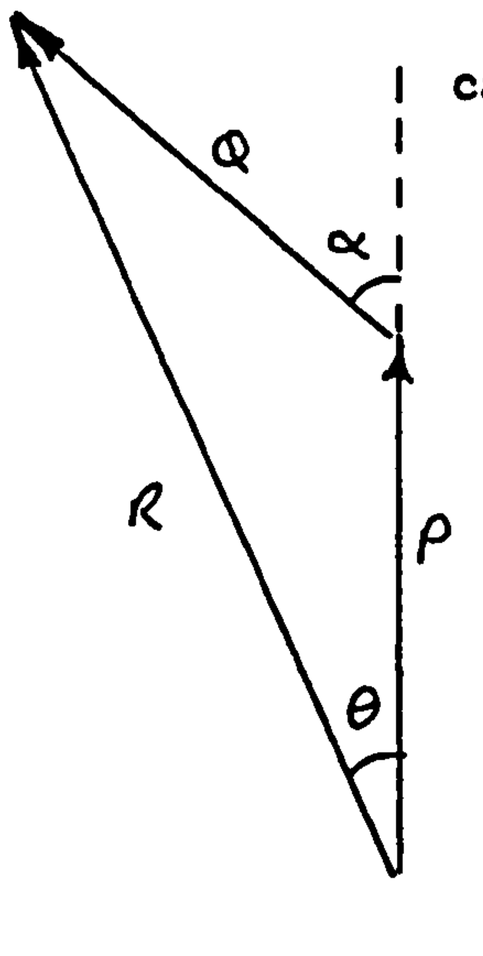

carriers P and Q from basestations Bp and Bq, and combined resultant R.

Fig. 7.5.2 Phasor Diagram of Carriers from Two Base Stations and their Resultant

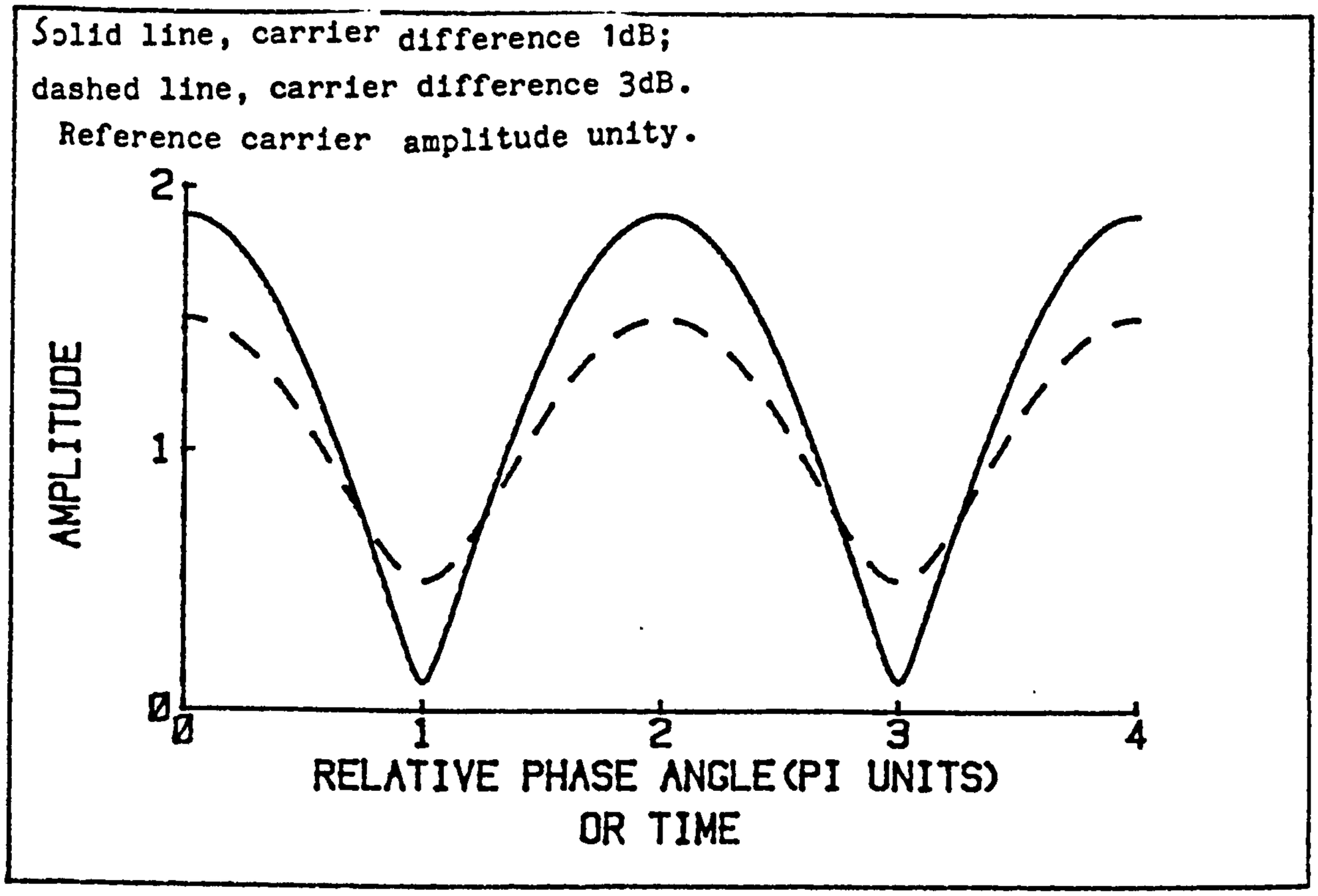

Fig. 7.5.3 Variation of Amplitude of Envelope of Resultant

Variation of noise power at the demodulator after ALC action. Solid line, carrier difference 1dB; dashed line, carrier difference 3dB. A single carrier of unity amplitude gives the reference noise power of 0dB.

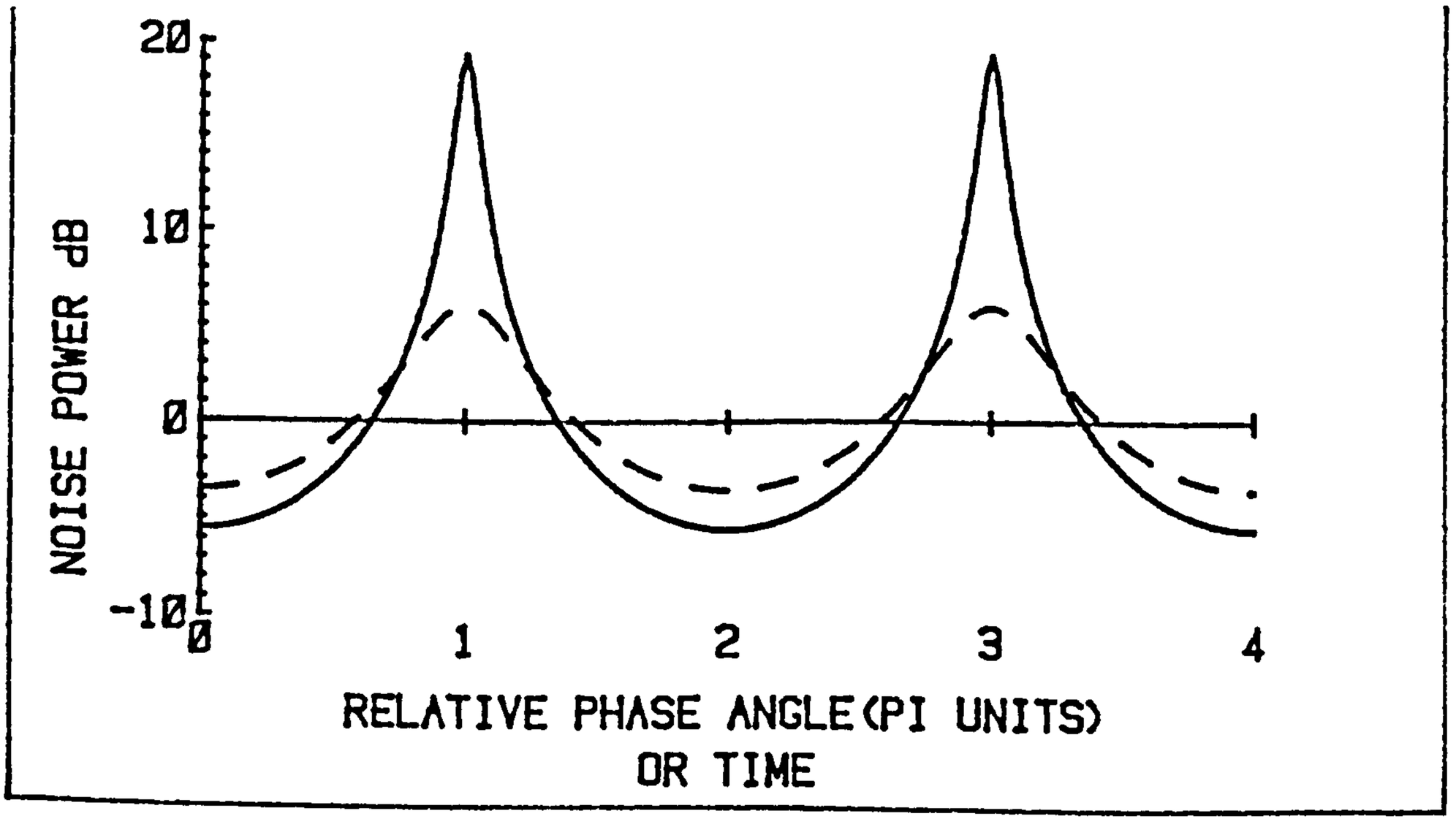

Fig. 7.5.4 Noise Power at the Demodulator after ALC

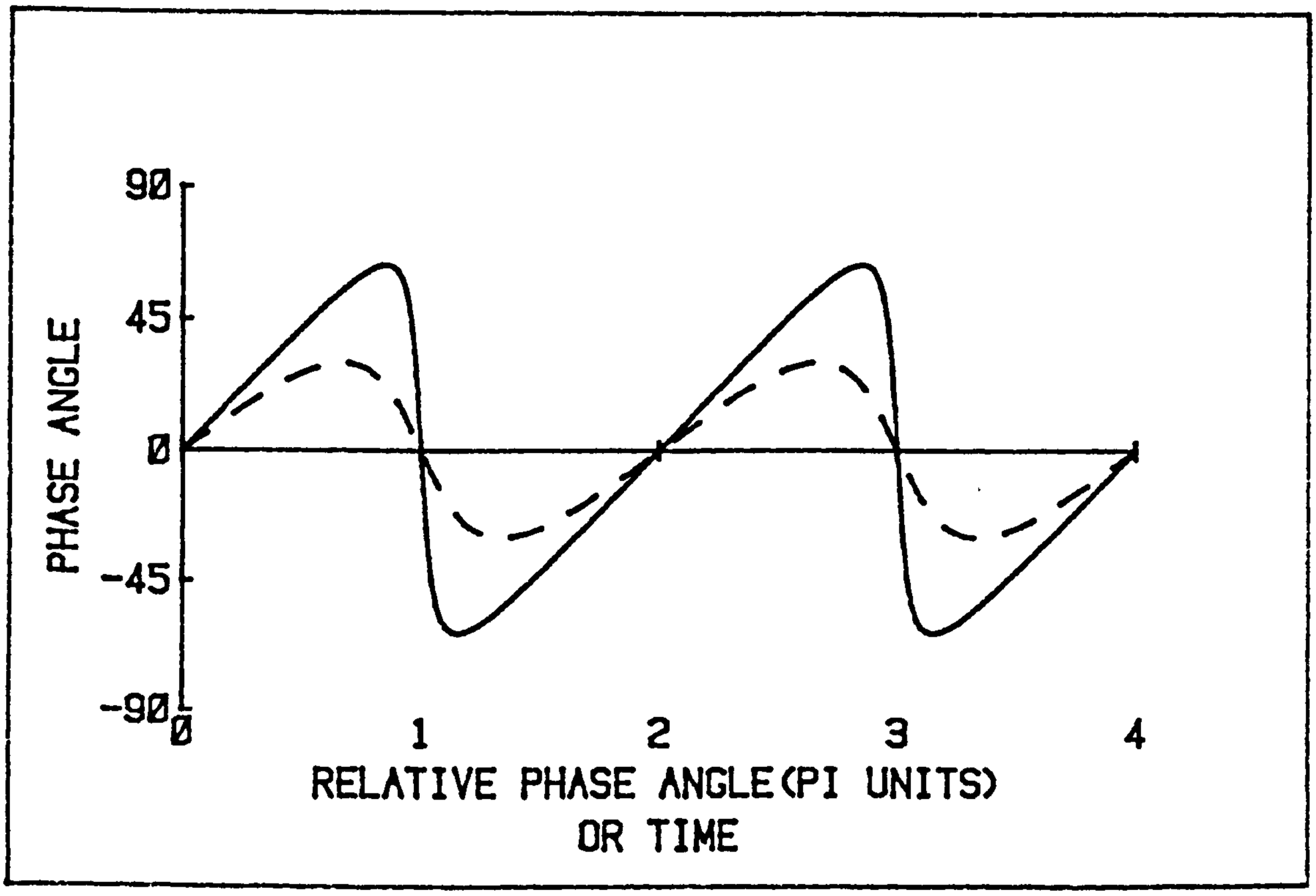

Solid line, carrier difference 1dB; dashed line, carrier difference 3dB.

Fig. 7.5.5 Phase Demodulator Output

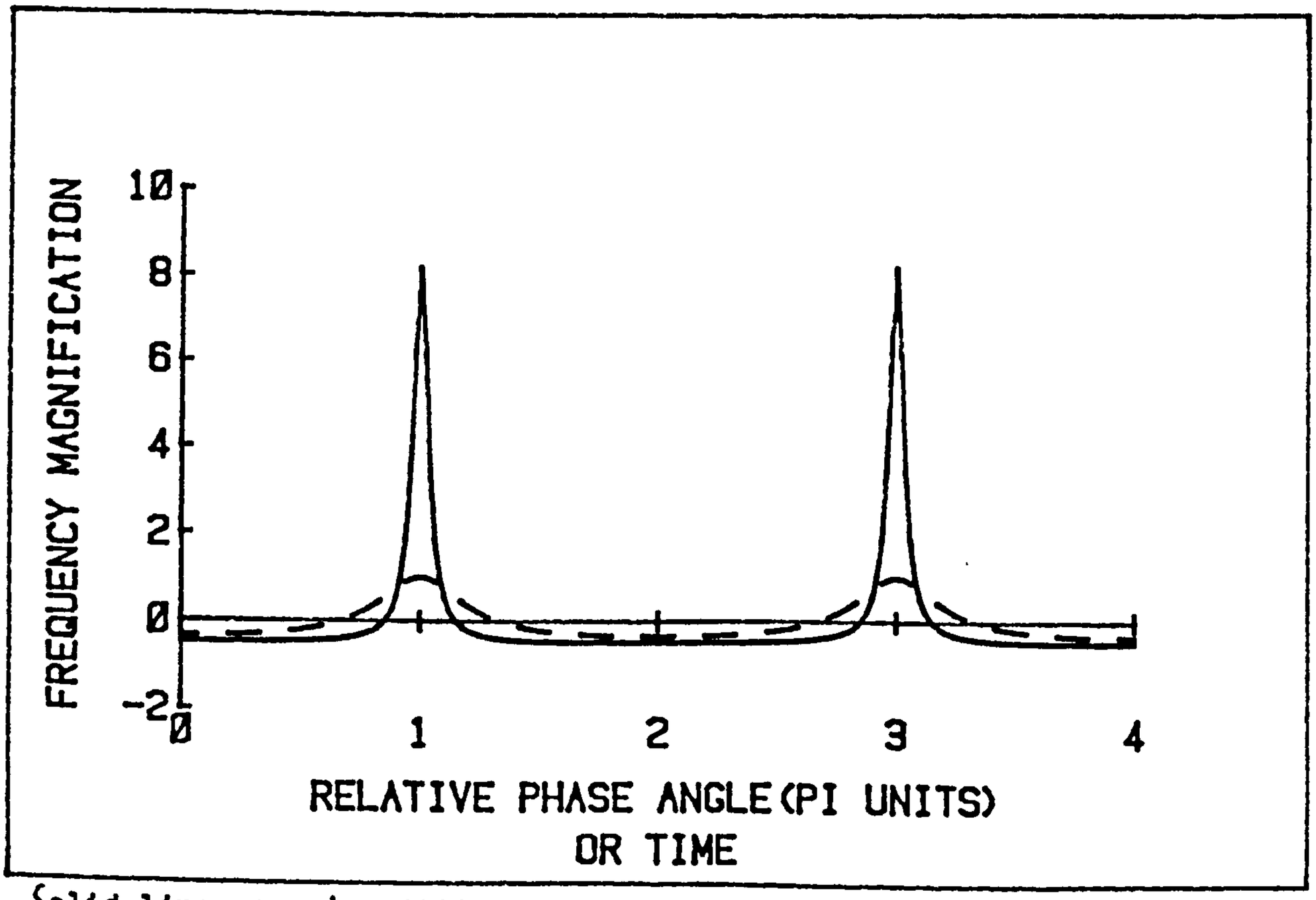

Solid line, carrier difference 1dB; dashed line, carrier difference 3dB.

Fig. 7.5.6 Frequency Demodulator Output

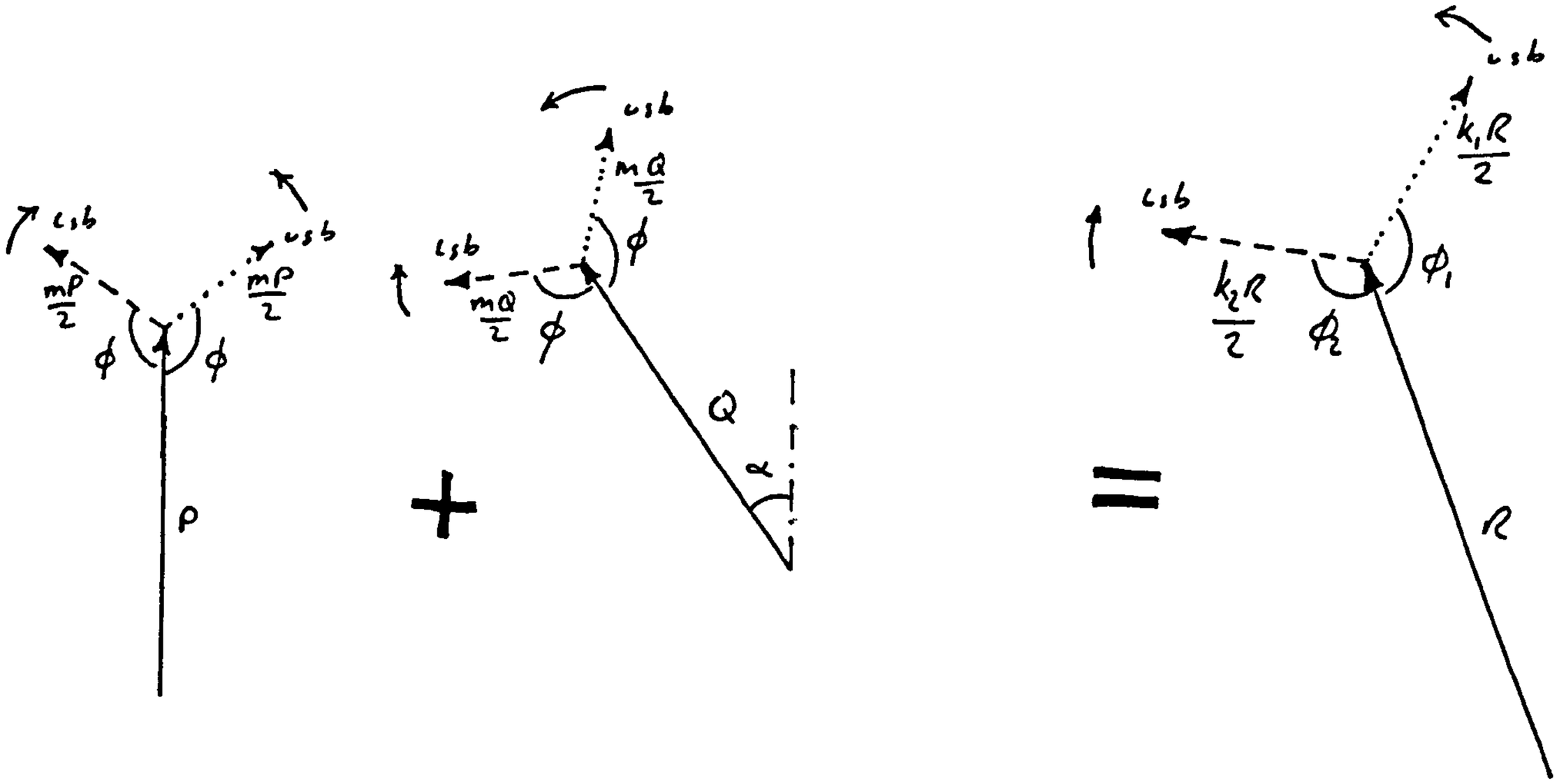

Fig. 7.5.7 Phasor Diagram for Identically Modulated Carriers

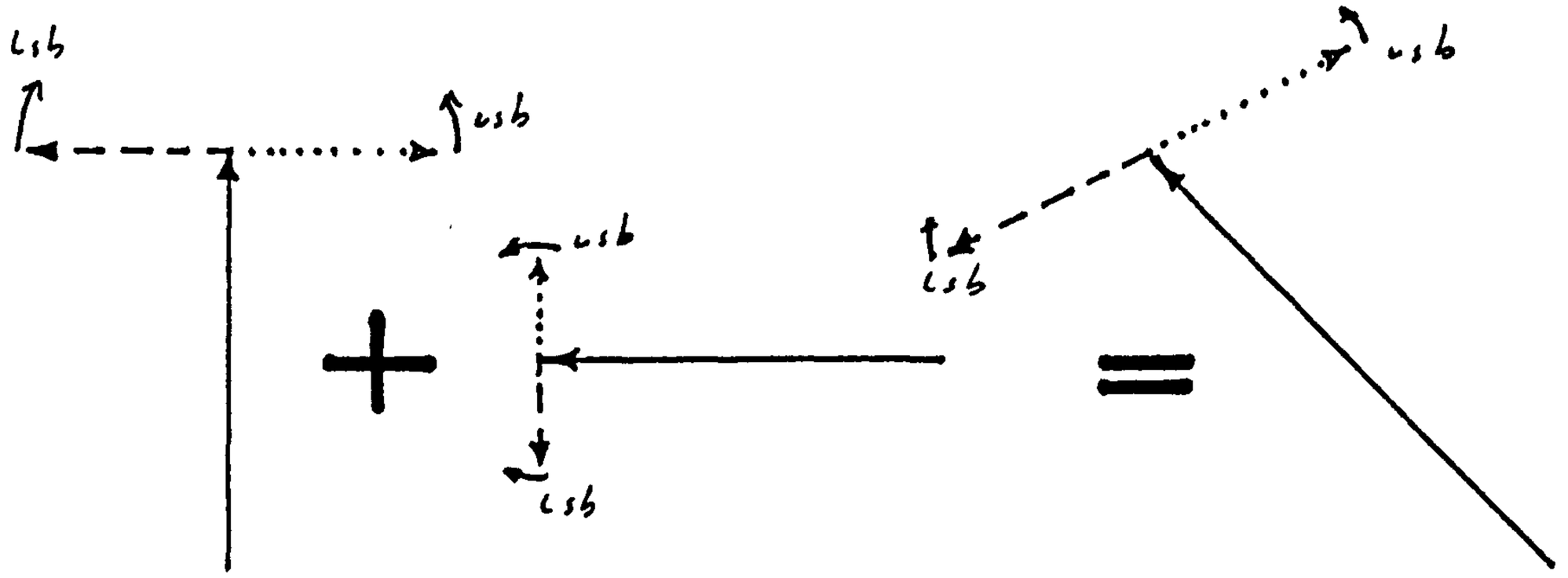

Fig. 7.5.8 Summation of Amlitude Modulations Differing by 2:1 (6 dB)

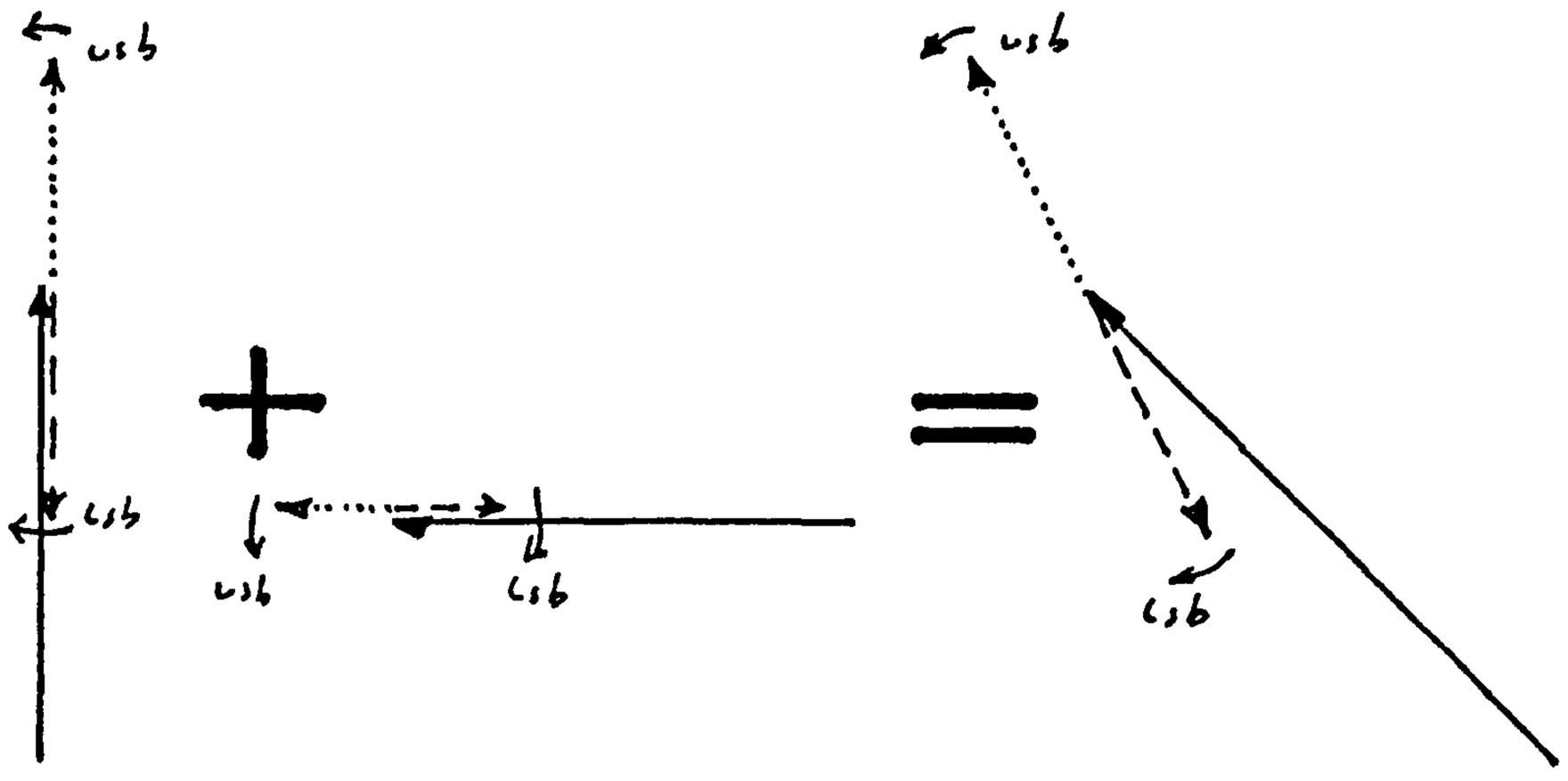

Fig. 7.5.9 Summation of Frequency Modulations Differing by 2:1 (6 dB)

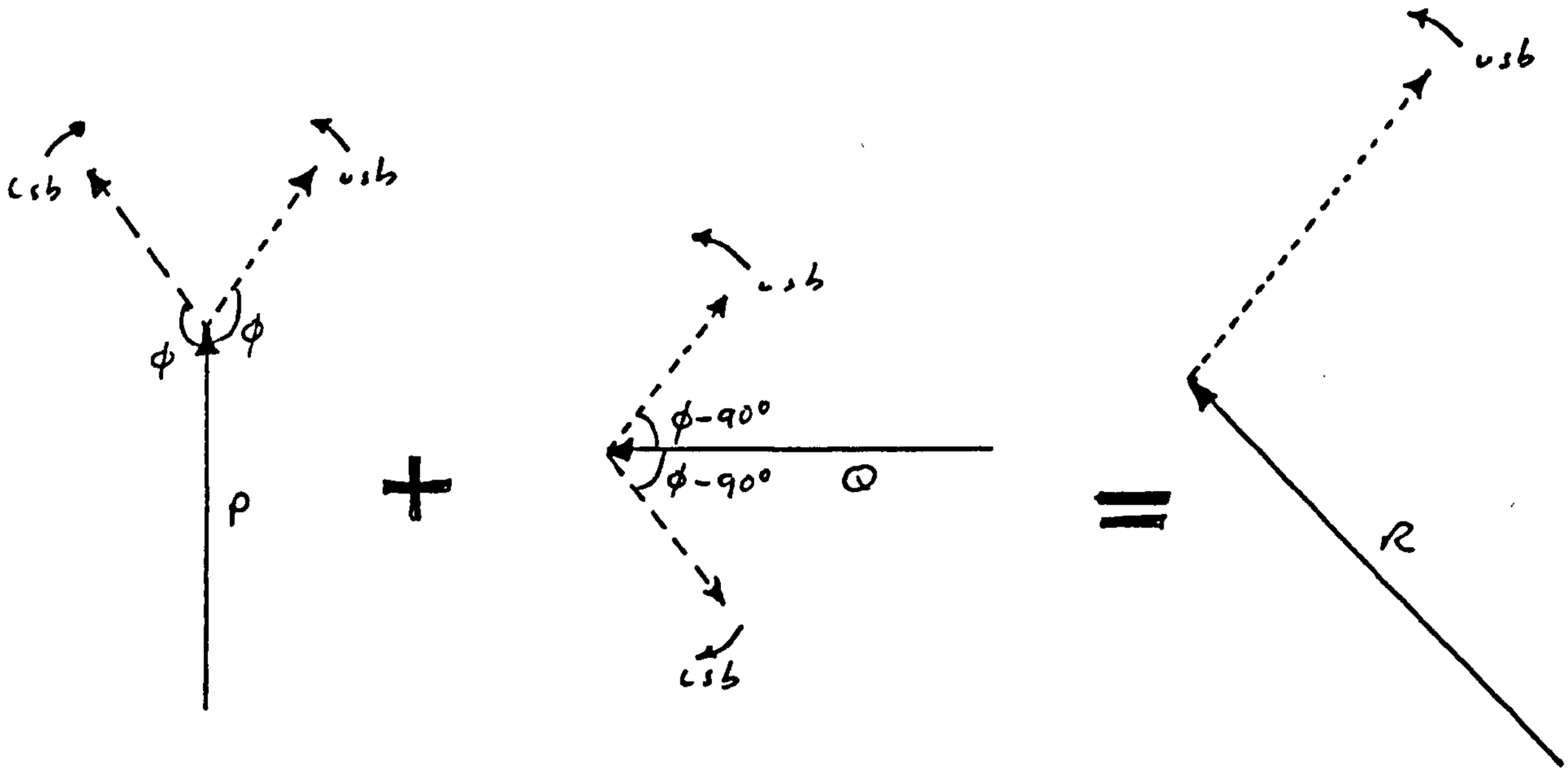

Fig. 7.5.10 Phasor diagam for Amplitude Modulations Differing by 90 degrees I

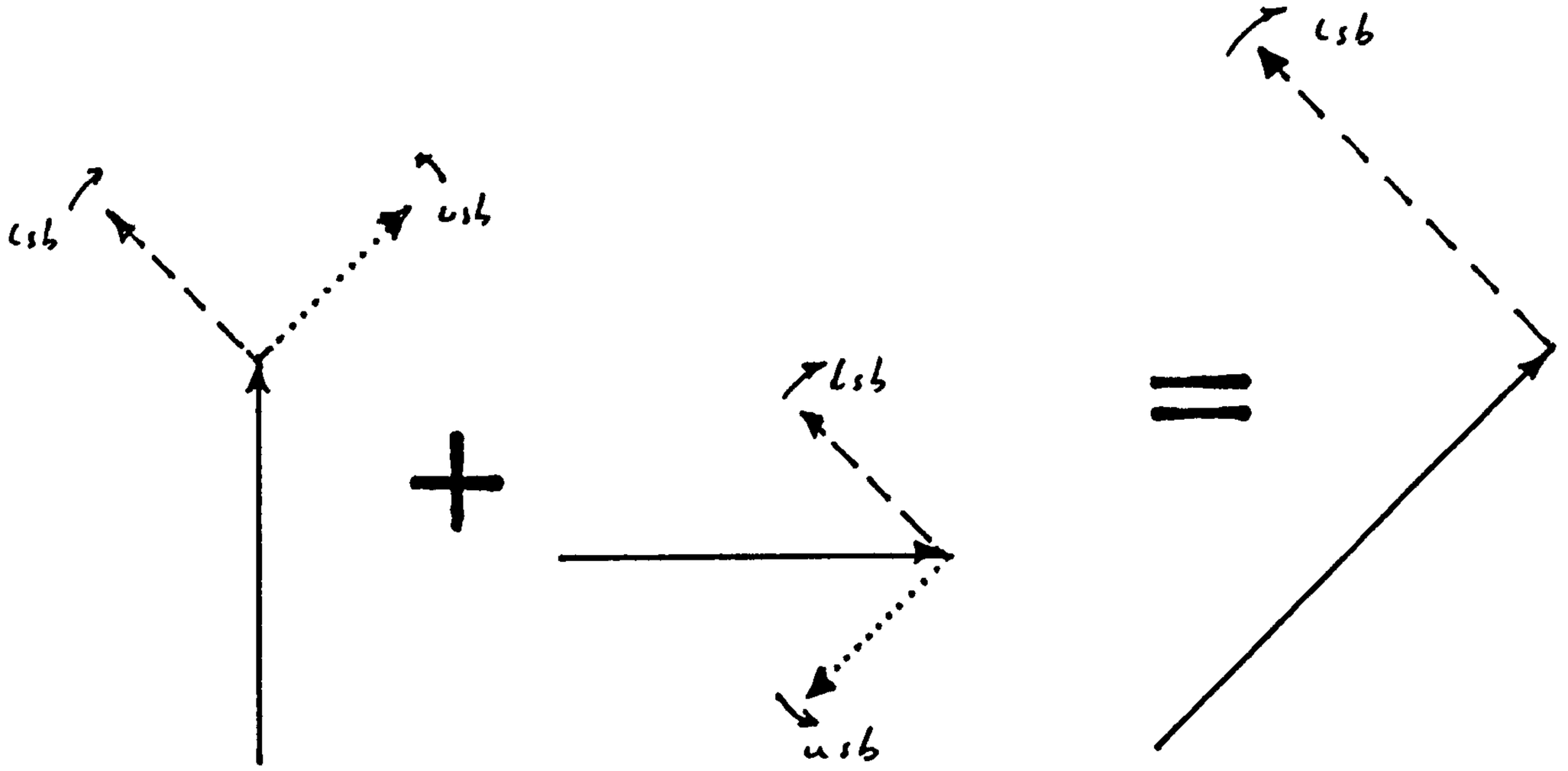

Fig. 7.5.11 Phasor diagam for Amplitude Modulations Differing by 90 degrees I

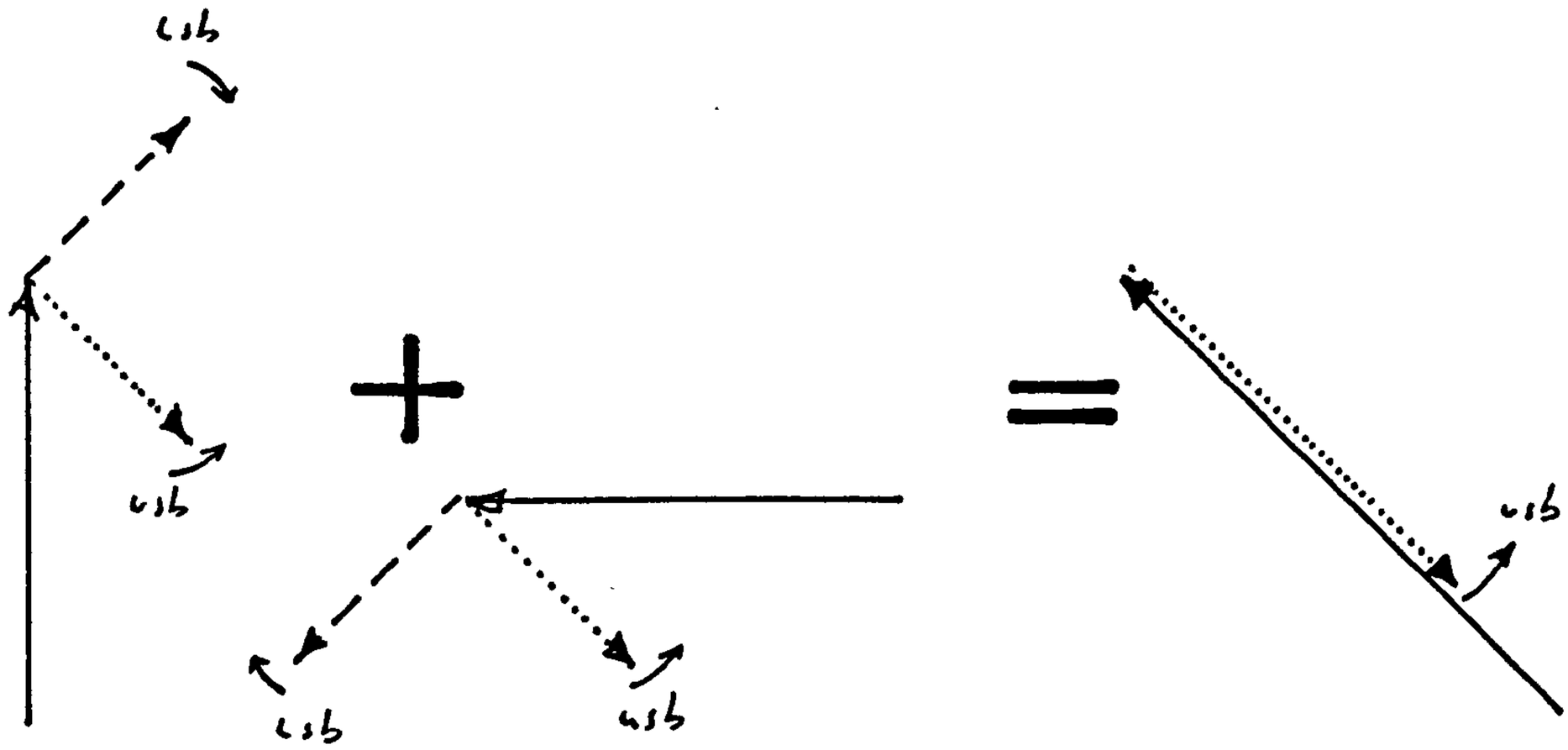

Fig. 7.5.12 Phasor diagam for Frequency Modulations Differing by 90 degrees II

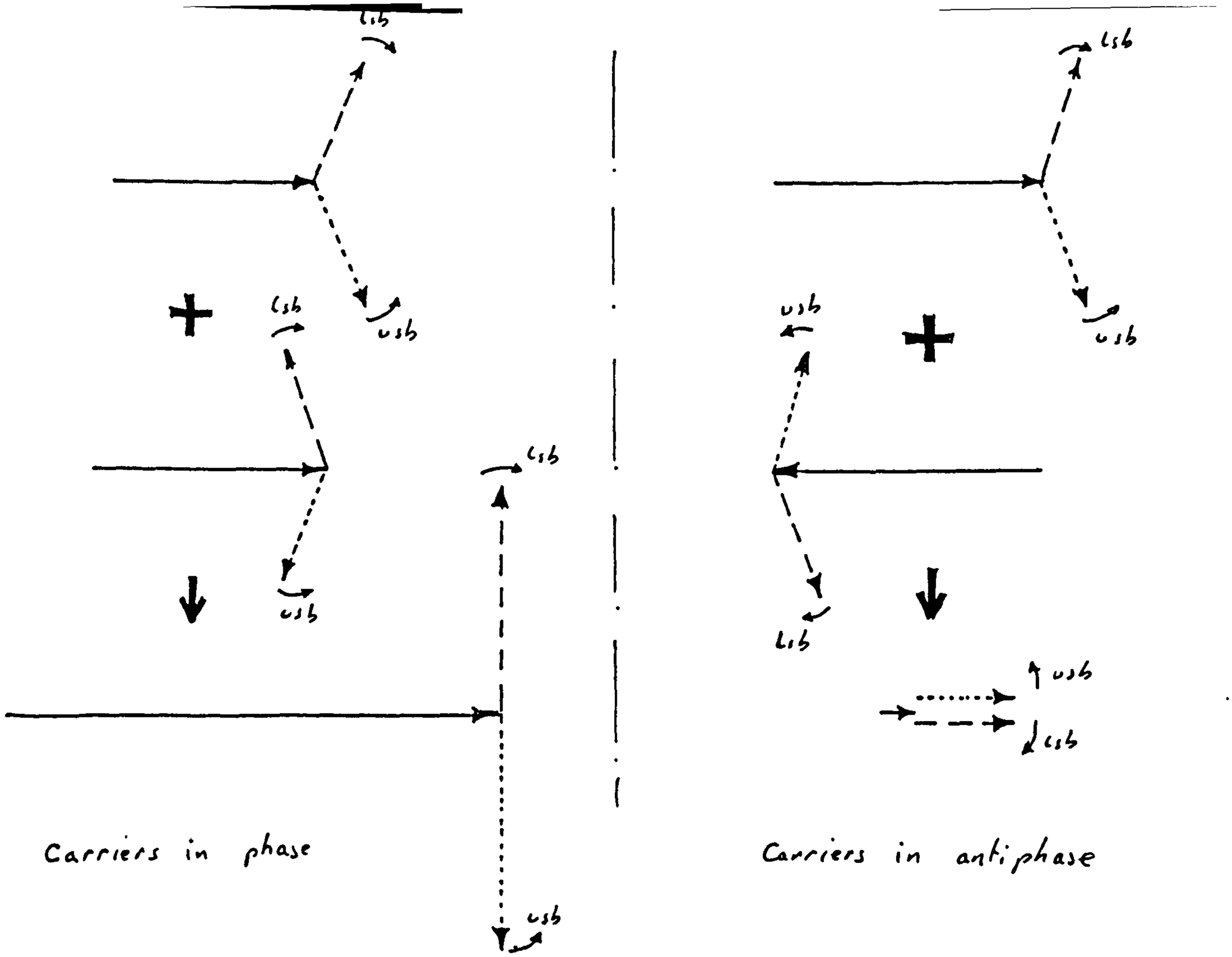

Carriers in phase

Carriers in antiphase

Fig. 7.5.13 Phasor Diagram for Phase mismatched Amplitude Modulations at Opposite Extremes of the Beat Cycle

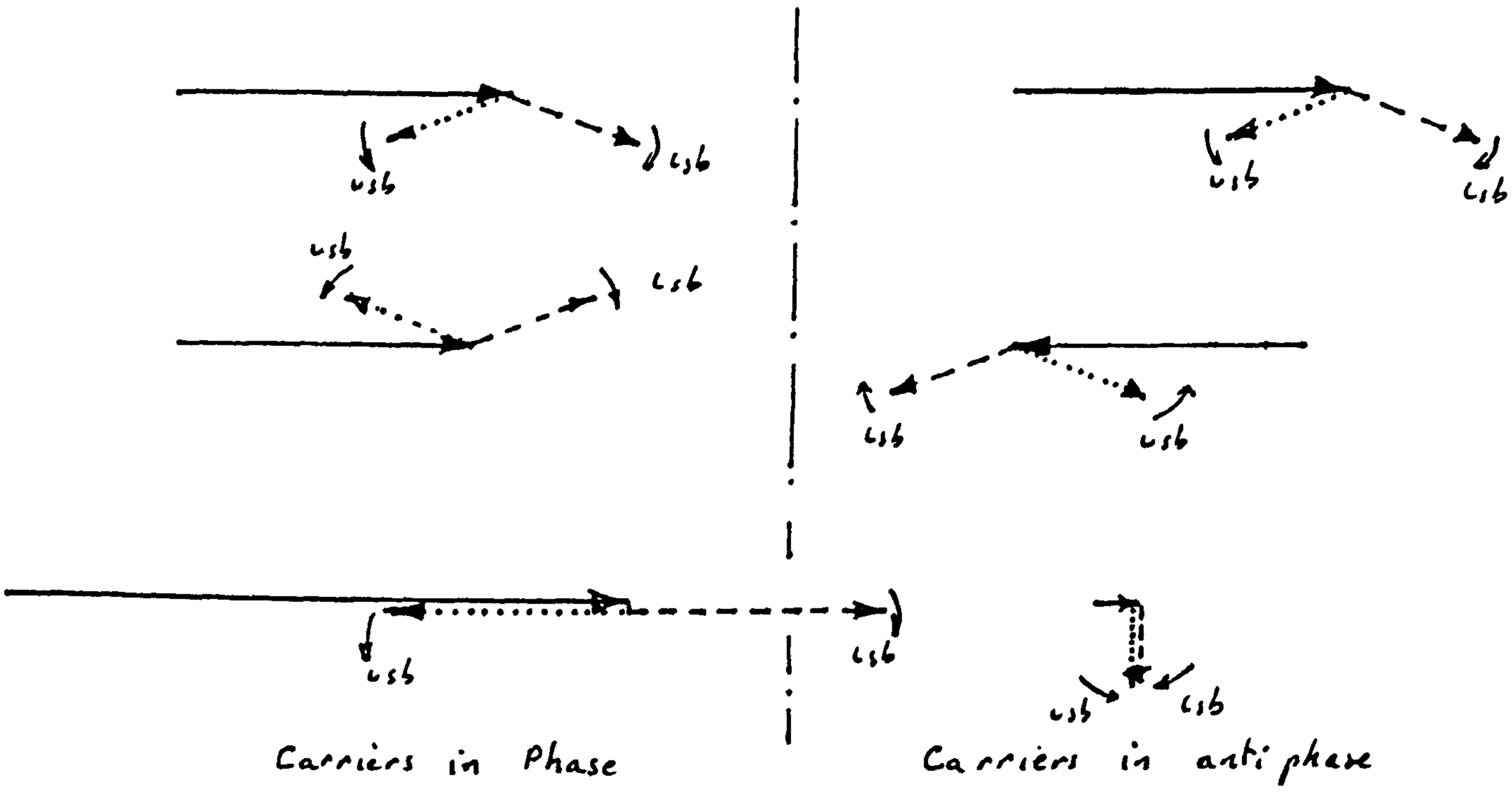

Fig. 7.5.14 Phasor Diagram for Phase mismatched Amplitude Modulations at Opposite Extremes of the Beat Cycle

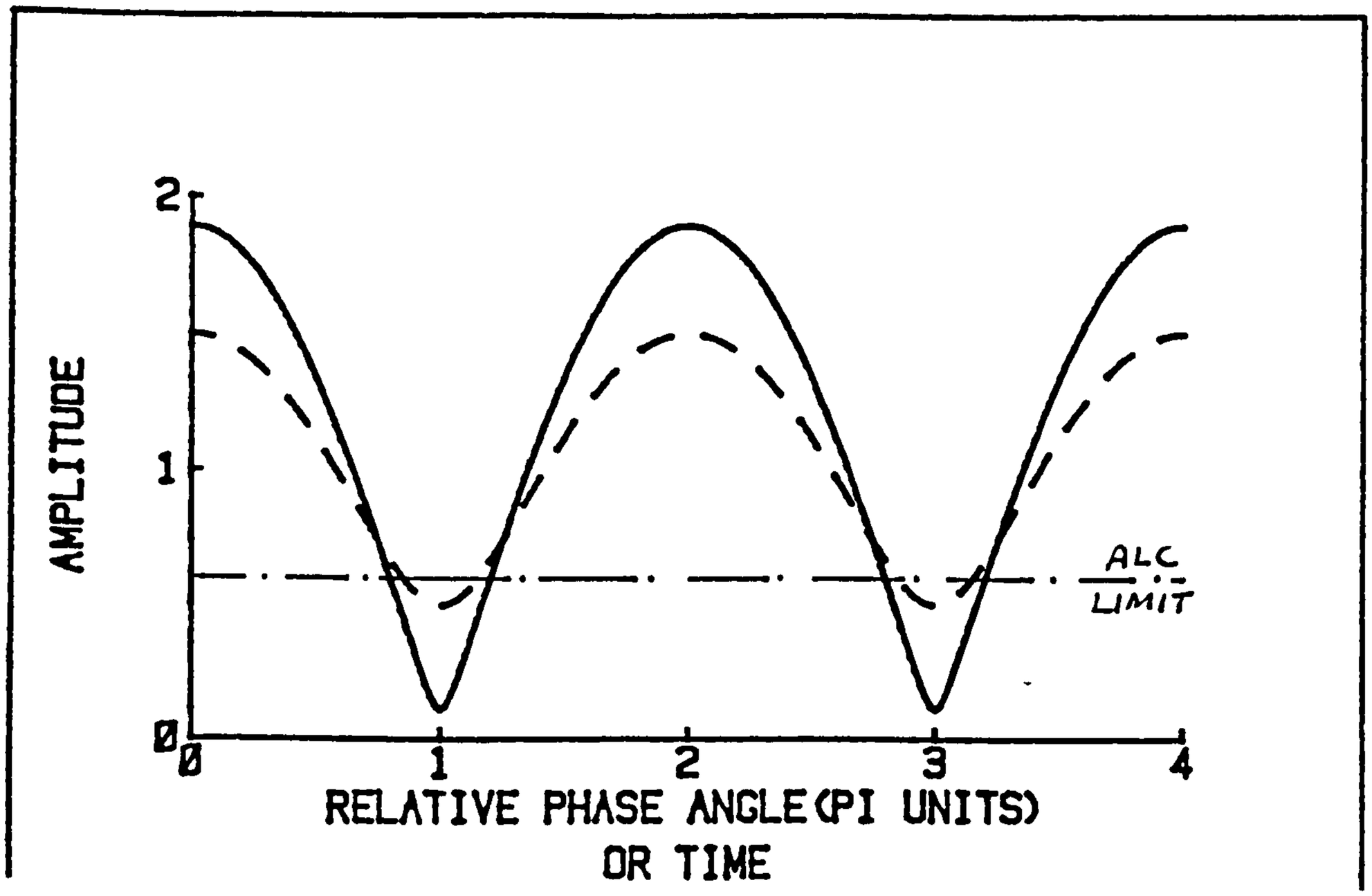

Fig. 7.5.15 Position of ALC Limits of Action on the Envelope

Variation of amplitude of envelope of resultant, Solid line, carrier difference 1dB; dashed line, carrier difference 3dB. Reference carrier amplitude unity.

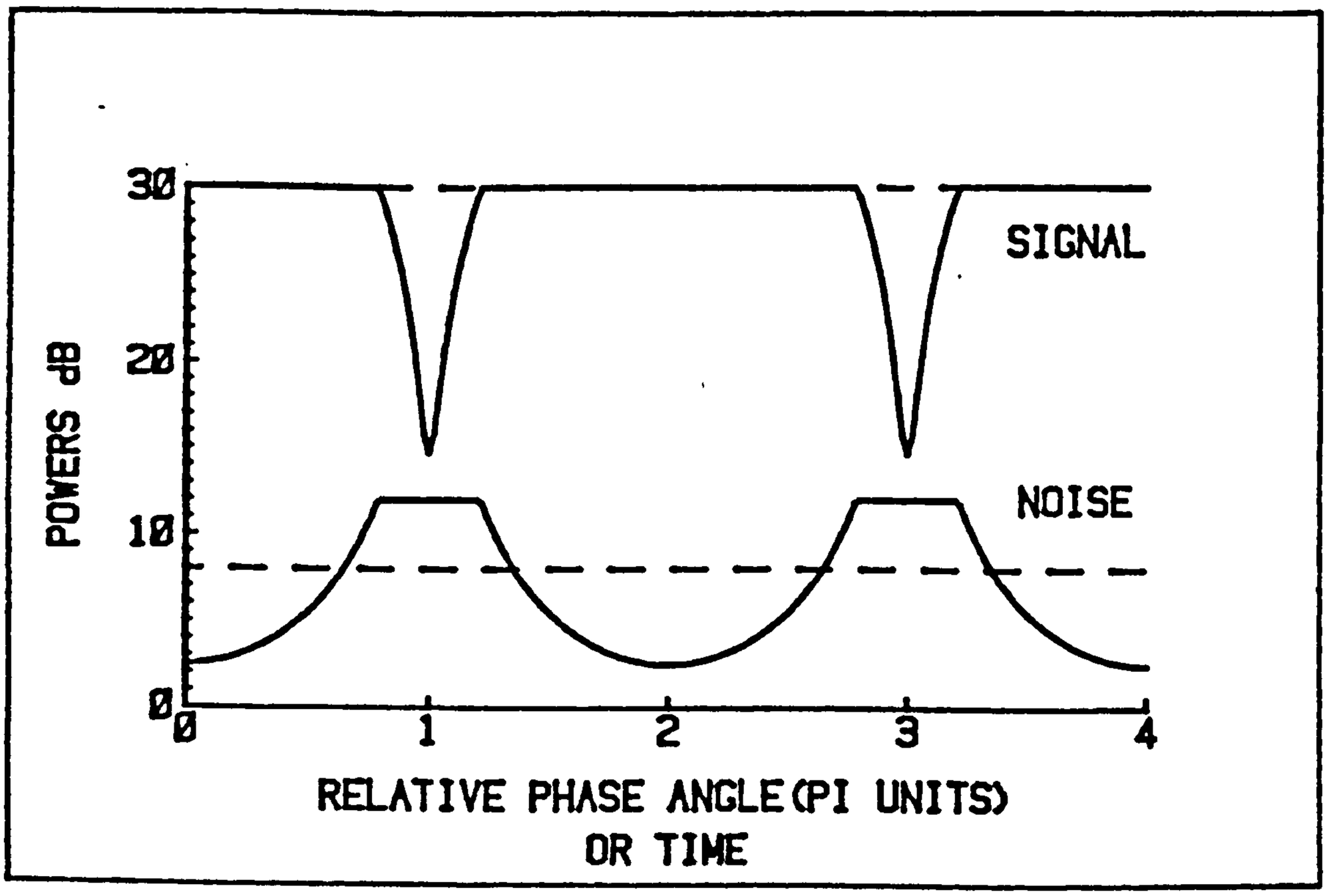

Fig. 7.5.16 Effect of ALC Limits of Action on the Envelope

Variation of signal and noise when ALC has a limited range of action. Solid lines show case of two carriers 1dB different in amplitude with signal level arbitrarily set at 30dB. Dashed curves show case for single carrier with 22 dB signal to noise ratio.

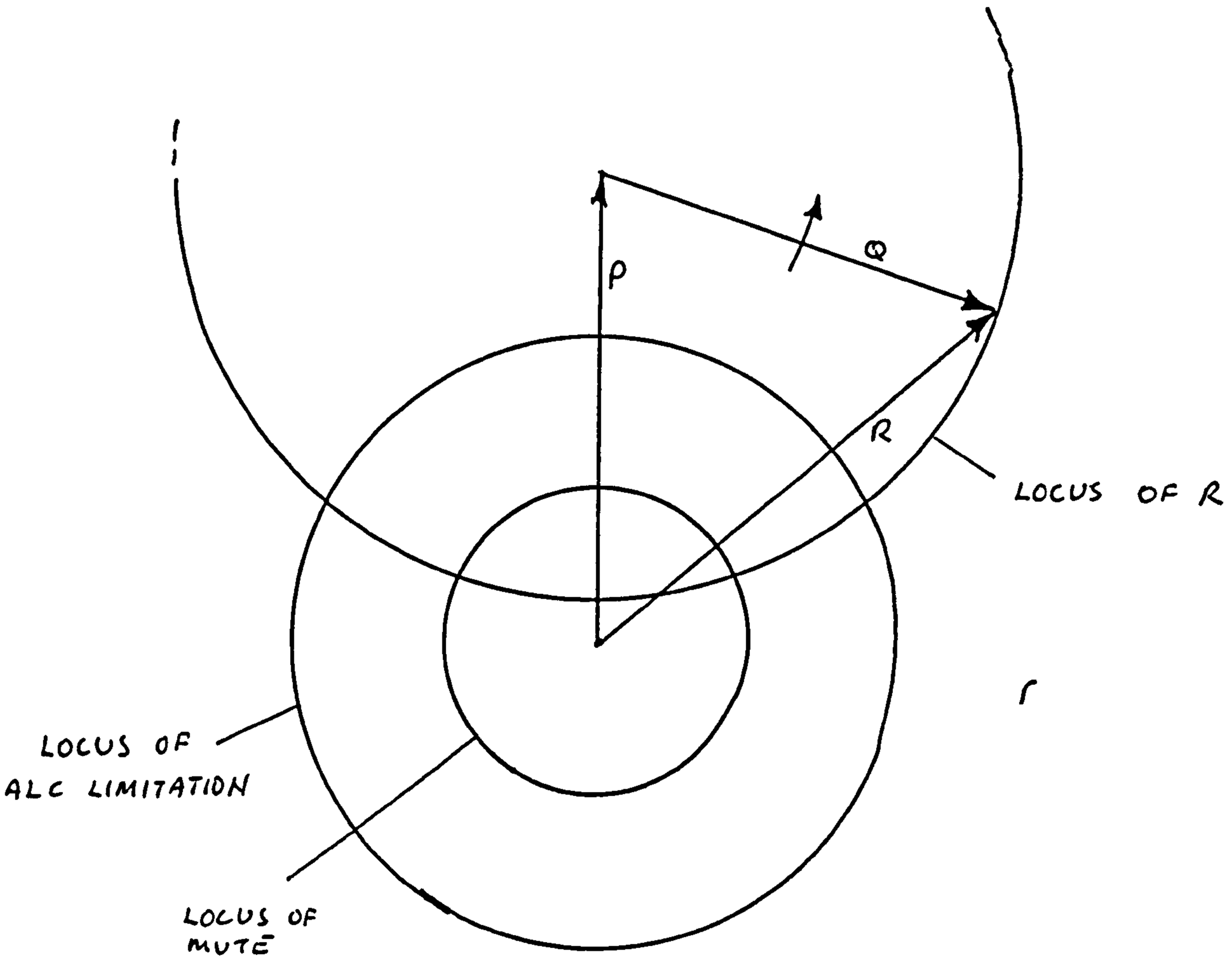

Fig. 7.5.17 Loci of Mute, ALC, and Resultant

mute ١٧٥ , ALC ٢٧٥, P 10dB above mute, Q 1dB below P.

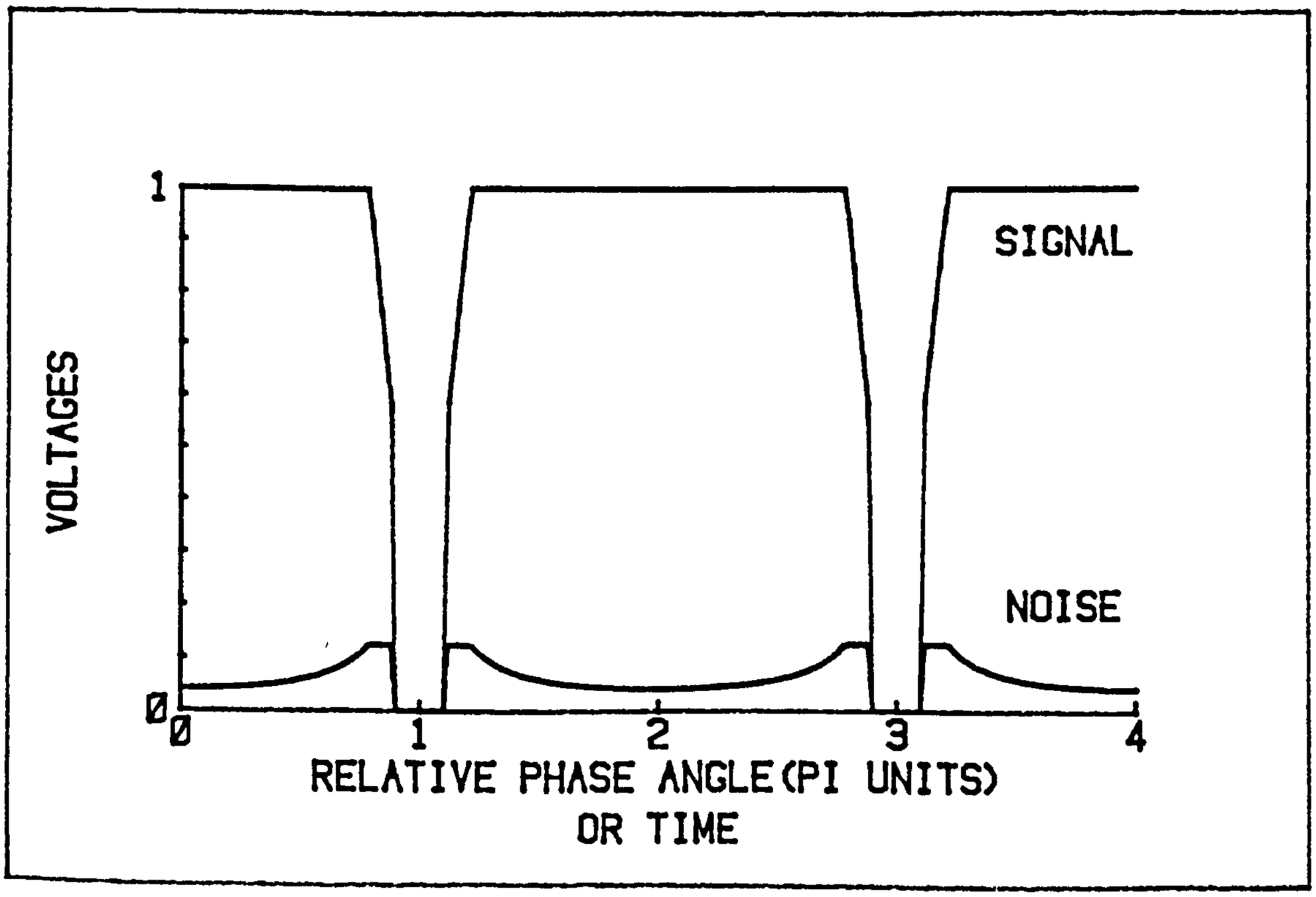

Fig. 7.5.18 Effect of Mute and ALC Limitation on AM Demodulator Output

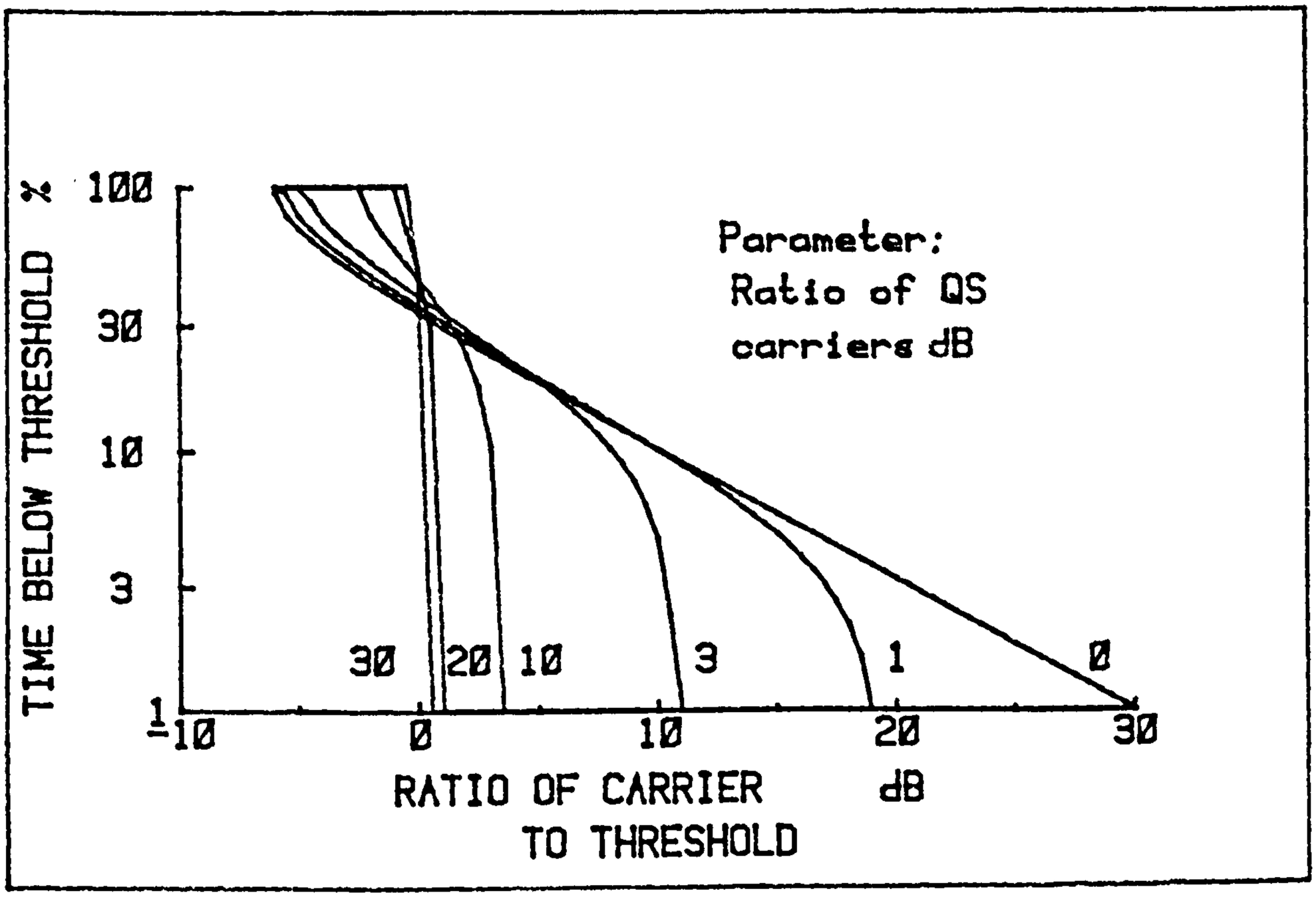

Fig. 7.5.19 Probability of Combined QS Carriers Falling Below a Theshold.

Various Ratios of QS Carriers

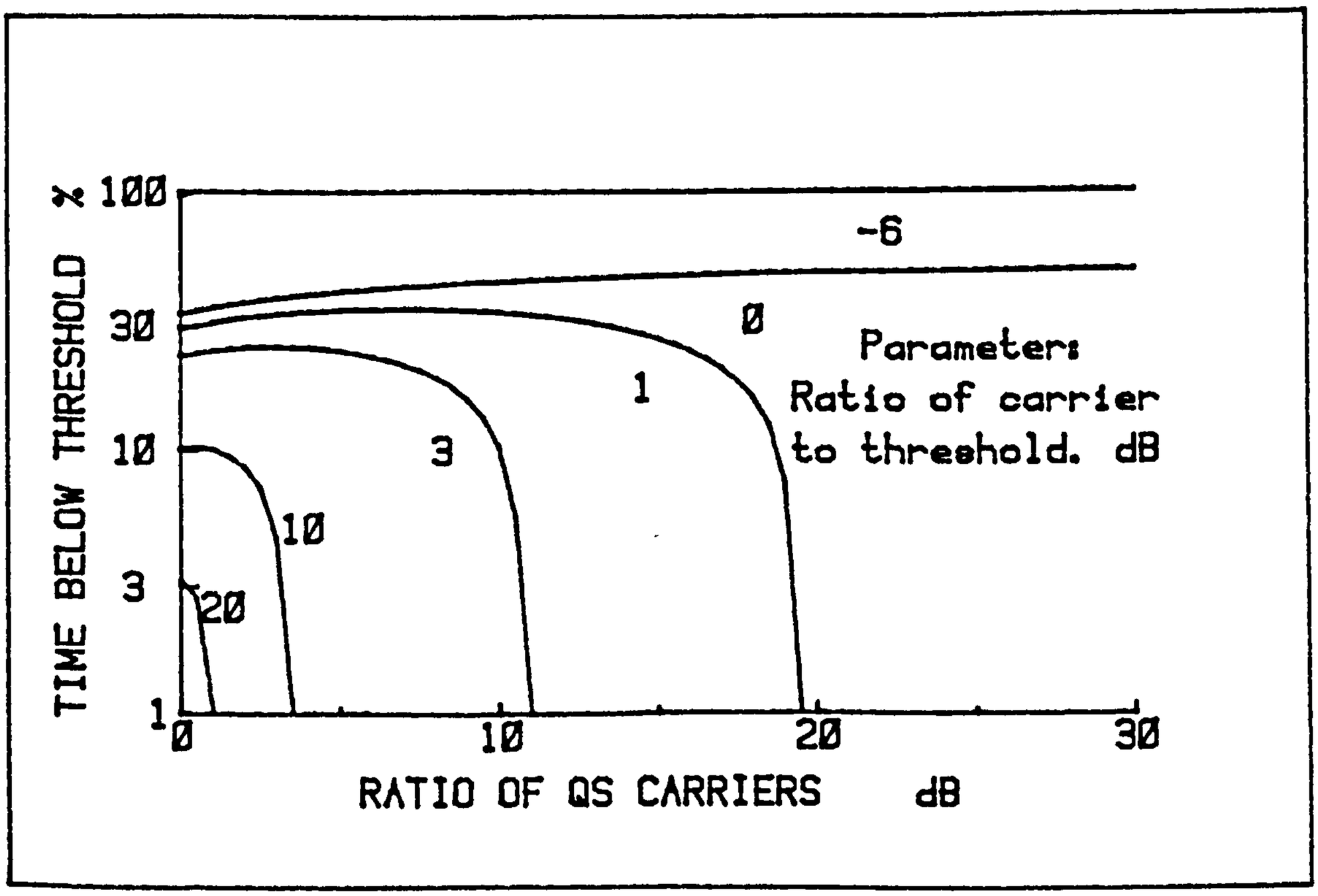

Fig. 7.5.20 Probability of Combined QS Carriers Falling Below a Theshold.

Various Ratios of Major Carrier to Threshold

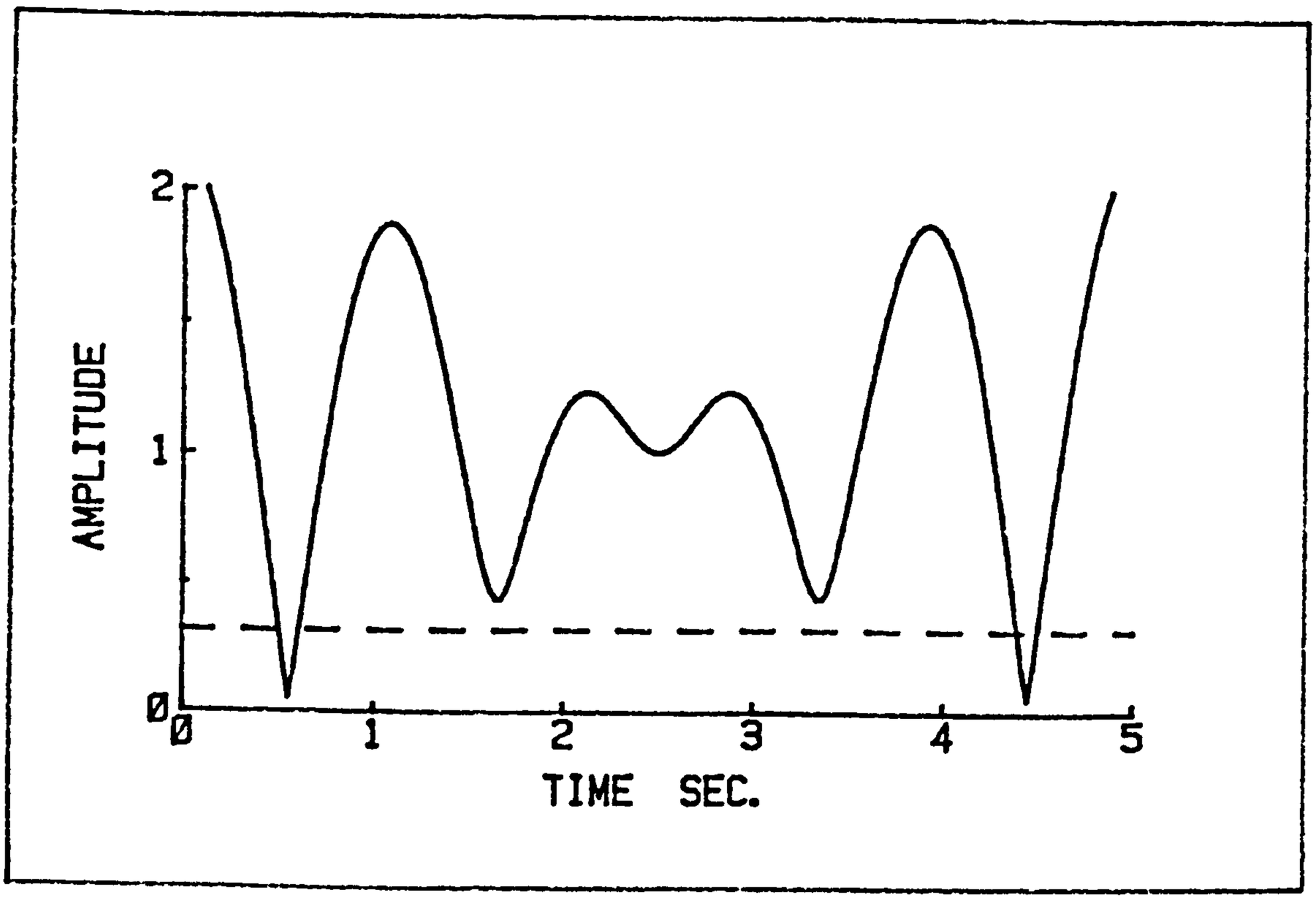

Fig. 7.5.21 Resultant Envelope of Three QS Carriers

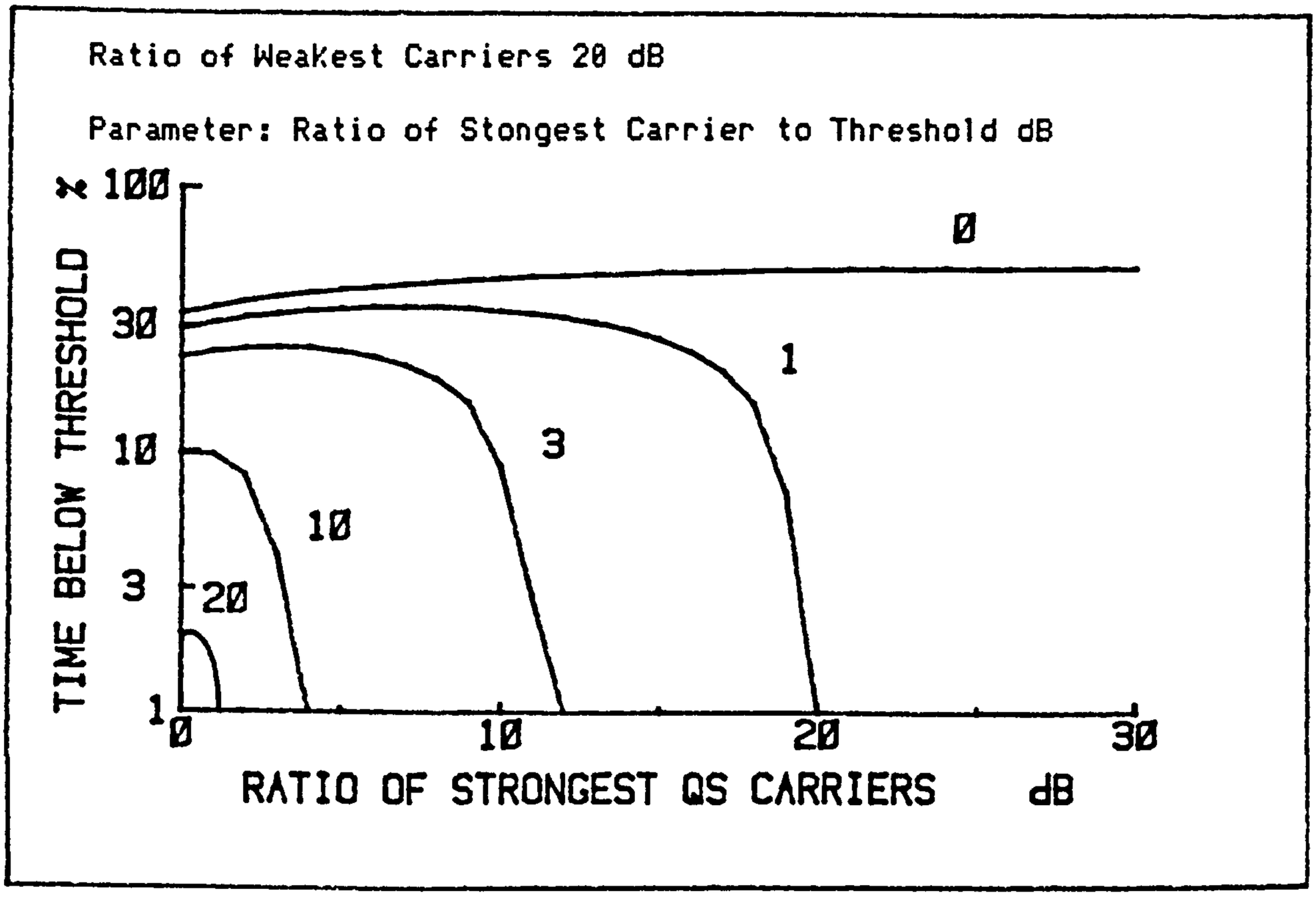

Fig. 7.5.22 Probability of Three QS Carriers Falling Below a Theshold. I

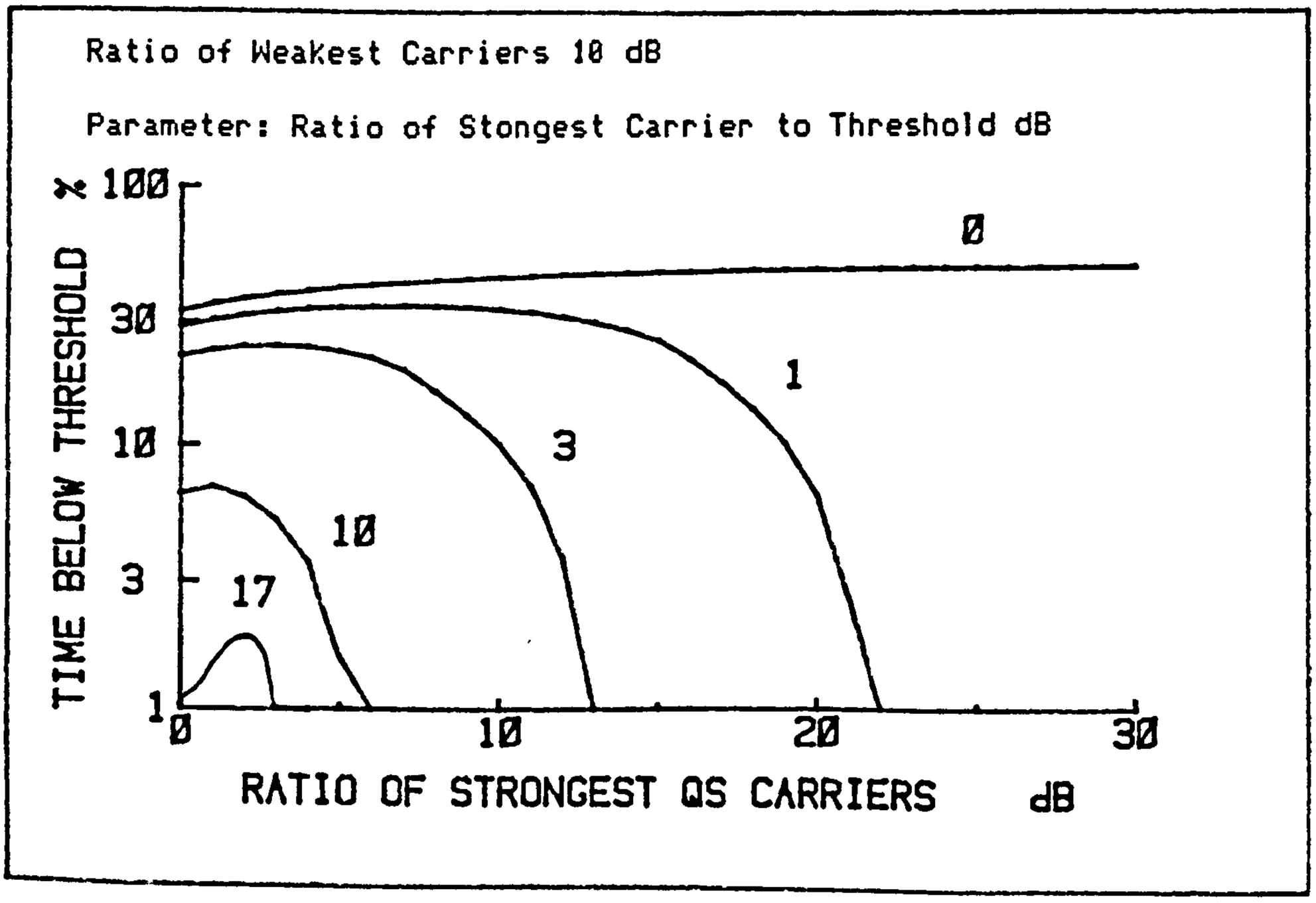

Fig. 7.5.23 Probability of Three QS Carriers Falling Below a Theshold. II

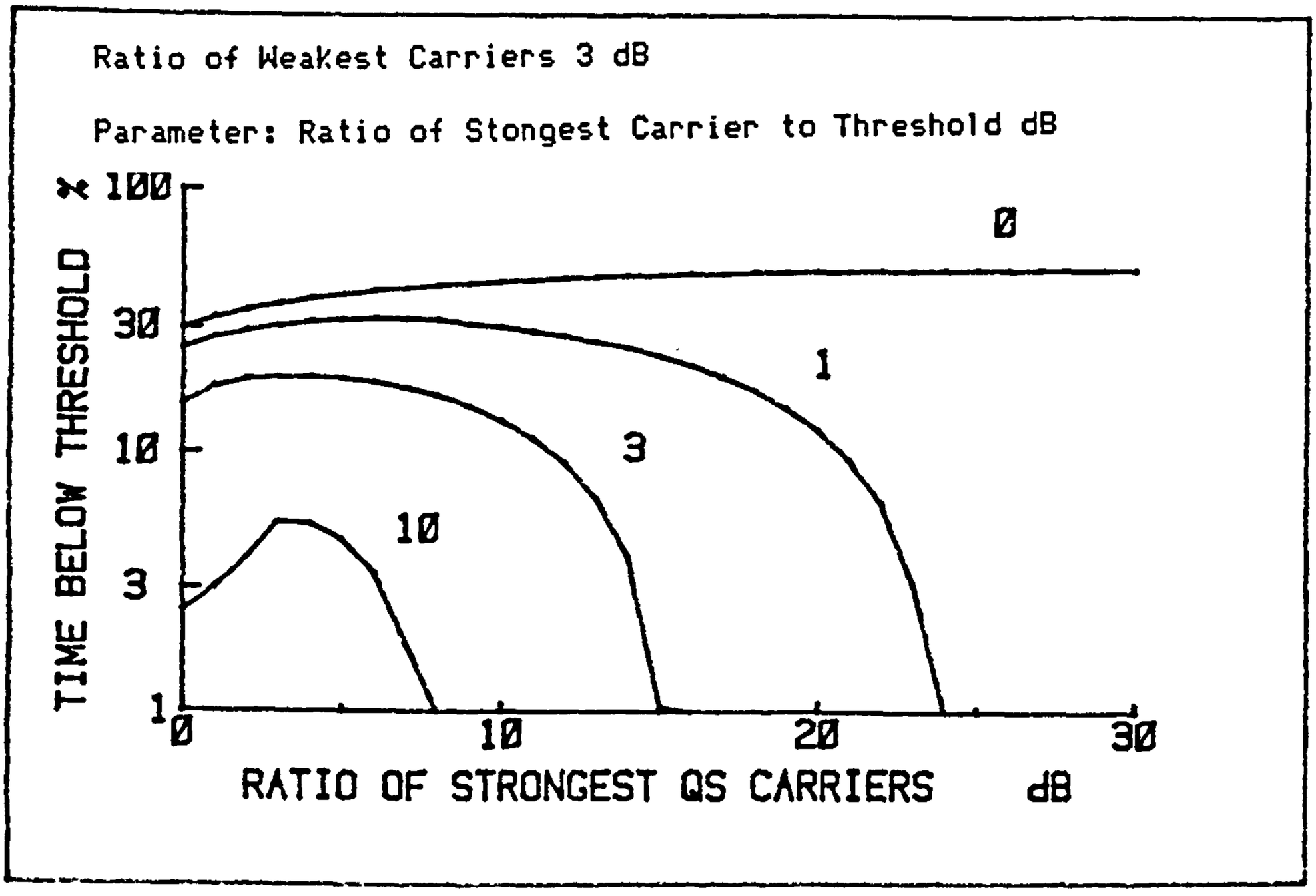

Fig. 7.5.24 Probability of Three QS Carriers Falling Below a Theshold. III

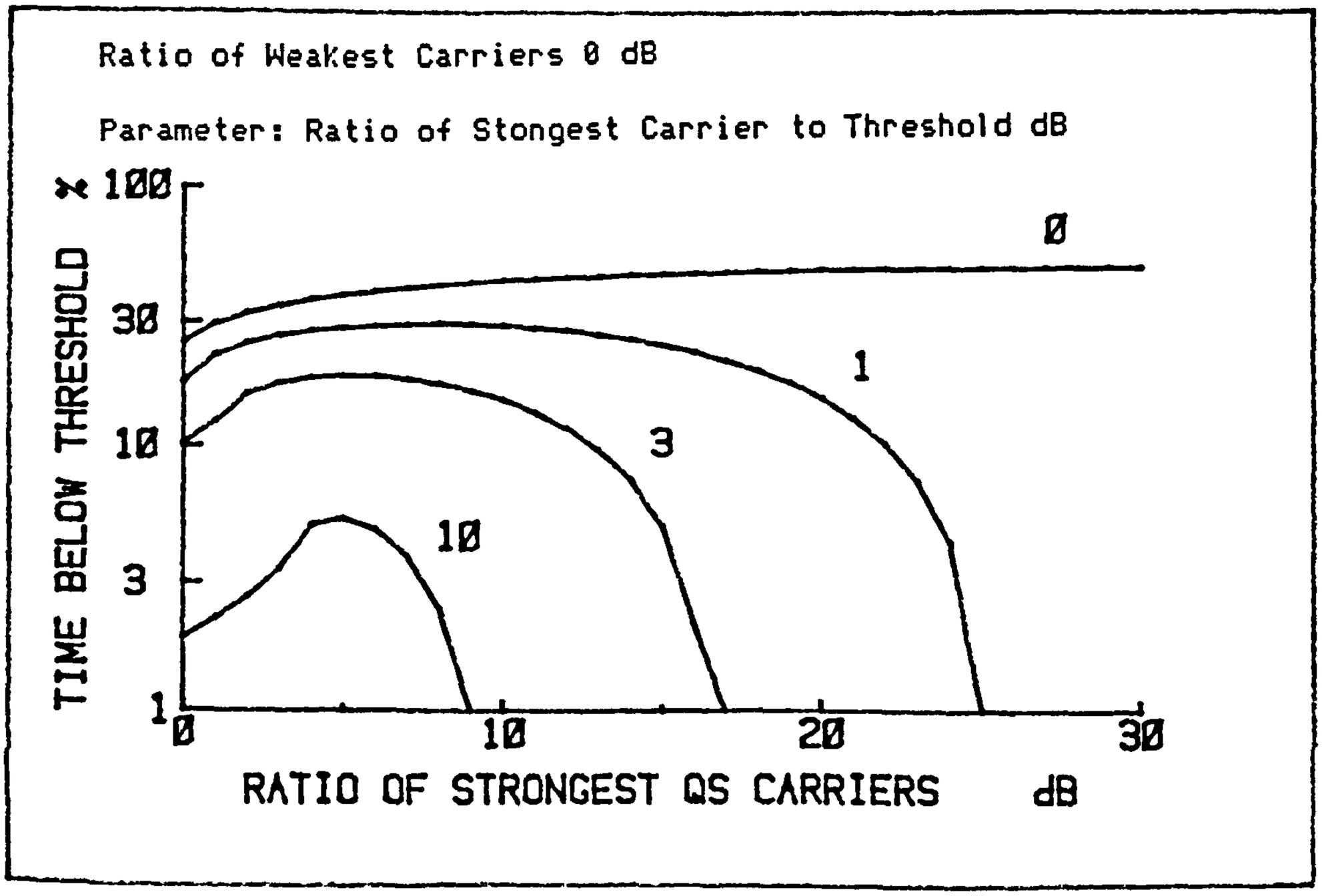

Fig. 7.5.25 Probability of Three QS Carriers Falling Below a Theshold. IV

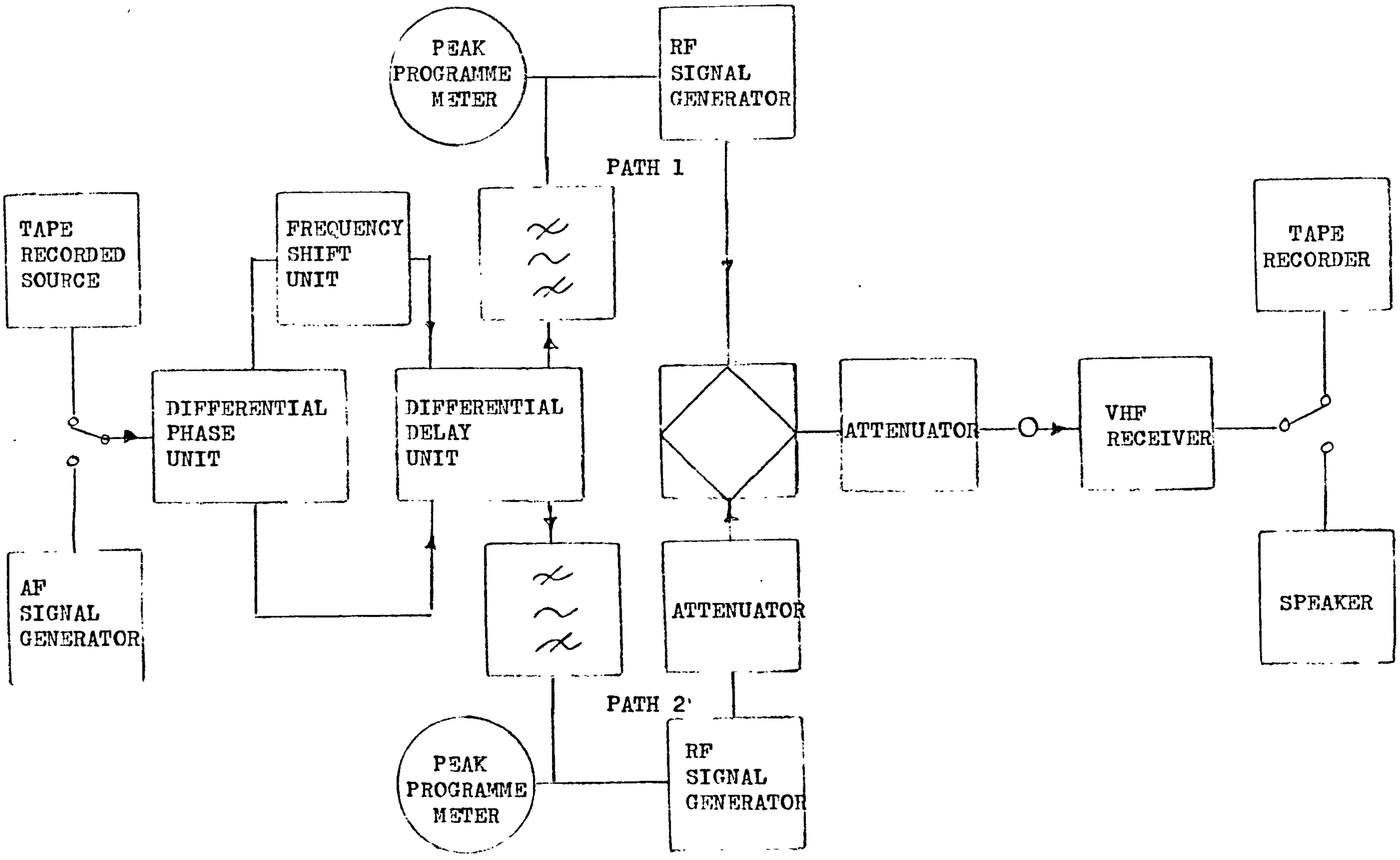

Fig. 7.7.1 Equipment for Laborarory Simulation of a Two Station QS Scheme

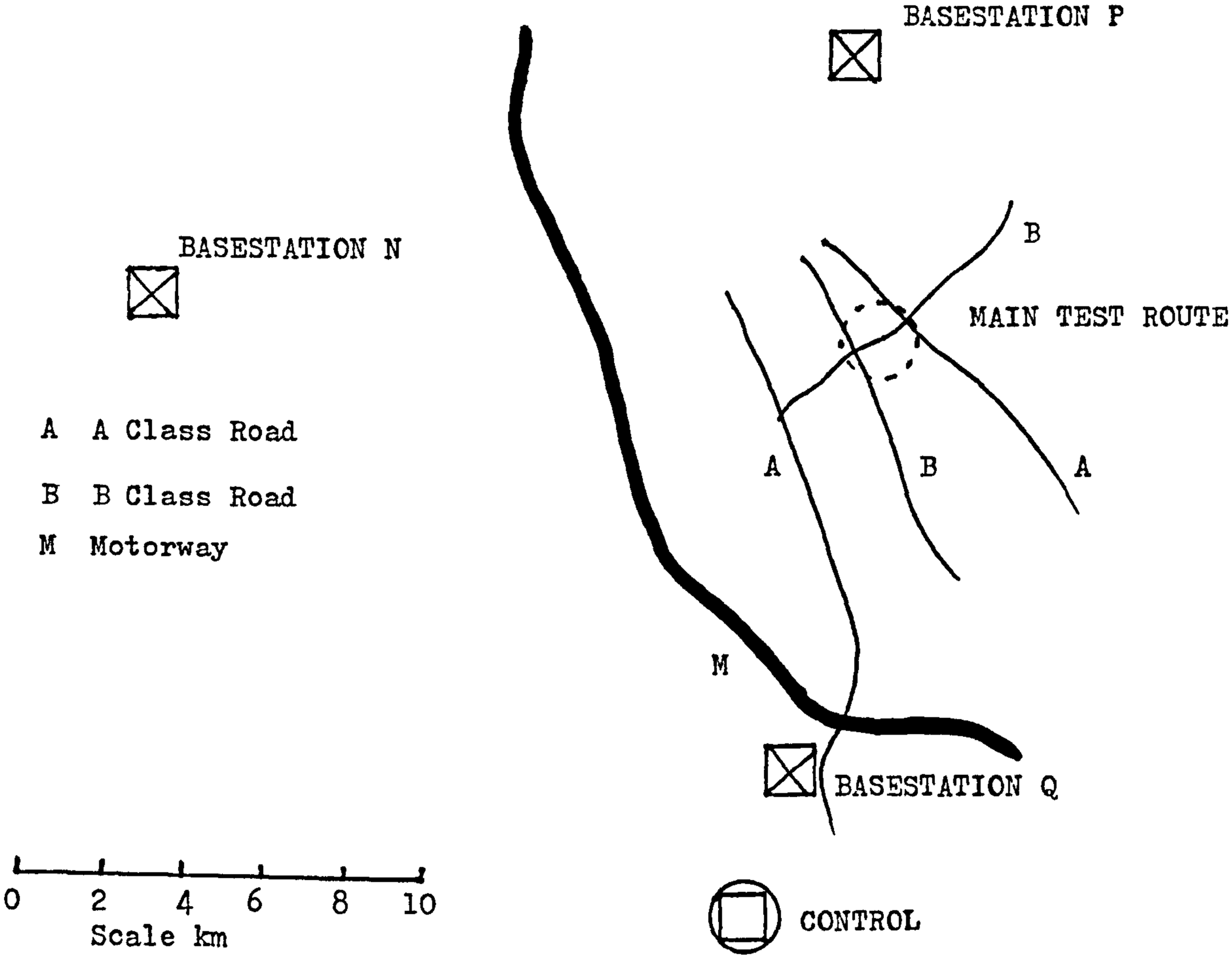

Fig. 7.7.2 Field Assessment Locations

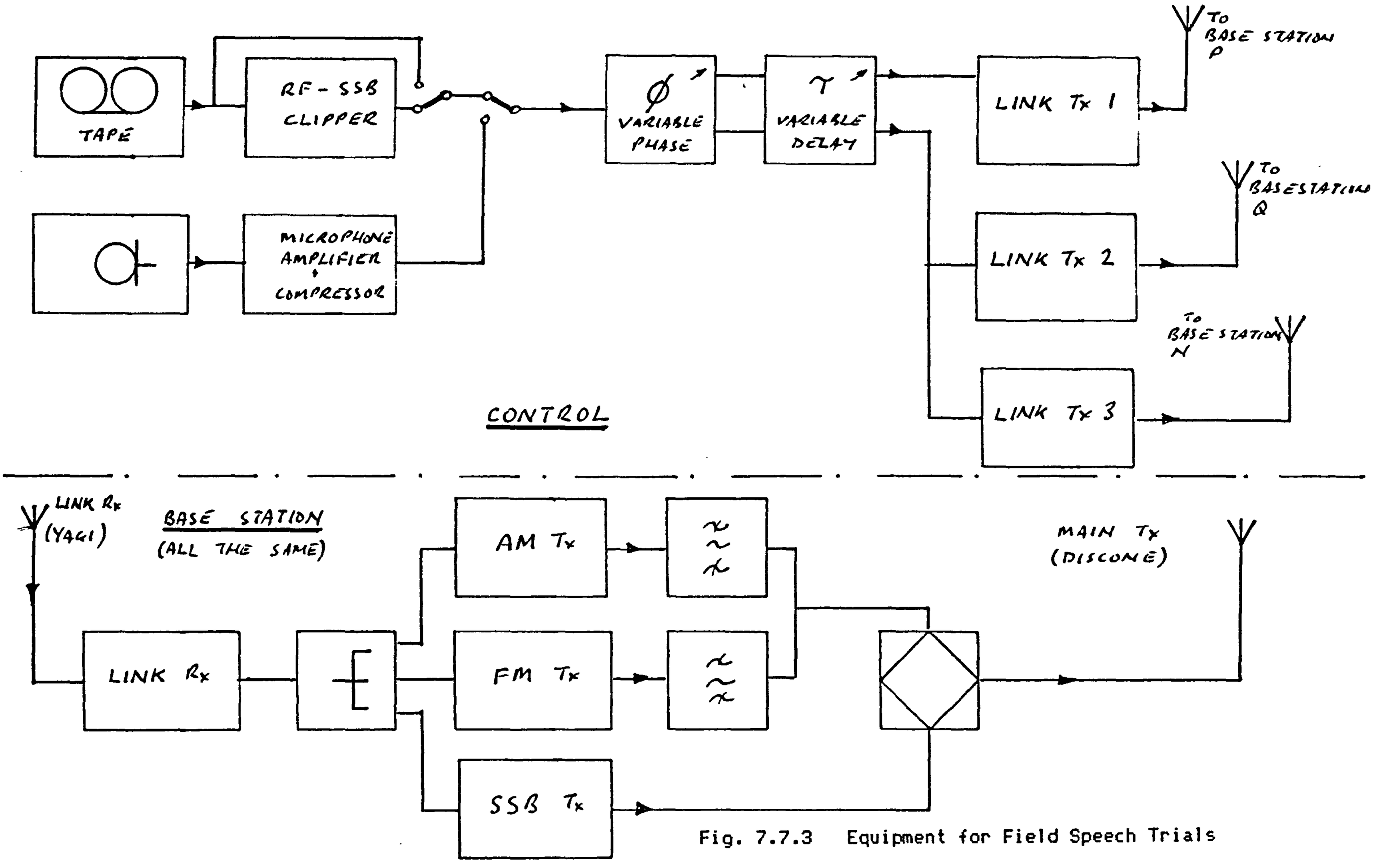

Fig. 7.7.3 Equipment for Field Speech Trials

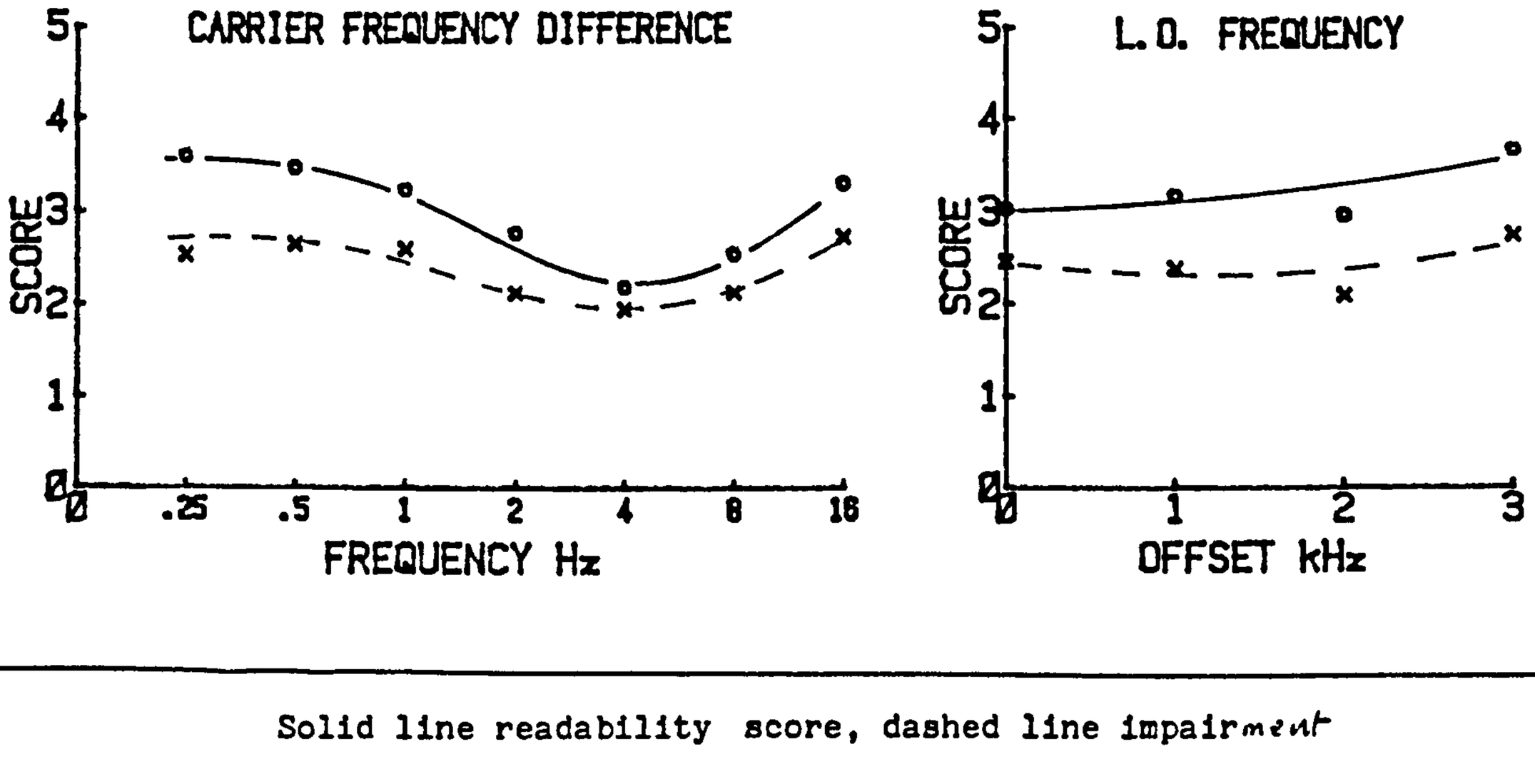

Solid line readability score, dashed line impairment

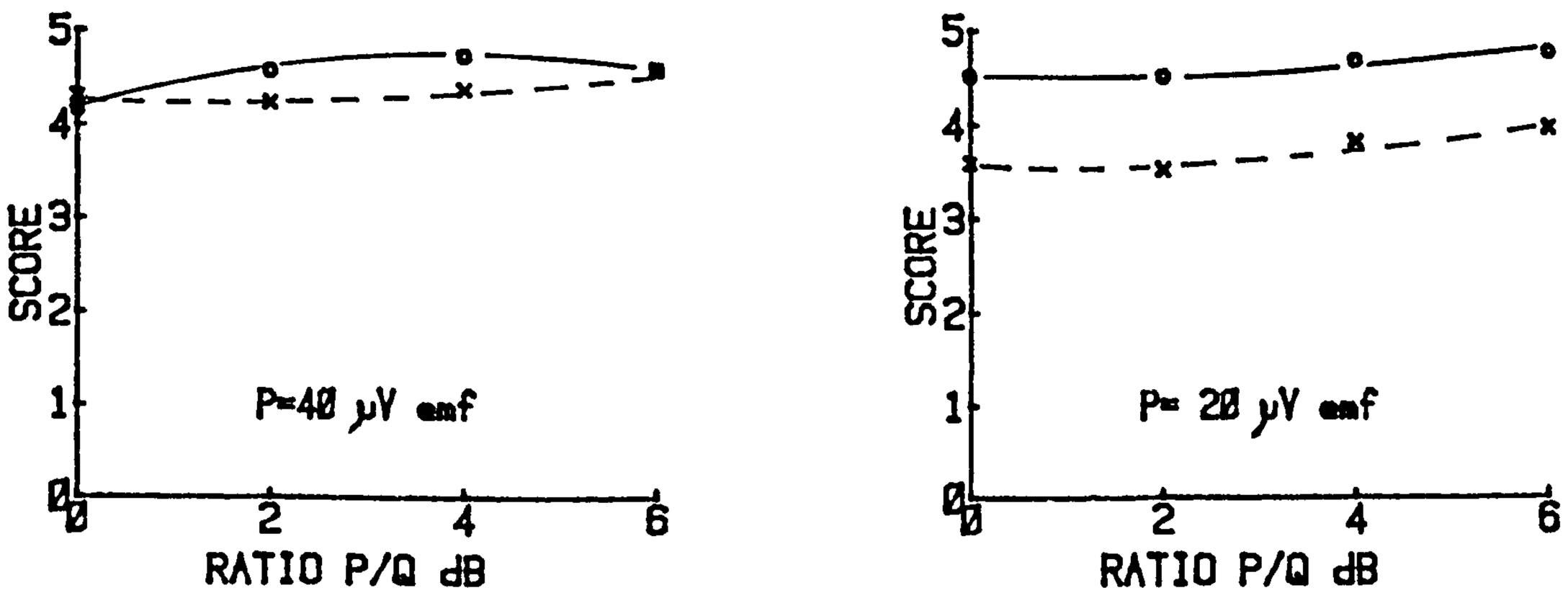

VARIATION OF CARRIER LEVELS

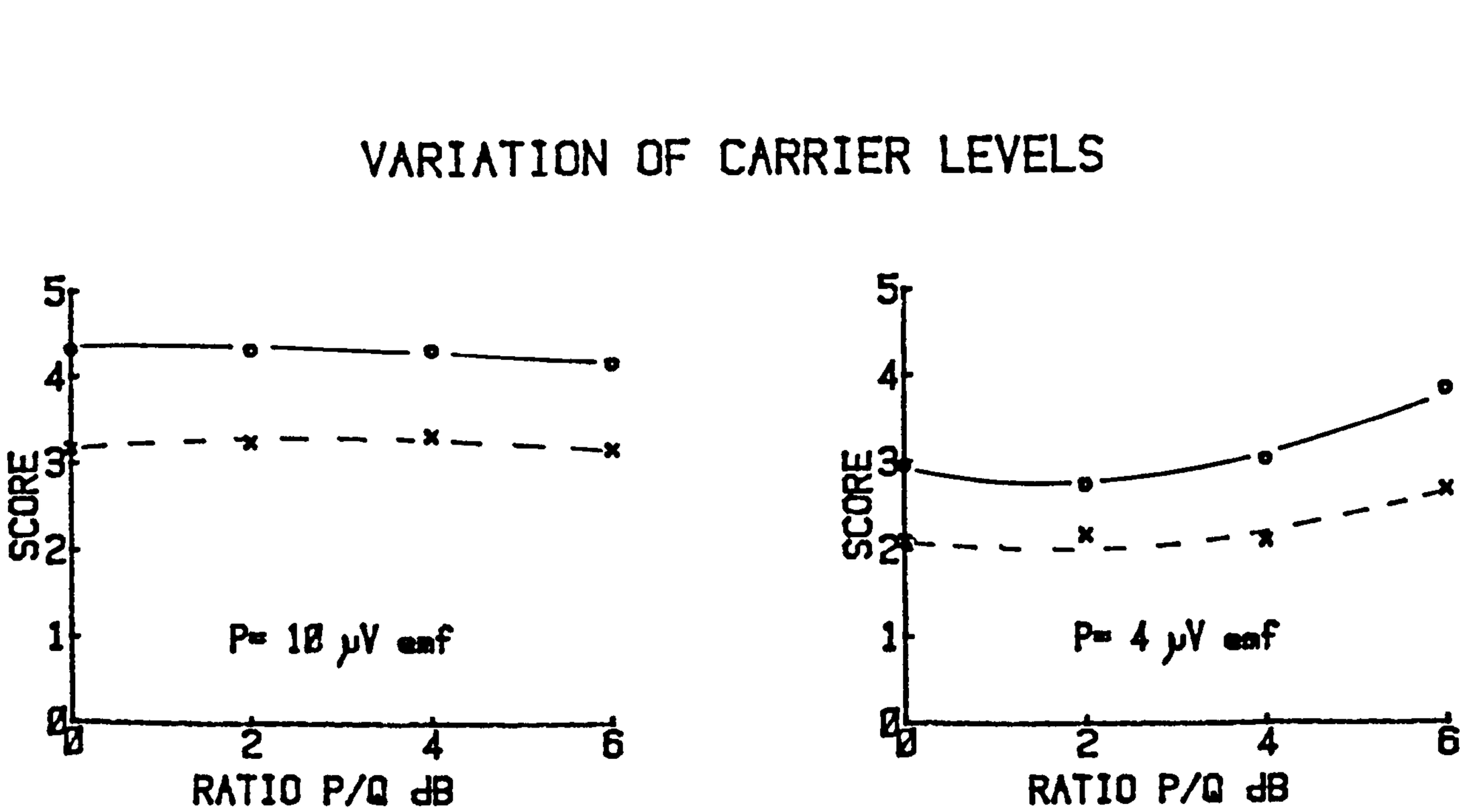

Fig. 7.8.1 Results of the Laboratry Bench AssessmentsI

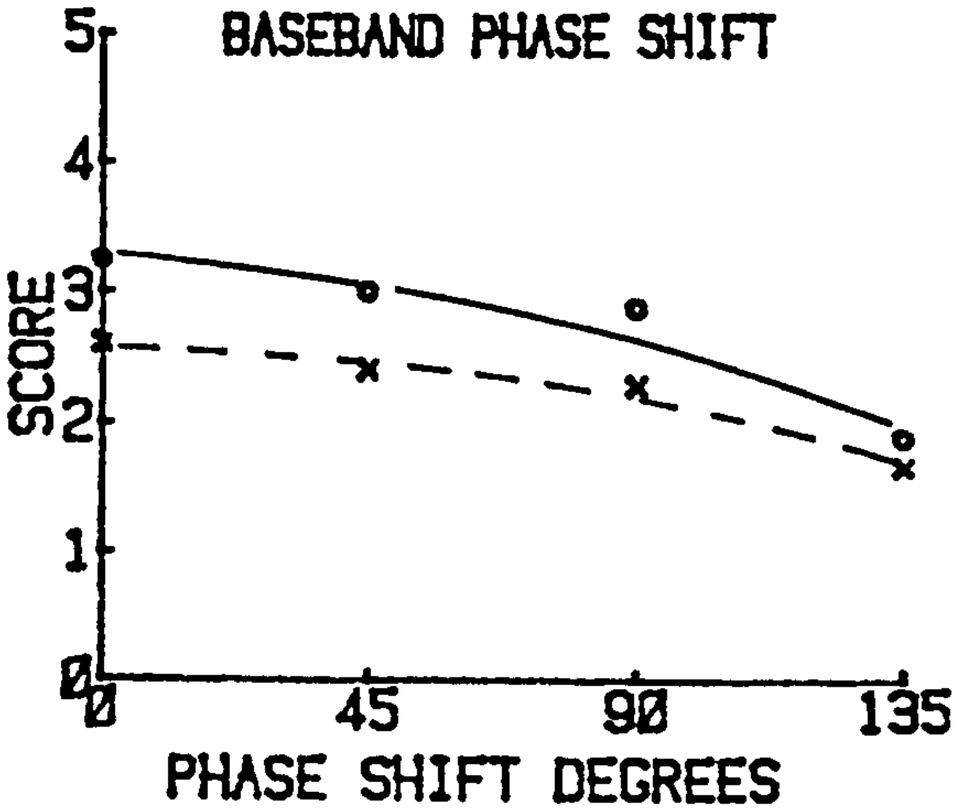

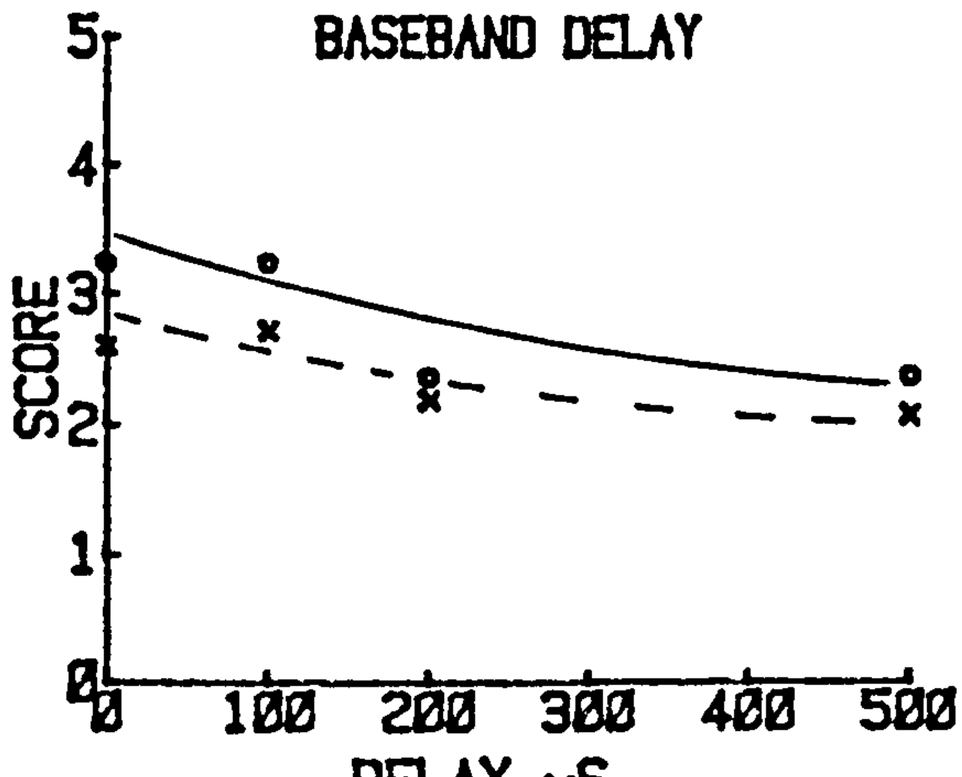

Solid line readability score, dashed line impairment score.

PHASE SHIFT AND DELAY COMBINED

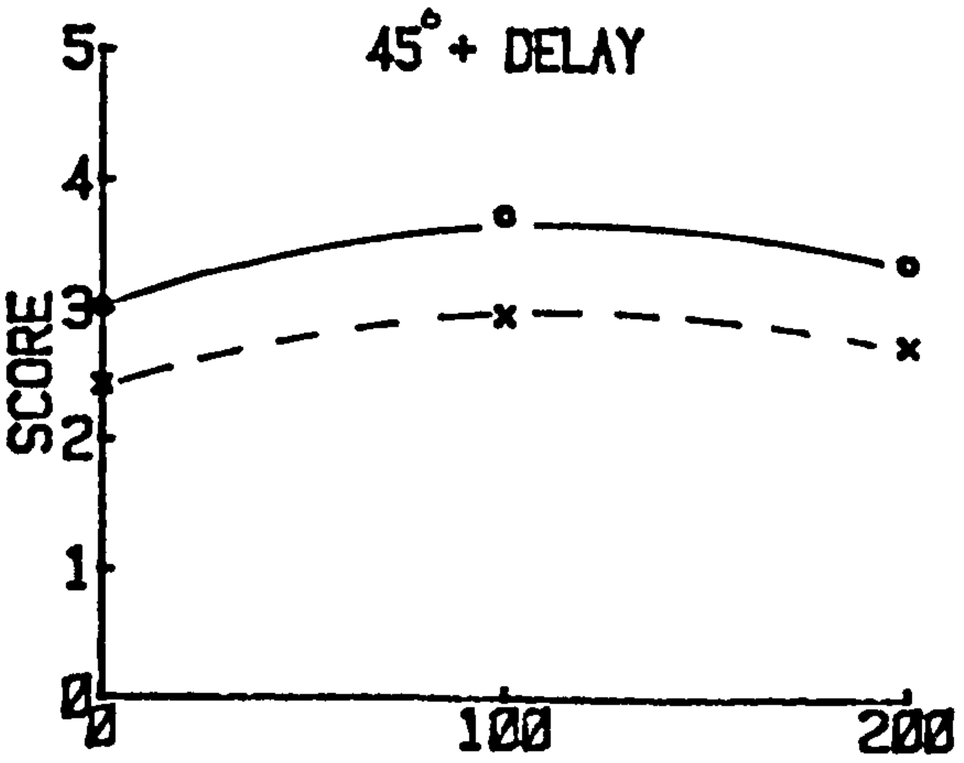

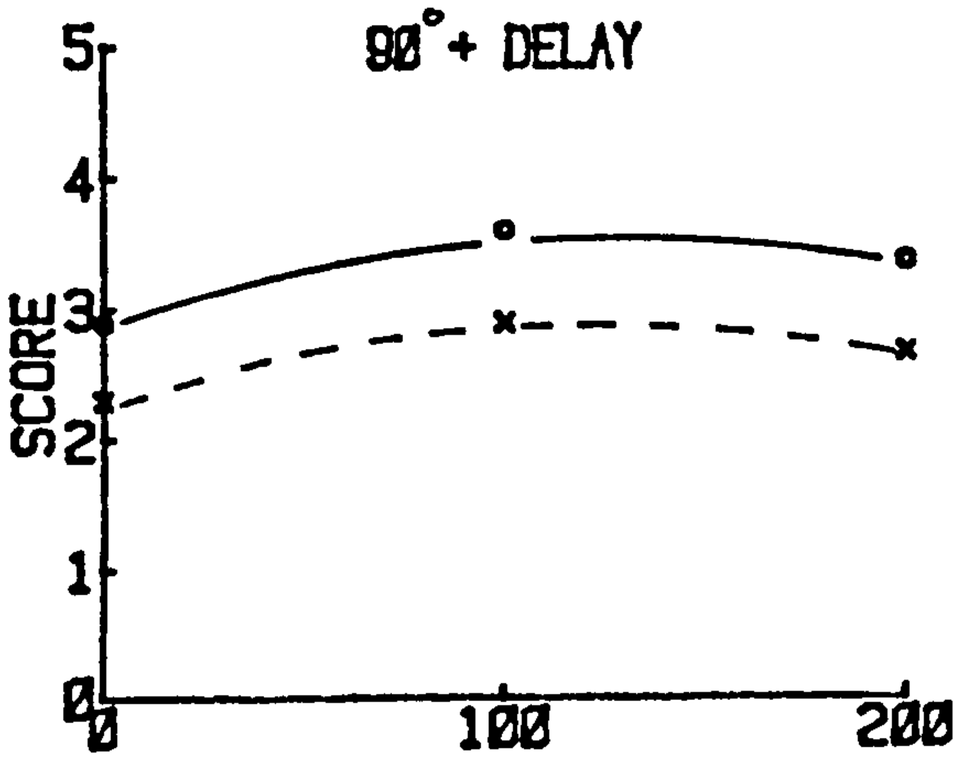

CARRIER OFFSET 4 Hz

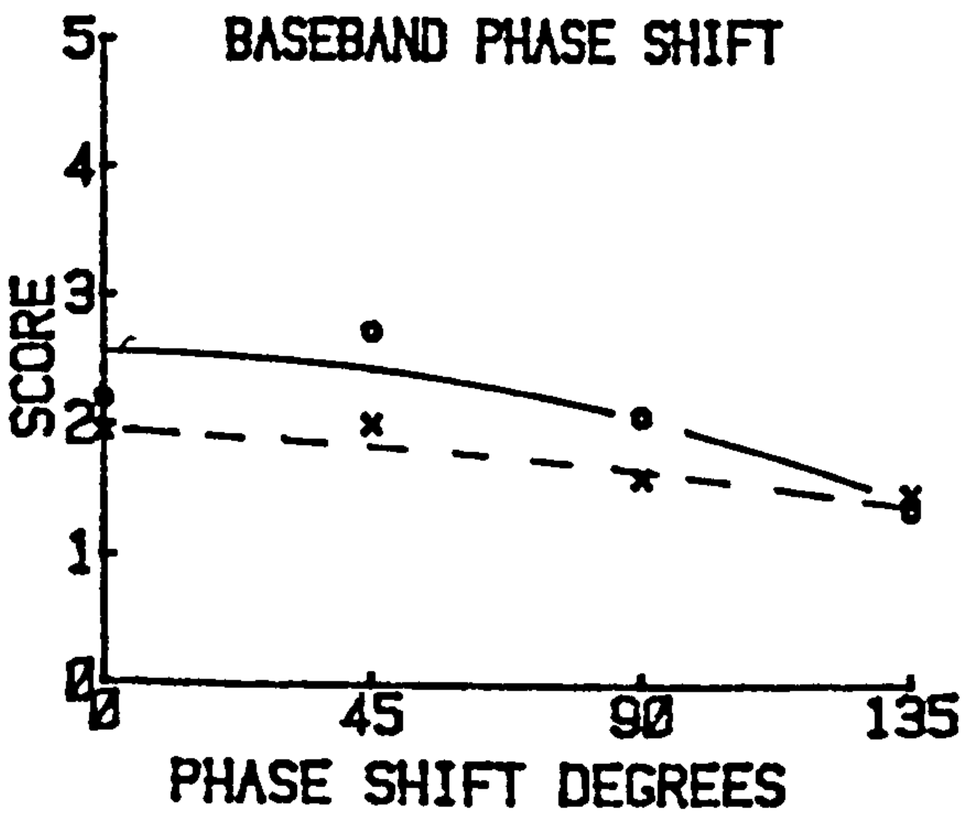

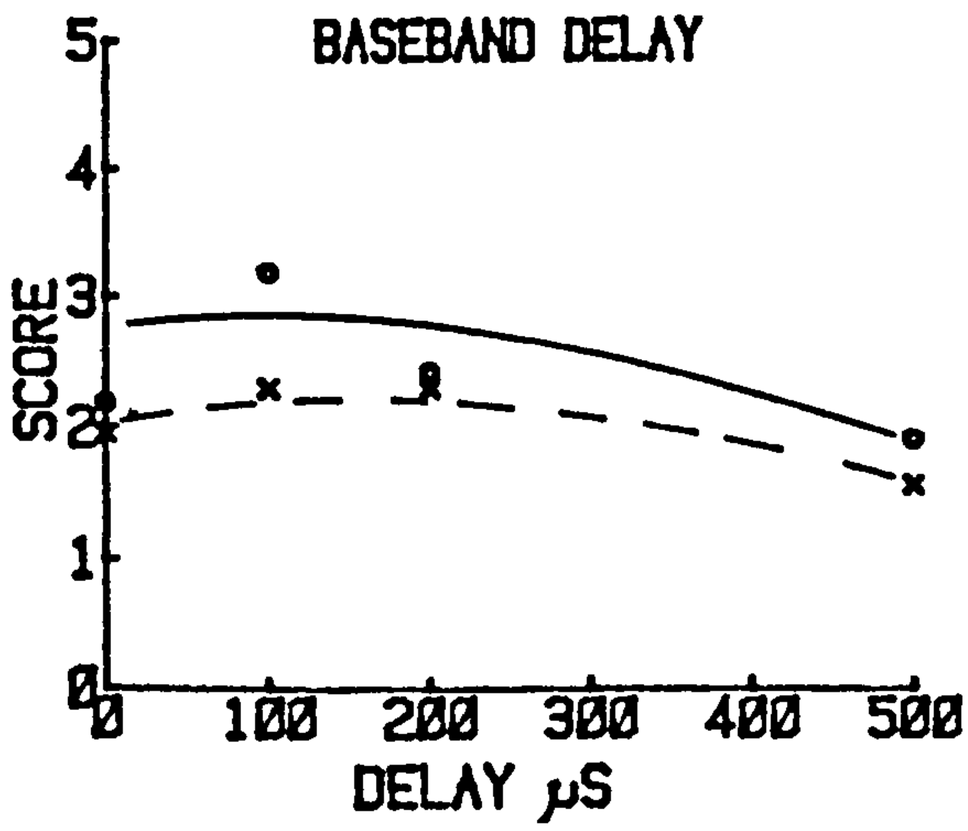

Fig. 7.8.2 Results of the Laboratory Bench Assessments II

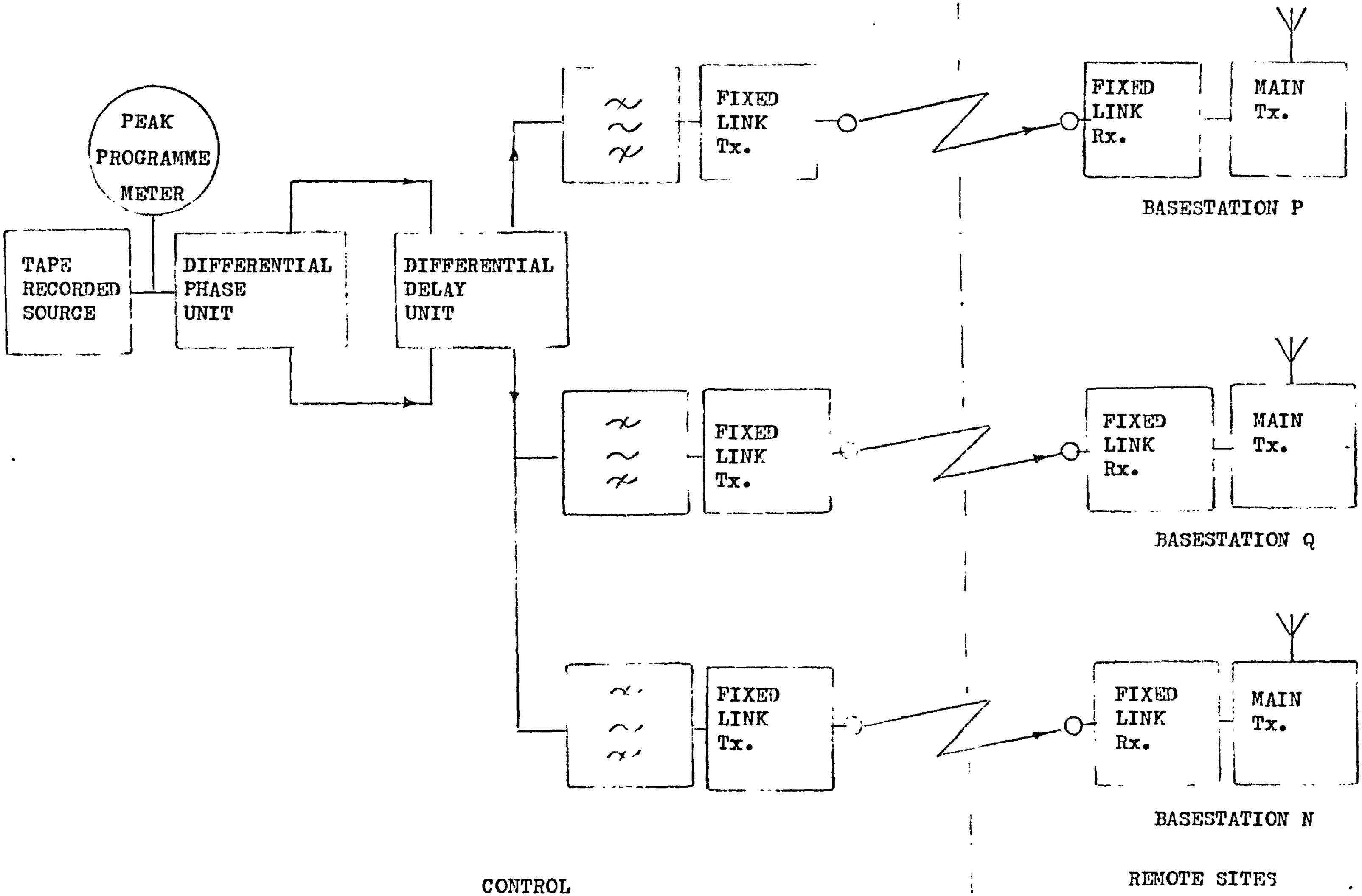

Fig. 7.8.3 Equipment Arrangment for the Field Assessment

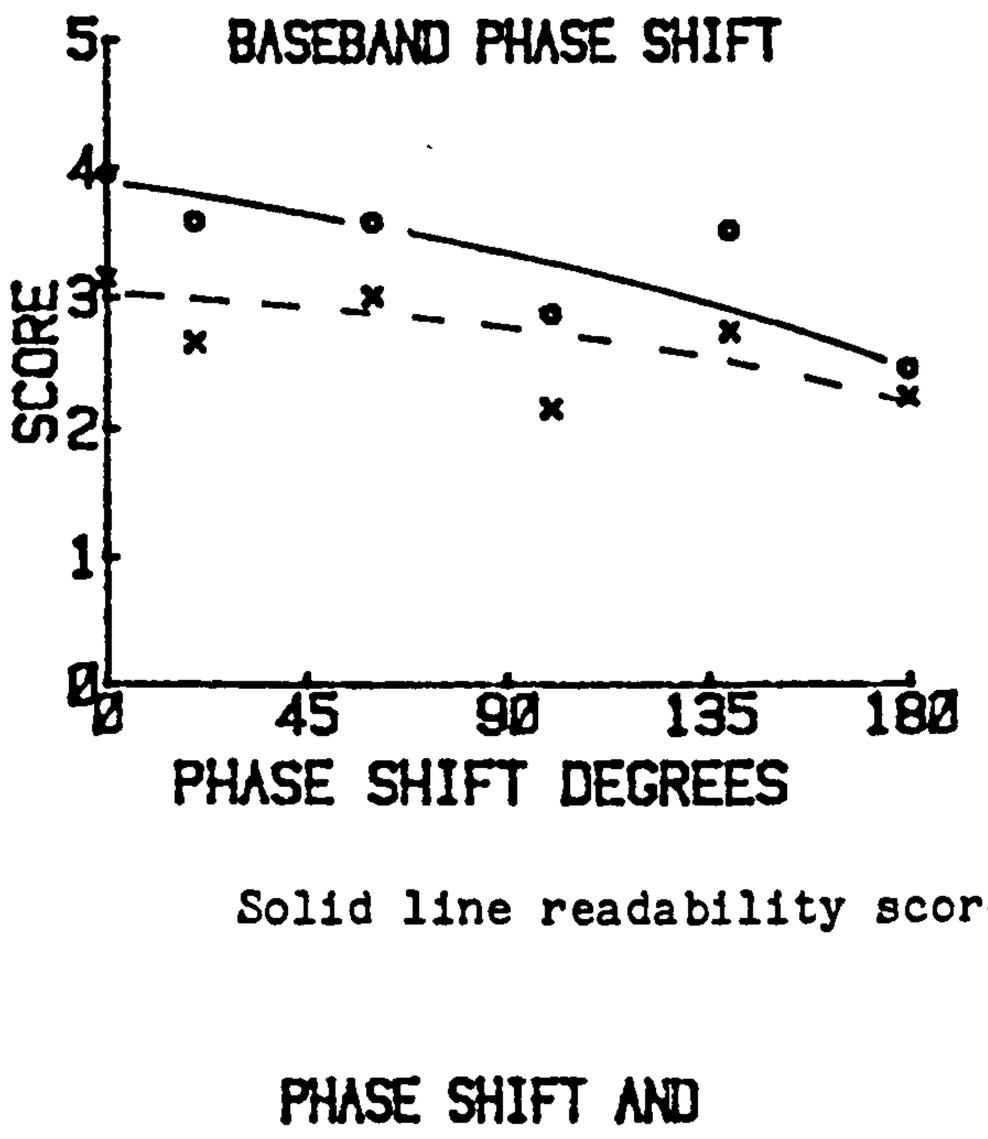

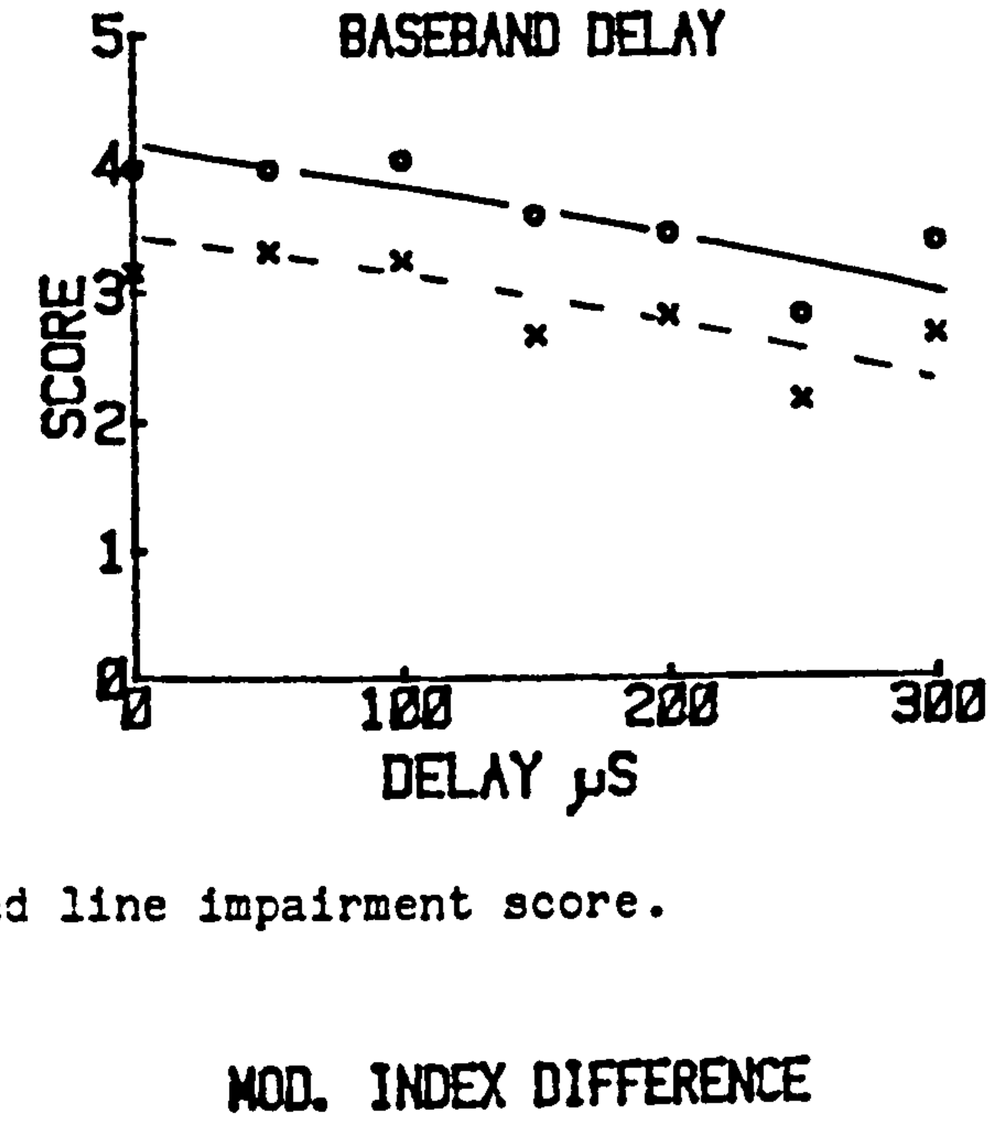

Solid line readability score, dashed line impairment score.

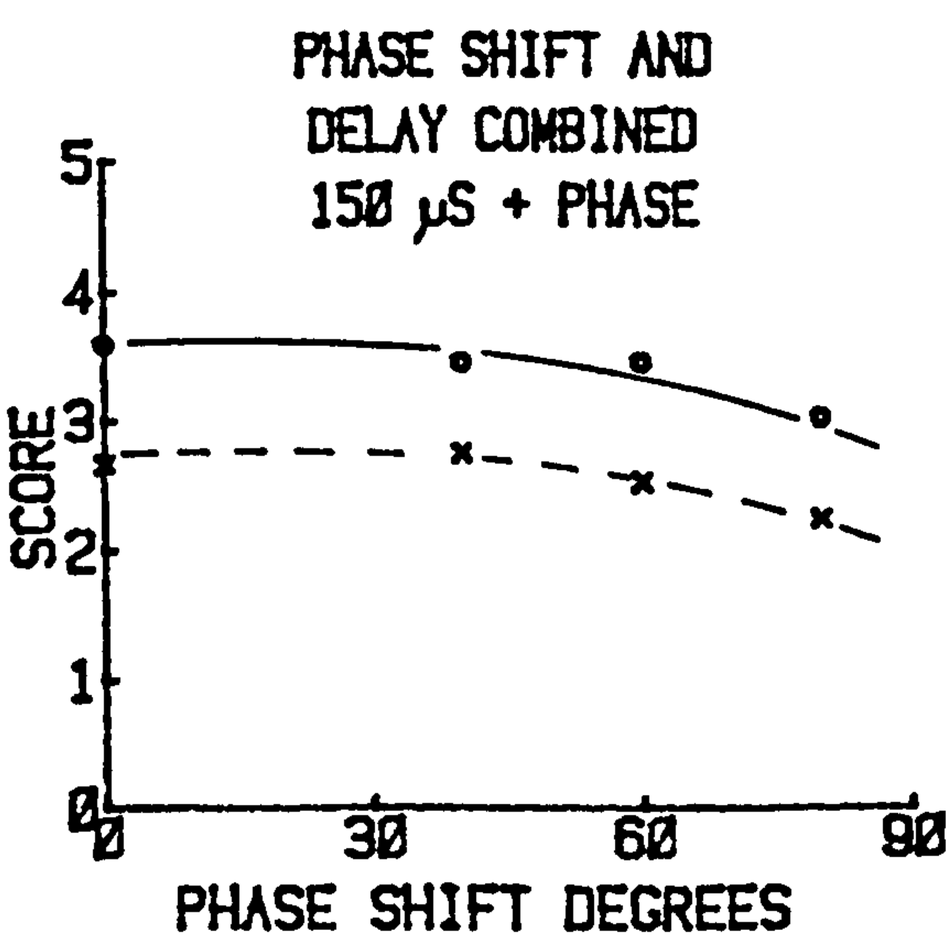

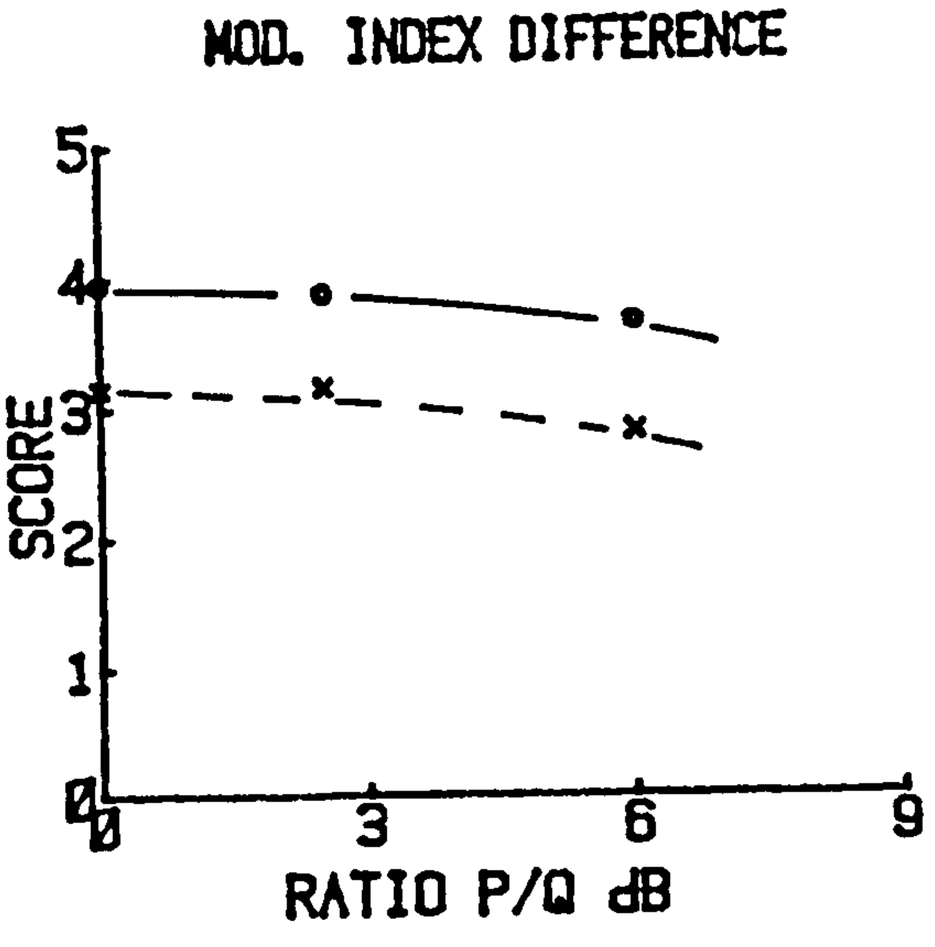

VARIATION OF CARRIER LEVELS

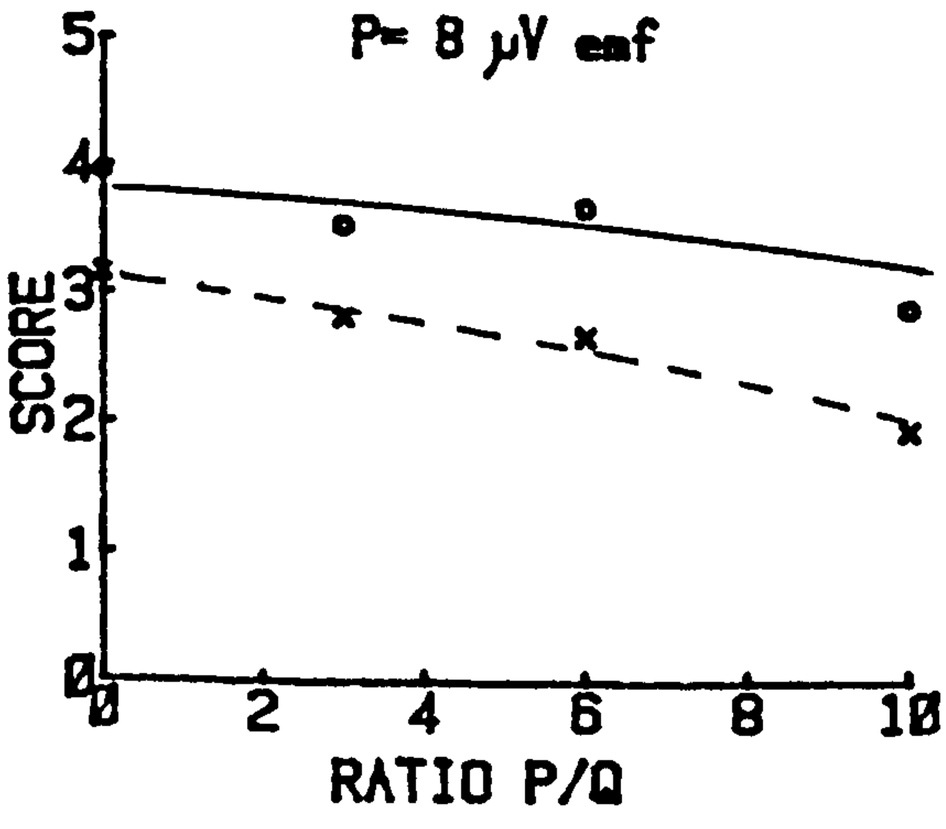

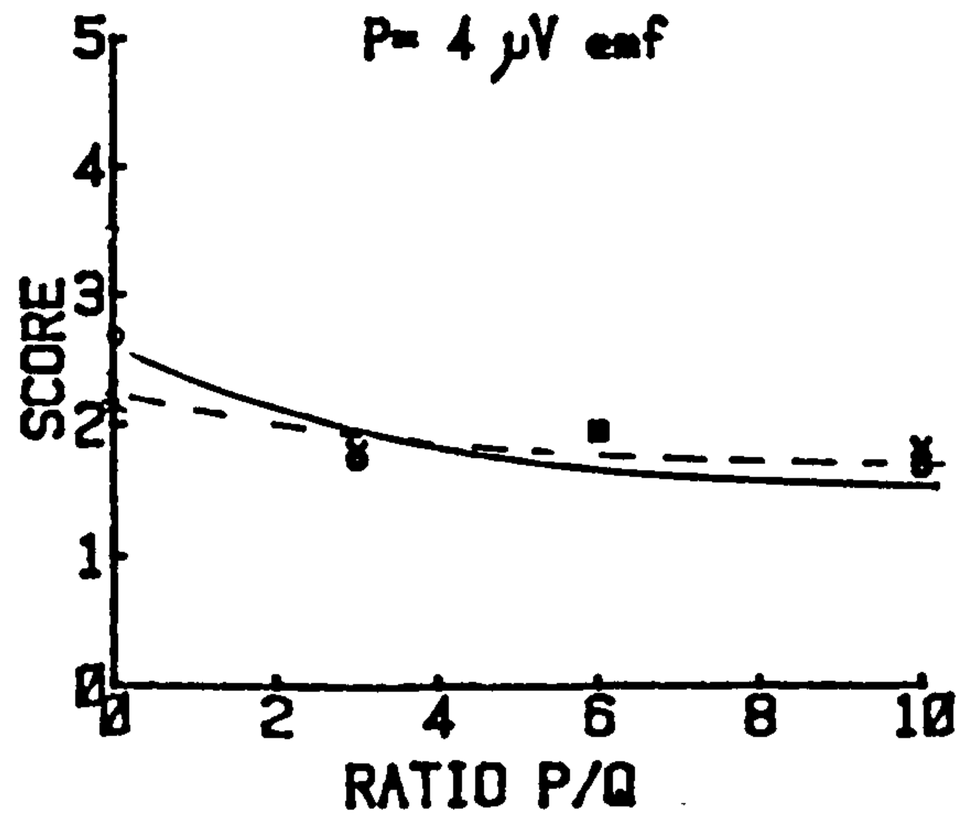

Fig. 7.8.4 Results of the Field Assessments

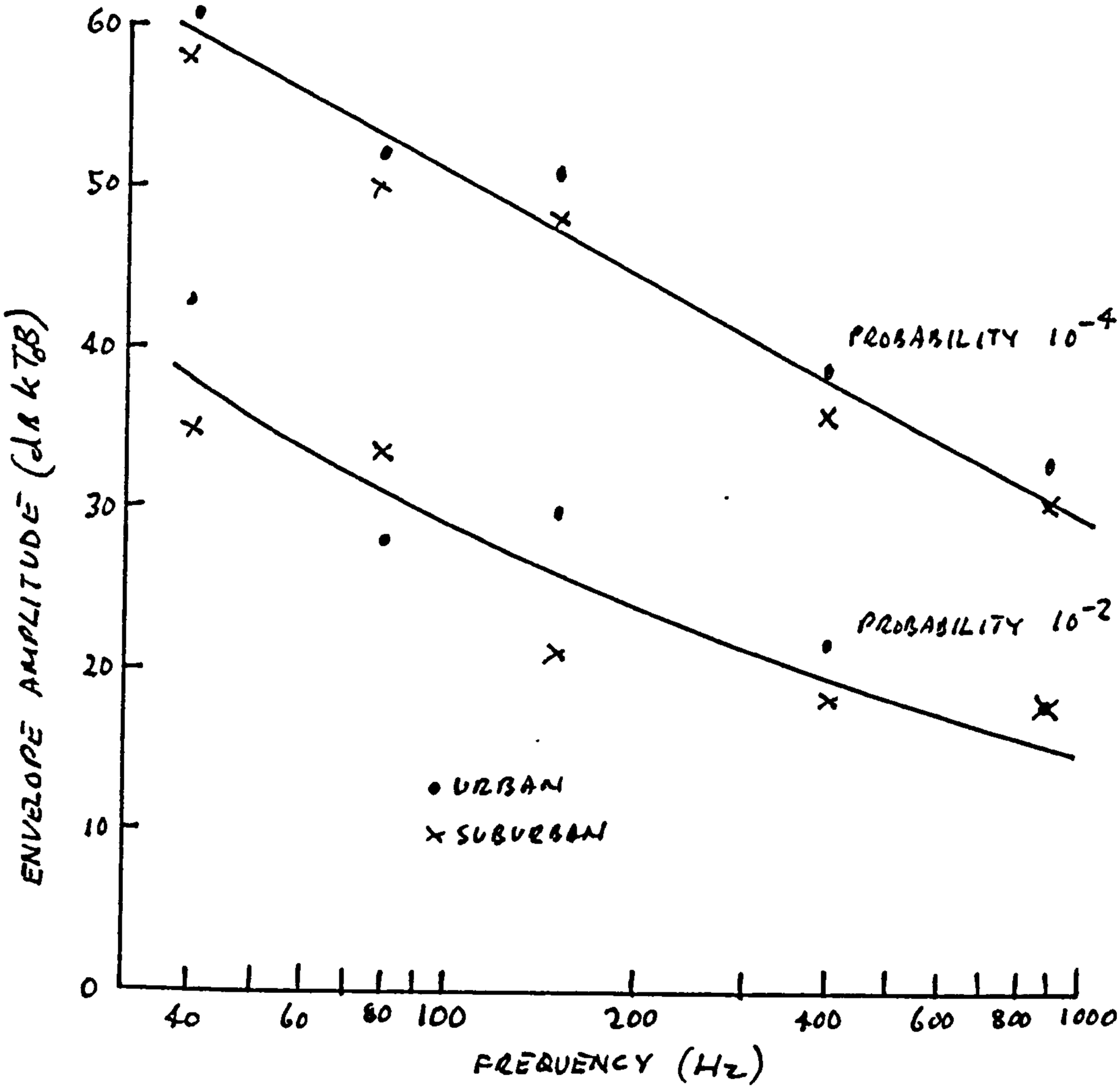

Fig. 8.2.1 Man-made Noise Level vs. Frequency

Fig. 8.2.2 Sporadic E Effects - Durations

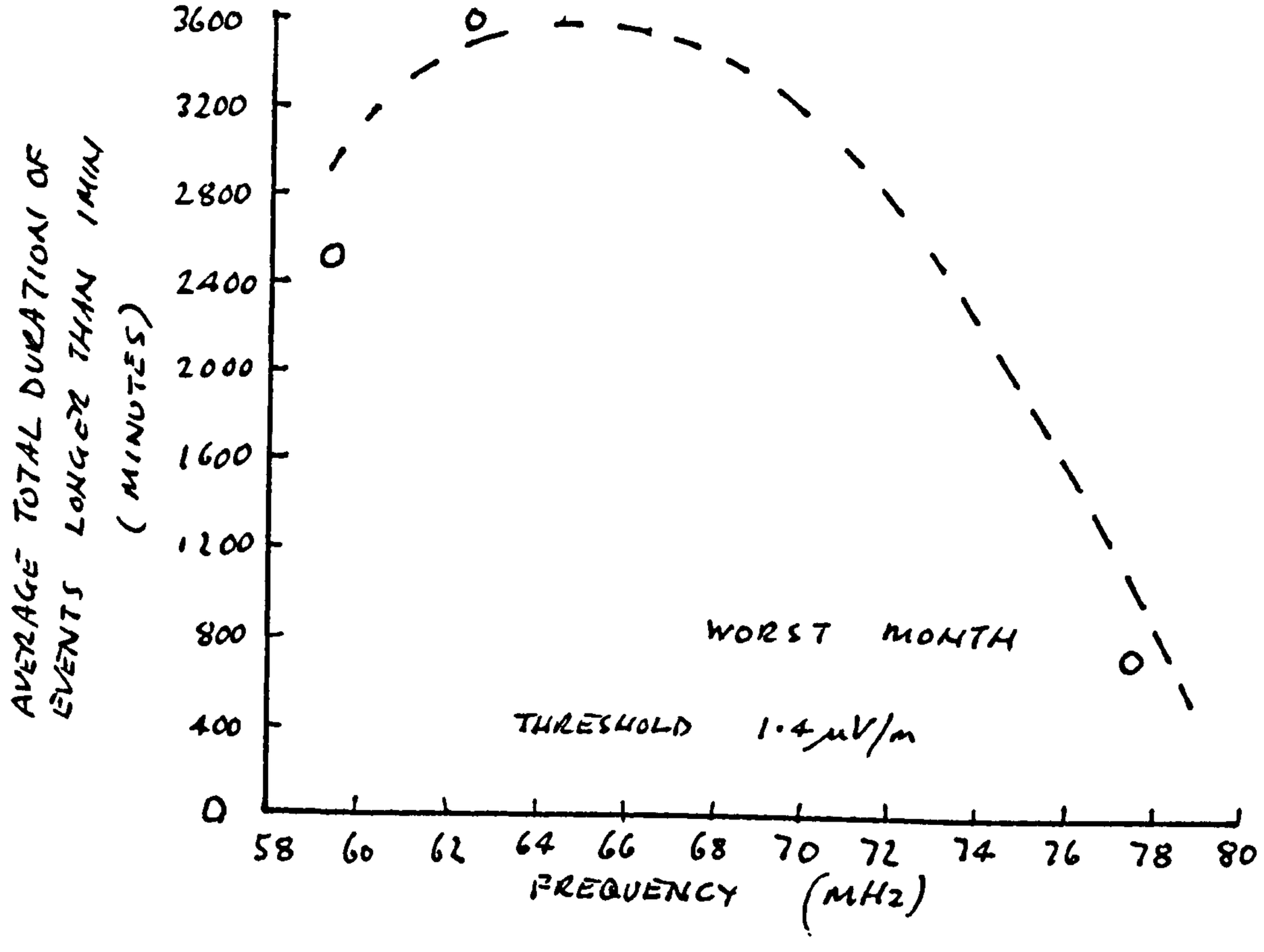

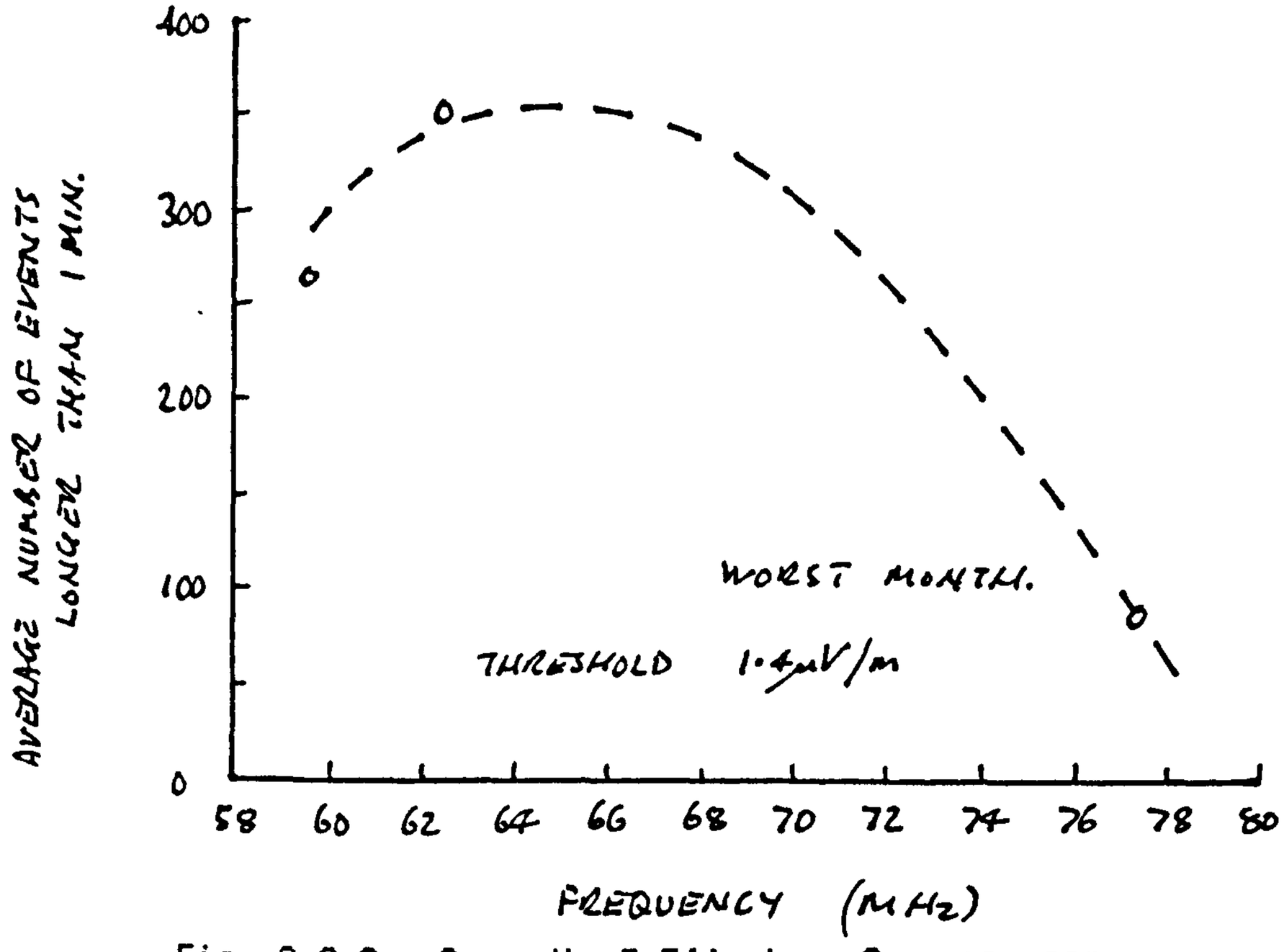

Fig. 8.2.3 Sporadic E Effects - Occurrrences

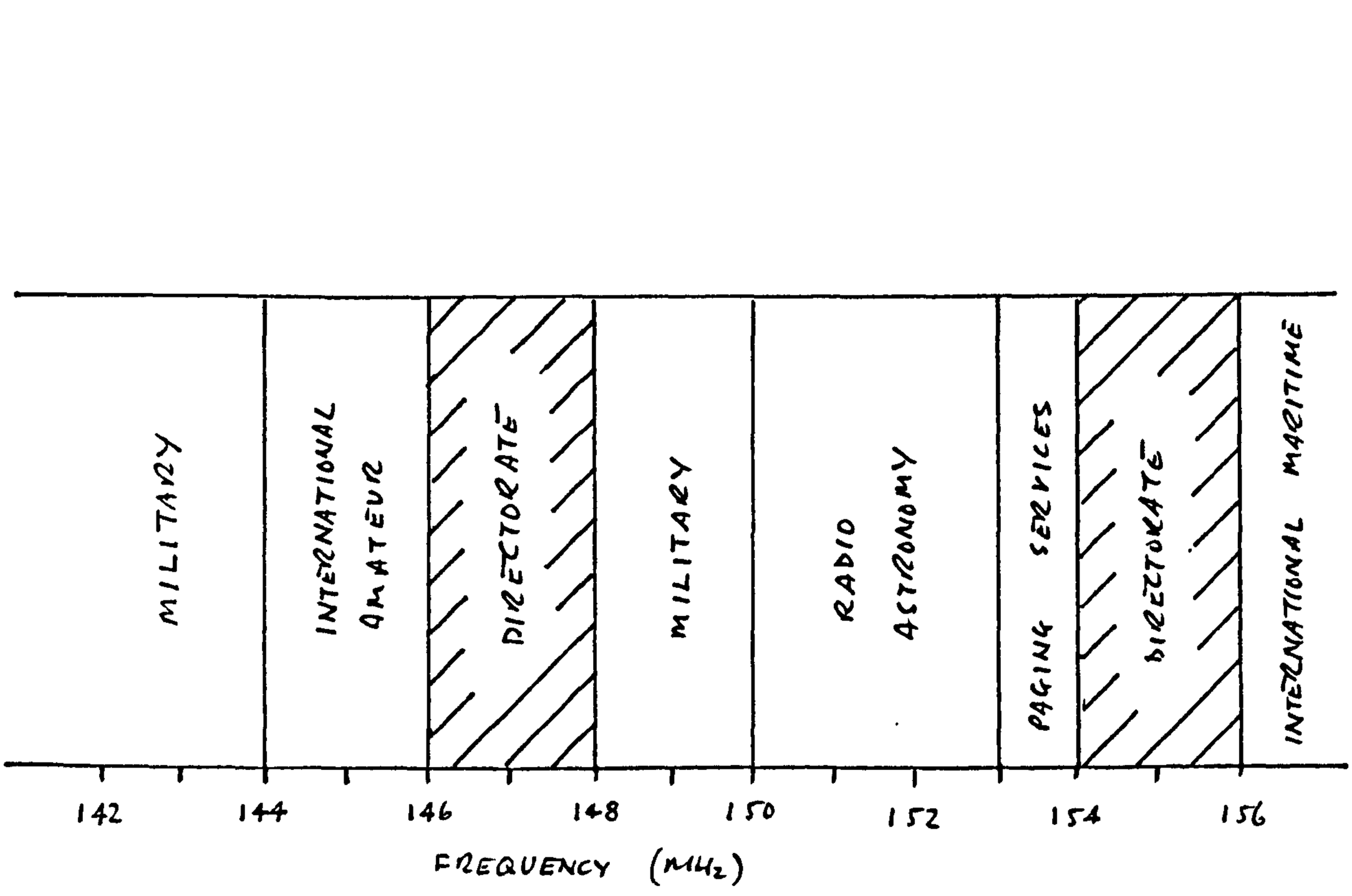

Fig. 8.4.1 UK Users of VHF Mid-band Spectrum

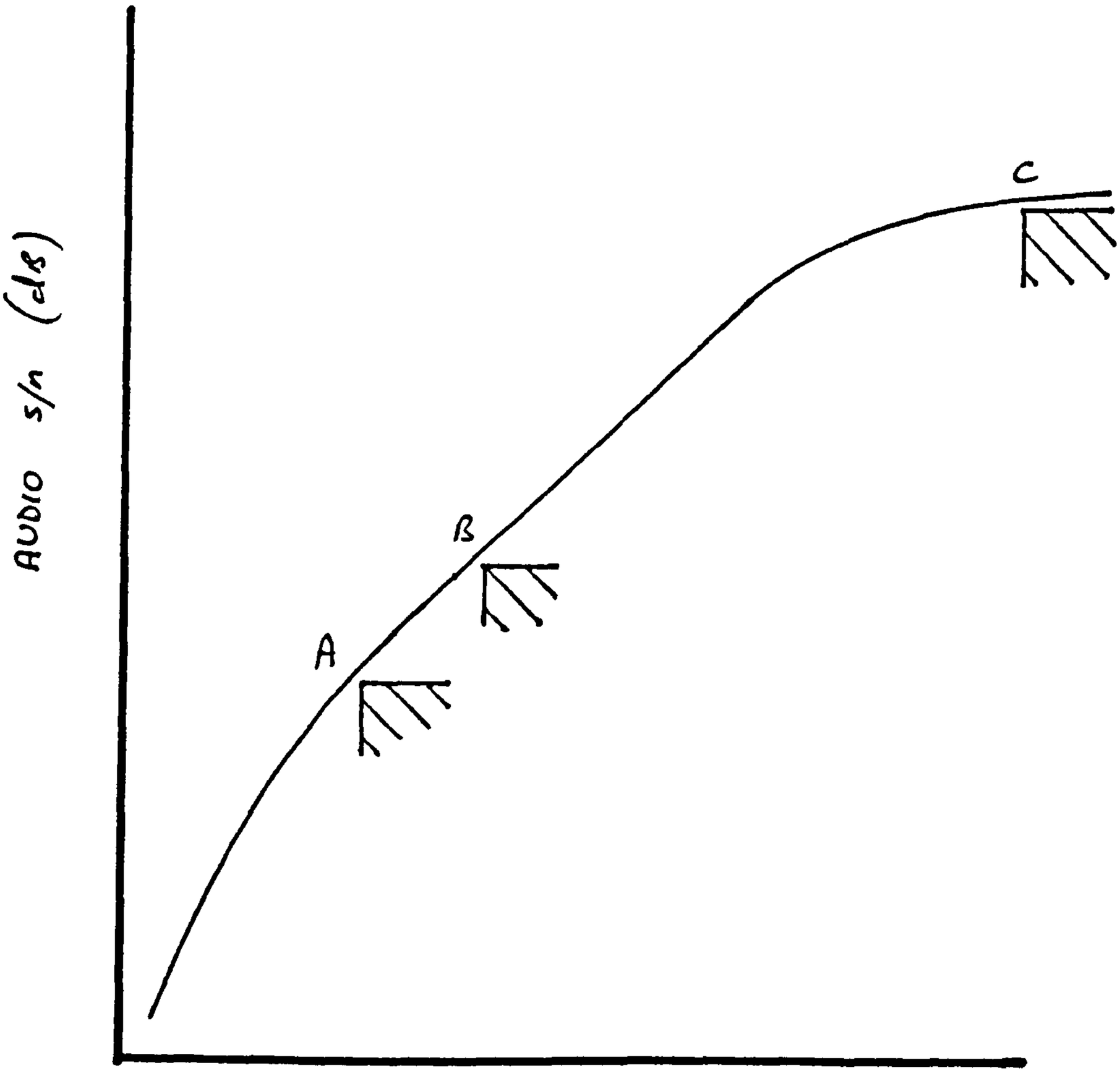

Fig. 9.4.1 SINAD Performance Secification Points

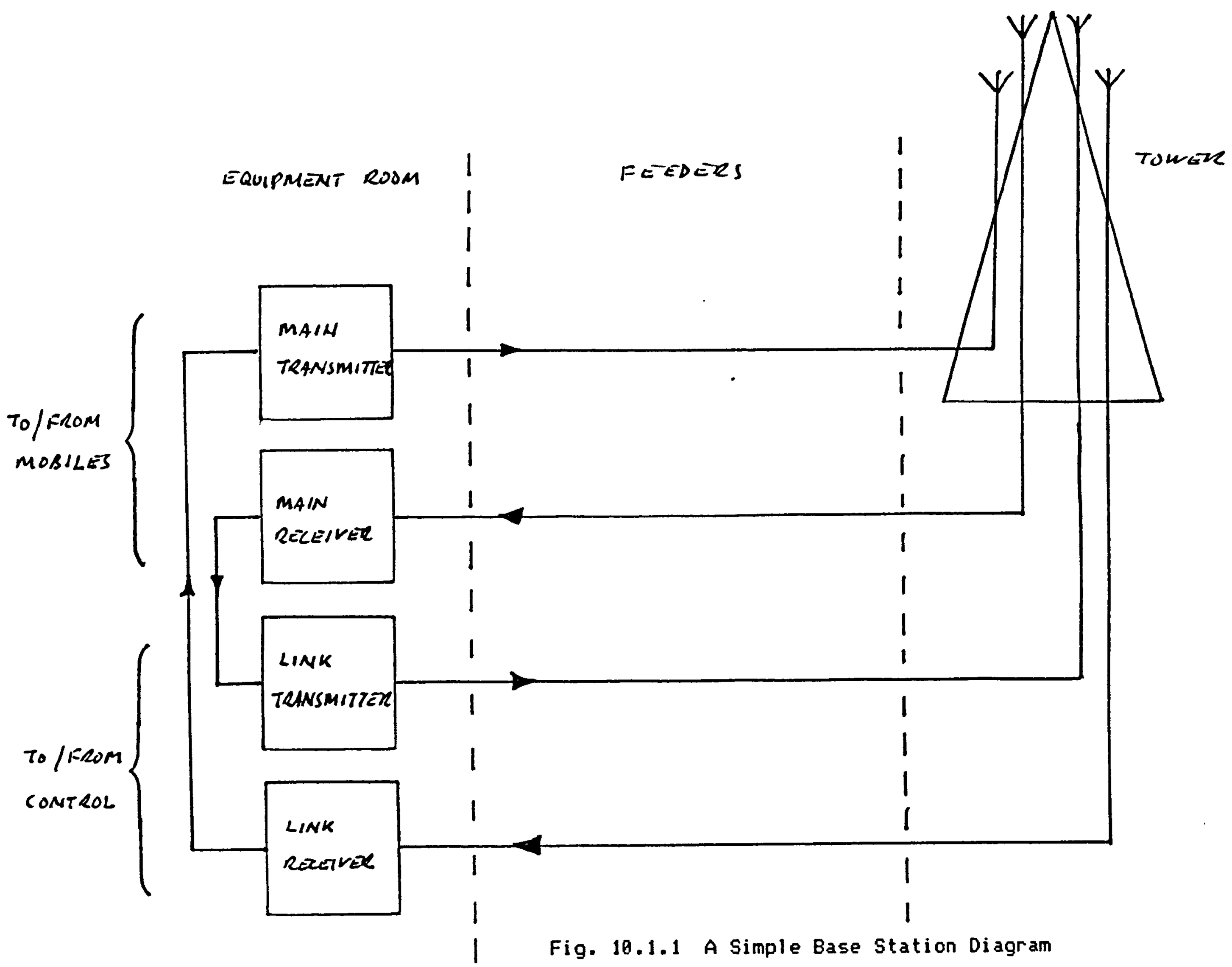

Fig. 10.1.1 A Simple Base Station Diagram

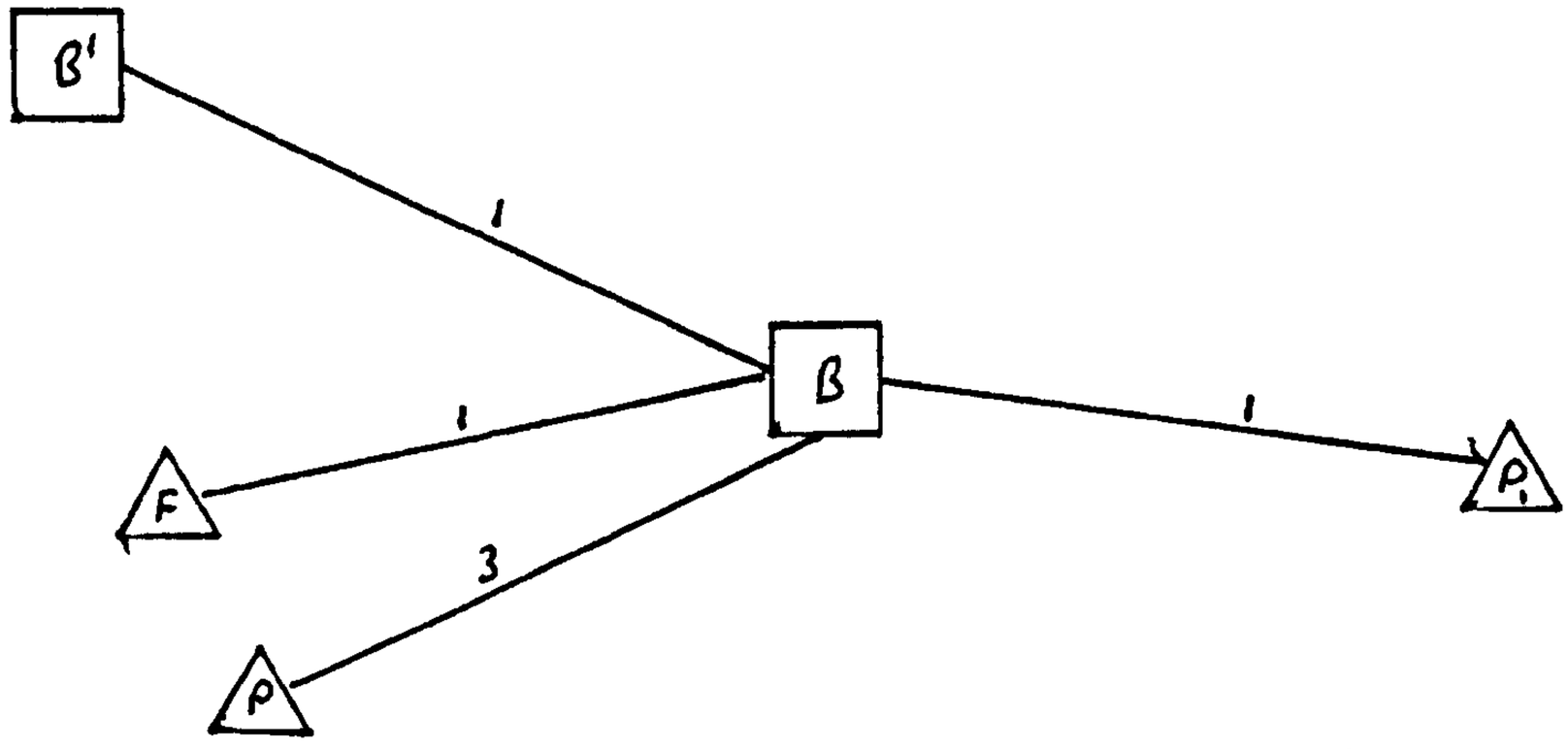

Fig. 10.1.2 Base Station Fixed Links

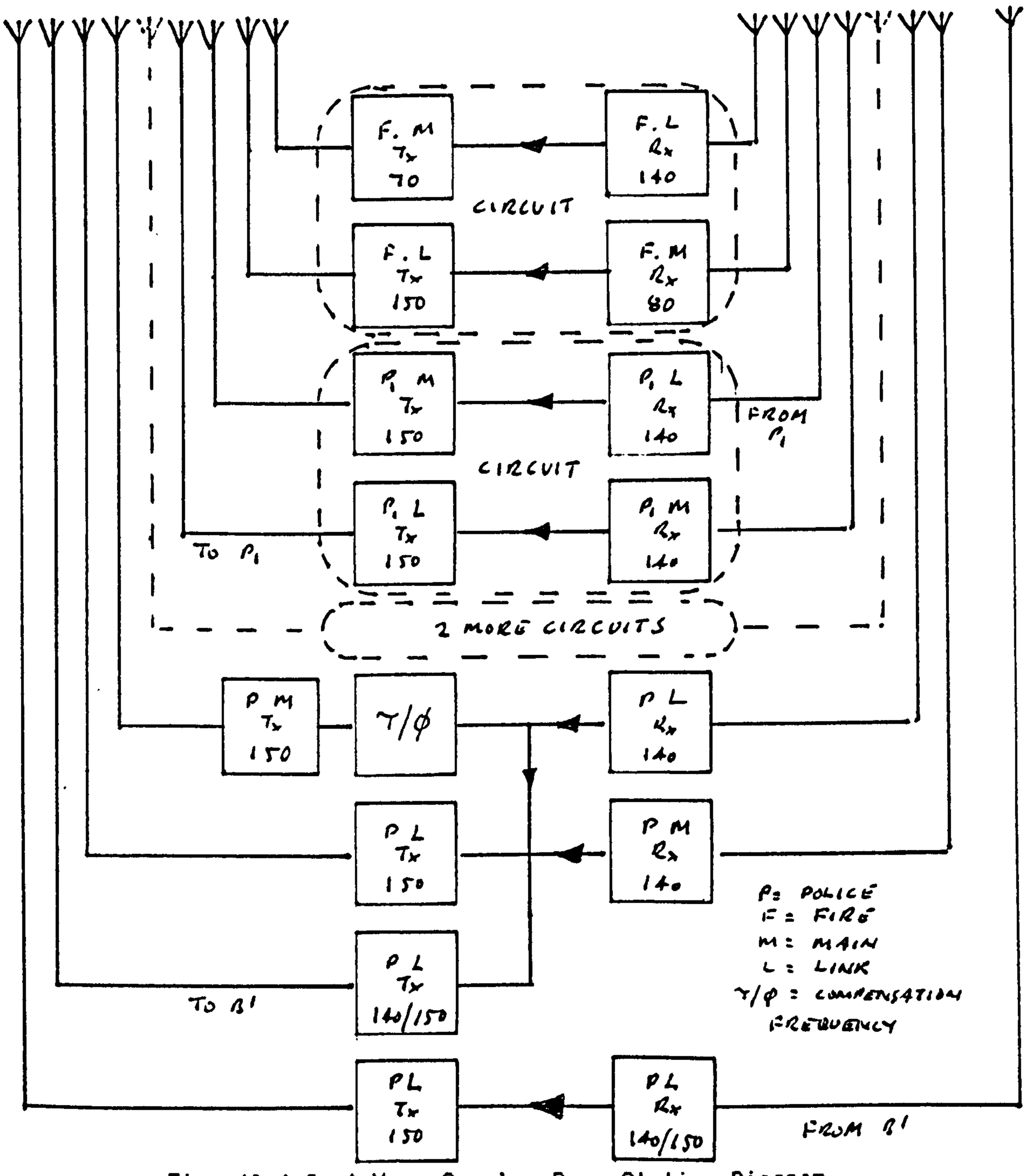

Fig. 10.1.3 A More Complex Base Station Diagram

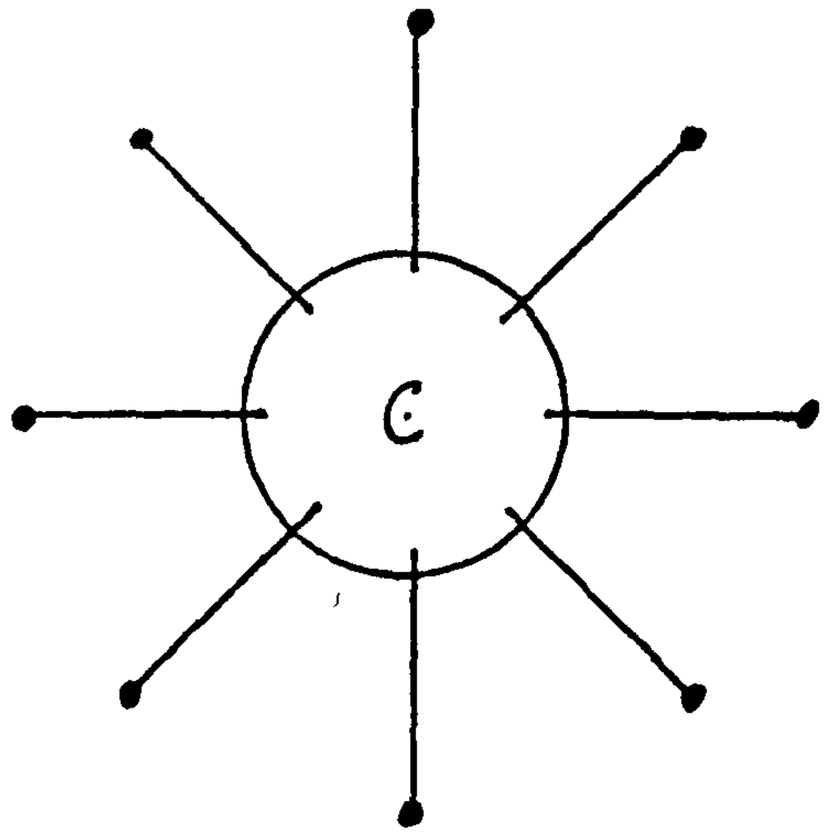

Fig. 10.2.1 Plan View of Aerial Elements and Combiner

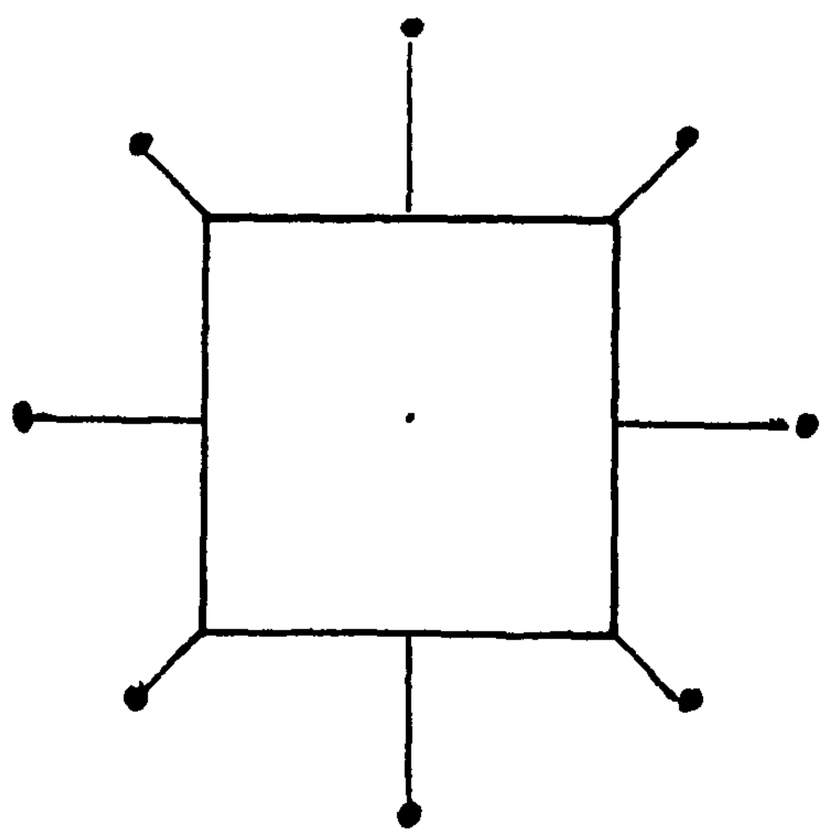

Fig. 10.2.2 Plan View Representing Eight Dipoles around a Square Tower

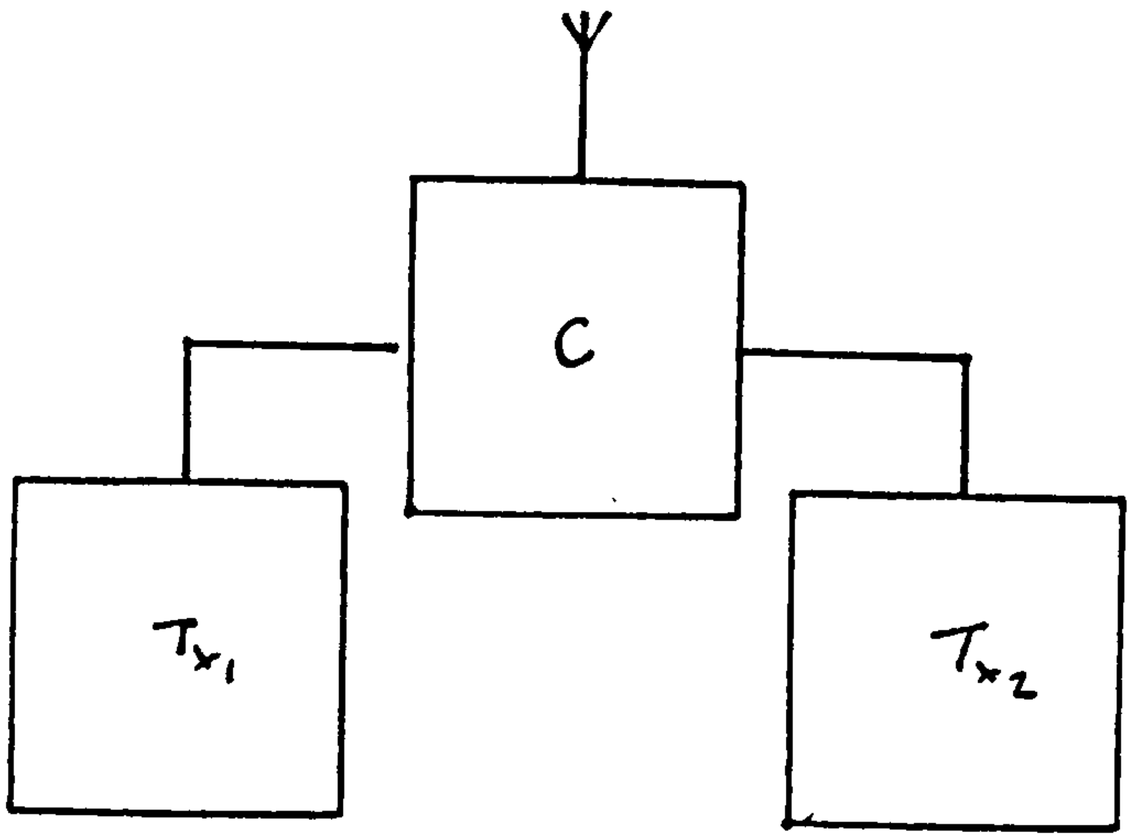

Fig. 10.3.1 Simple Combiner

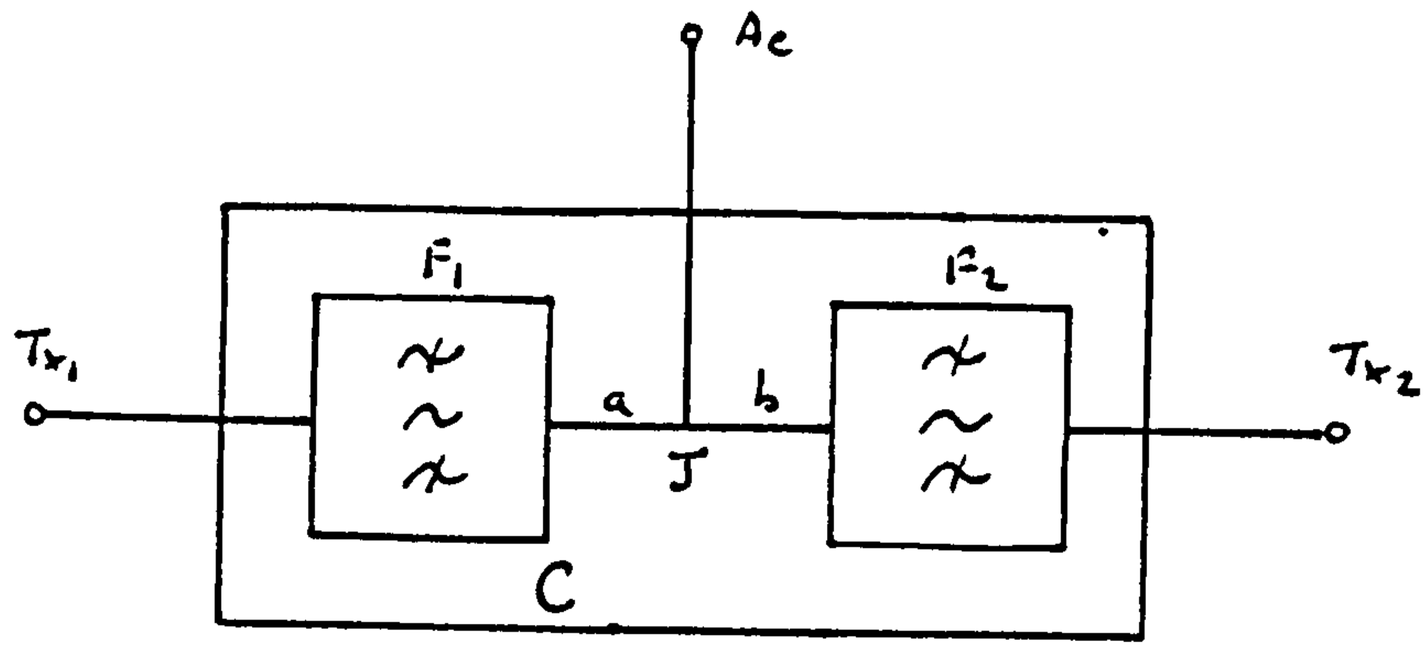

Fig. 10.3.2 Details of Filter Combiner

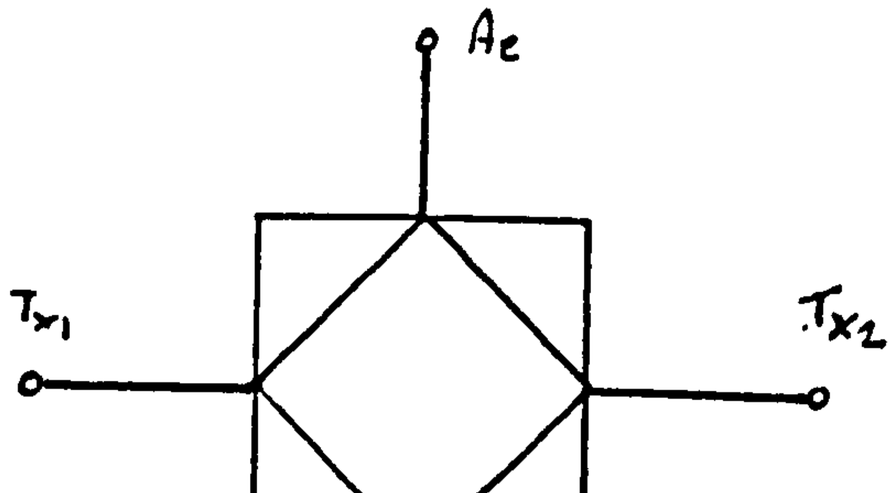

Fig. 10.3.3 Hybrid as a Combiner

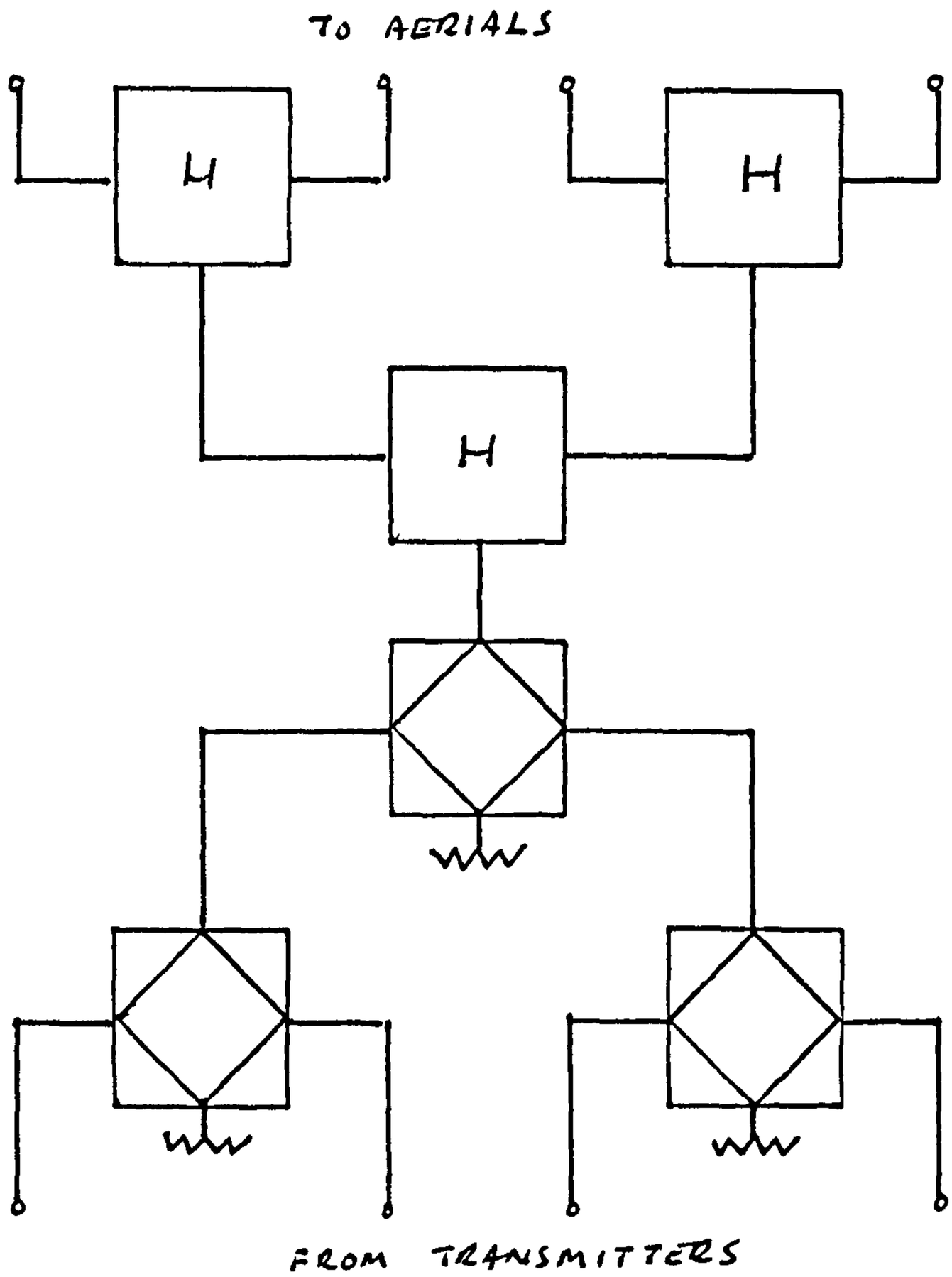

Fig. 10.3.4 Complex Combiner

Fig. 10.3.5 Butler Matrix Combiner

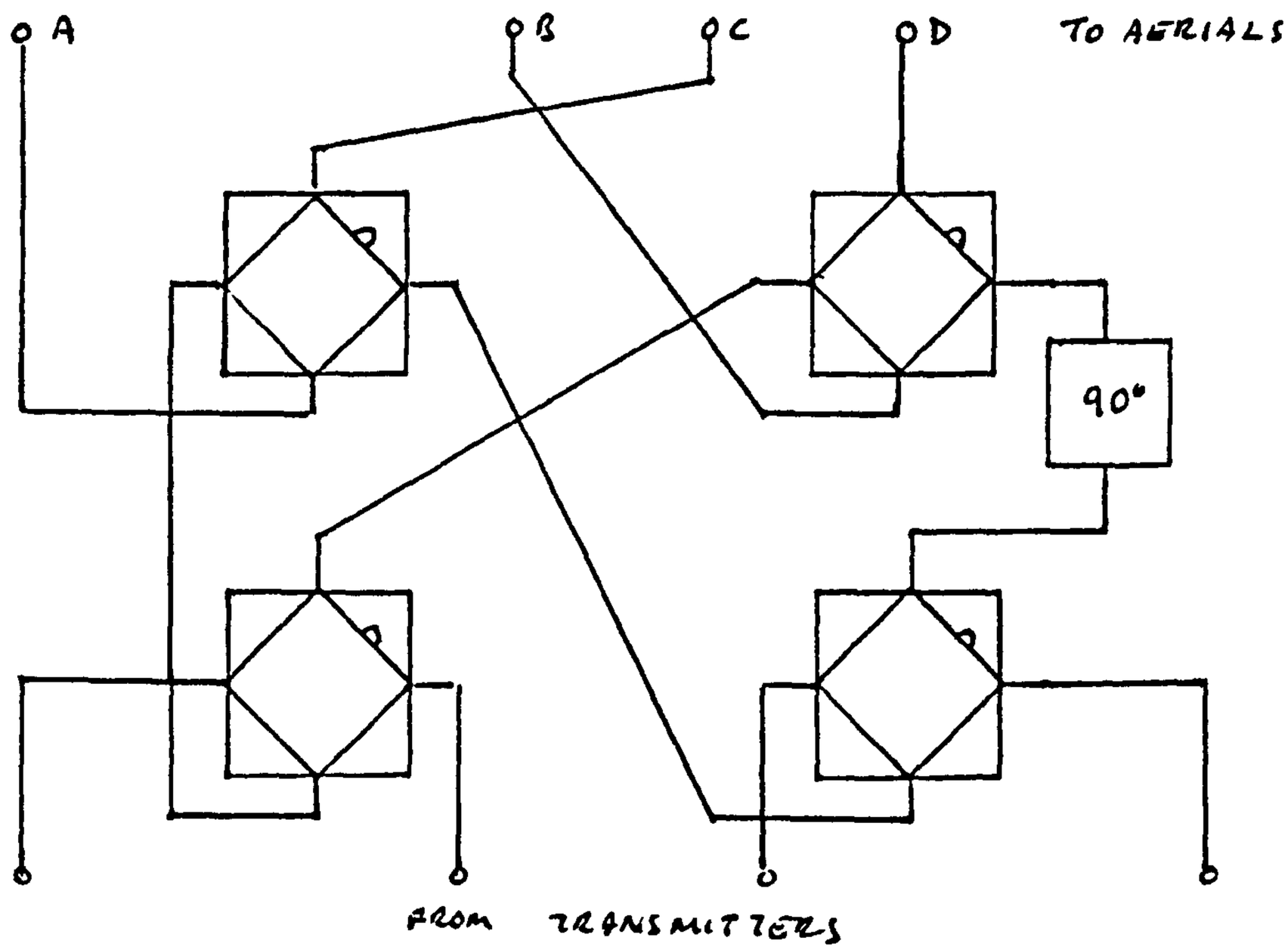

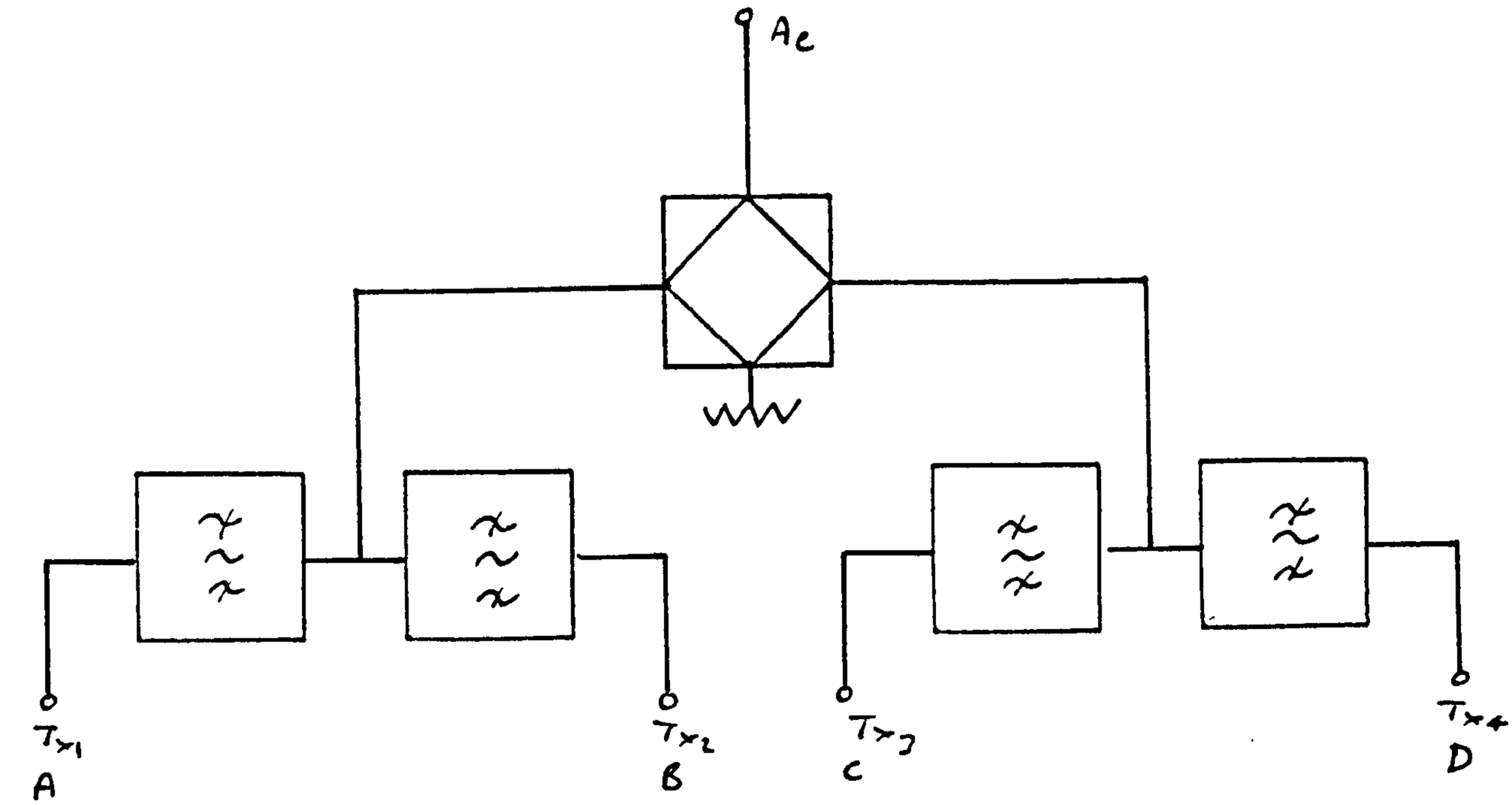

Fig. 10.3.6 Combination of Simple Techniques

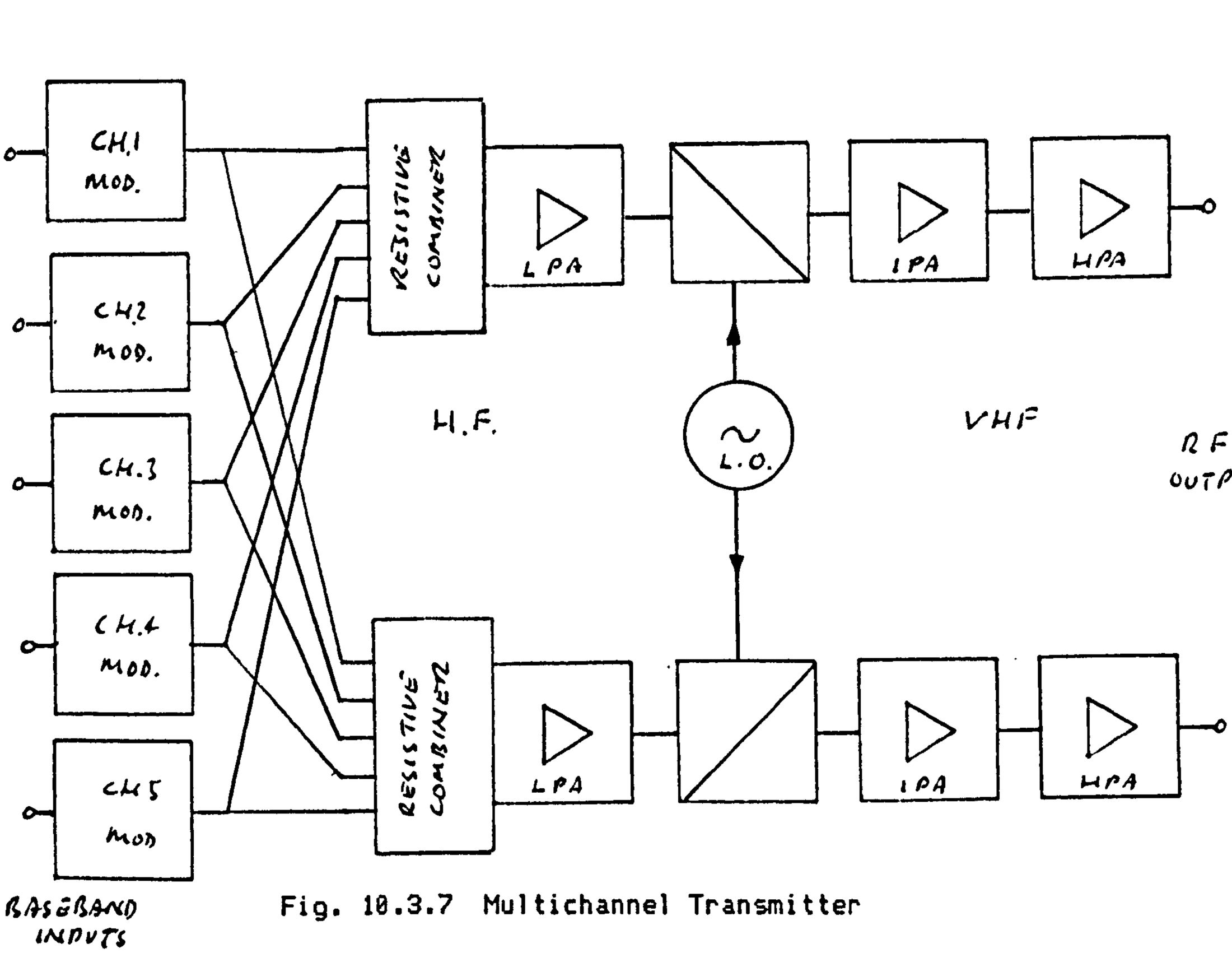

Fig. 10.3.7 Multichannel Transmitter

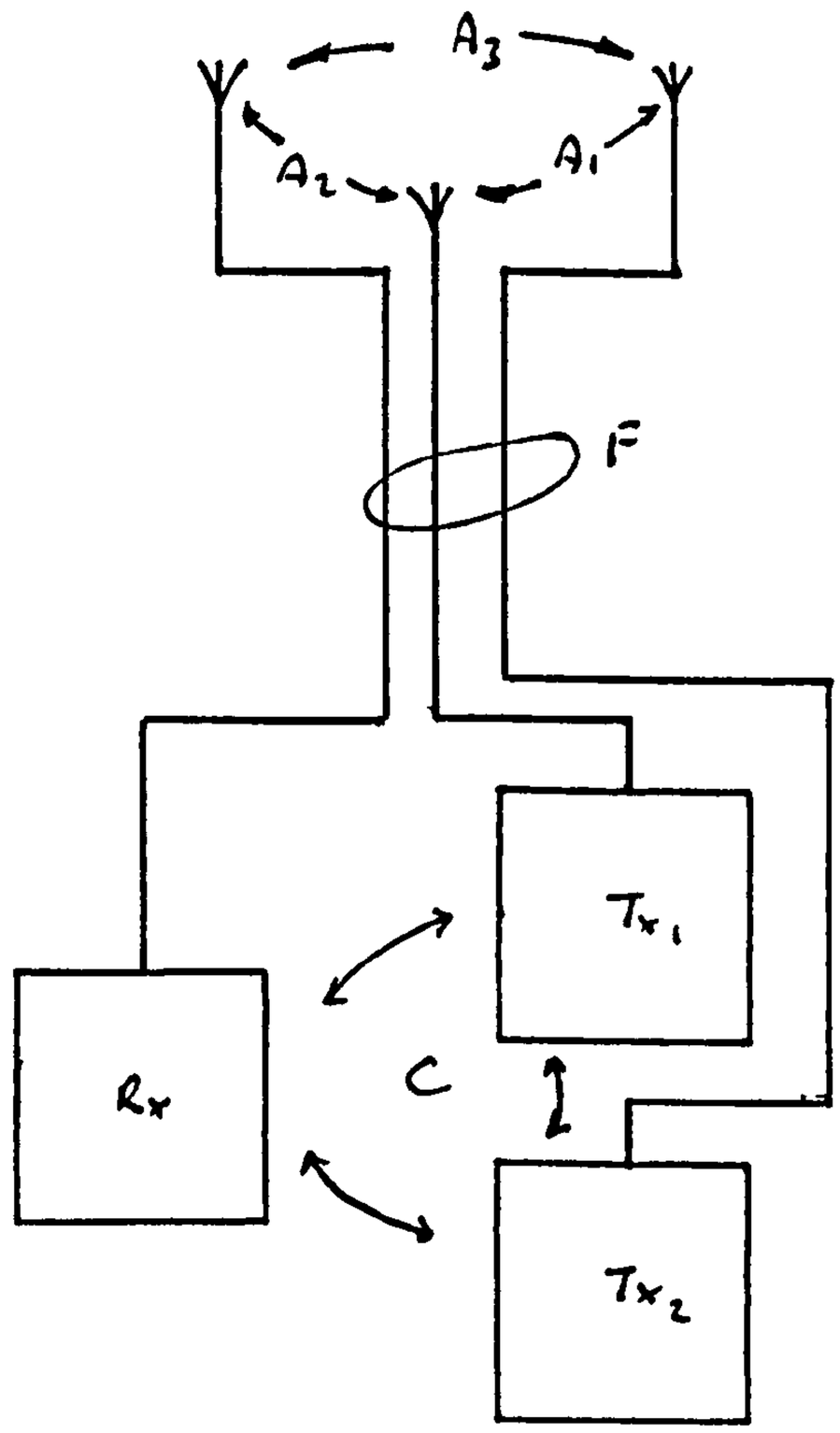

Fig. 10.5.1 Coupling Mechanisms for Generation of Intermods by Active Devices

Fig. 10.5.2 Conversion Loss of Valve Transmitter (T55)

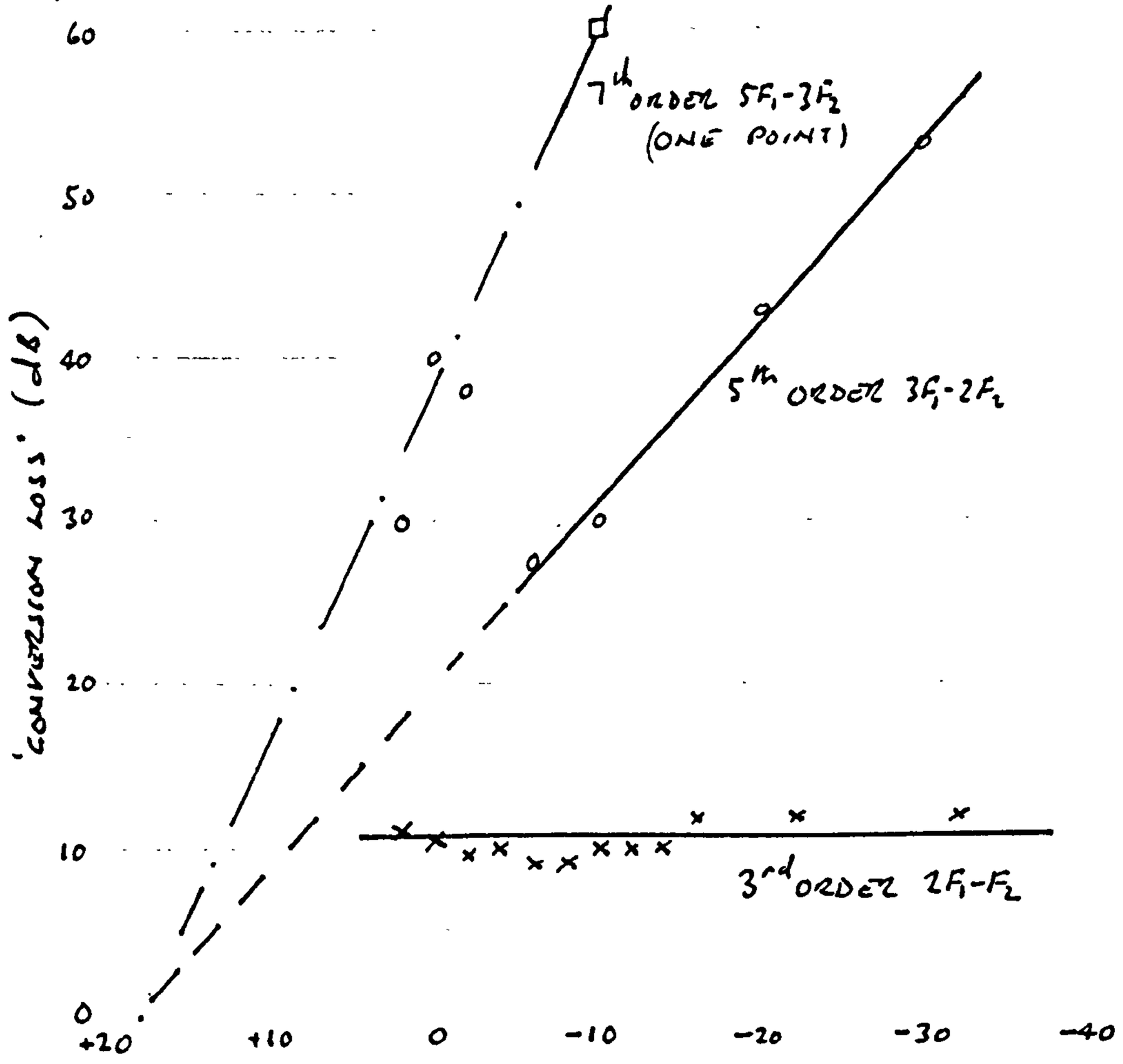

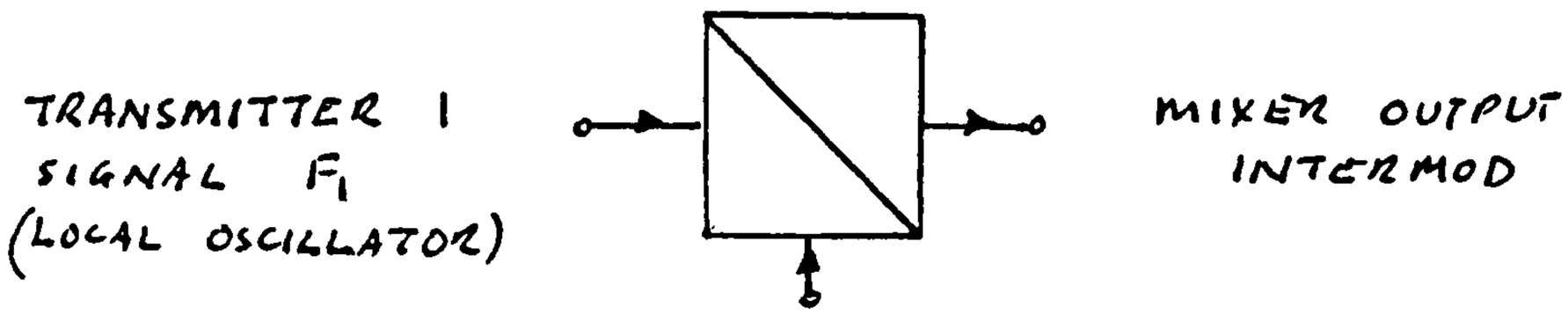

Fig. 10.5.3 Intermodulation Viewed as a Mixing Process

Fig. 10.5.4 Intermodulation Levels of Valve Transmitter (T55)

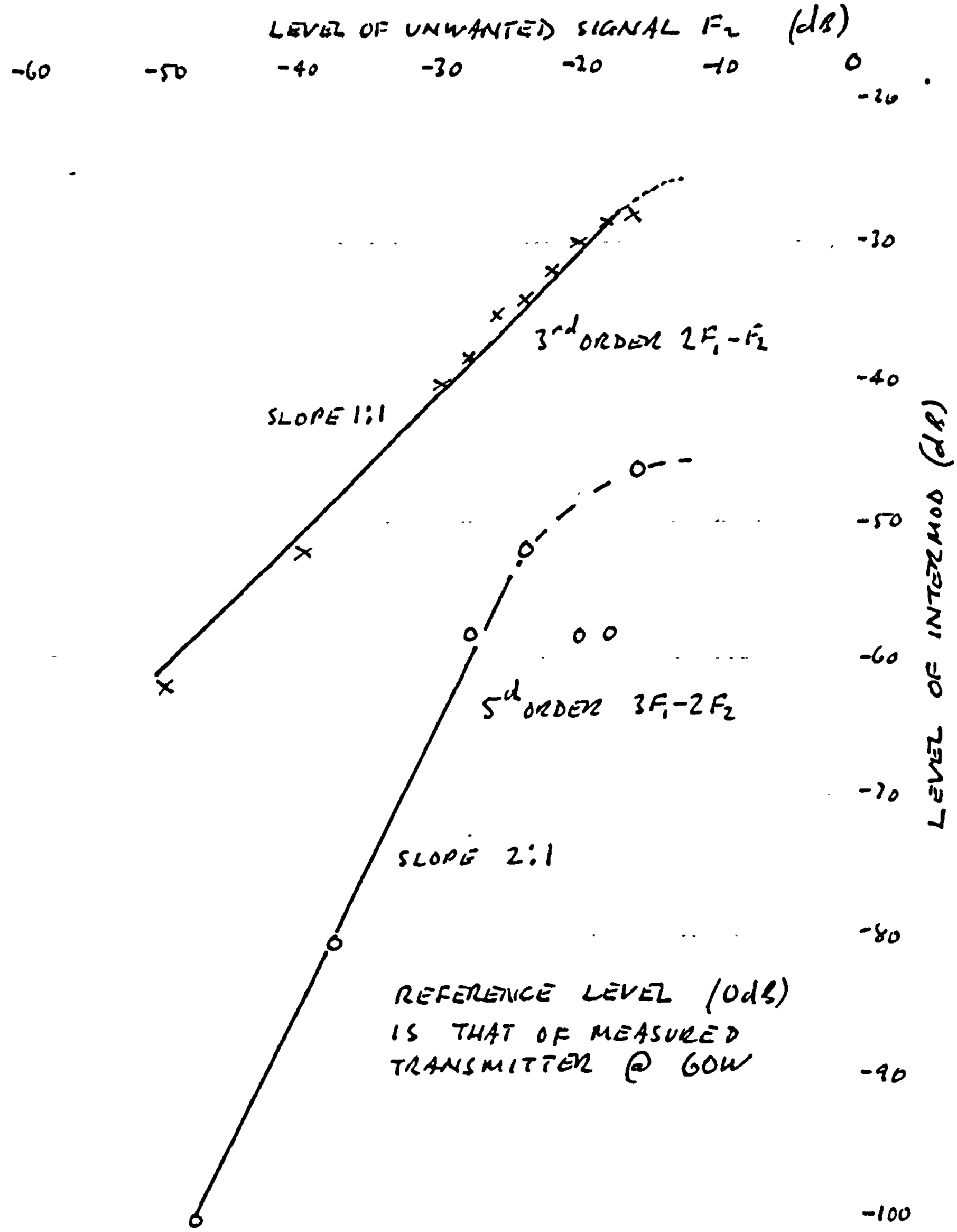

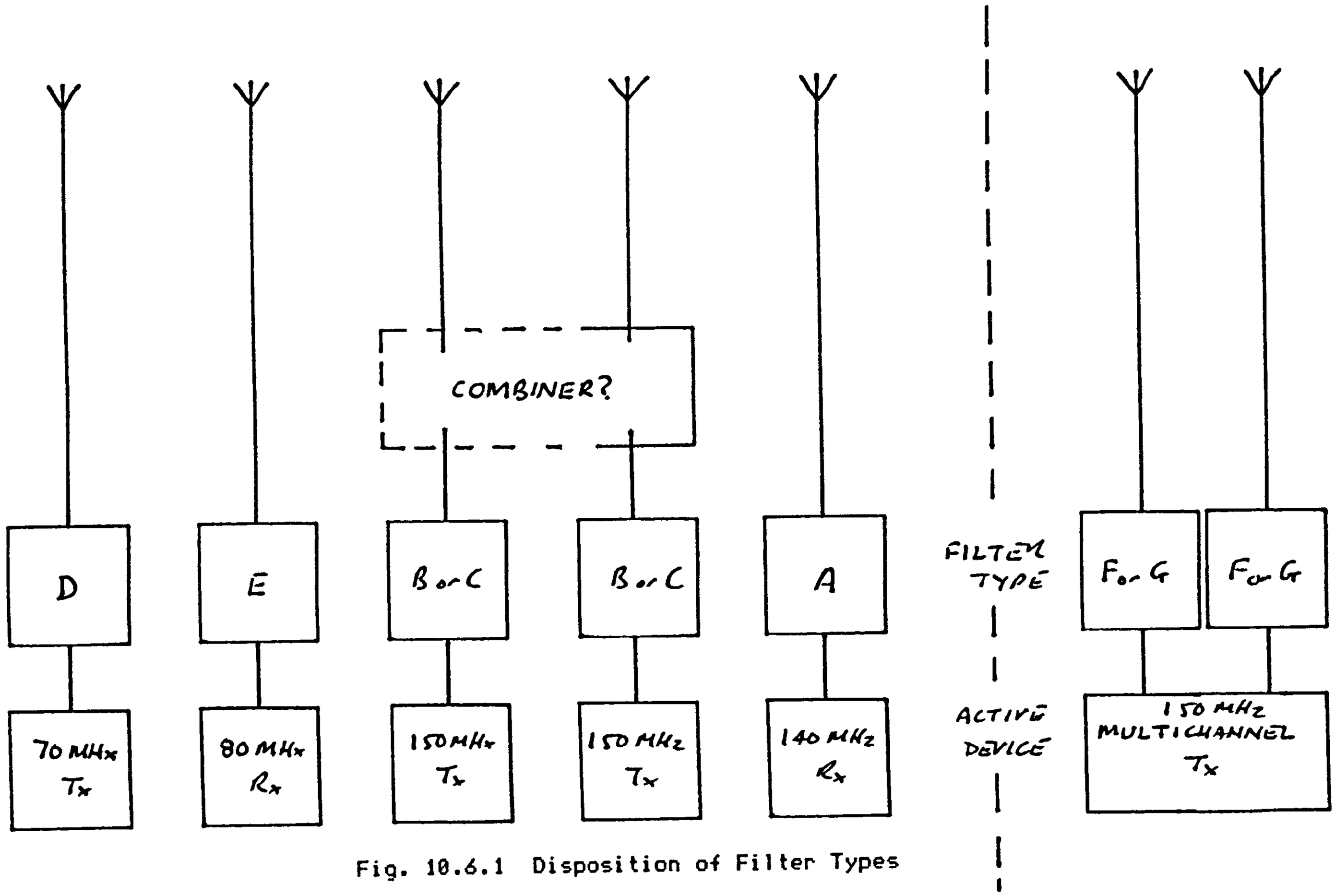

Fig. 10.6.1 Disposition of Filter Types

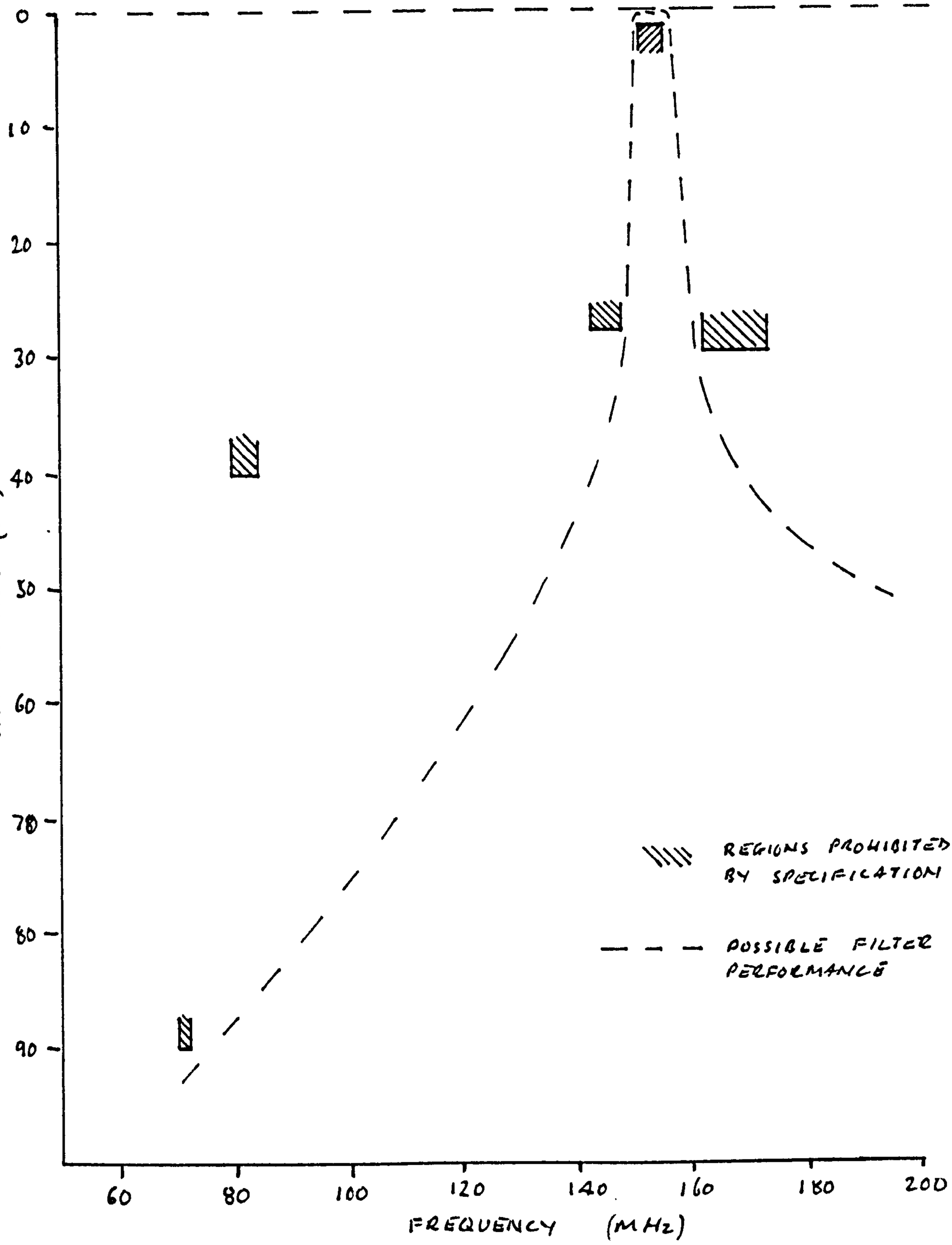

Fig. 10.6.2 Filter Performance Mask for Filter Type 'B'

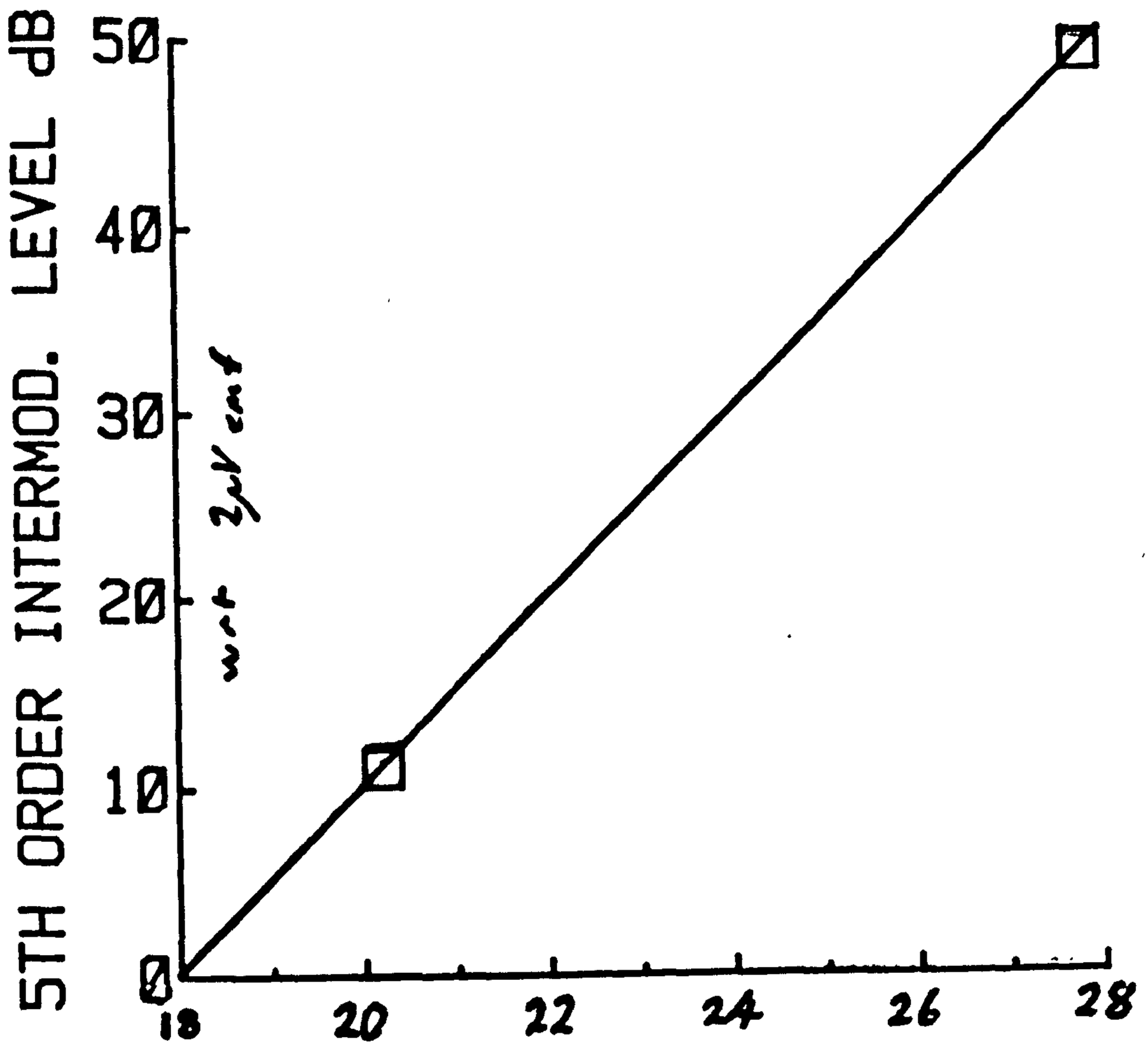

Fig. 11.1.1 Early 5th Order Intermodulation Measurement

Fig. 11.2.1 Susequent Intermodulation Test Set

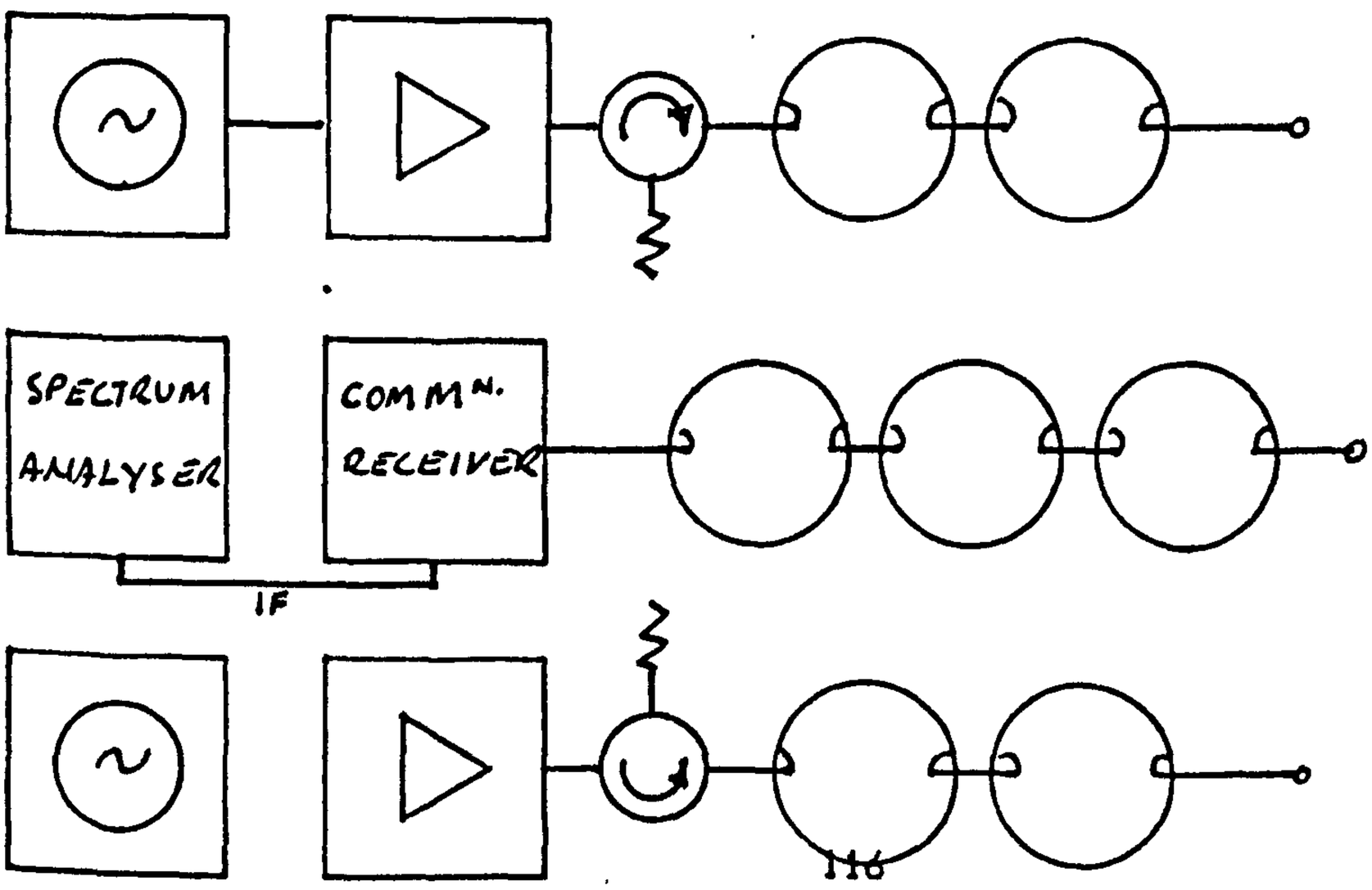

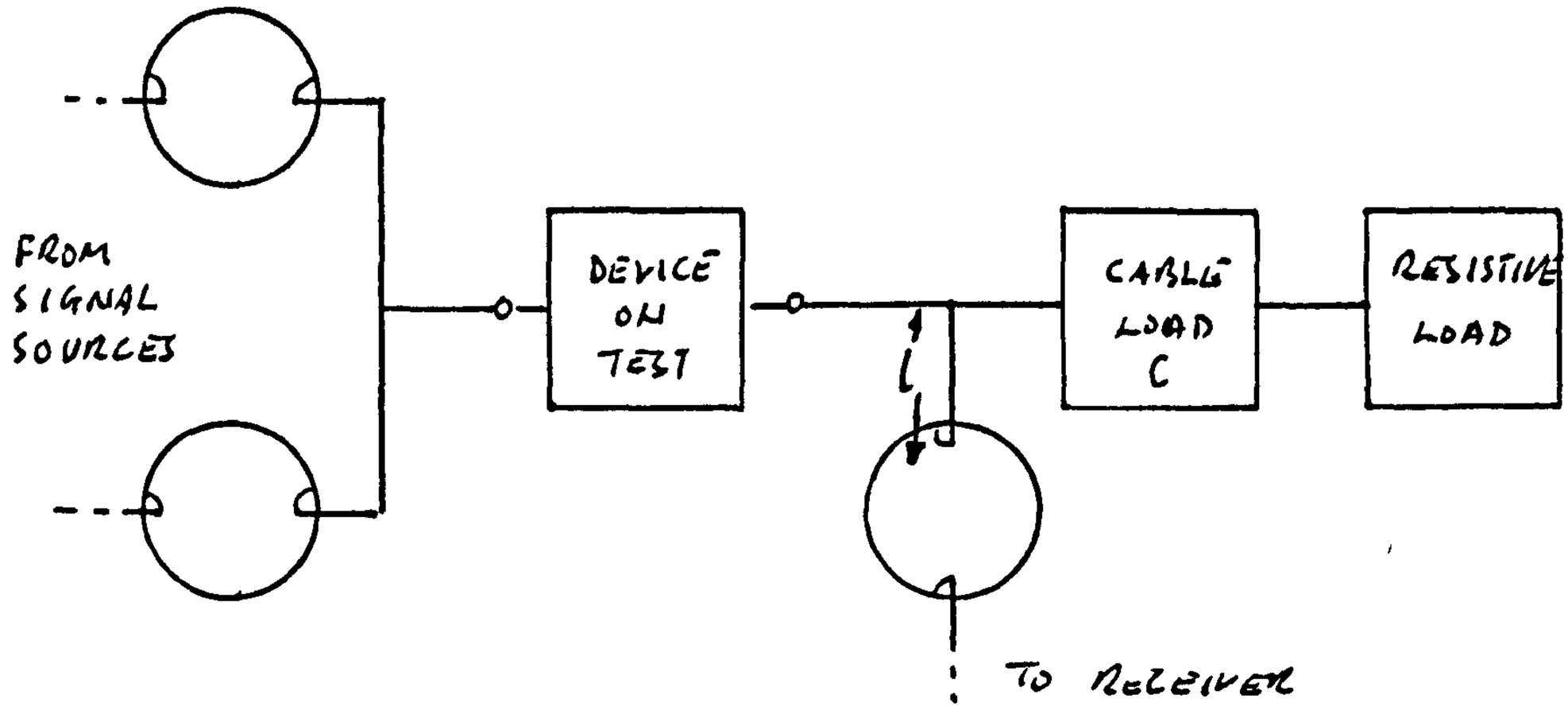

Fig. 11.2.2 Arrangement for Testing a Two-port

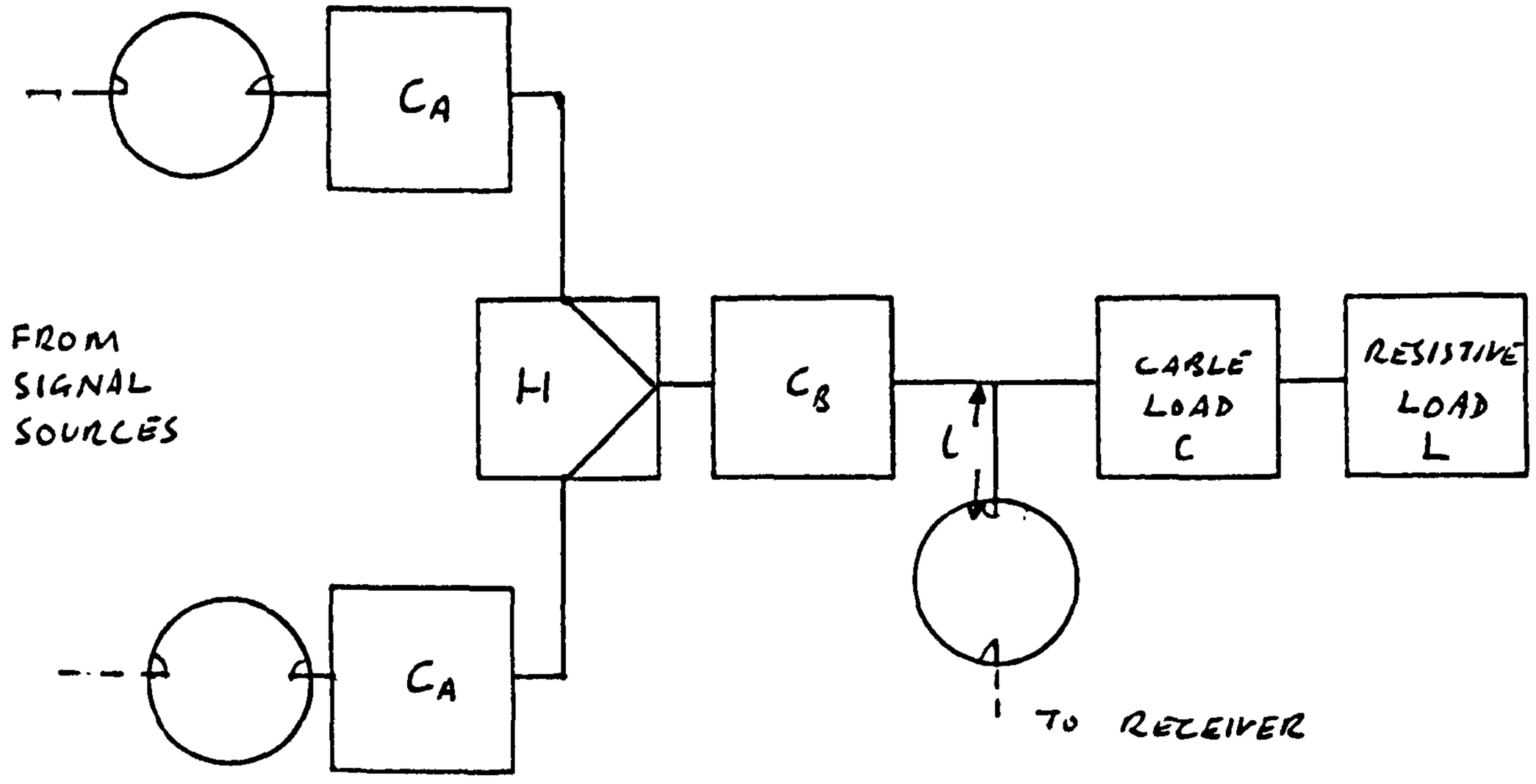

Fig. 11.2.3 Calibreation of Test Set

Section	Location/Comments	Tx Power watts	Tx-Tx Aerial Isolation dB	Tx-Rx Aerial Isolation dB	Product level (max relative to 2μV pd for order number: dB					
					5	7	9	11	13	15
A	Harrow (min, max)									
	dipoles dry	27	21	26/30	-15, 0	-25, -10	-28, -16	-30, -15		
	dipoles wet	27	21	26/30	+10, +20	0, +10	-10, - 2	-30, -15		
B	Cheveley									
	dipoles	31	20	29/30	+50	+20	+15	+10	0	-10
	dipoles	31	50	33/38	+50	+40	+20	+ 5		
C	Tx slots, Rx dipole	31	40	42/60	+20	+15	+10	0		
	Tx slots, Rx slot	31	40	32/44	+ 7	-10	-15	<-20		
	Tx common, Rx slot	31	-	-	0	-5	< -30	<-30		
D	Ousden									
	dipoles	31	22	30	+42	+14	+8	+2		
	dipoles (receiver on separate tower)	31	20	℄	-10	-12	-5	-10		
	dipoles Tx and Rx on one tower, Tx on other	31	-	-	<-30	<-30	-	-		

Fig. 11.3.1 Compendium of Intermodulation Results

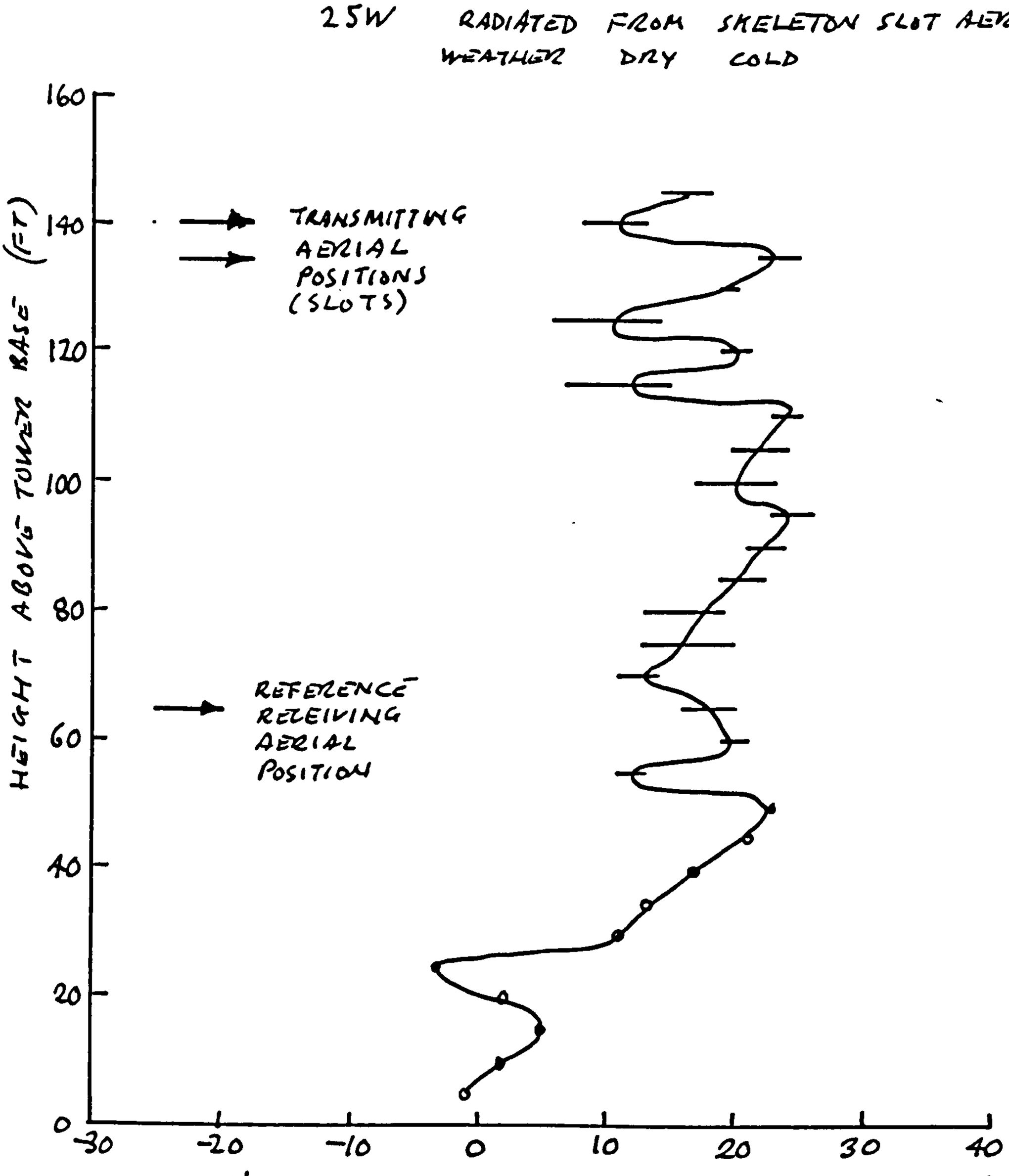

Fig. 11.3.2 3rd Order Intermodulation Variation with Height I

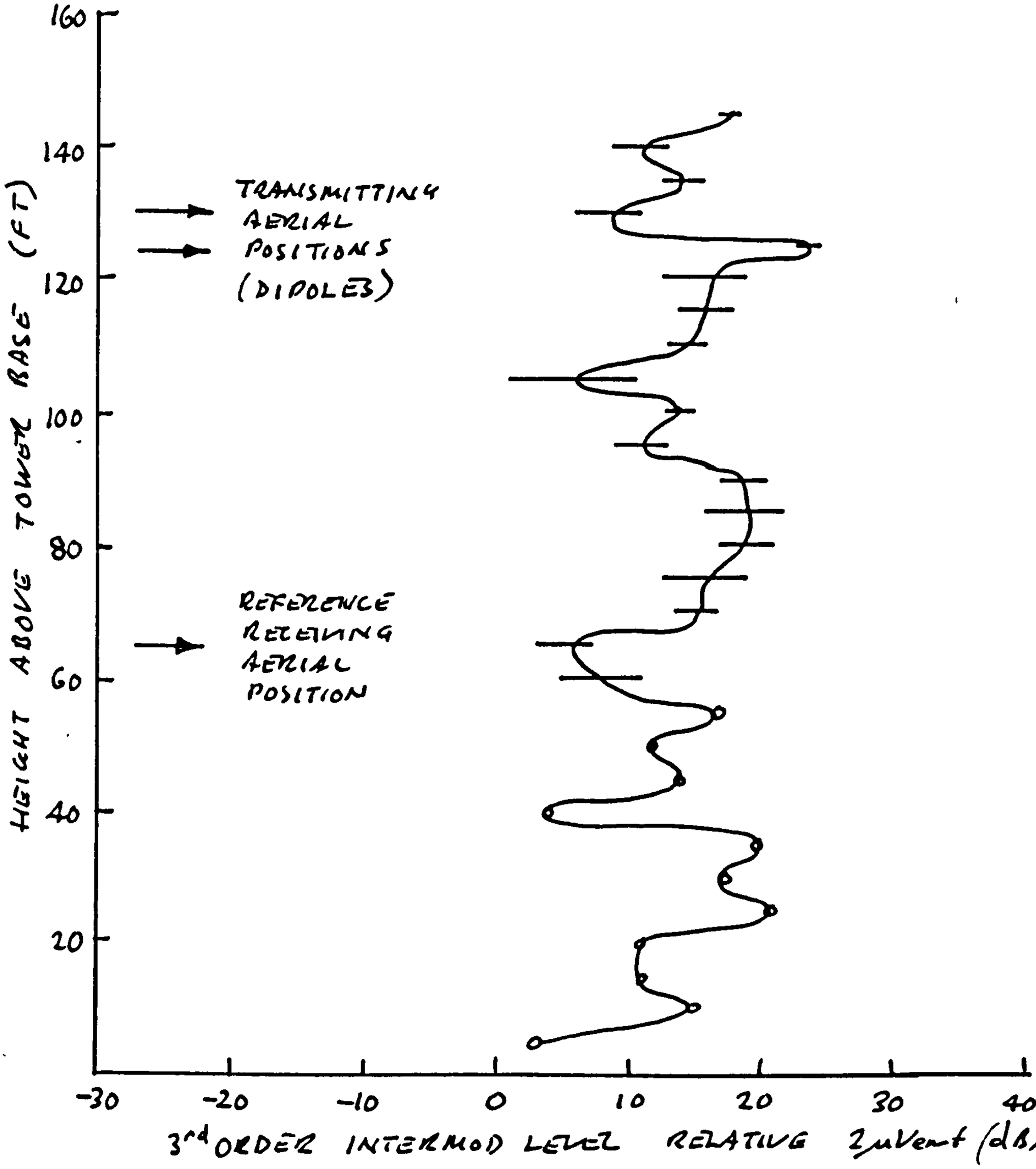

Fig. 11.3.3 3rd Order Intermodulation Variation with Height II

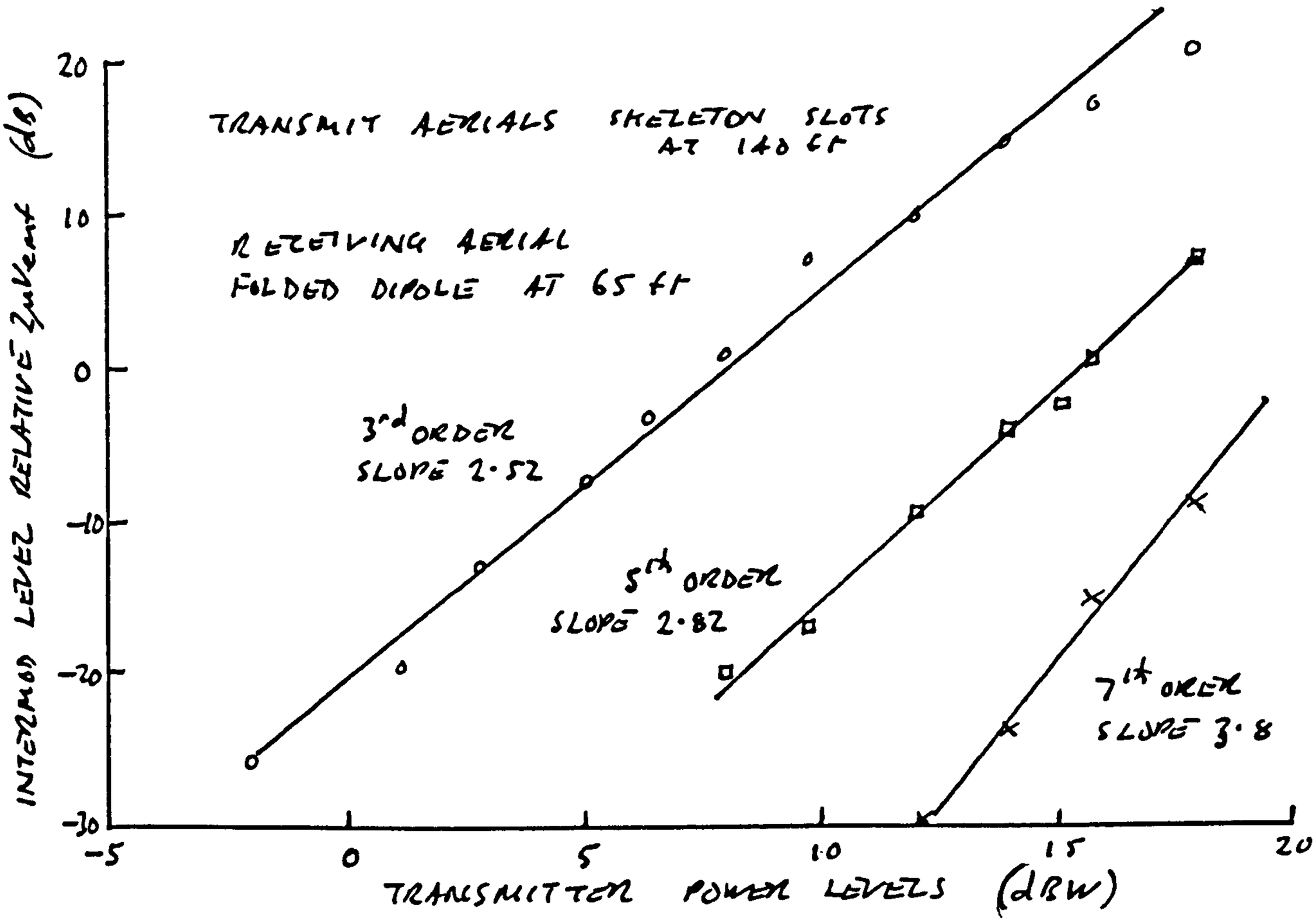

Fig. 11.3.4 Intermodulation Variation with Power - Various Orders

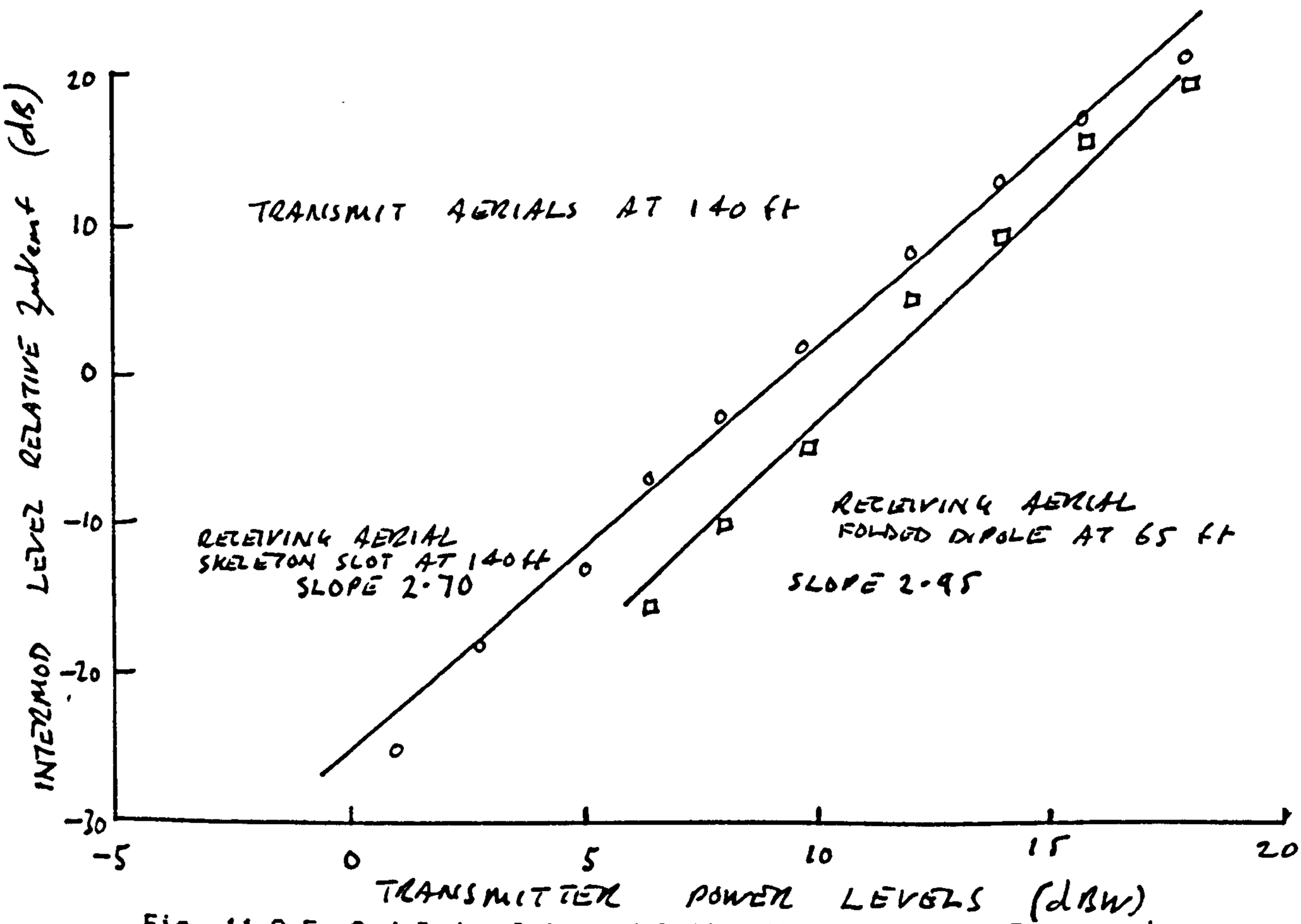

Fig. 11.3.5 3rd Order Intermodulation Variation with Power and Aerial Type/Position

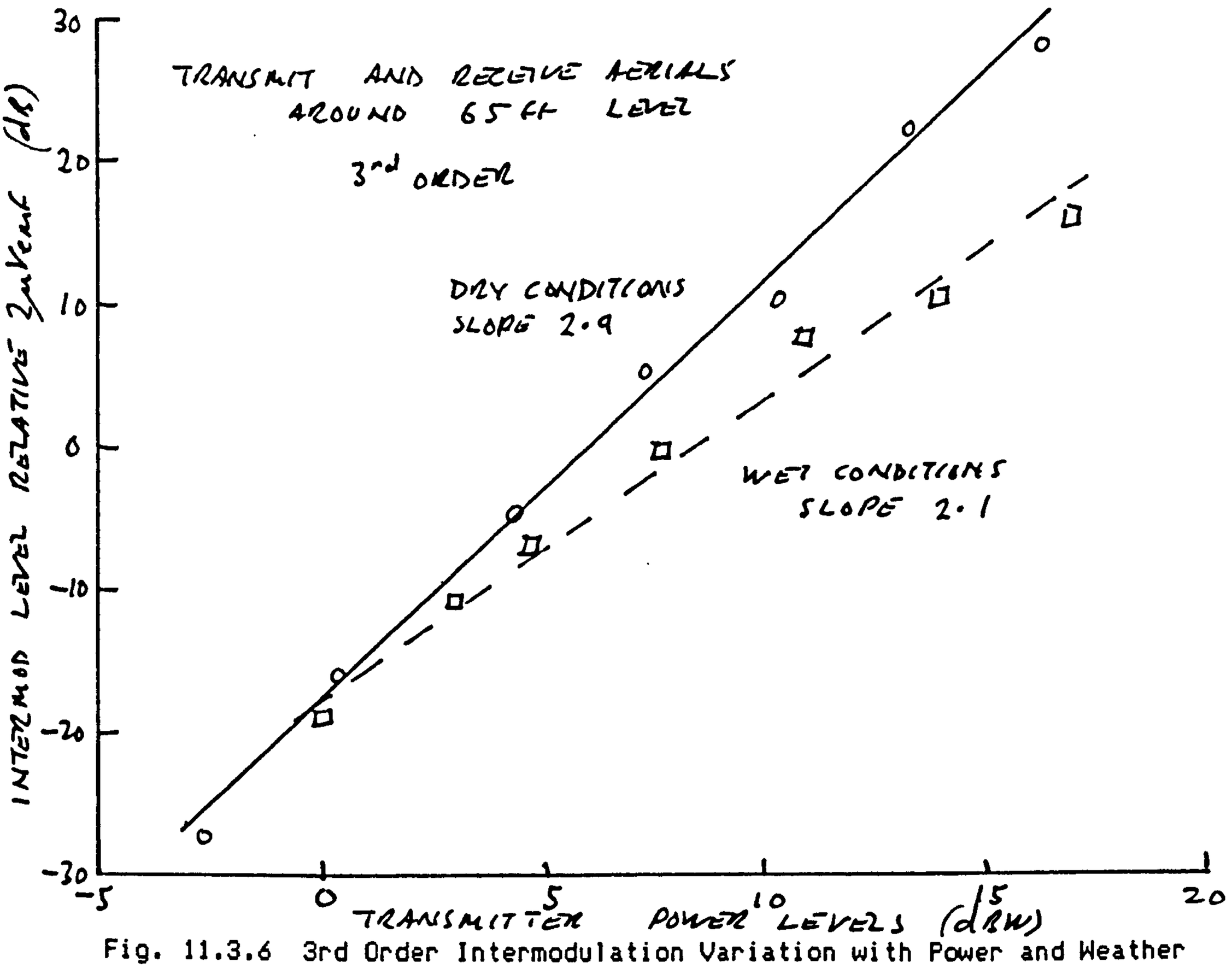

Fig. 11.3.6 3rd Order Intermodulation Variation with Power and Weather

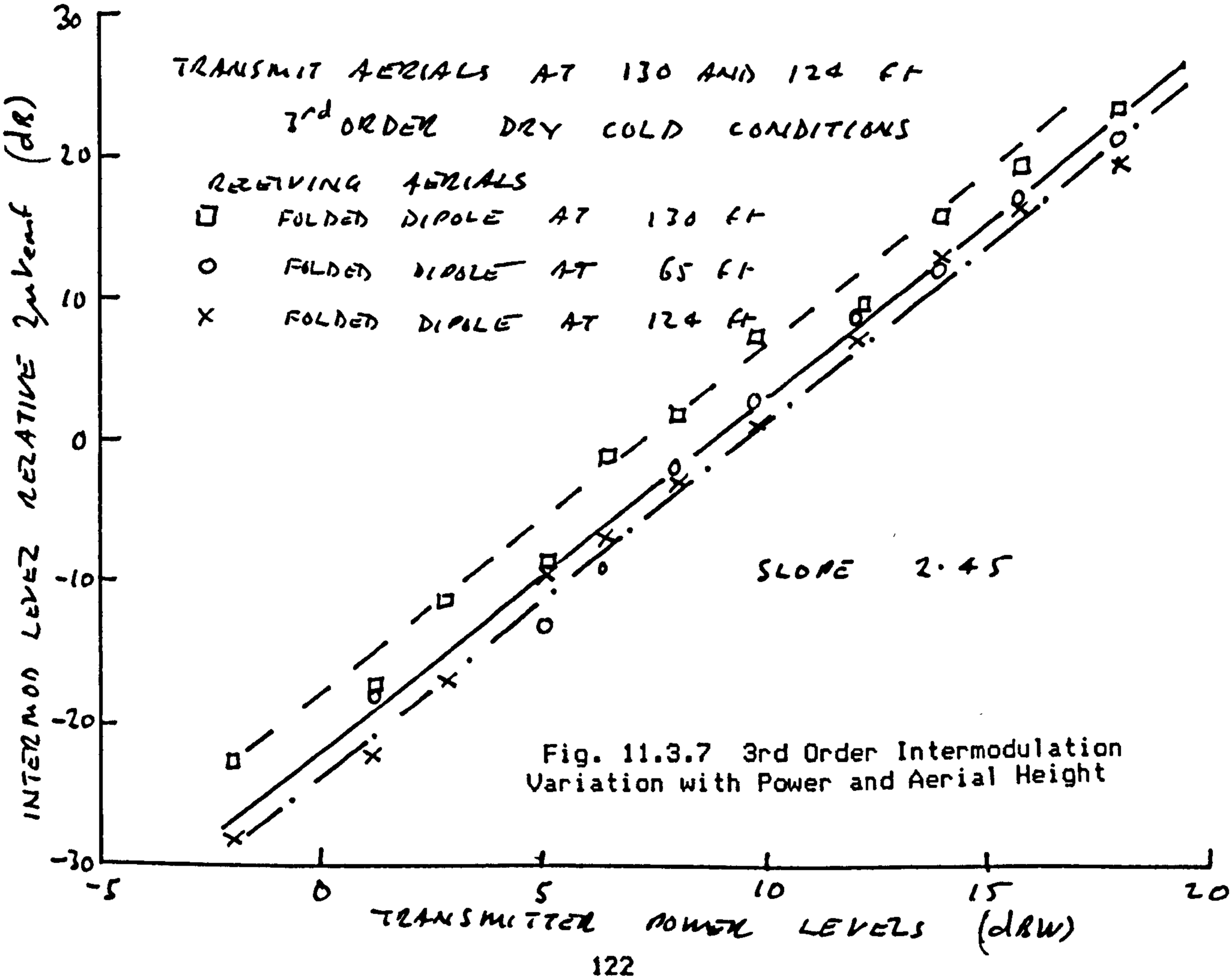

Fig. 11.3.7 3rd Order Intermodulation Variation with Power and Aerial Height

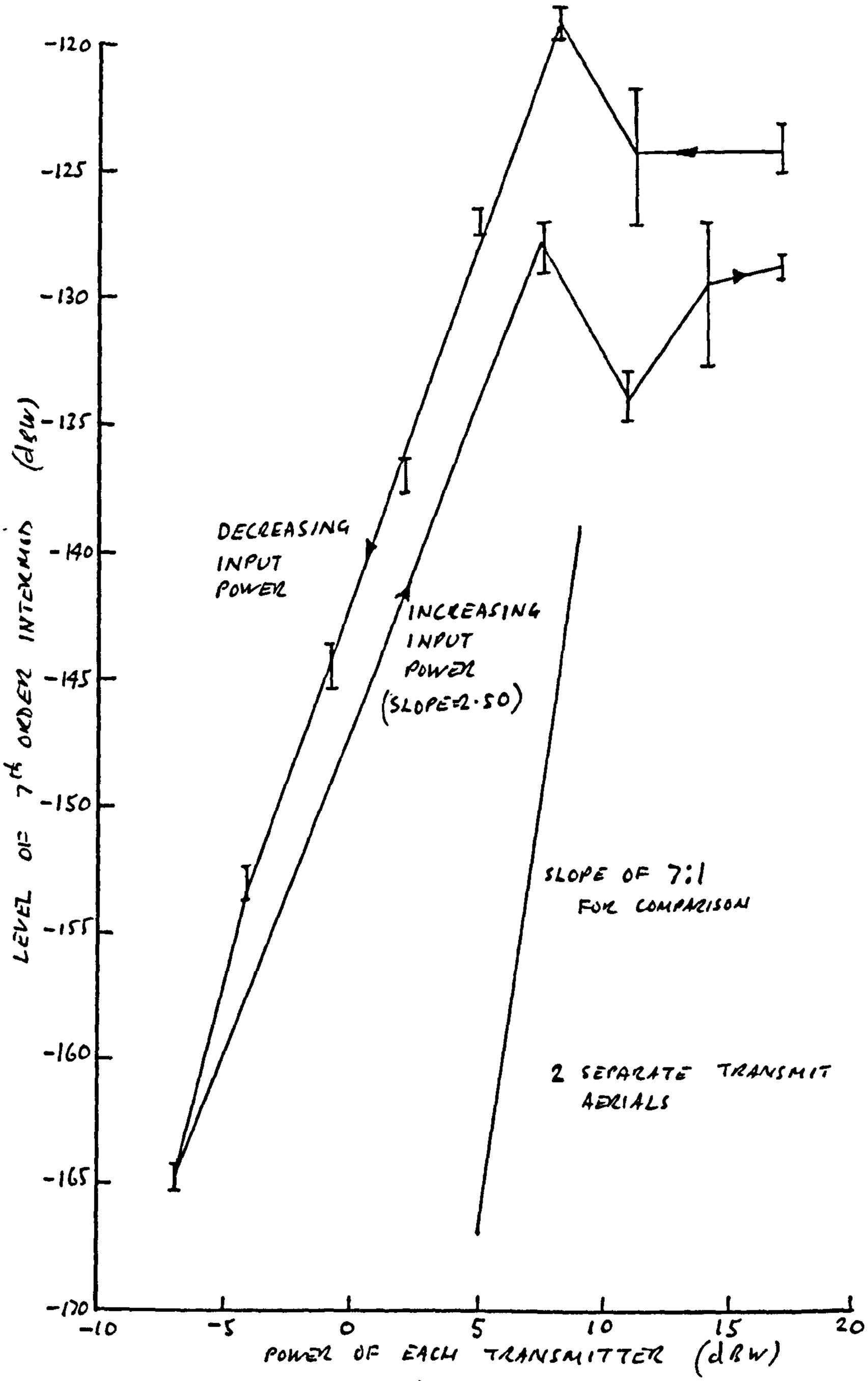

Fig. 11.3.8 7th Order Variation with Power

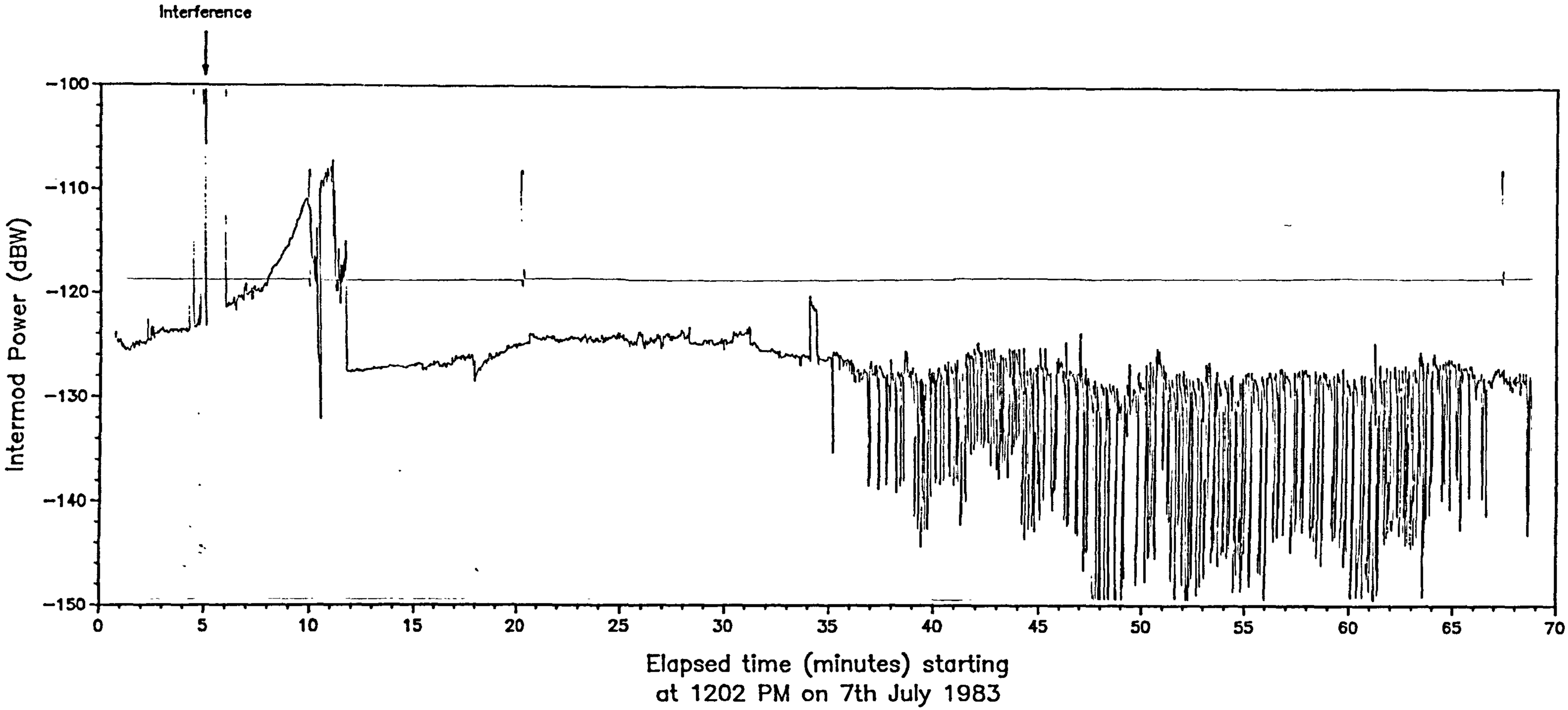

Relative Humidity 64%
Temp. 77 Fahrenheit

Fig. 11.3.9 3rd Order Intermodulation Variation with Time I

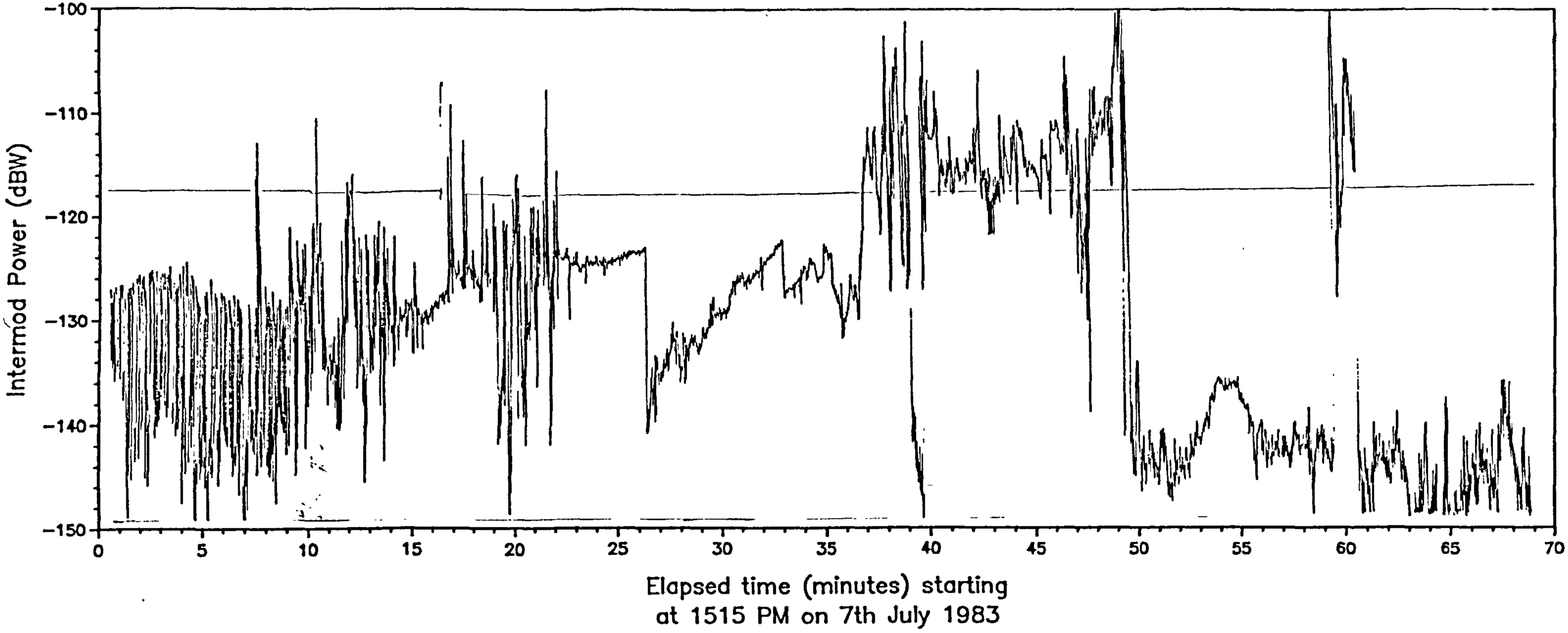

Relative Humidity 60%
Temp. 75 Fahrenheit

Fig. 11.3.10 3rd Order Intermodulation Variation with Time II

DAY 1 GROUND WET (BOTH DAYS CALM) DAY 2 GROUND DRY

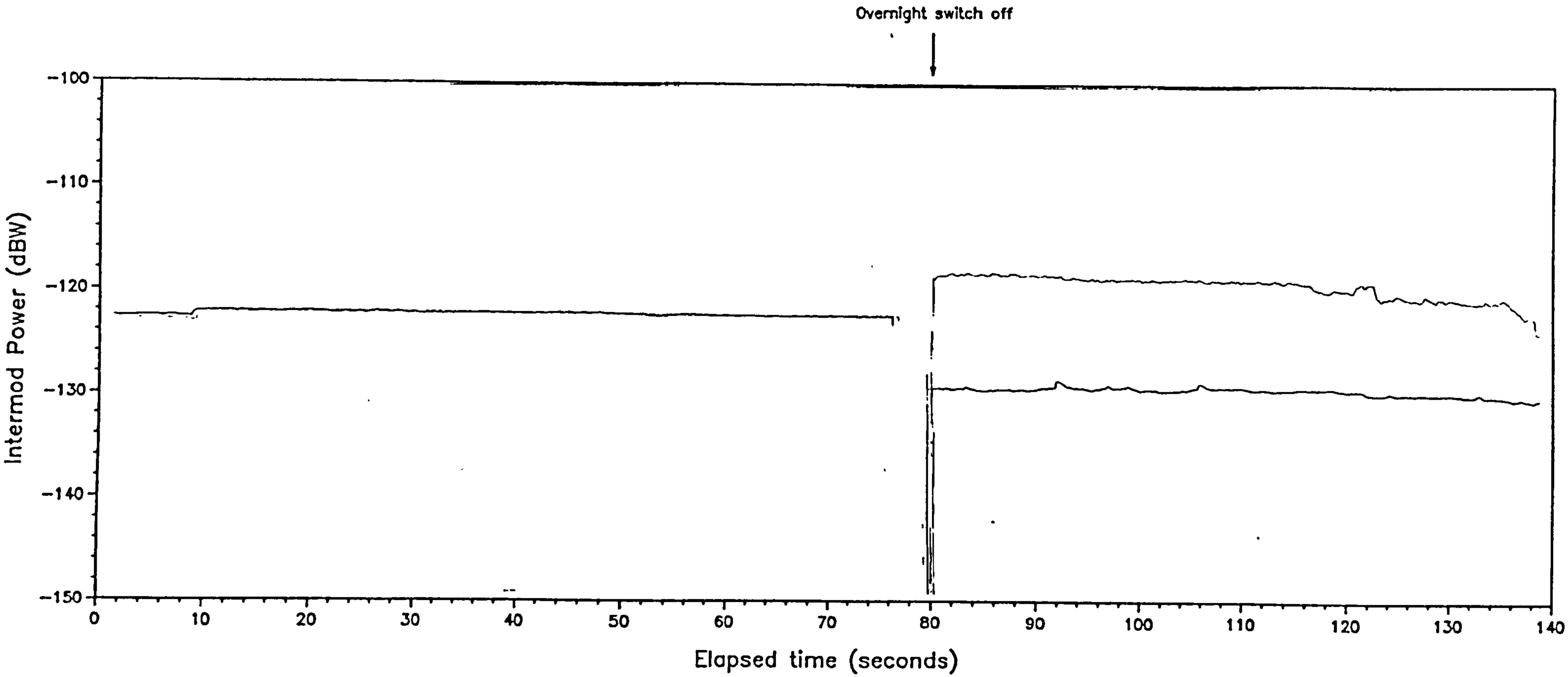

Light trace = 5th order on 161.9375 MHz
Heavy trace = 3rd order on 158.800 MHz (20 dB attenuation)

Tx aerial H
Rx aerial C

Fig. 11.3.11 3rd Order Intermodulation Variation with Time III

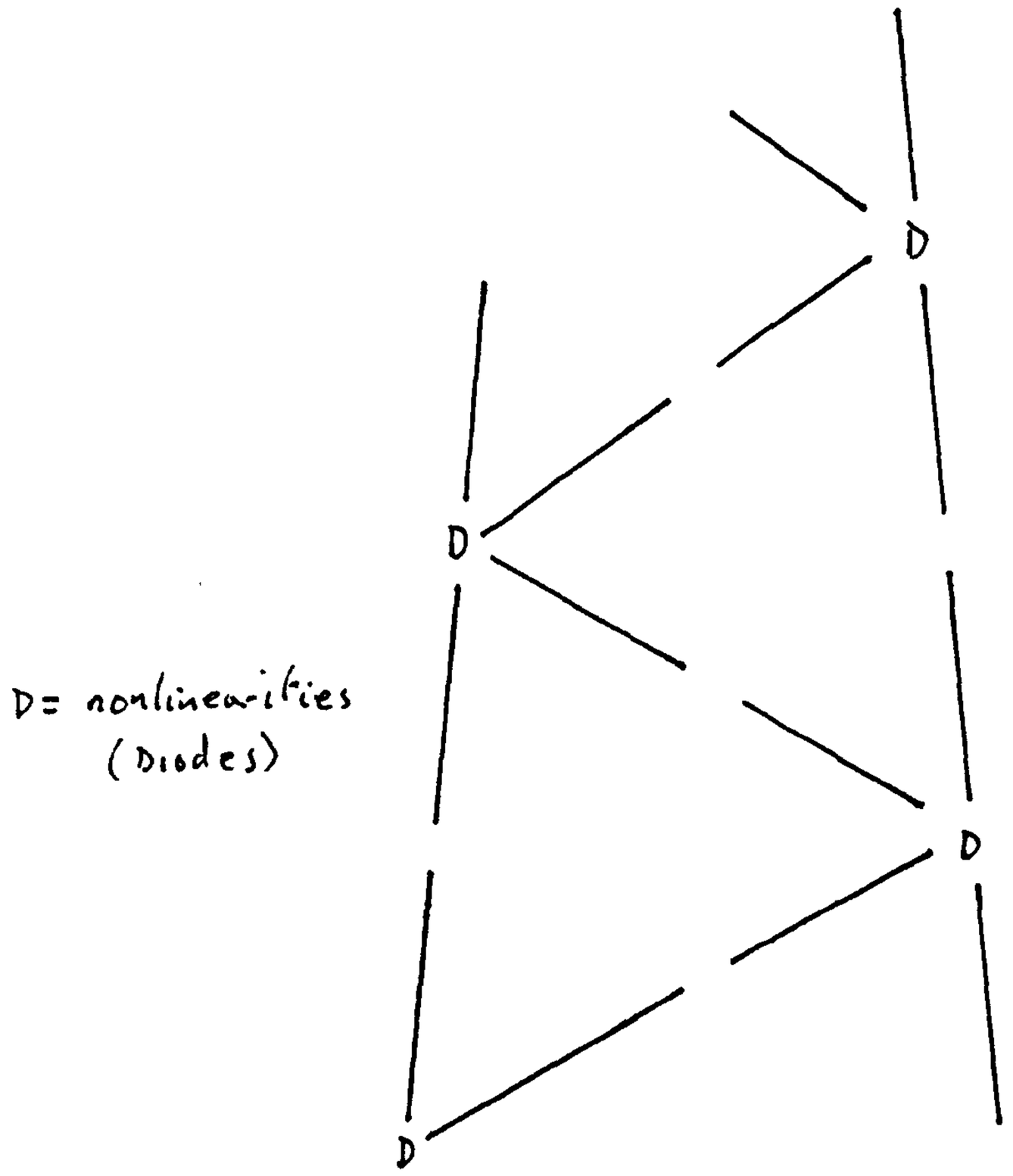

Fig. 11.4.1 Tower Construction Showing Possible Sources of Non Linearities

Fig. 11.4.2 Tower Construction Showing Other Possible Sources of Non Linearities

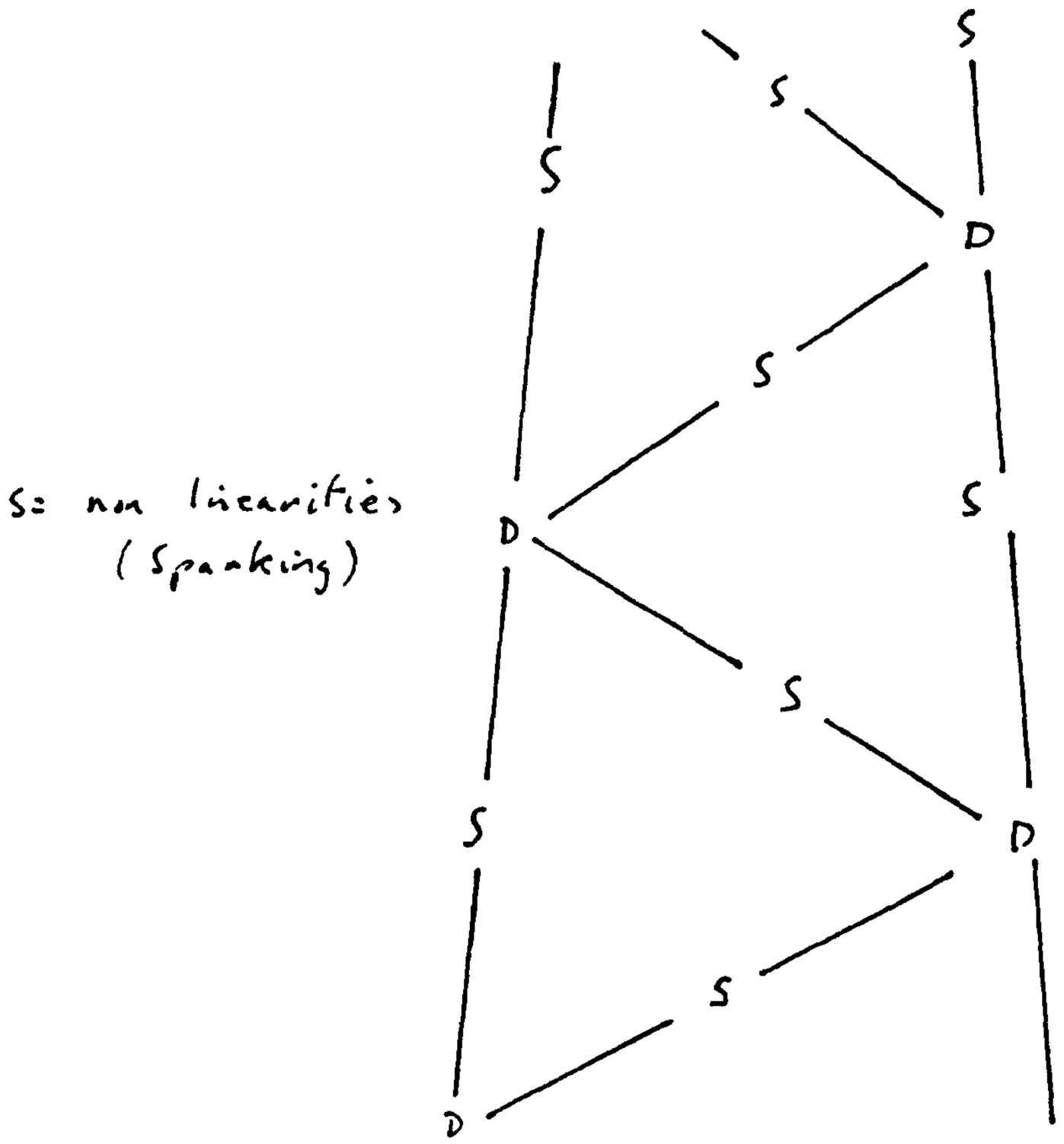

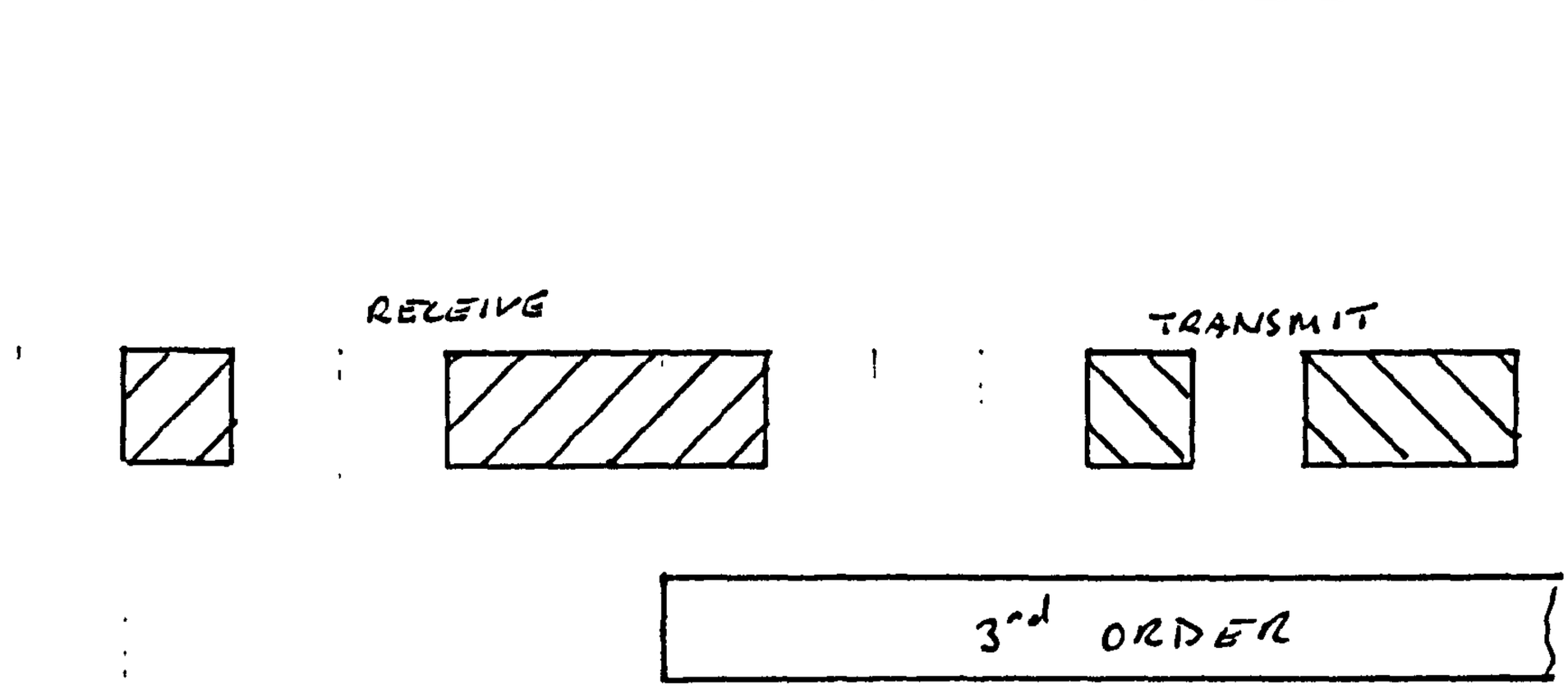

Fig. 11.5.1 Intermodulation Frequency Bands

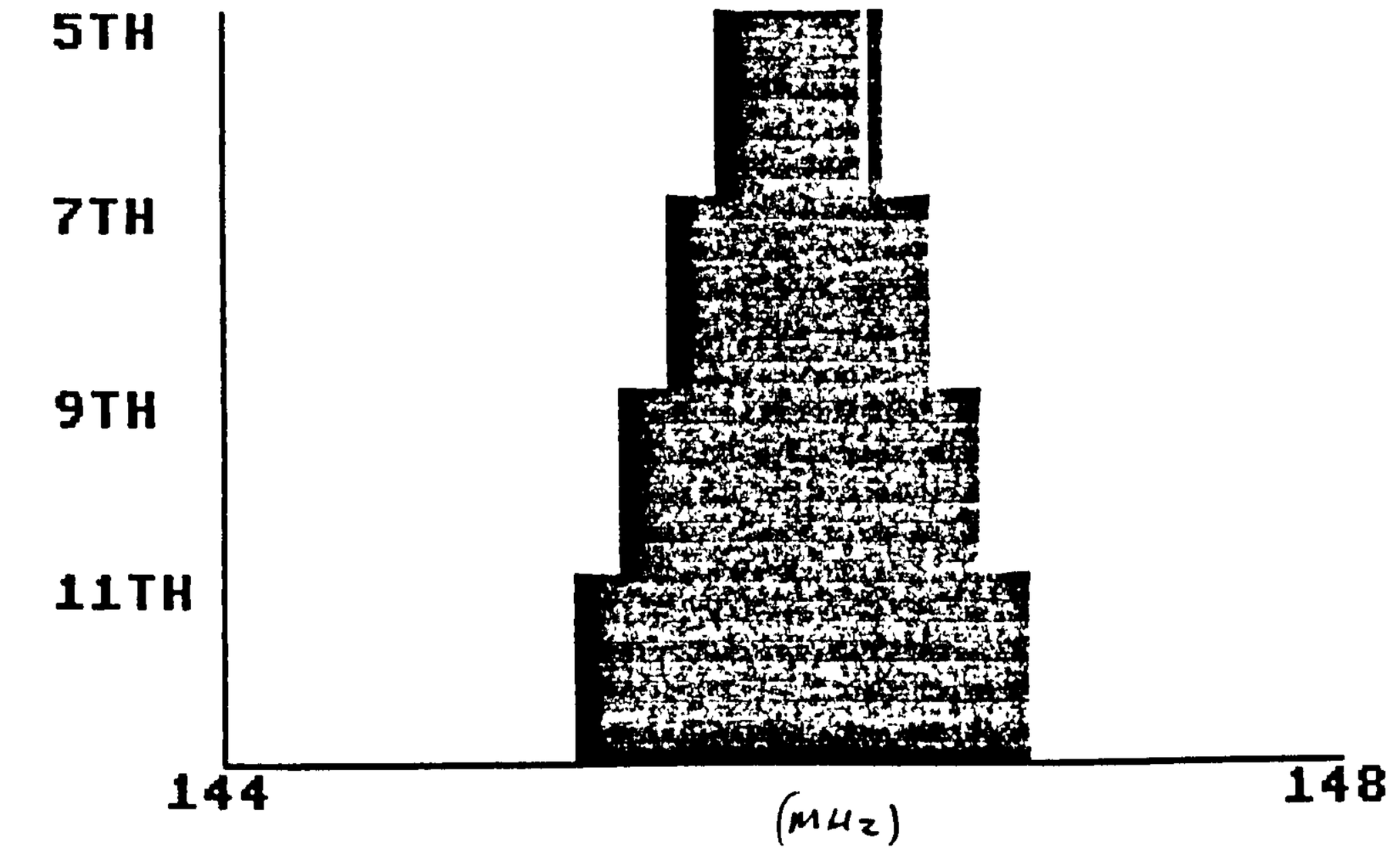

No OF INBAND PRODUCTS	TRANSMISSION FREQUENCIES (MHz) 155.1625 155.3000 155.3250 152.1500 152.2250
5TH 24	
7TH 60	
9TH 132	
11TH 228	

Fig. 11.5.2 Intermodulation Spectrum - 5 Transmissions

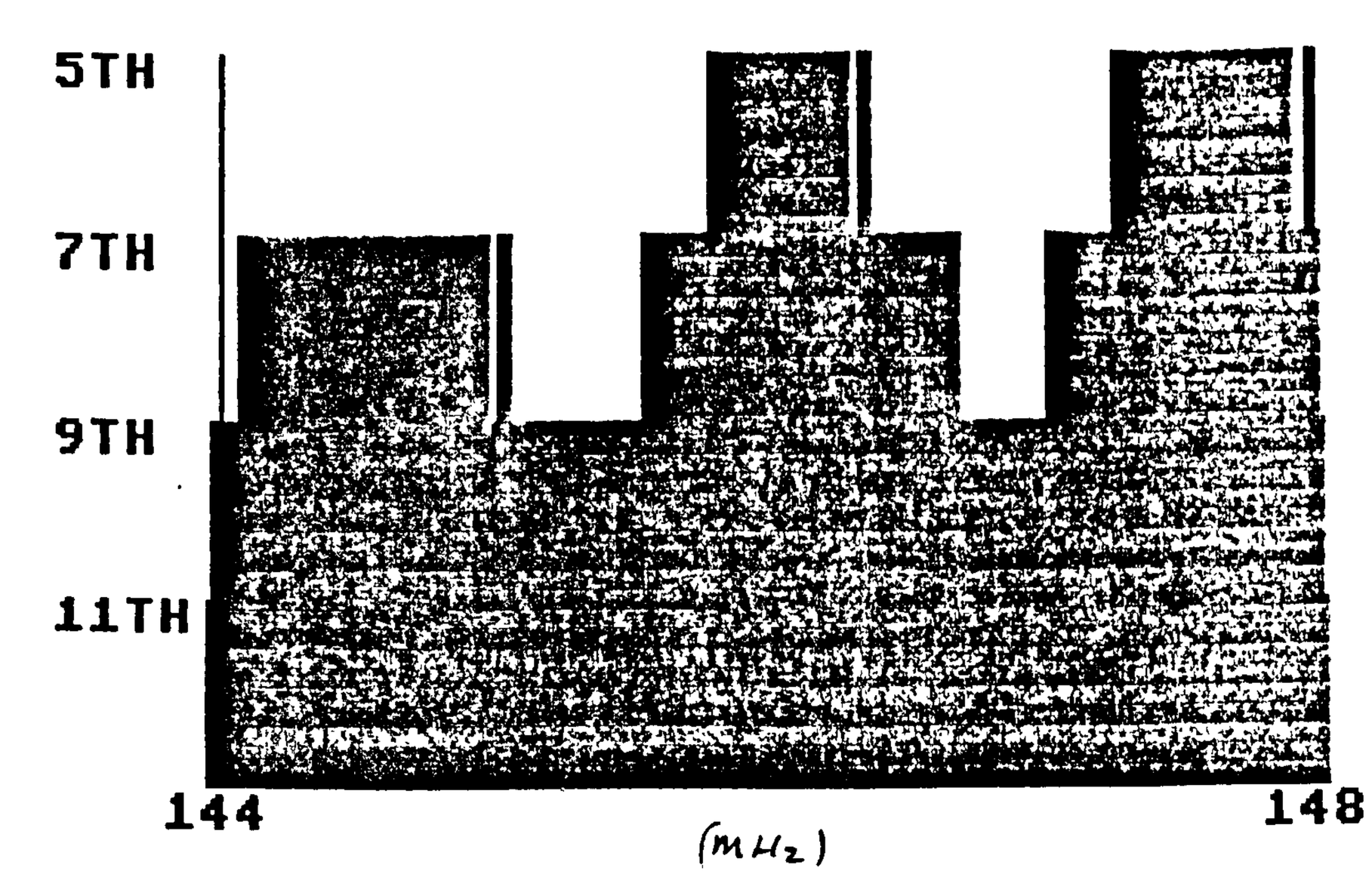

No OF INBAND PRODUCTS	TRANSMISSION FREQUENCIES (MHz) 155.1625 155.3000 155.3250 152.1500 152.2250 153.8500
5TH 414	
7TH 277	
9TH 1099	
11TH 1572	

Fig. 11.5.3 Intermodulation Spectrum - 6 Transmissions

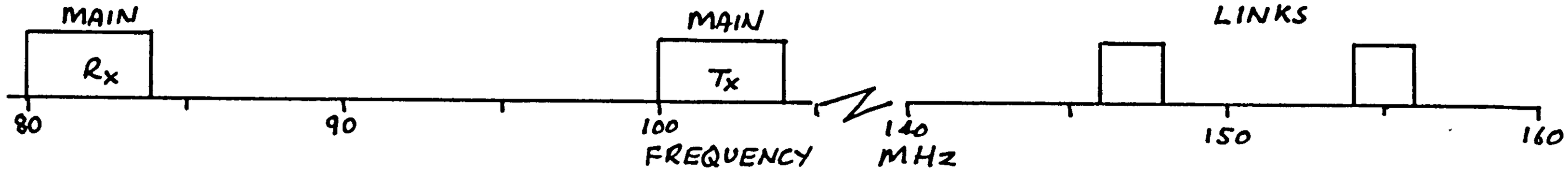

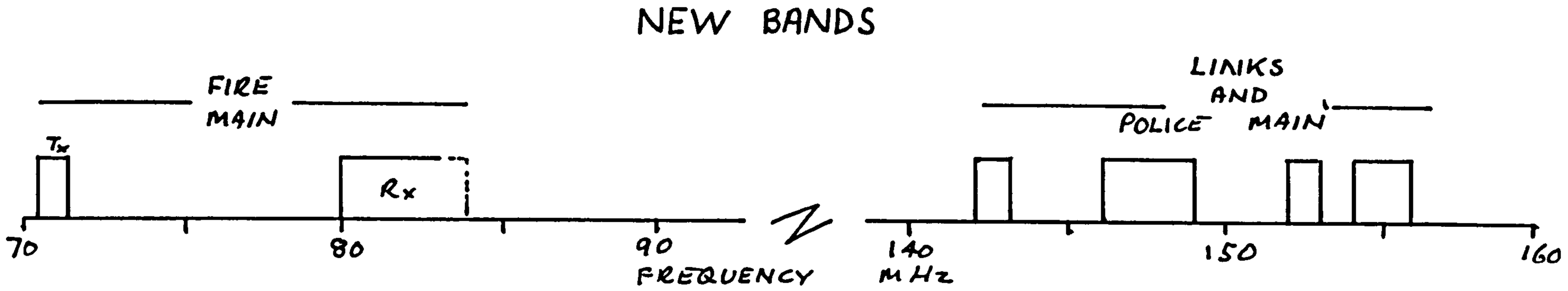

Fig. 12.1.1 Old and New Frequency Bands

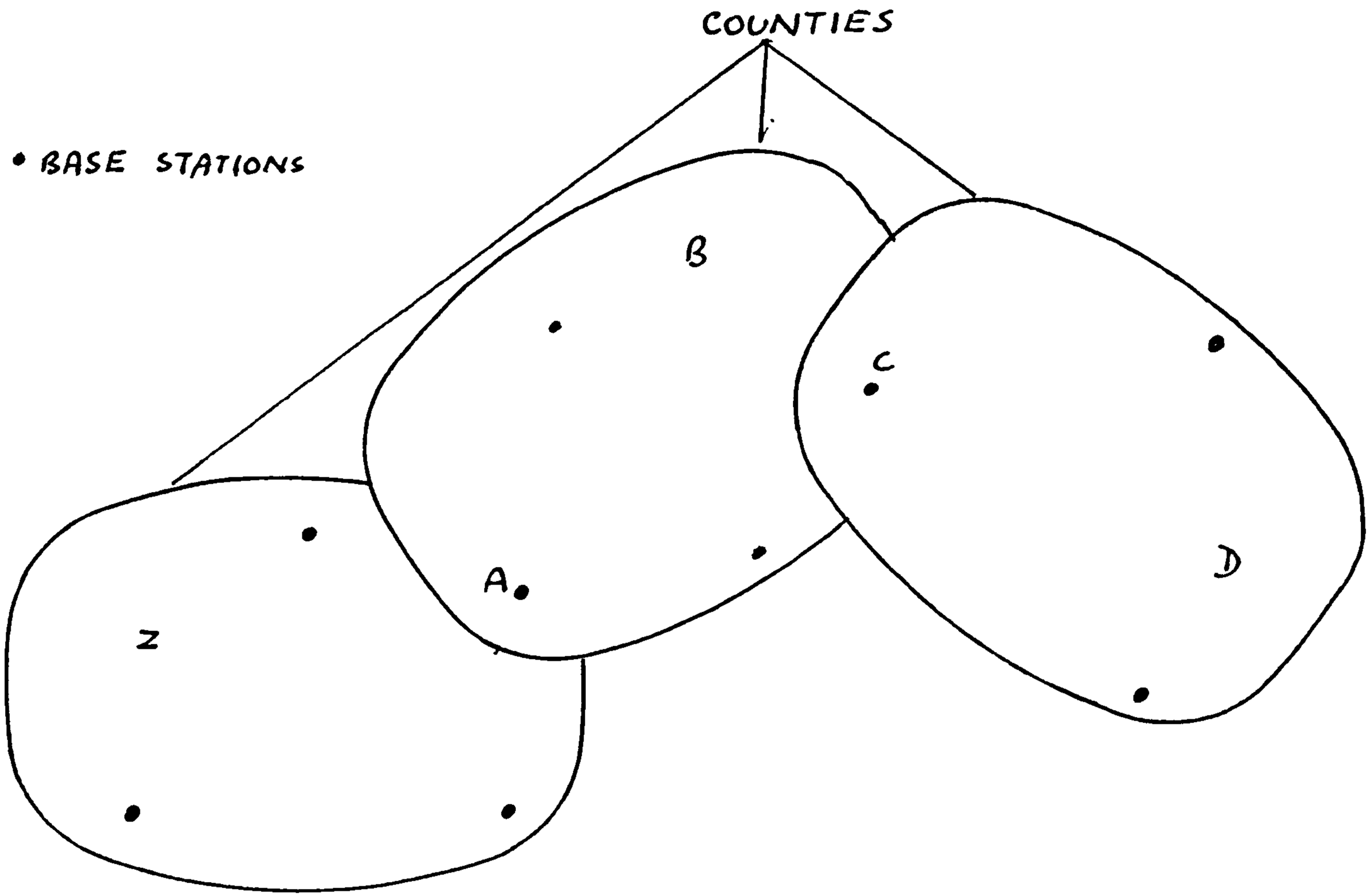

Fig. 12.1.2 Chaining

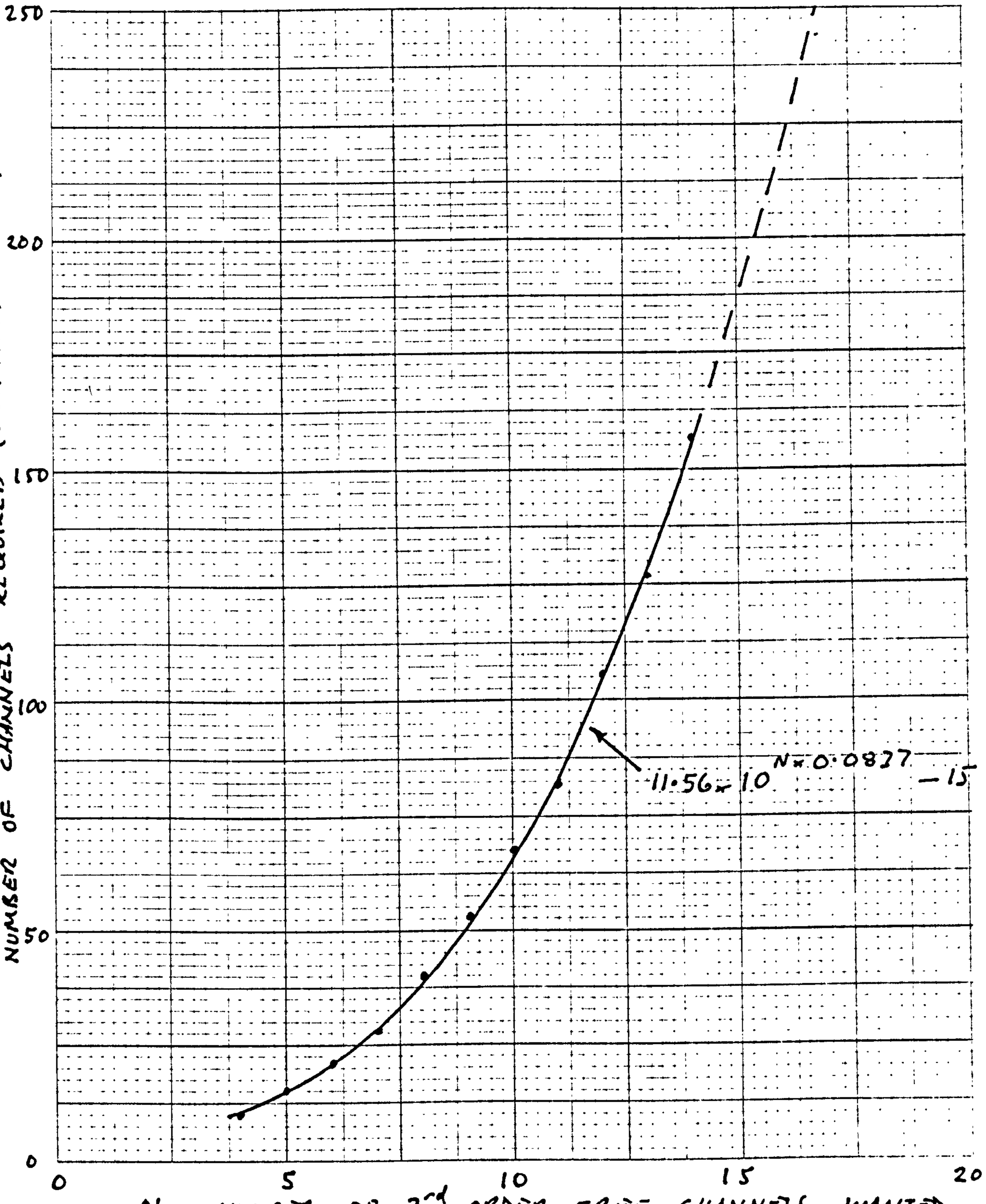

Fig. 12.2.1 Required Switching Range vs.Number of Channels

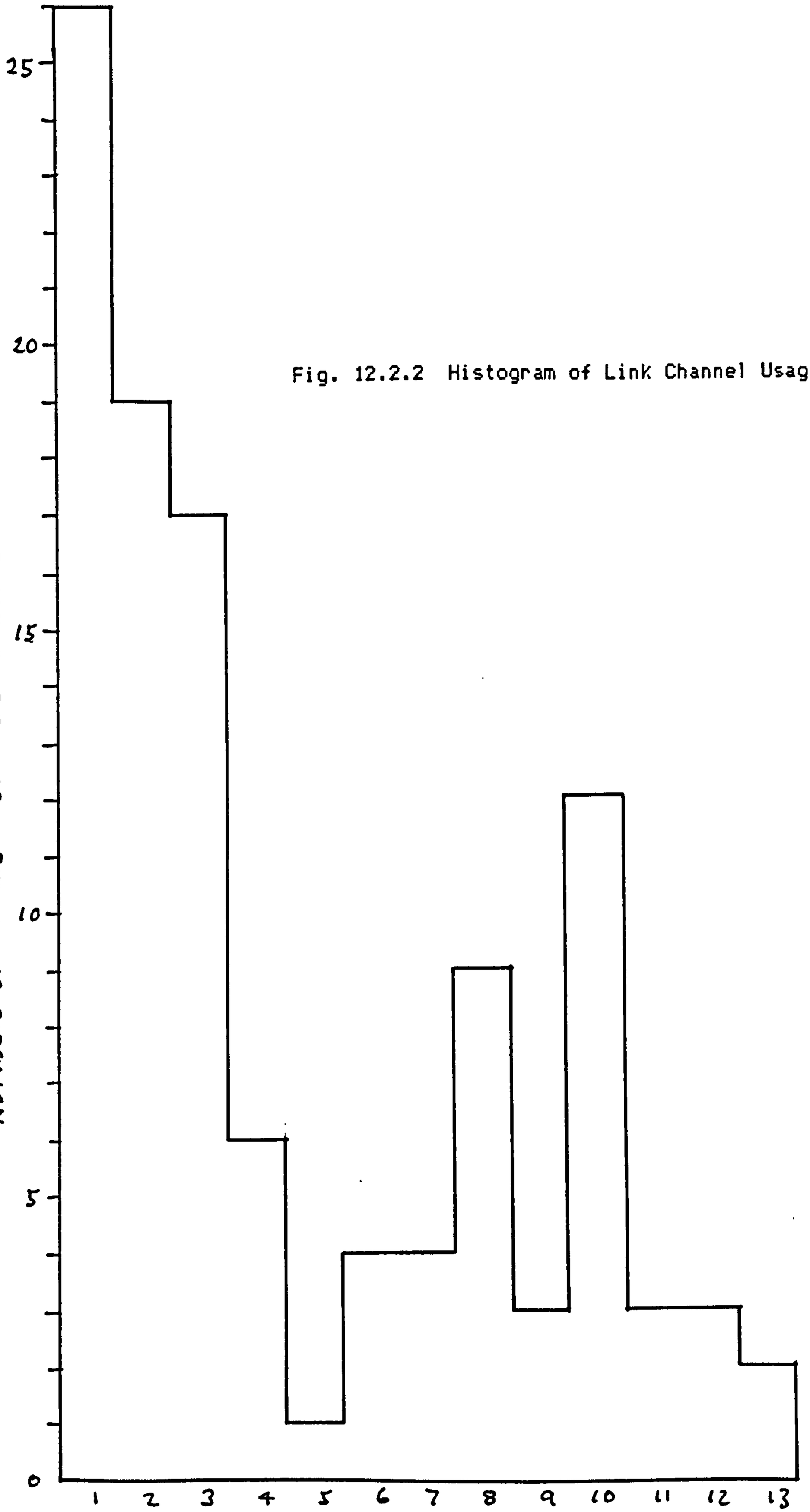

Fig. 12.2.2 Histogram of Link Channel Usage

INTERMODULATION BANDS

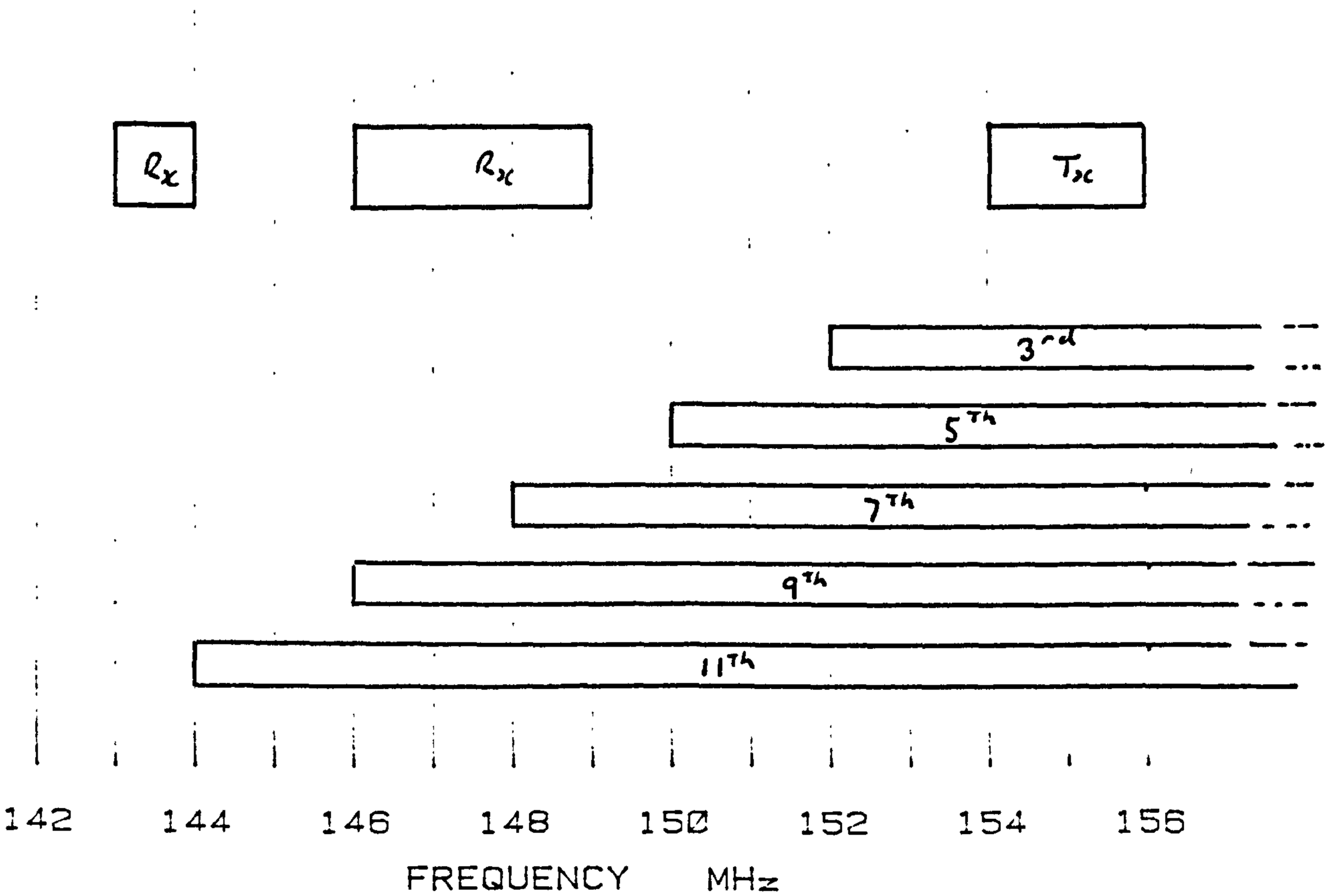

Fig. 12.3.1 Intermodulation Distribution (154-156MHz)

INTERMODULATION BANDS

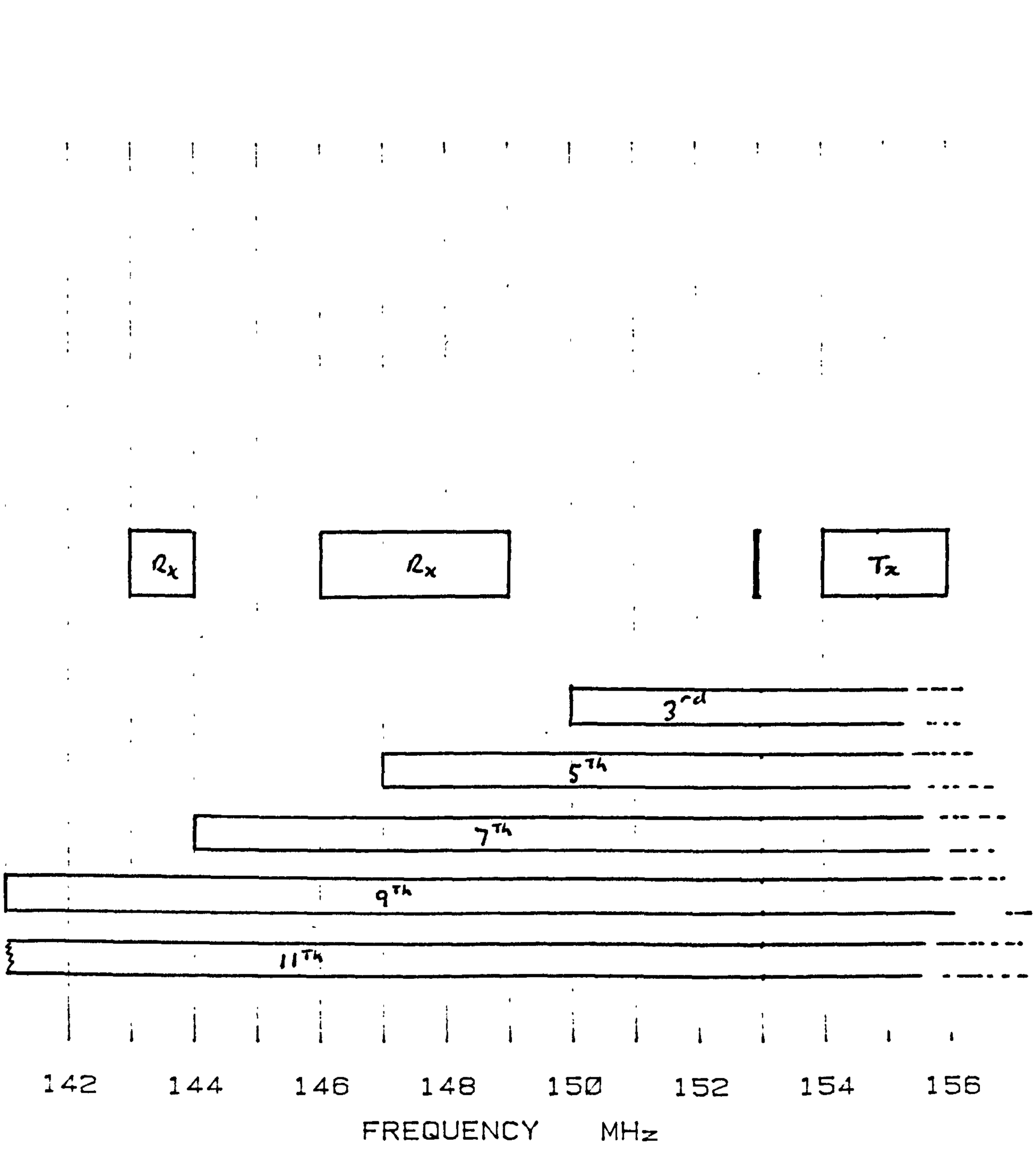

Fig. 12.3.2 Intermodulation Distribution (153+154-156MHz)

INTERMODULATION BANDS

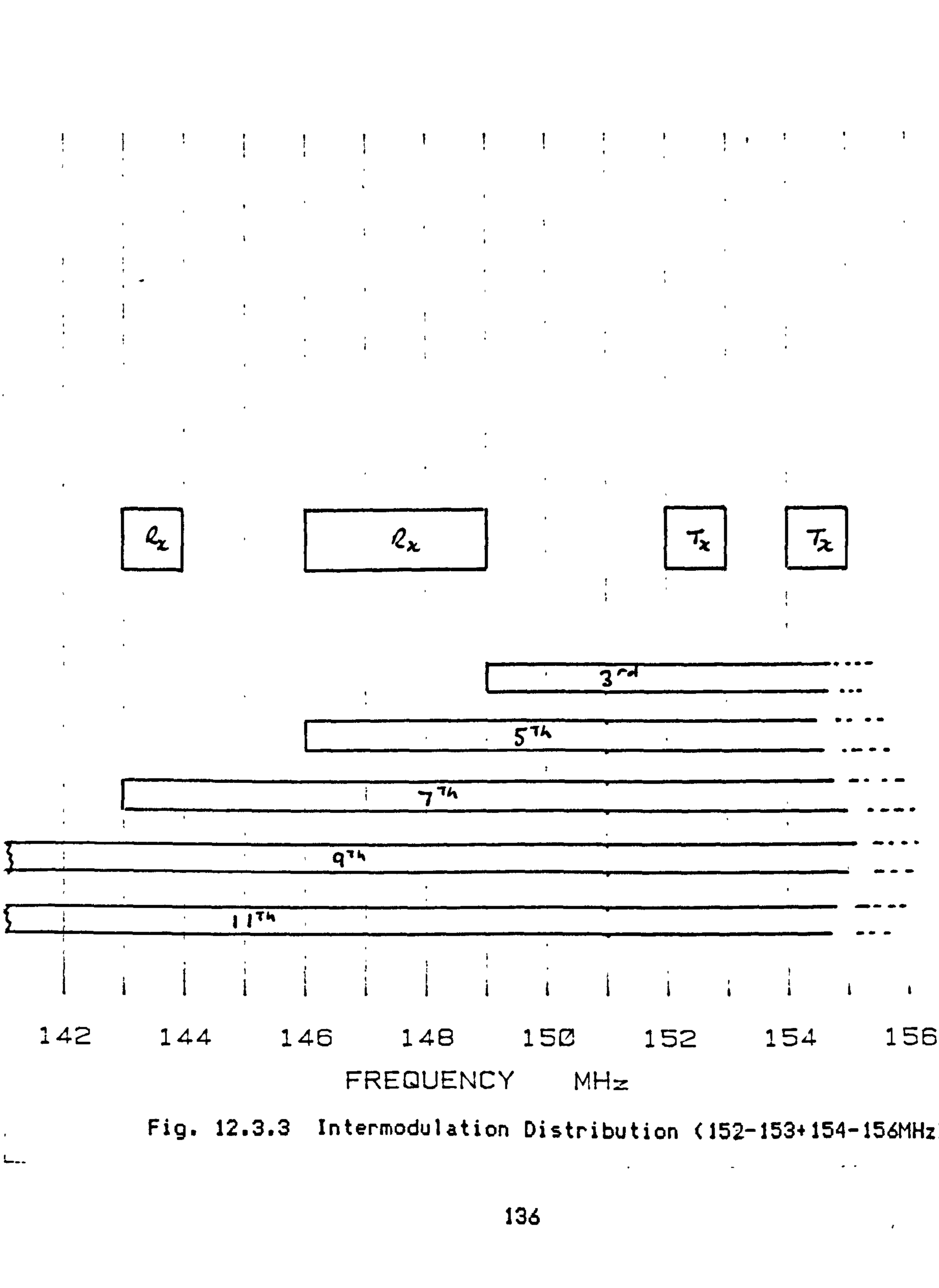

Fig. 12.3.3 Intermodulation Distribution (152-153+154-156MHz)

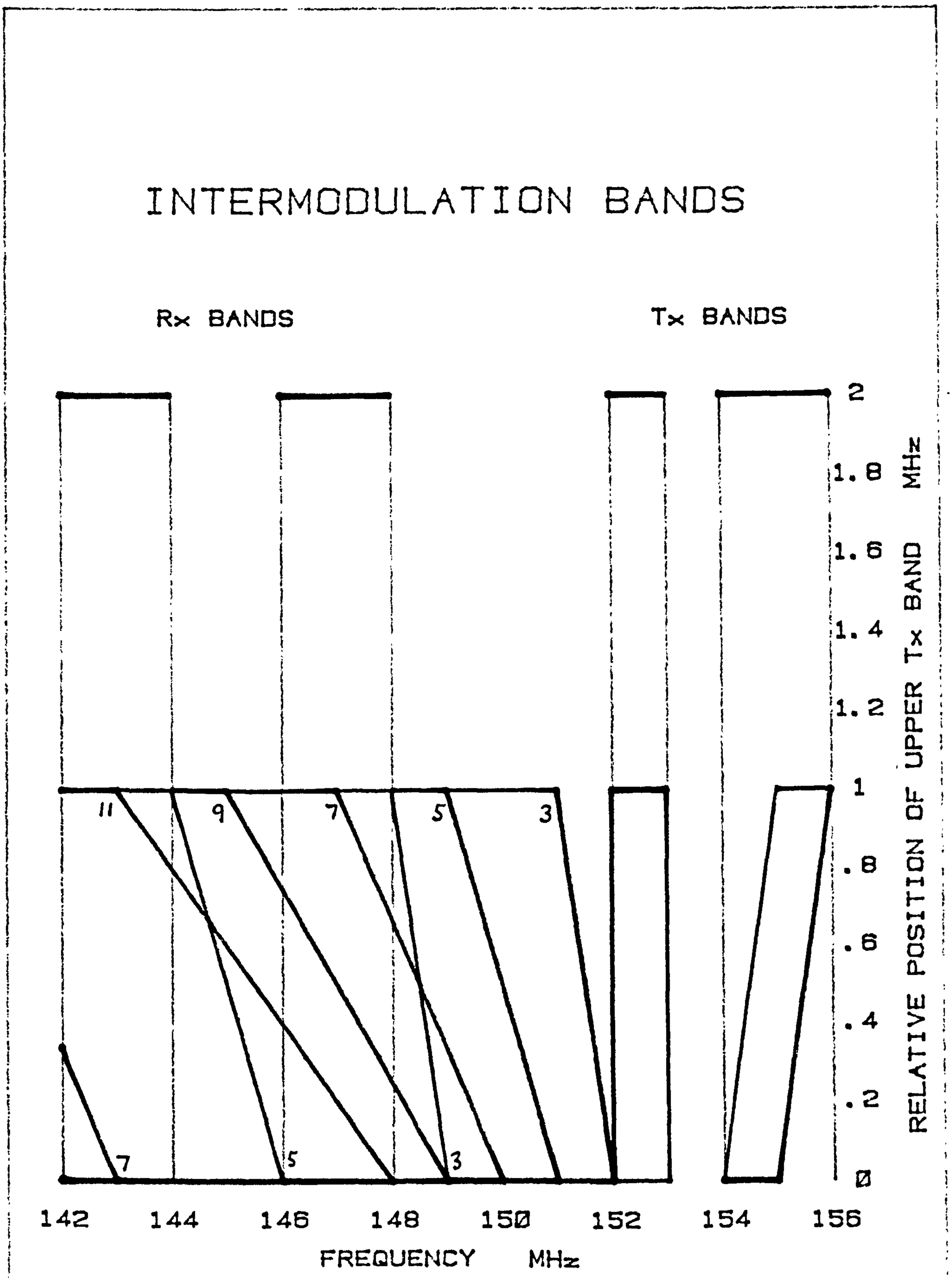

Fig. 12.3.4 Intermodulation Bands (152-153+1MHz)

INTERMODULATION BANDS

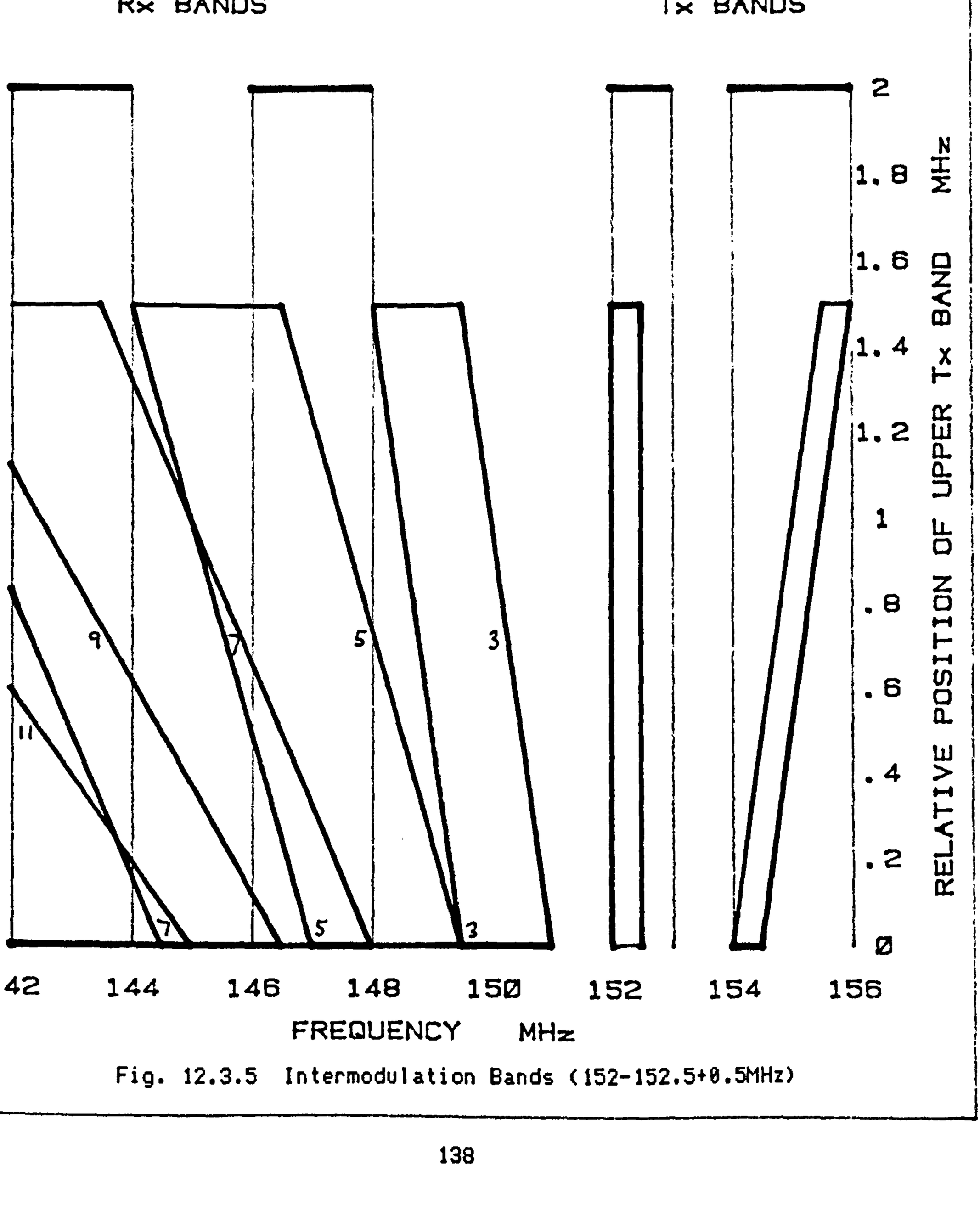

Fig. 12.3.5 Intermodulation Bands (152-152.5+0.5MHz)

INTERMODULATION BANDS

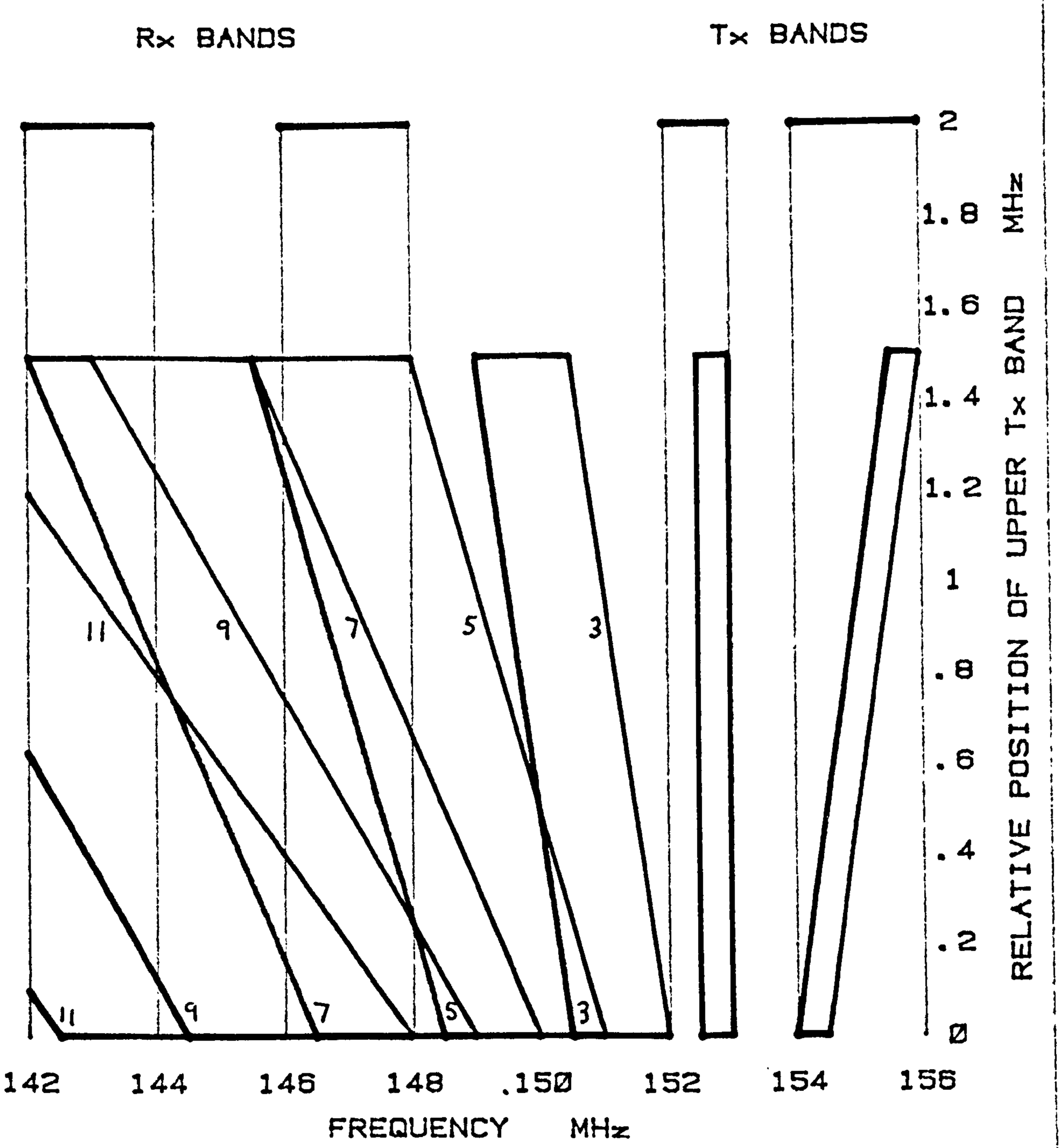

Fig. 12.3.6 Intermodulation Bands (152.5-153+0.5MHz)

$B-A = D-C = F-E$

TRANSMISSIONS (FUNDAMENTALS)	A B C D E F
TRANSMITTERS TURNED ON ACD AEF BCD BEF	
CAB CEF DAB DEF	
EAB ECD FAB FCD	
NUMBER OF PRODUCTS	2 2 2 2 2 2 2 2 2 2 2 2

Fig. 12.4.1 3rd Order Intermodulation - Stacking

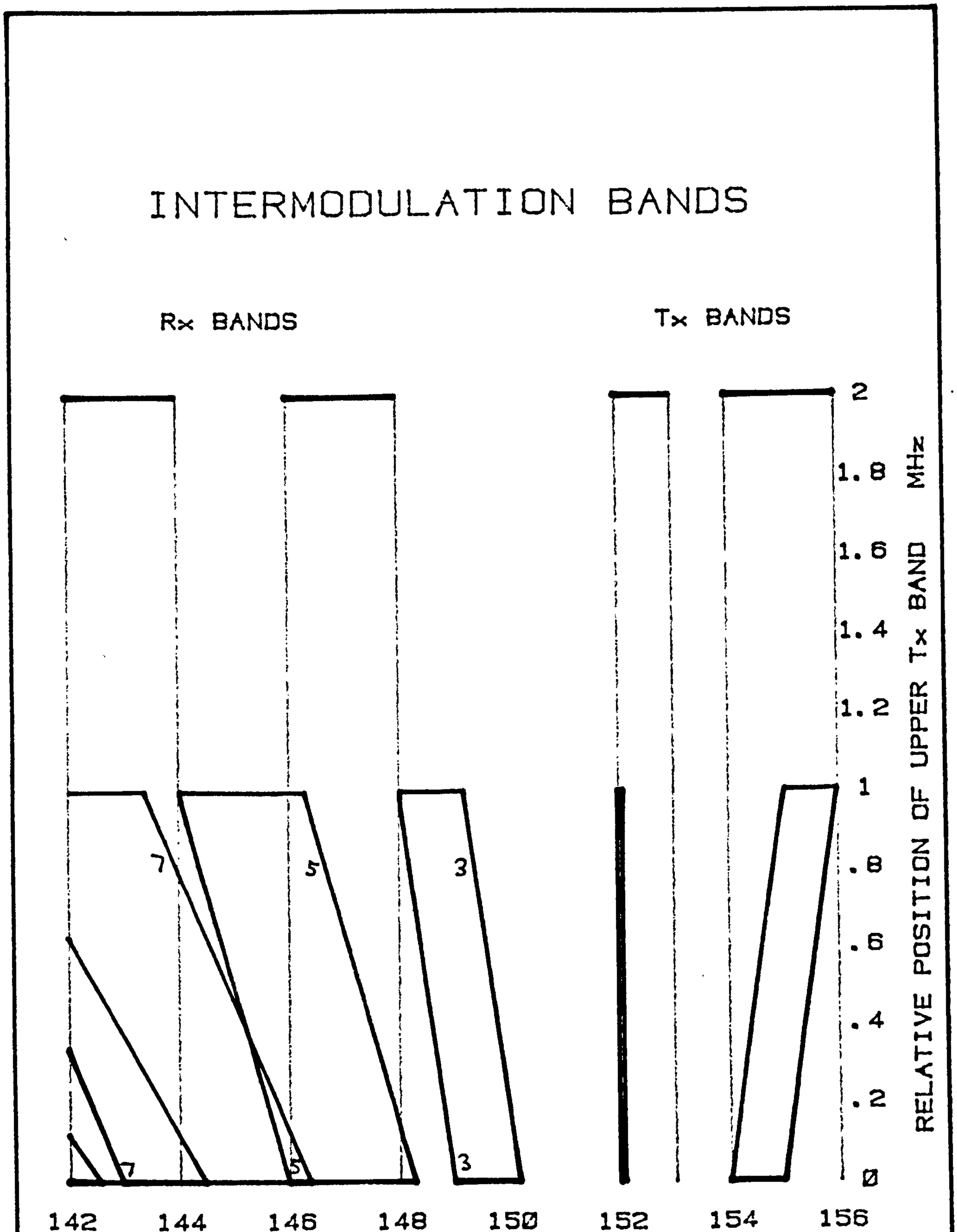

Fig. 12.4.2 Intermodulation Bands (152-152.1+1MHz)

INTERMODULATION BANDS

Fig. 12.4.3 Intermodulation Bands (152.5-152.6+1MHz)

INTERMODULATION BANDS

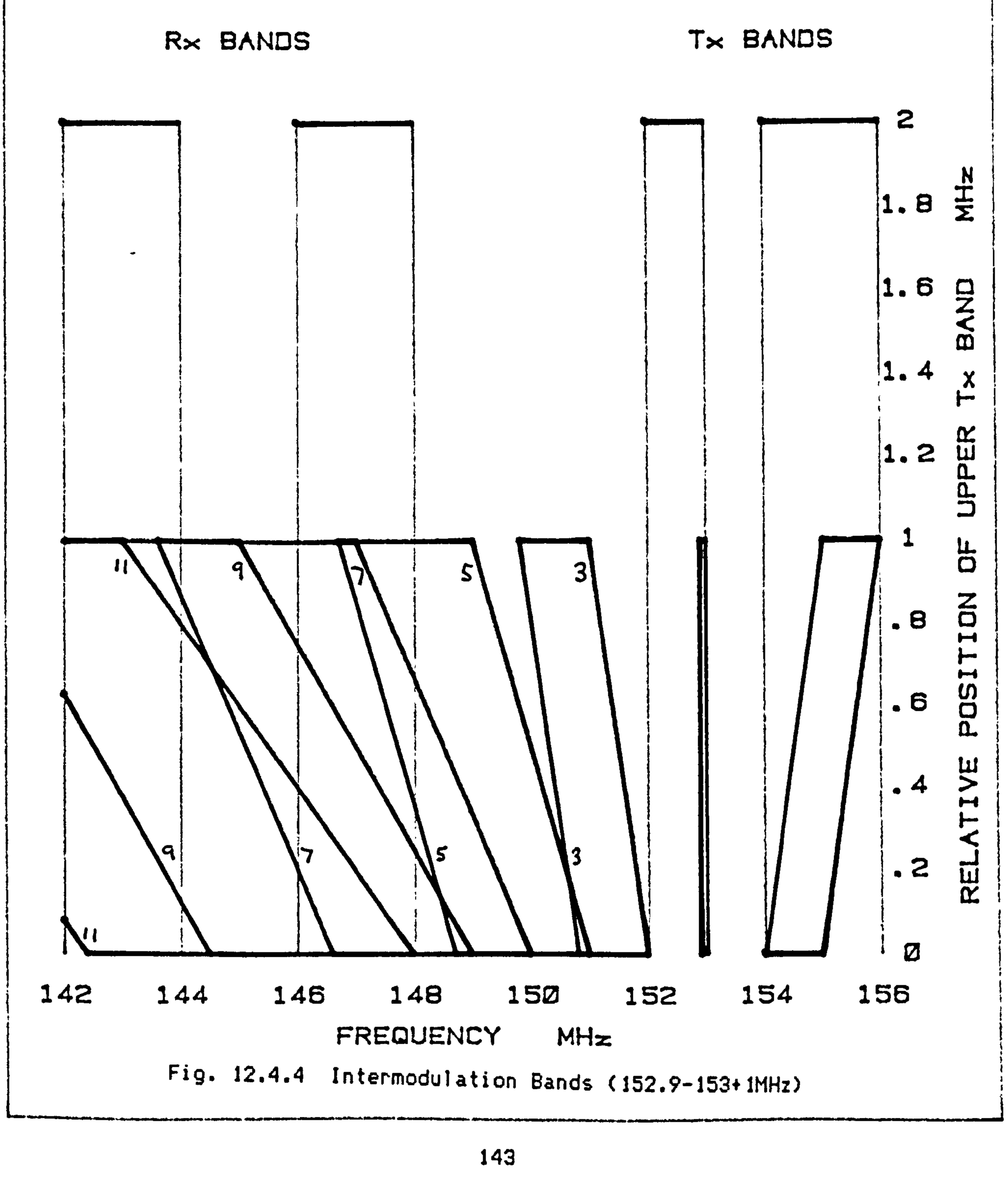

Fig. 12.4.4 Intermodulation Bands (152.9-153+1MHz)

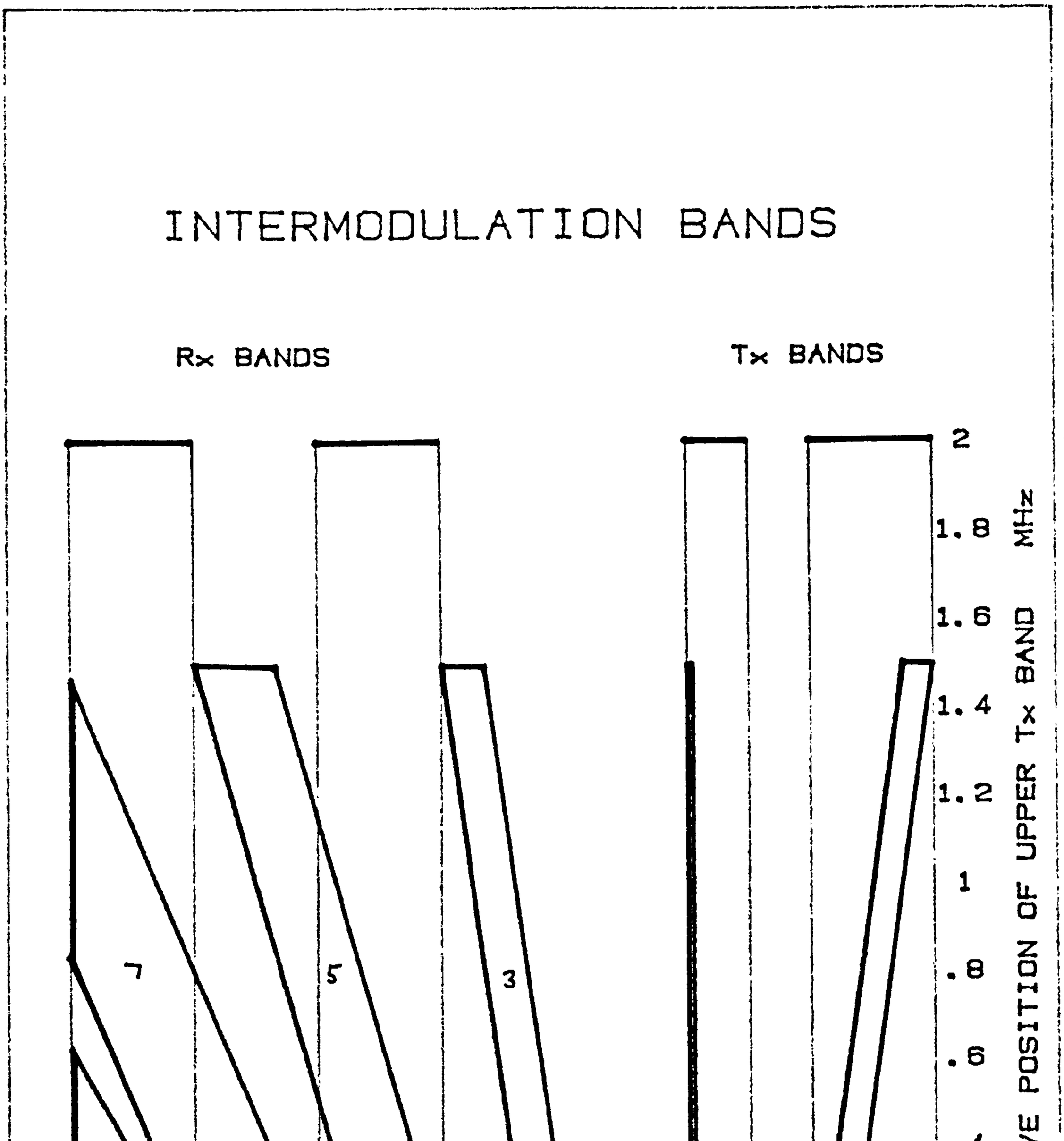

Fig. 12.4.5 Intermodulation Bands (152-152.1+0.5MHz)

INTERMODULATION BANDS

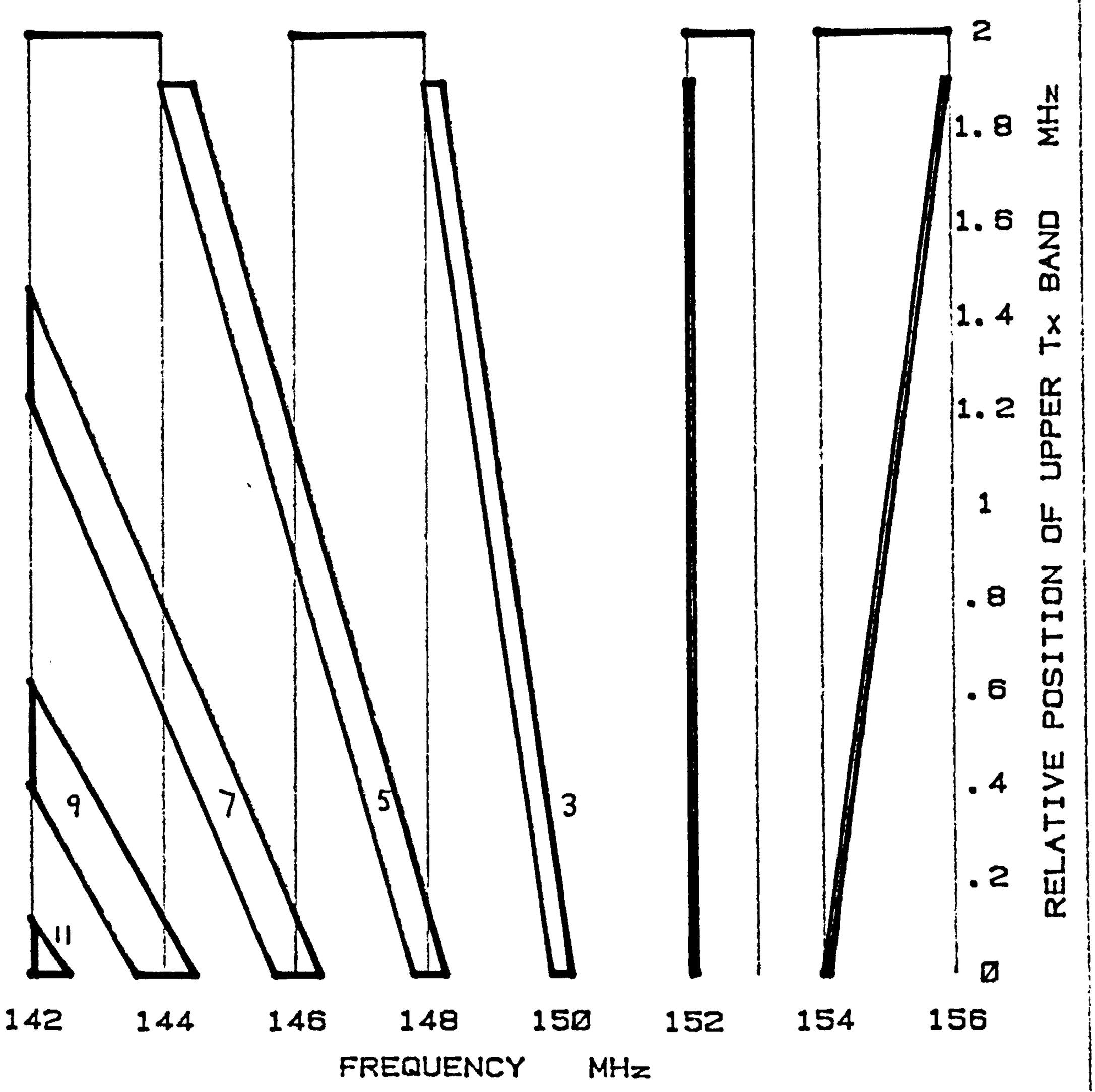

Fig. 12.5.1 Intermodulation Bands (152-152.1+0.1MHz)

INTERMODULATION BANDS

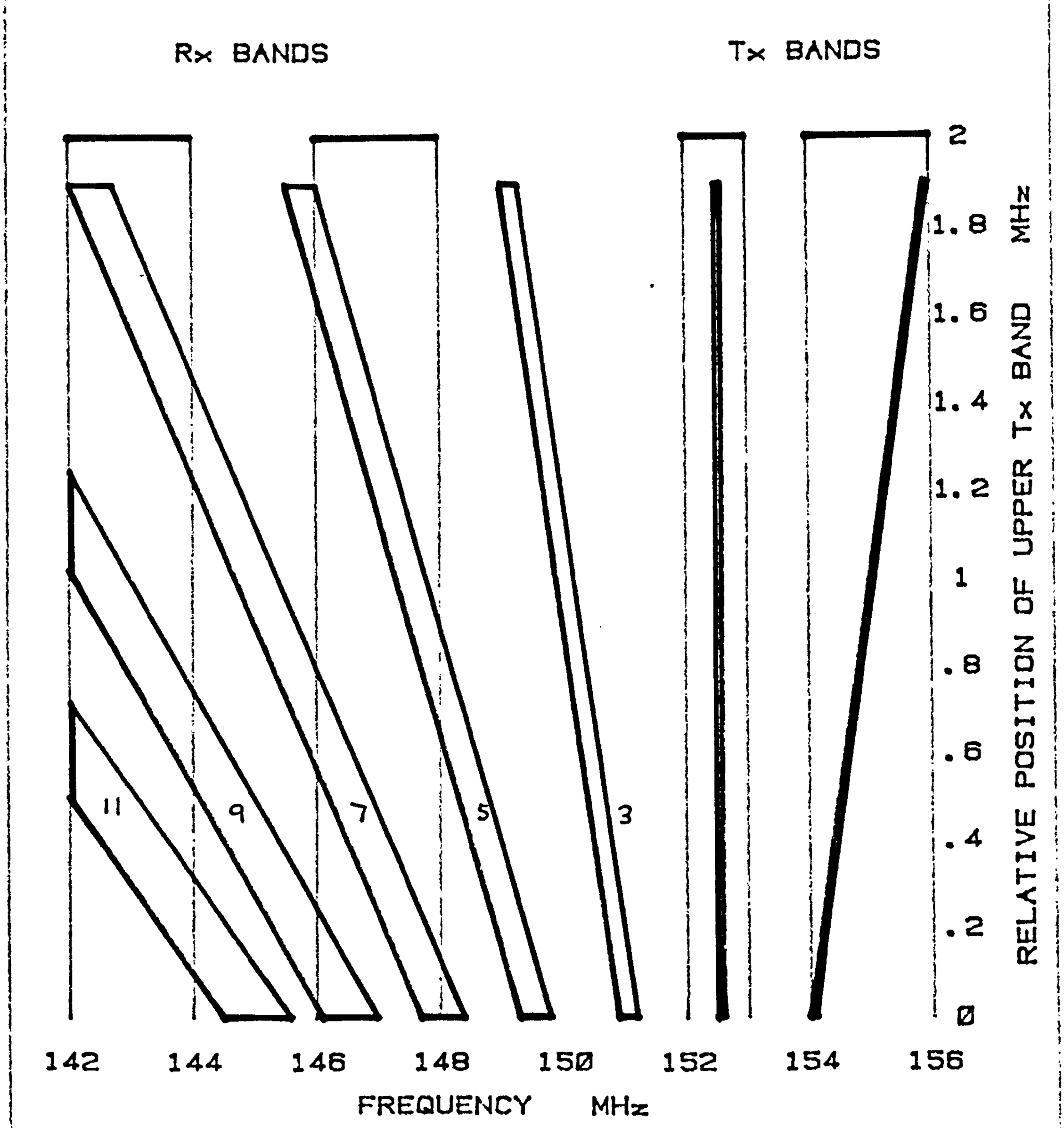

Fig. 12.5.2 Intermodulation Bands (152.5-152.6+0.1MHz)

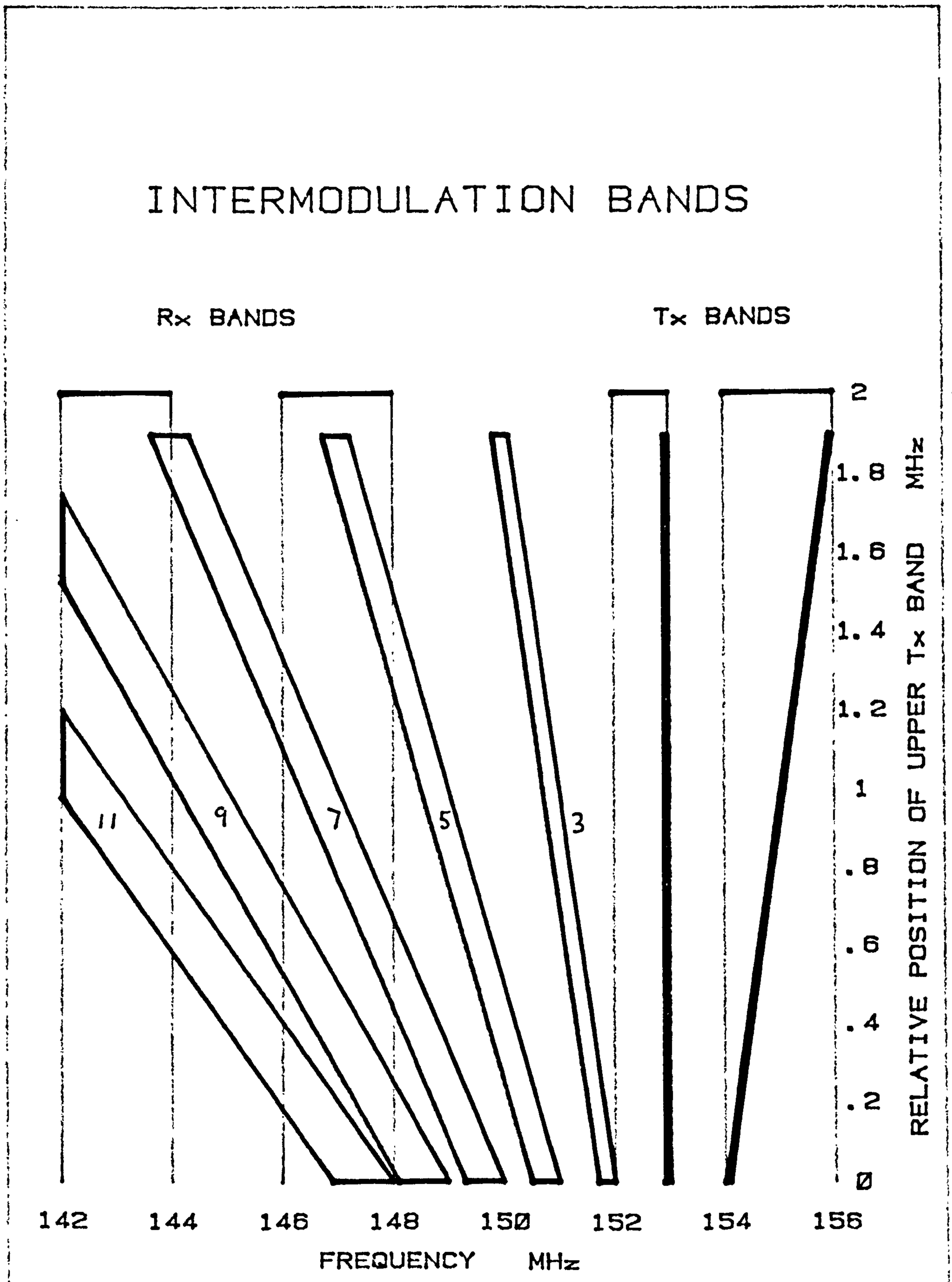

Fig. 12.5.3 Intermodulation Bands (152.7-153+0.1MHz)

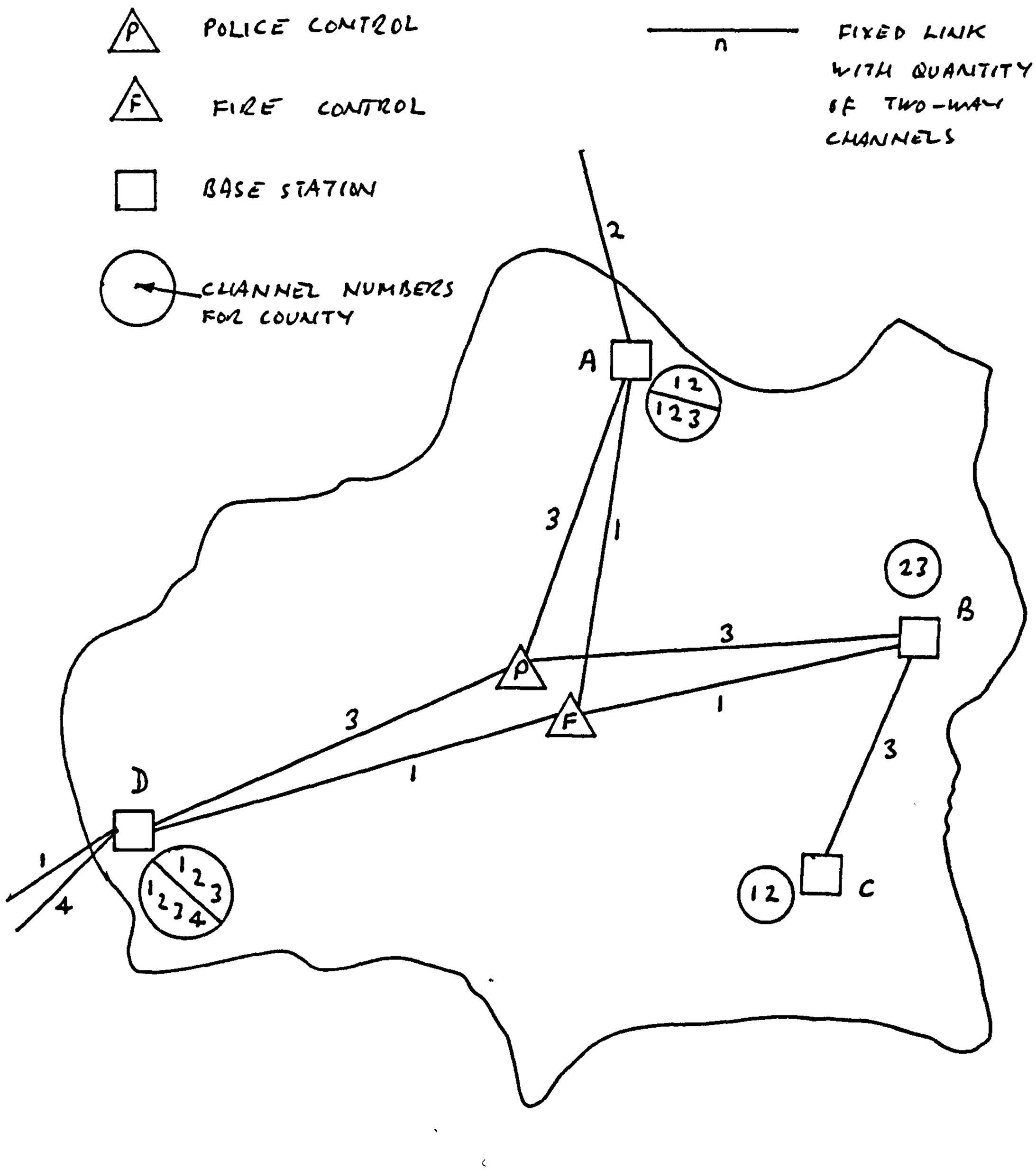

Fig. 13.1.1 An Illustrative County

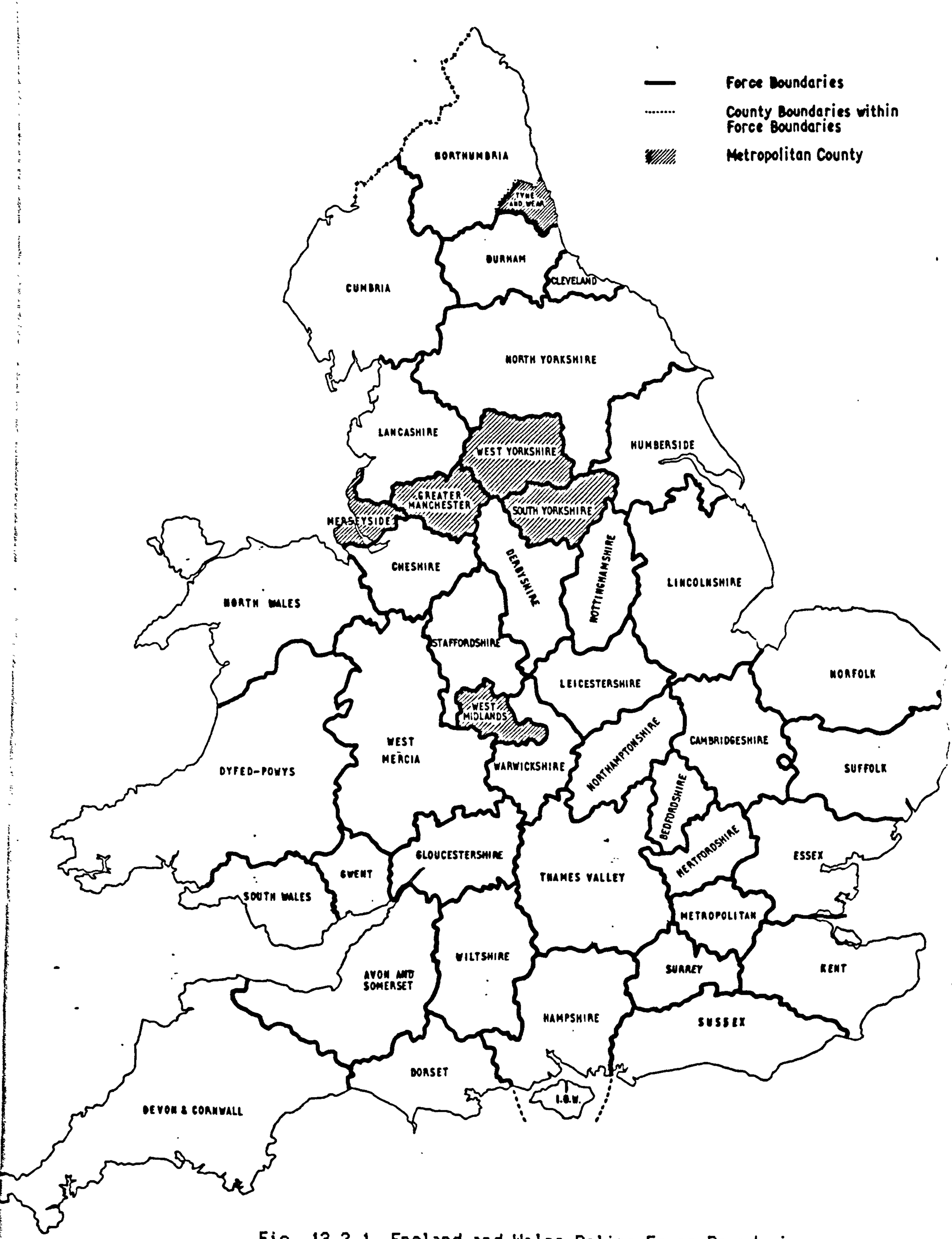

Fig. 13.2.1 England and Wales Police Force Boundaries

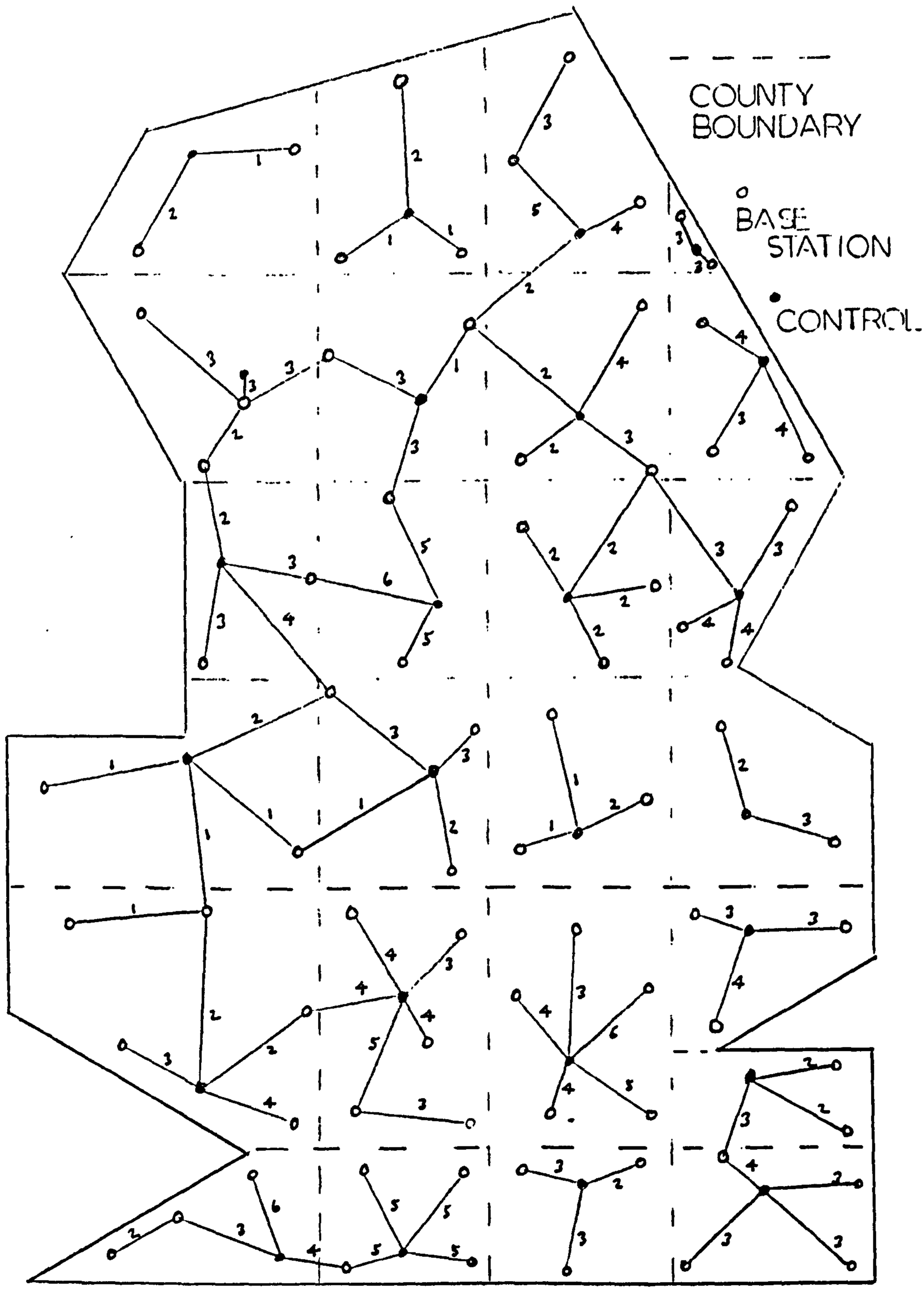

Fig. 13.2.2 Idealised Link Map of England and Wales

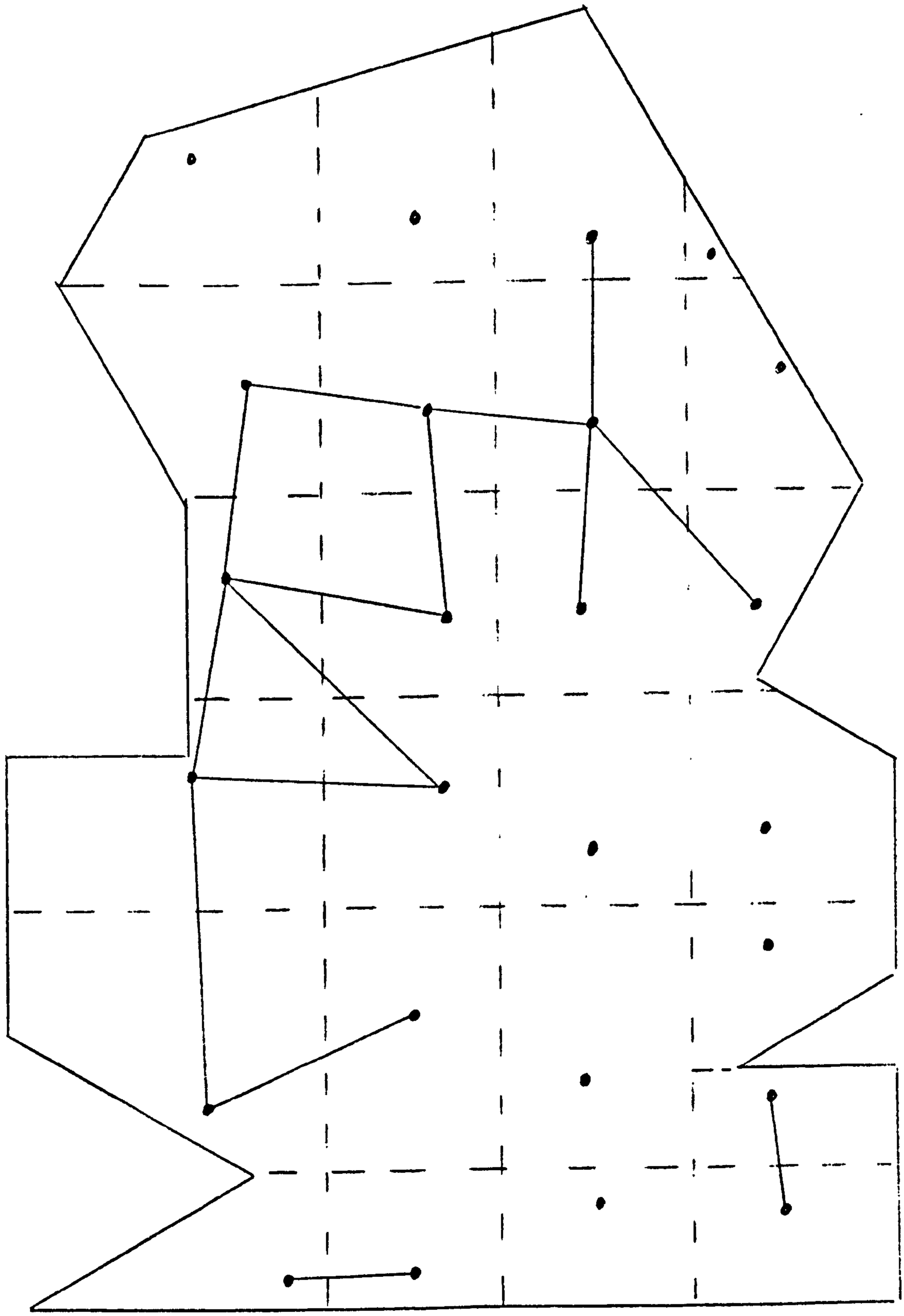

Fig. 13.2.3 Idealised Chaining Map of England and Wales

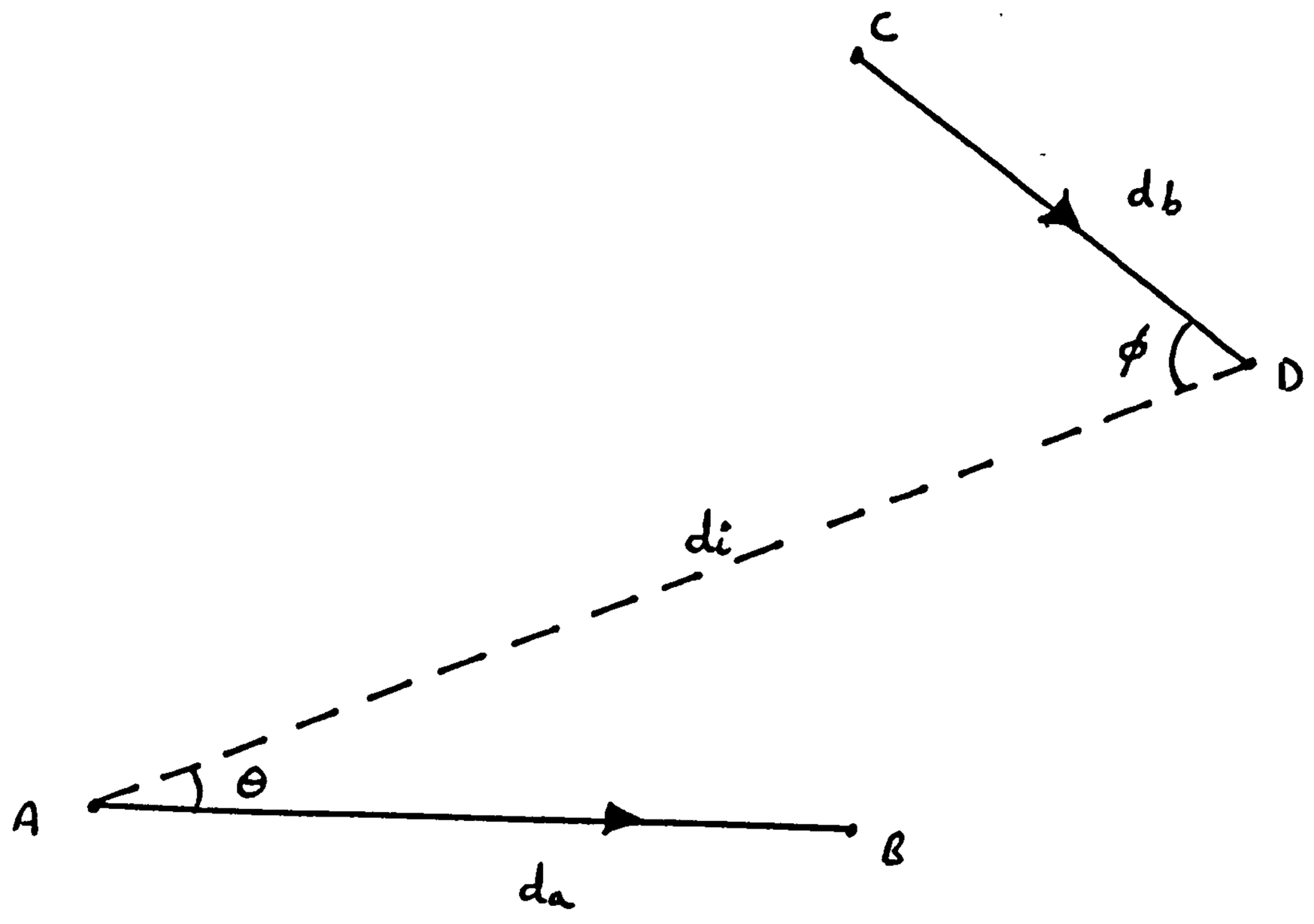

Fig. 13.3.1 Link Reuse Diagram

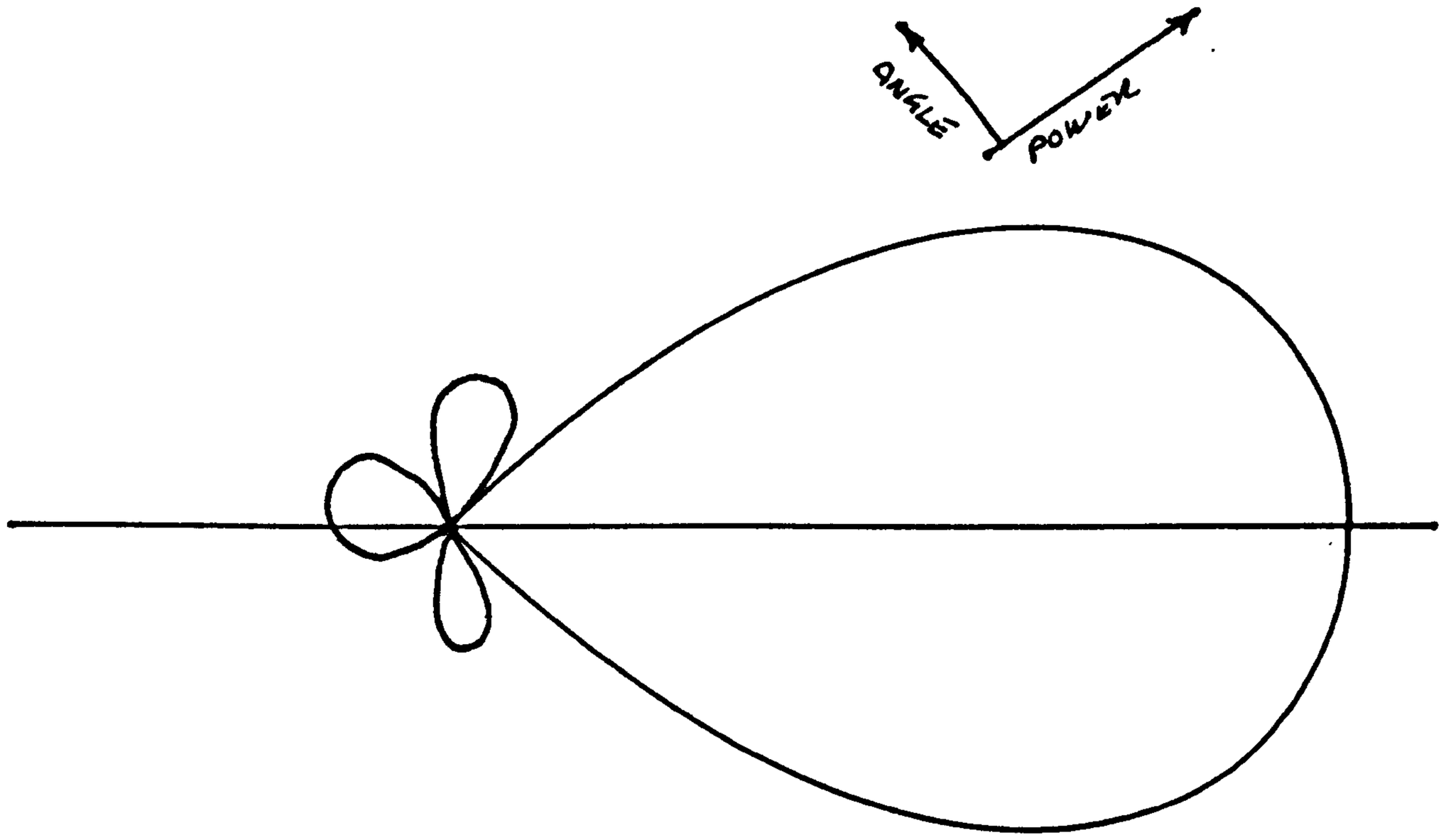

Fig. 13.3.2 Polar Response of 6 Element Yagi Aerial

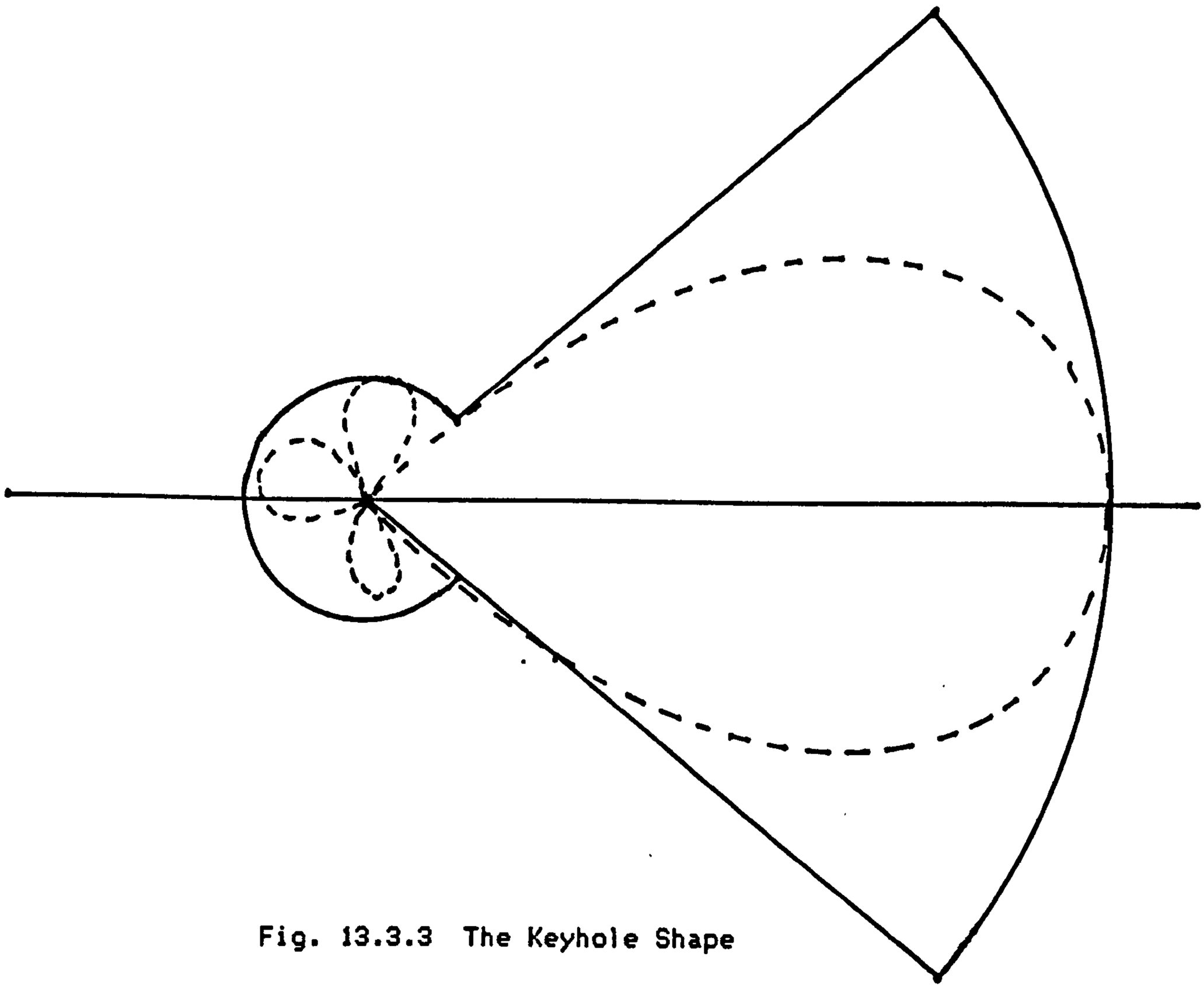

Fig. 13.3.3 The Keyhole Shape

Fig. 13.3.4 The Keyhole with Protection Ratio Scale

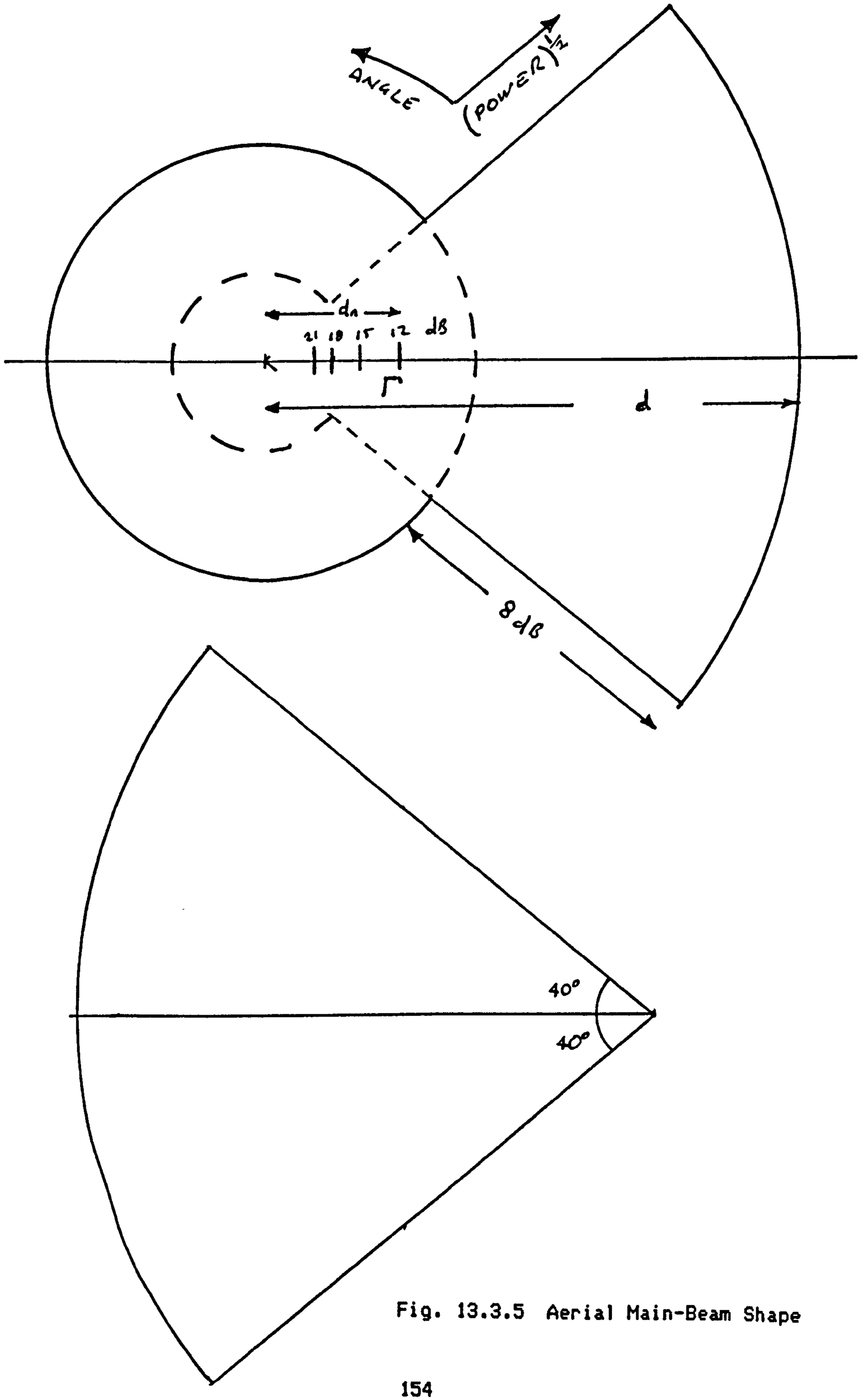

Fig. 13.3.5 Aerial Main-Beam Shape

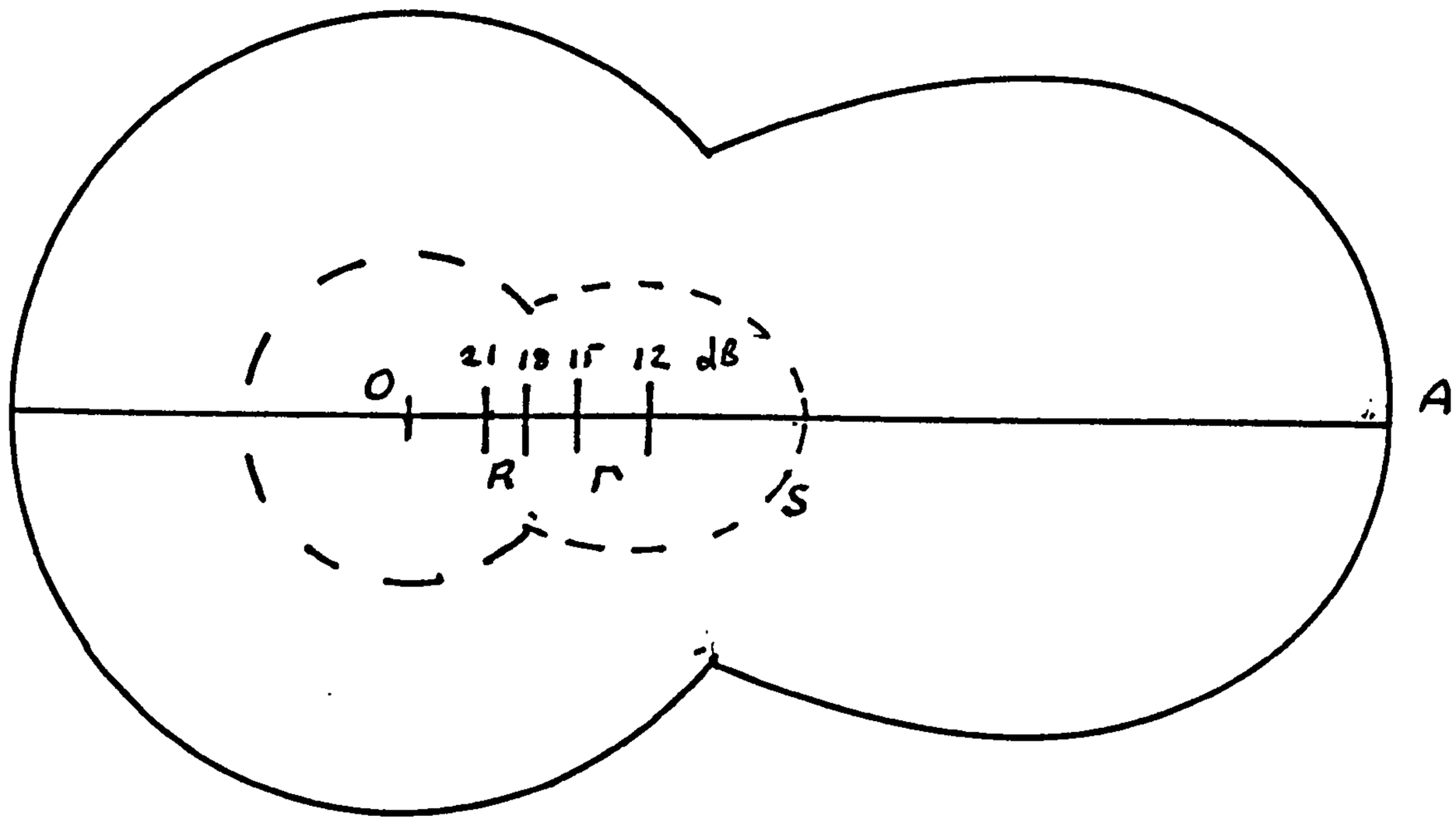

Fig. 13.3.6 The Refined Keyhole

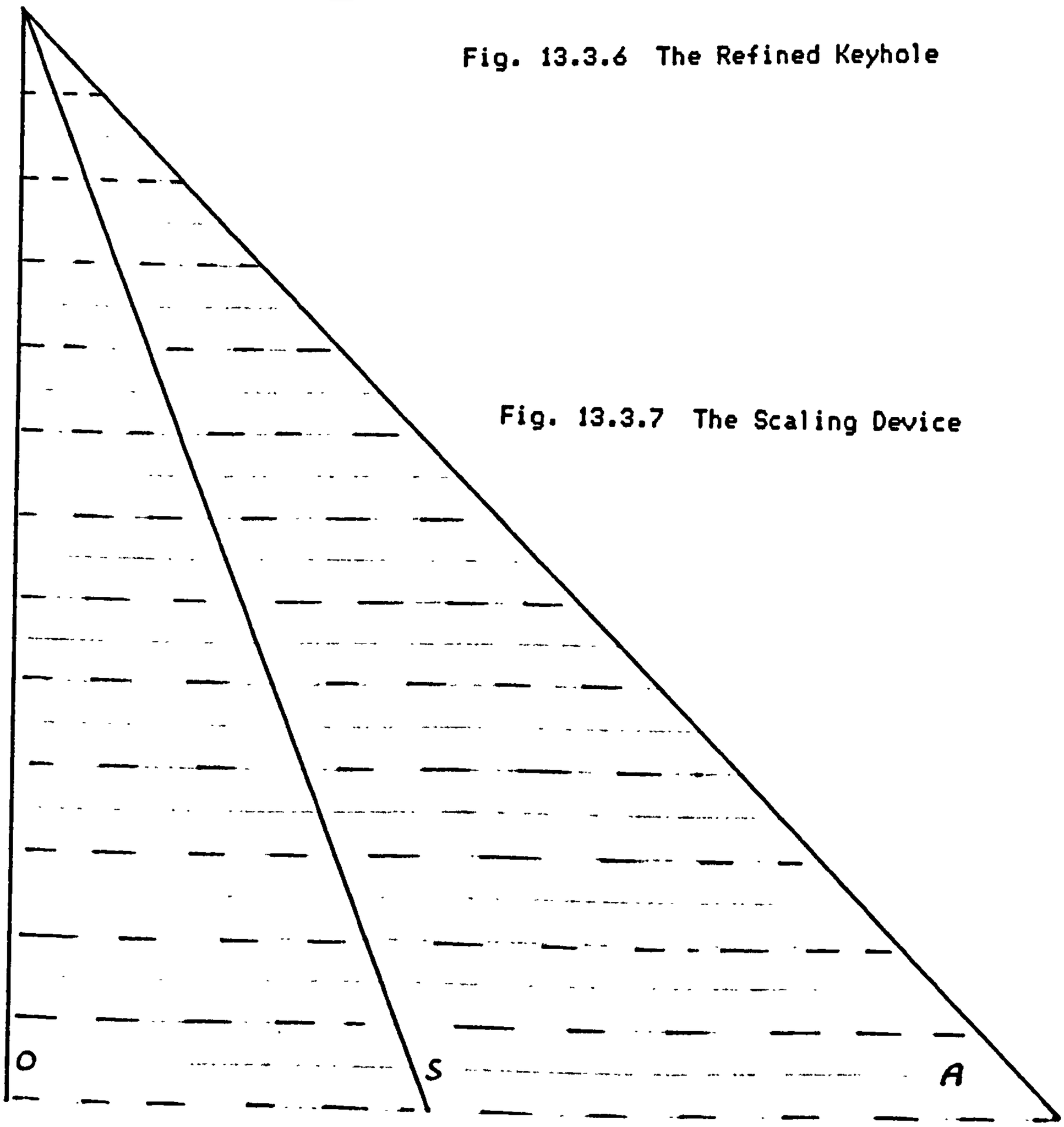

Fig. 13.3.7 The Scaling Device

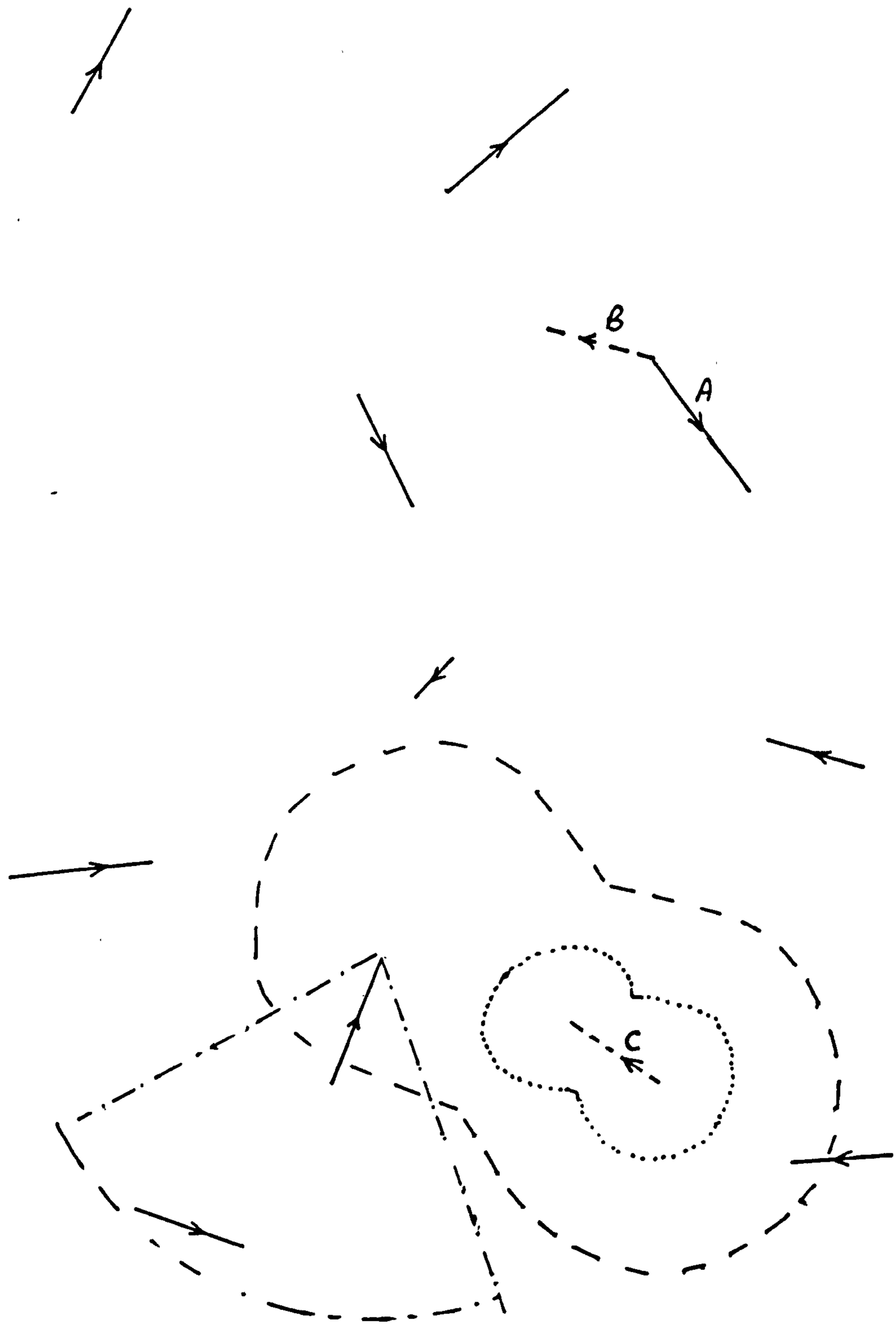

Fig. 13.3.8 Use of Link Reuse Overlay and Keyhole

Channel No. / Location	37	38	39	40	41	42	43	44	45	46	47
County M											
Site V			1	3			3	2	1		
County N								→			

Fig. 13.4.1 Channel Allocation at a Shared Site

Channel No. / Location	37	38	39	40	41	42	43	44	45	46	47
County M		4	2	1	3						
Site V				1	3		3	2	1		
County N							3	2	1	5	4

Fig. 13.4.2 Channel Allocation for Counties at a Shared Site

Channel No. / Location	31	32	33	34	35	36	37	38	39	40	41	42	43	44	45	46	47	48	49	50	51
County L	2	3	5	1	4	6															
Site U				1	4	6			2	1											
County M								4	2	1	3										
Site V										1	3		3	2	1						
County N													3	2	1	5	4				
Site W															1	5	4		2	1	
County O																			2	1	3

Fig. 13.4.3 Channel Allocation for Several Chaining Counties

Channel Number	
Location, County or Site No.	
C1	
S1	
C2	
S2	
C3	
S3	
C4	
S4	
C5	
S5	
C6	
S6	
C7	
S7	
C8	
S8	
C9	
S9	
C10	
S10	
C11	
S11	
C12	
S12	
C13	
S13	
C14	
S14	
C15	
S15	

Fig. 13.4.4 Form of Main Transmit Channel Allocations

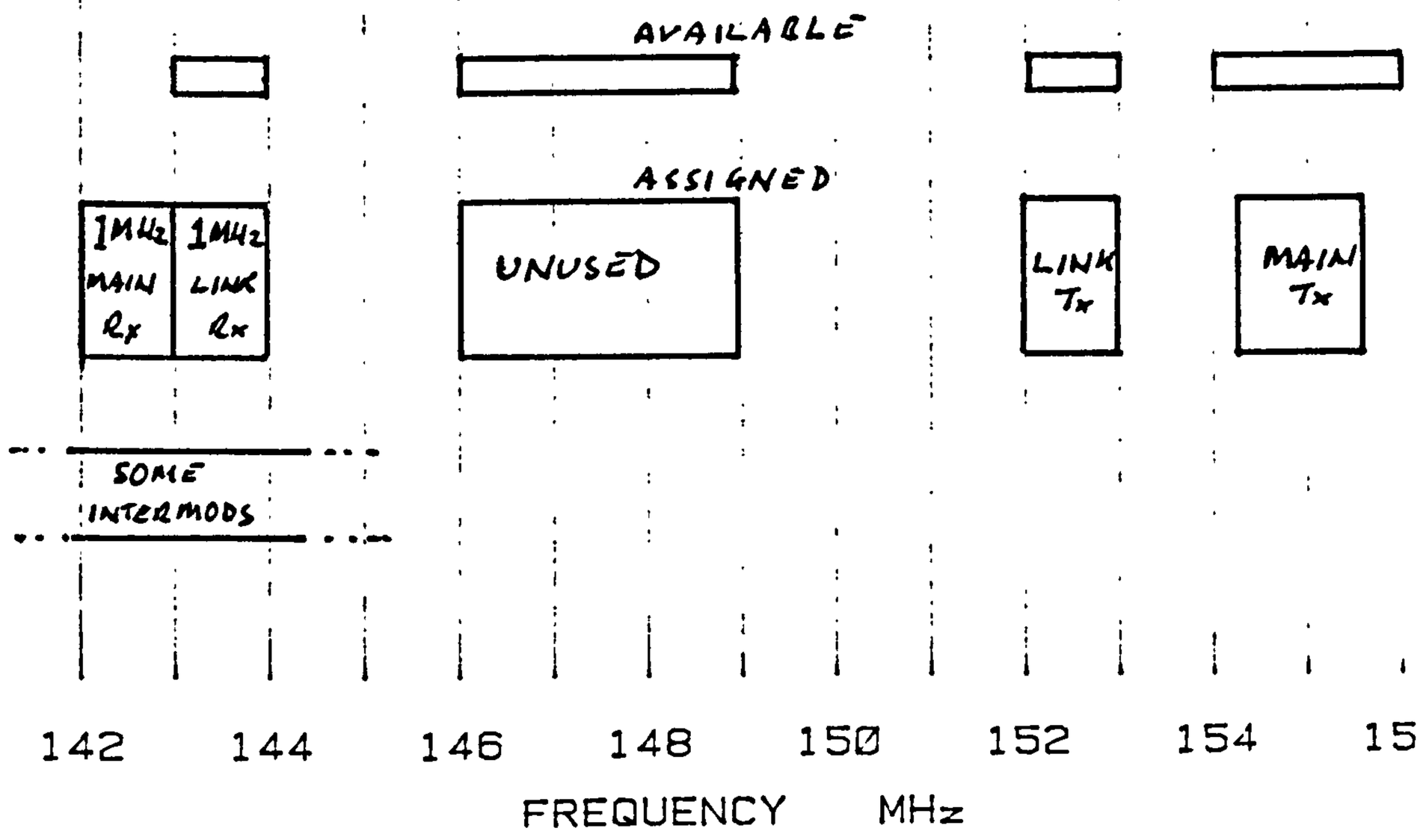

Fig. 13.7.1 Spectral Disposition of Block Assignments - to Date

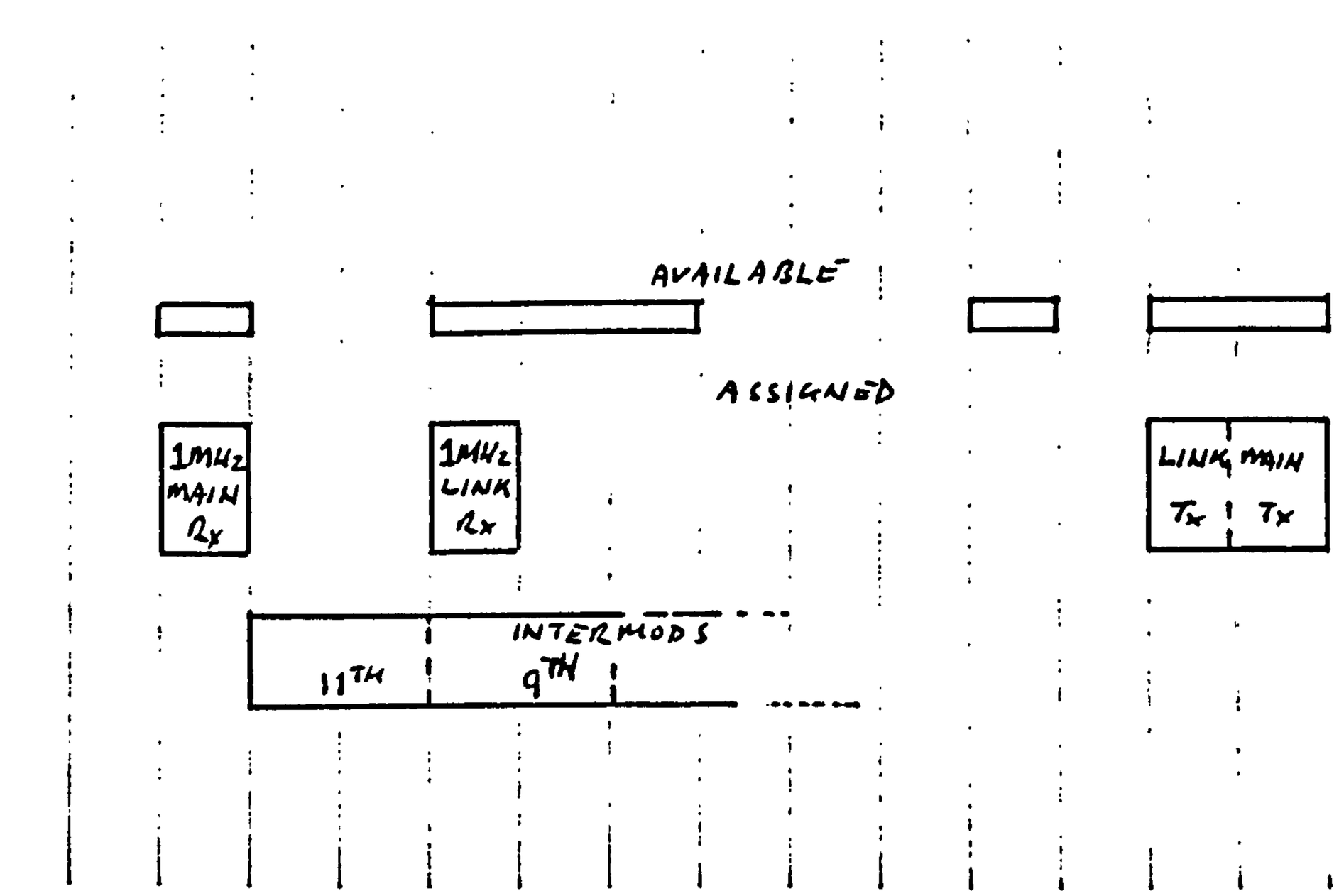

Fig. 13.7.2 An Alternative Spectral Disposition of Block Assignments

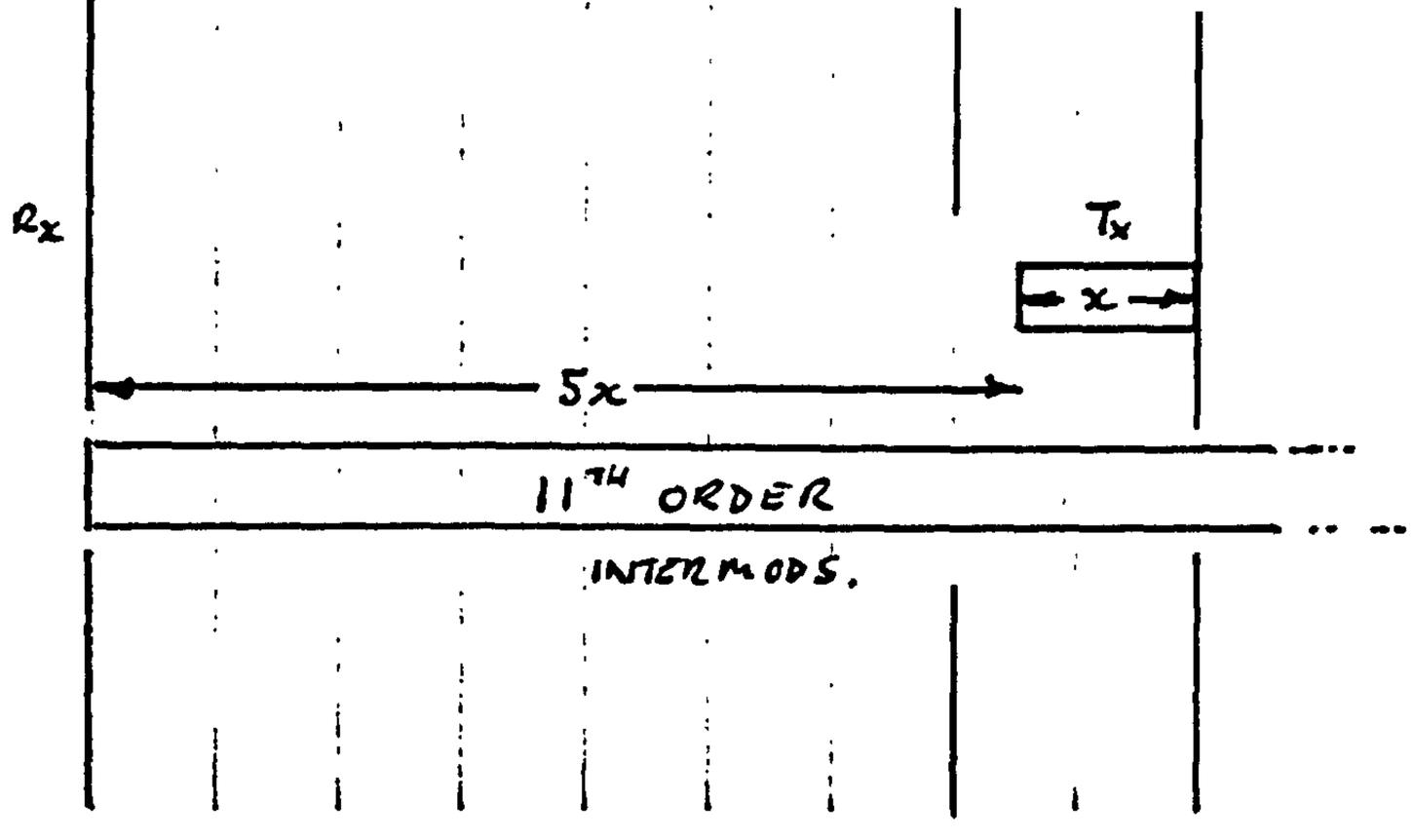

Fig. 13.7.3 High Order Intermodulation Situation

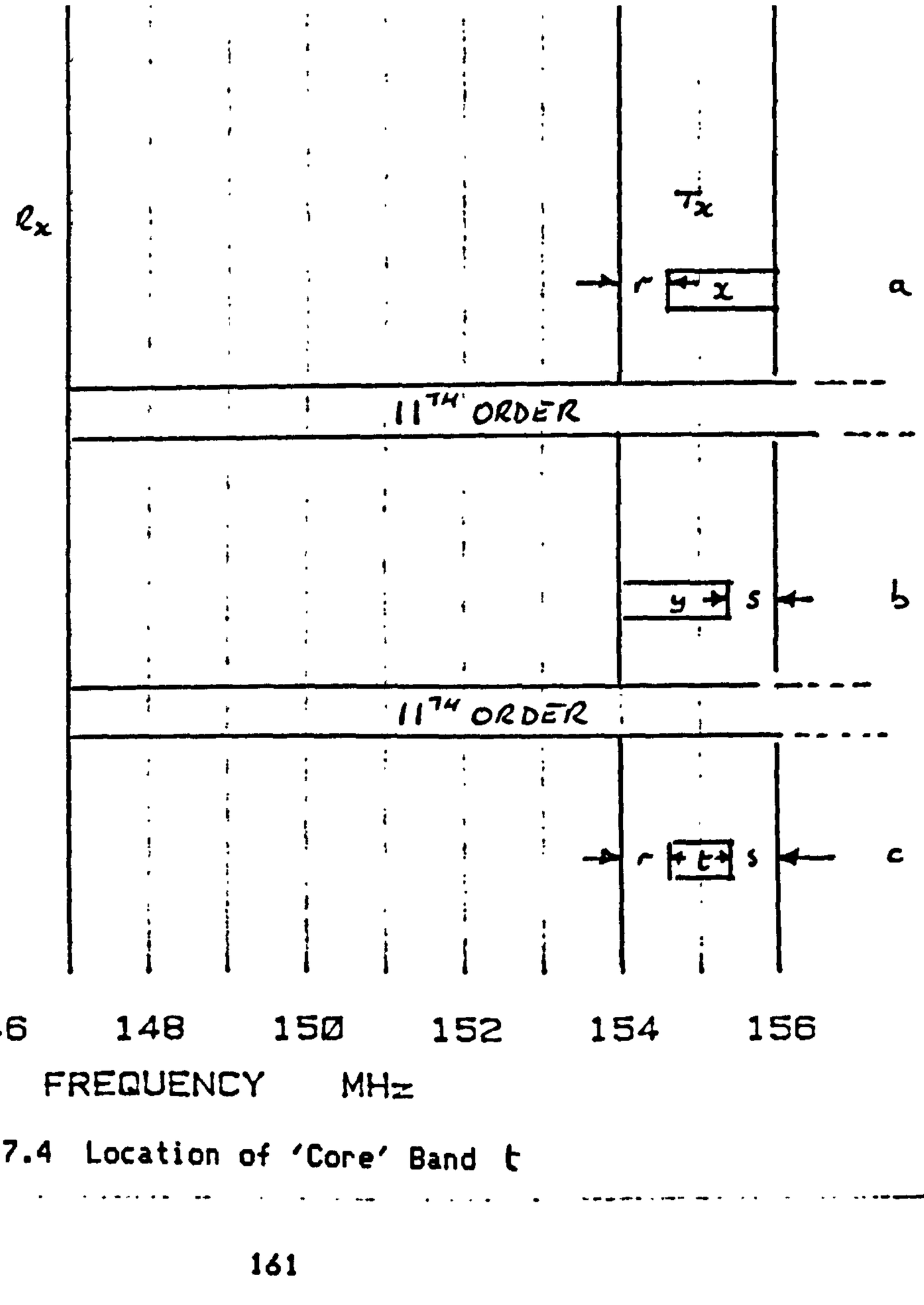

Fig. 13.7.4 Location of 'Core' Band t

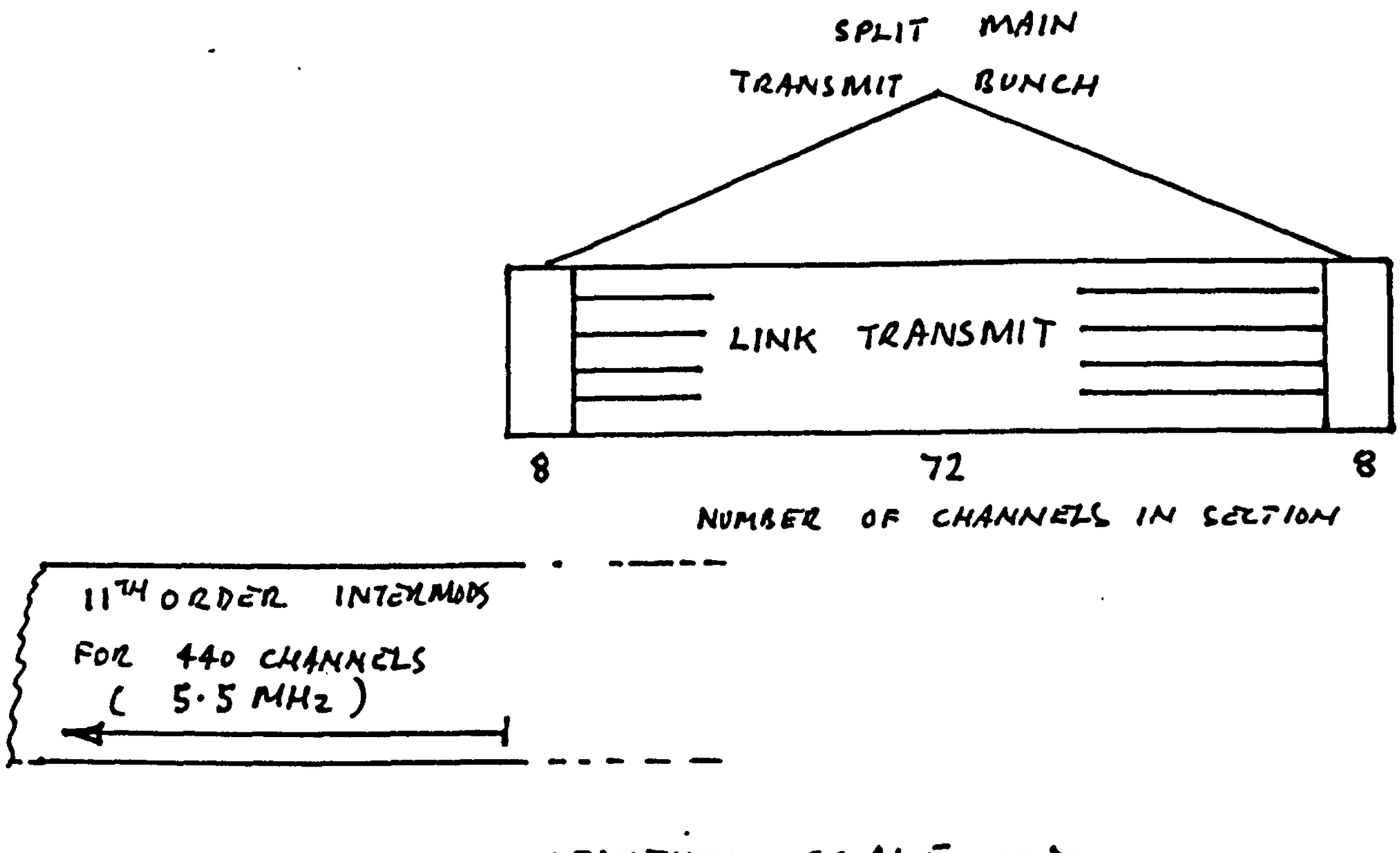

Fig. 13.7.5 A Split Chaining Allocation

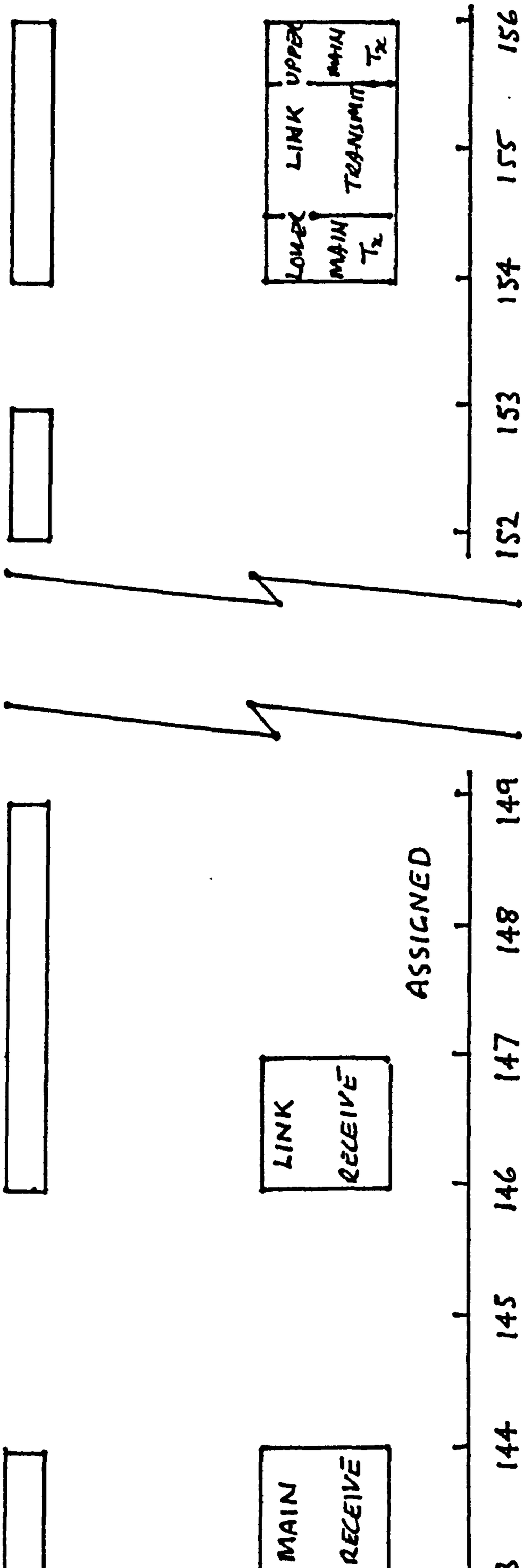

Fig. 13.7.6 A Better Spectral Disposition of Block Assignments

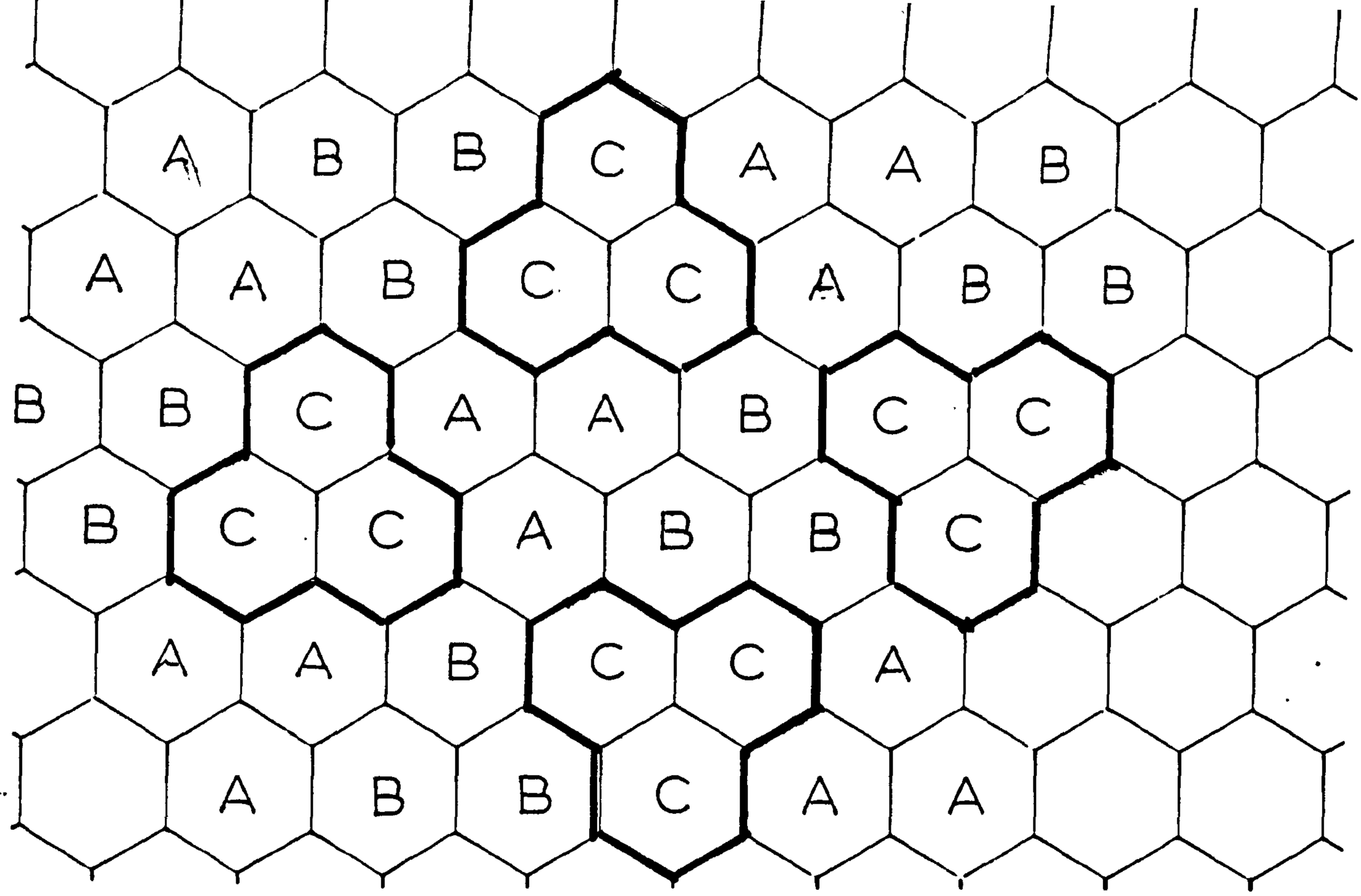

Fig. B.1(a) 3 Cell Cluster 3 Cluster Conglomerate

Fig. B.1(b) 3 Cell Cluster 4 Cluster Conglomerate

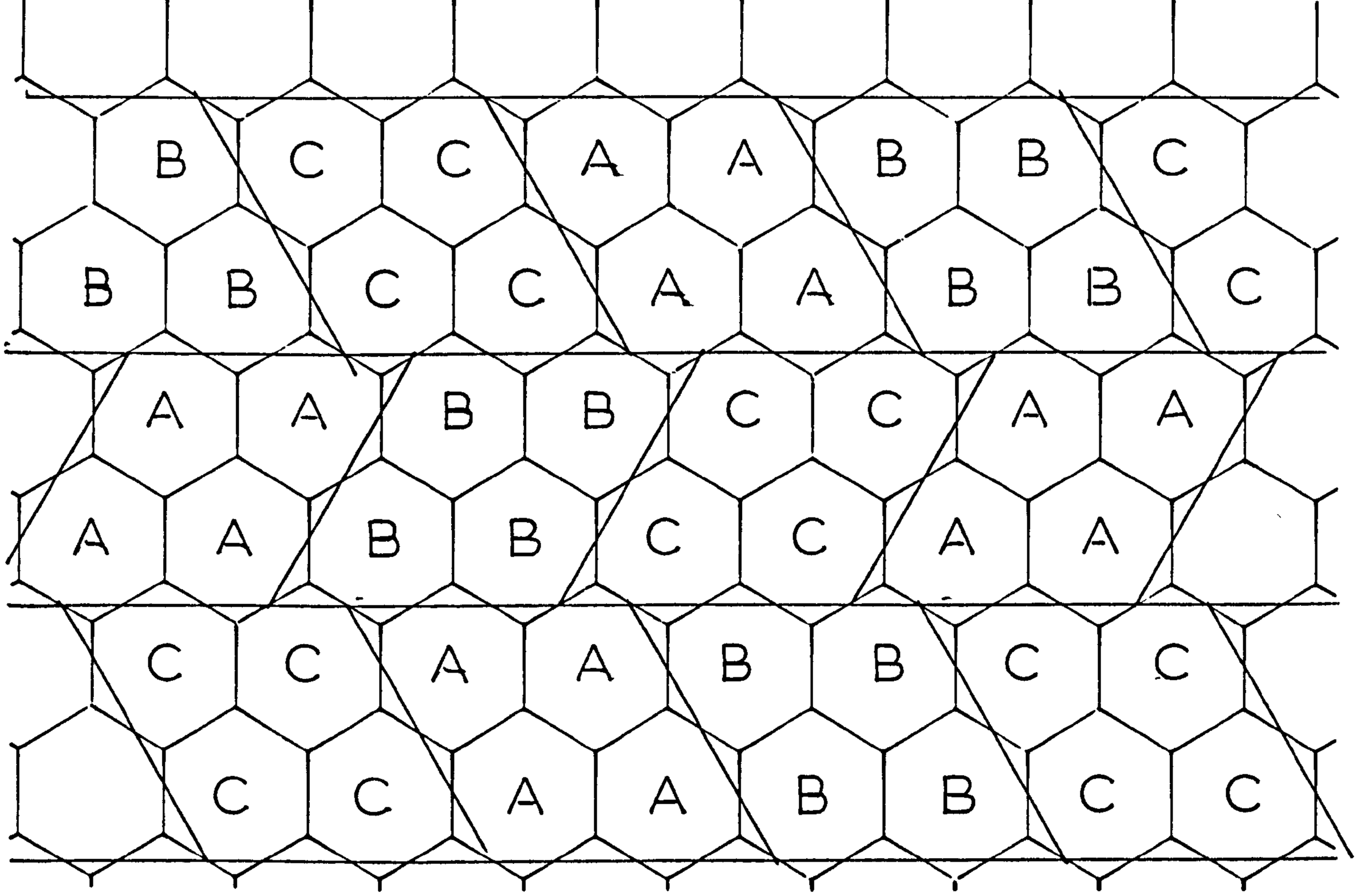

Fig. B.2 4 Cell Cluster 3 Cluster Conglomerate

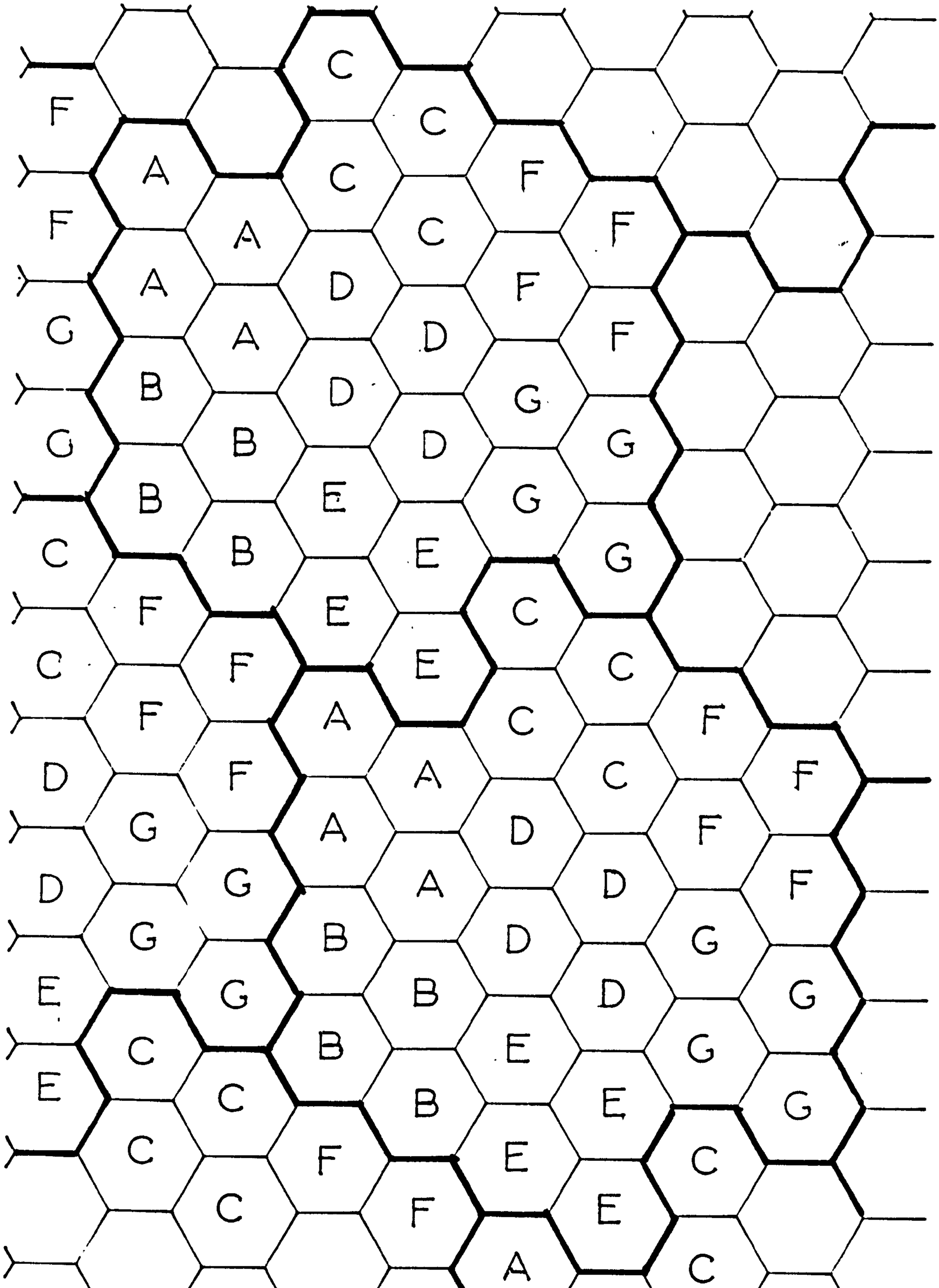

Fig. B.3 4 Cell Cluster 7 Cluster Conglomerate

Fig. B.4 7 Cell Cluster 3 Cluster Conglomerate

Fig. B.5 7 Cell Cluster 4 Cluster Conglomerate

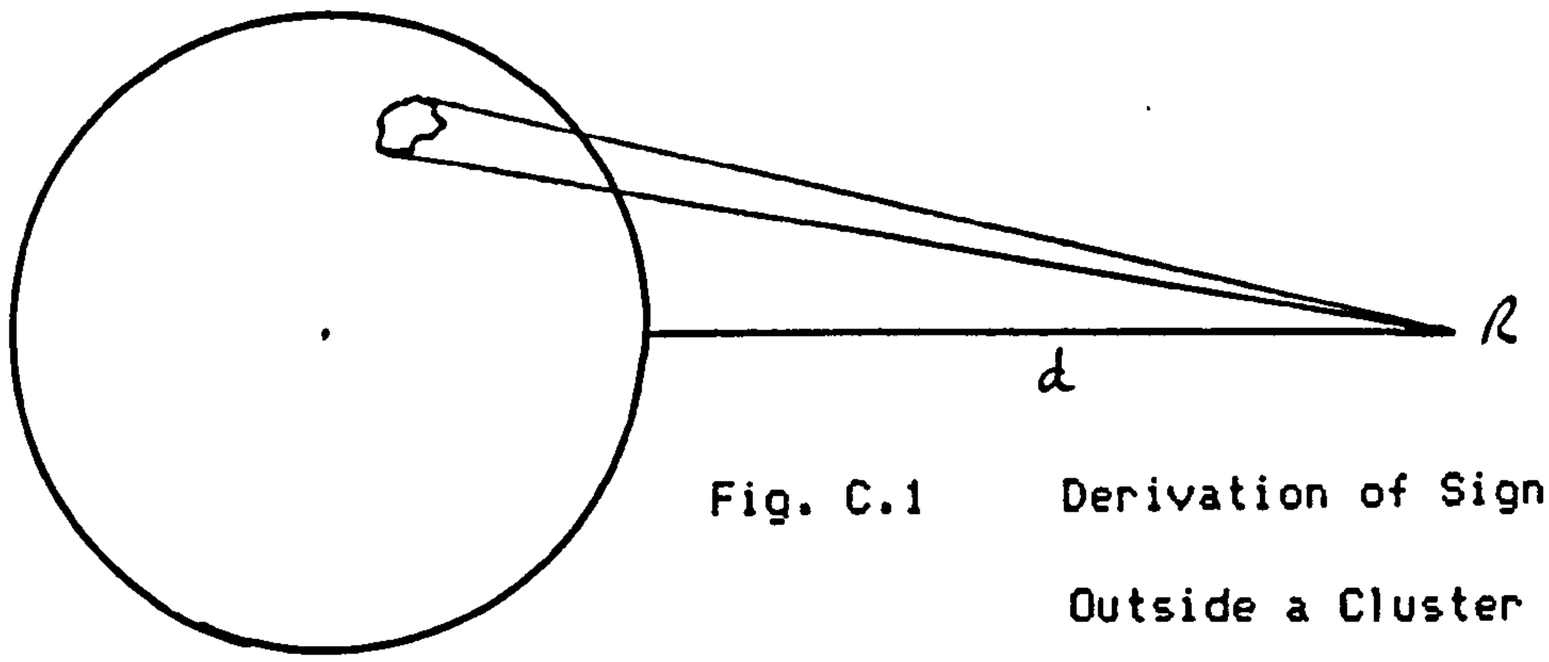

Fig. C.1 Derivation of Signal Level Outside a Cluster

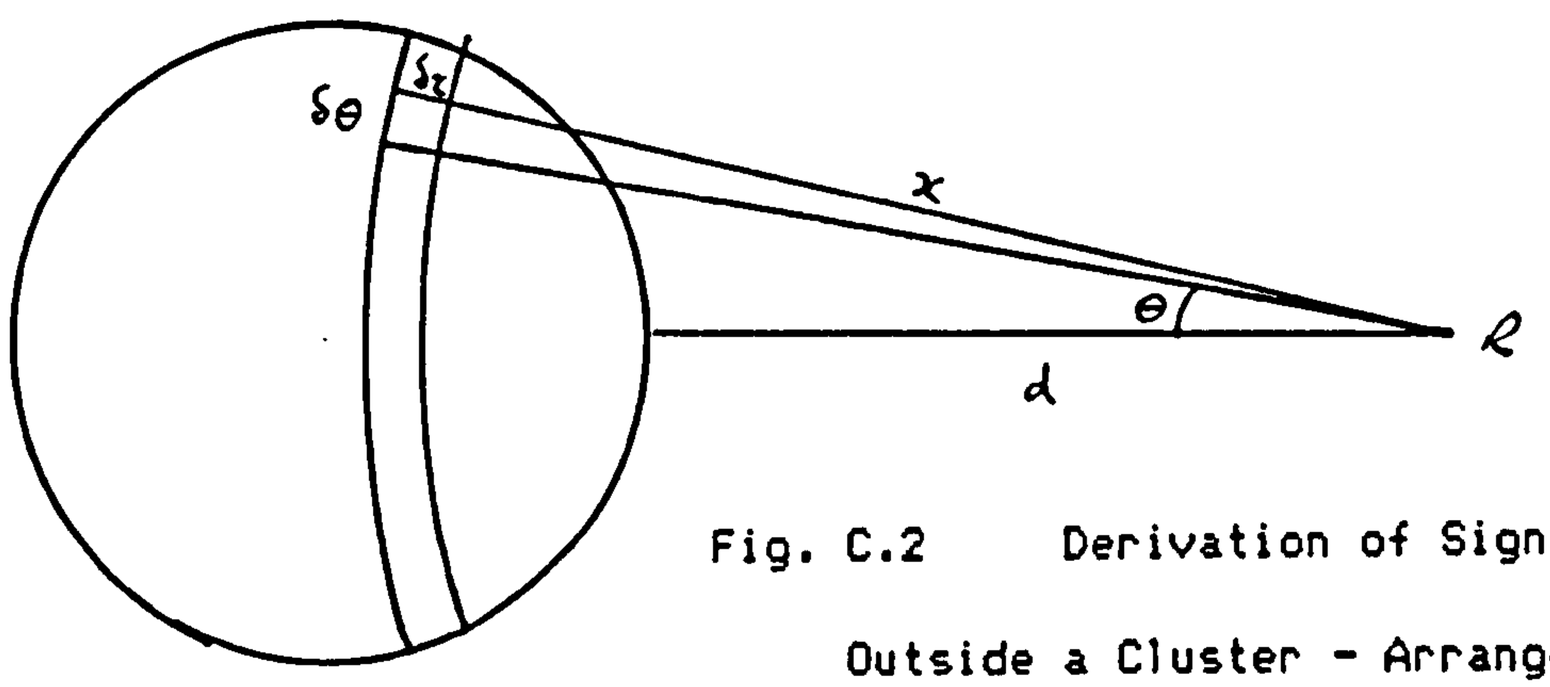

Fig. C.2 Derivation of Signal Level Outside a Cluster - Arrangement I

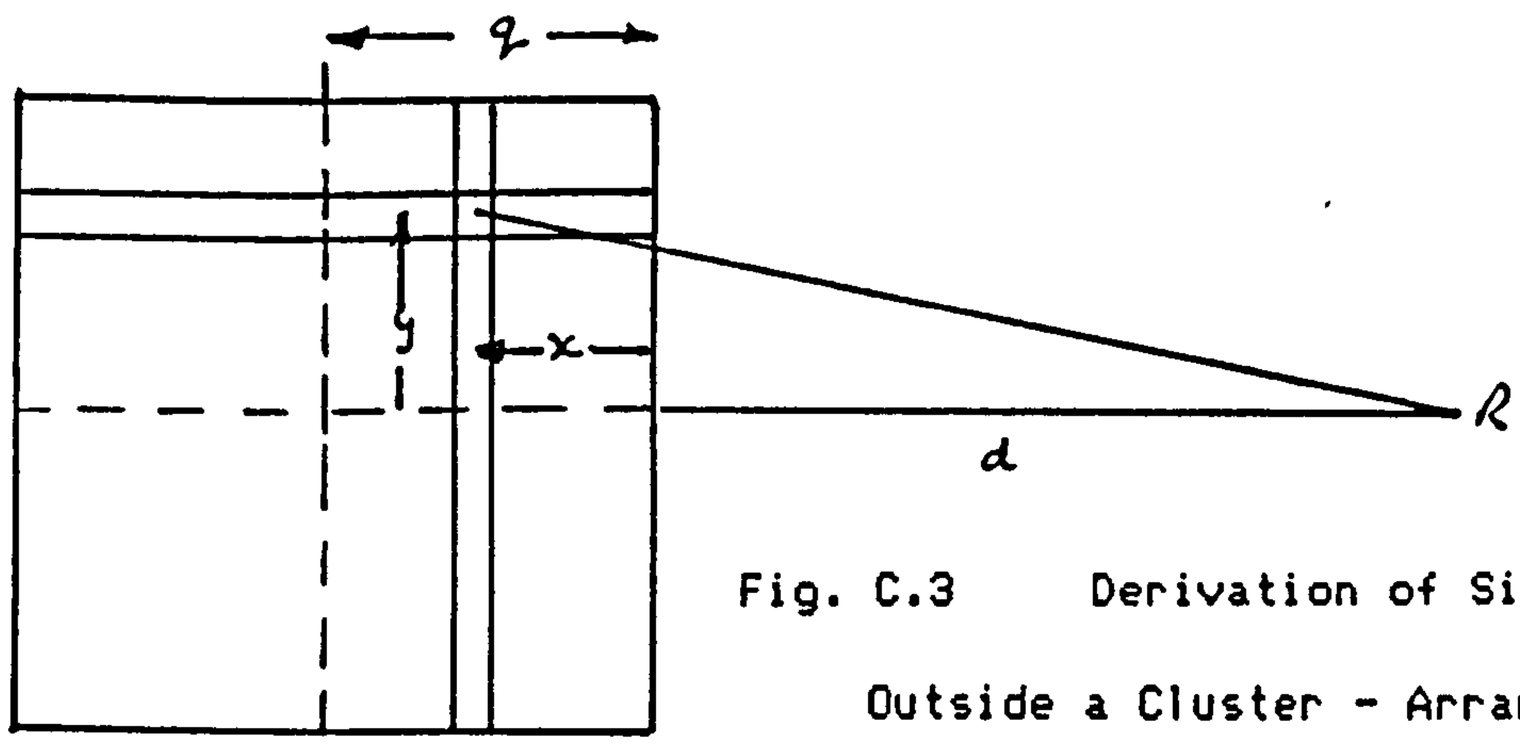

Fig. C.3 Derivation of Signal Level Outside a Cluster - Arrangement II

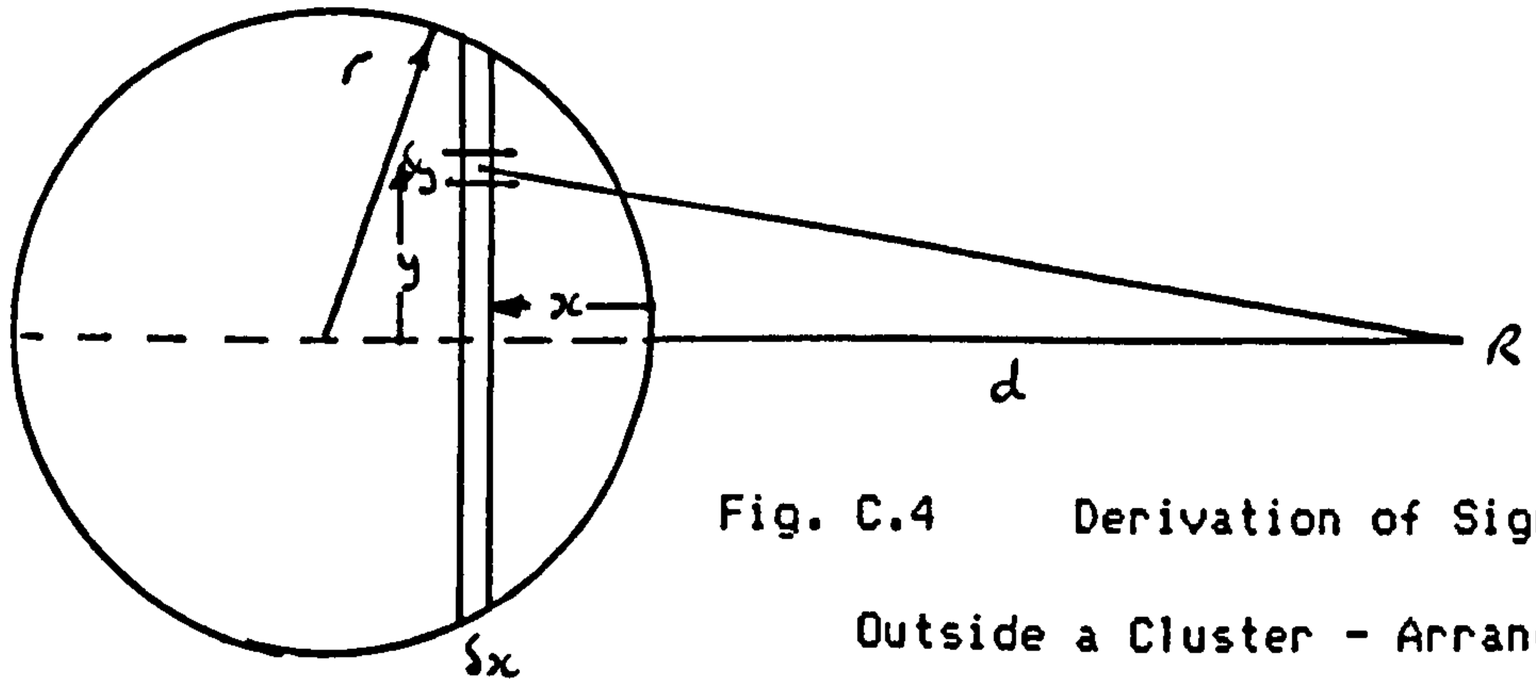

Fig. C.4 Derivation of Signal Level Outside a Cluster - Arrangement III

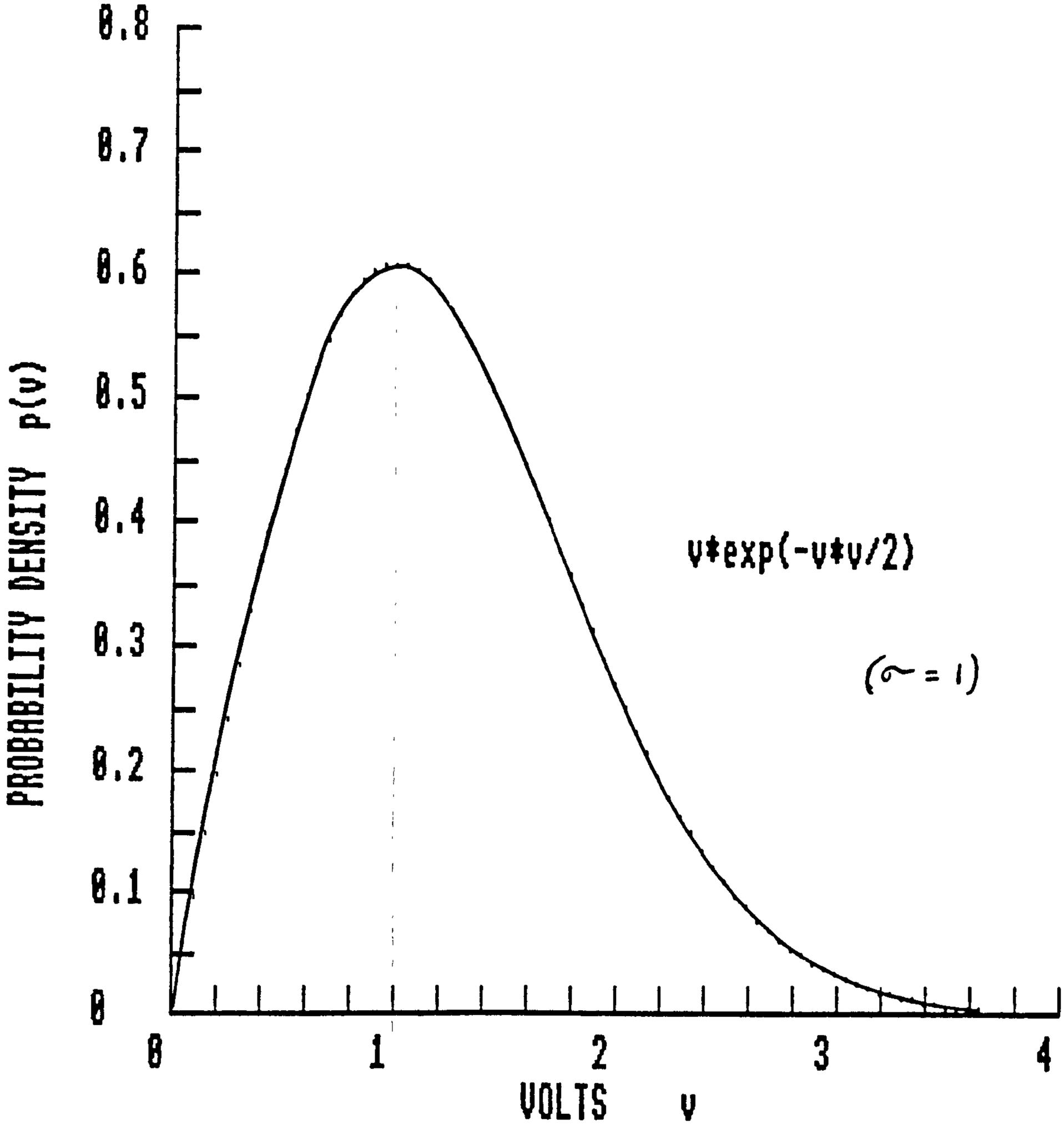

Fig. D.1 Rayleigh Probability Density Function

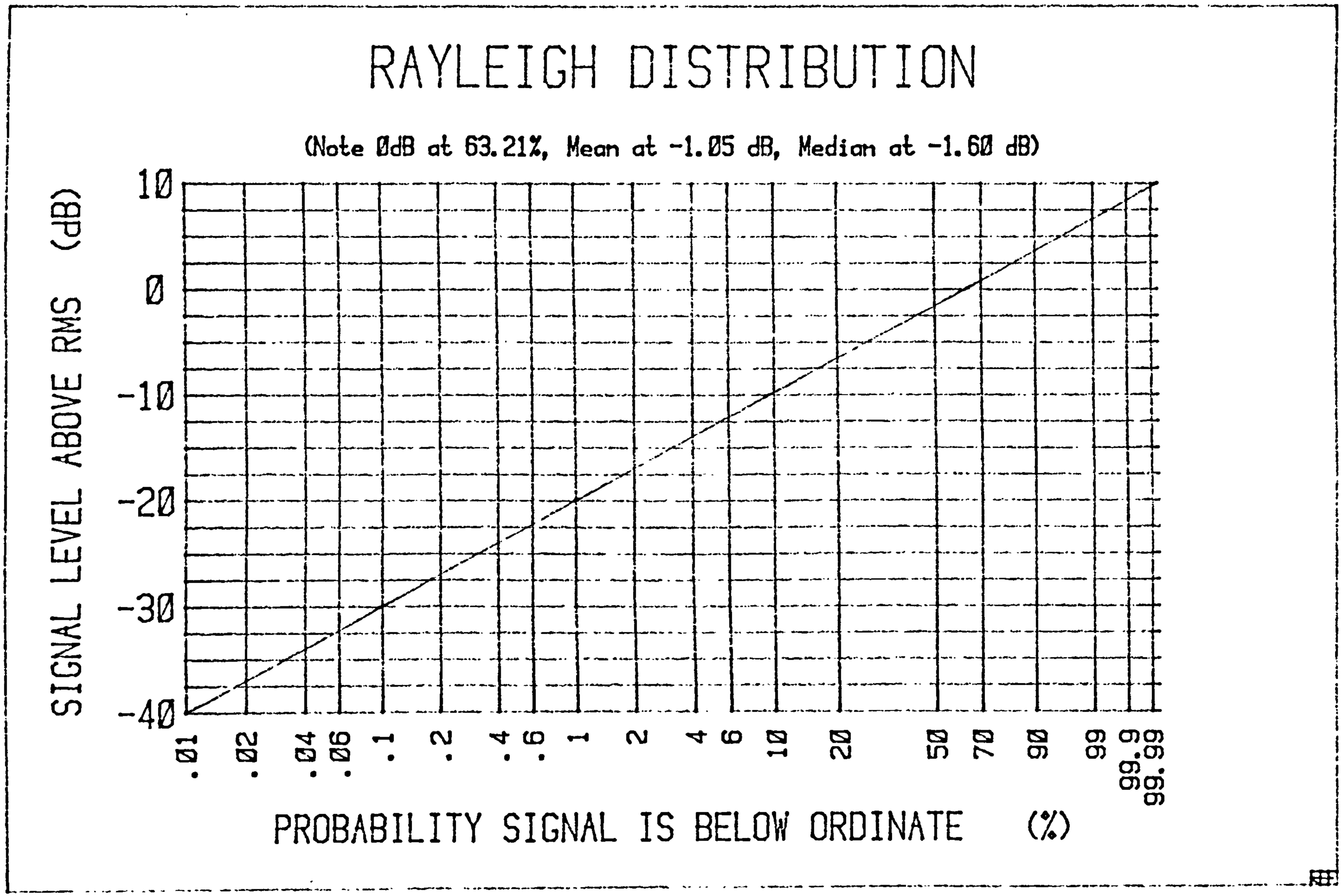

Fig. D.2 Rayleigh Cumulative Probability Function

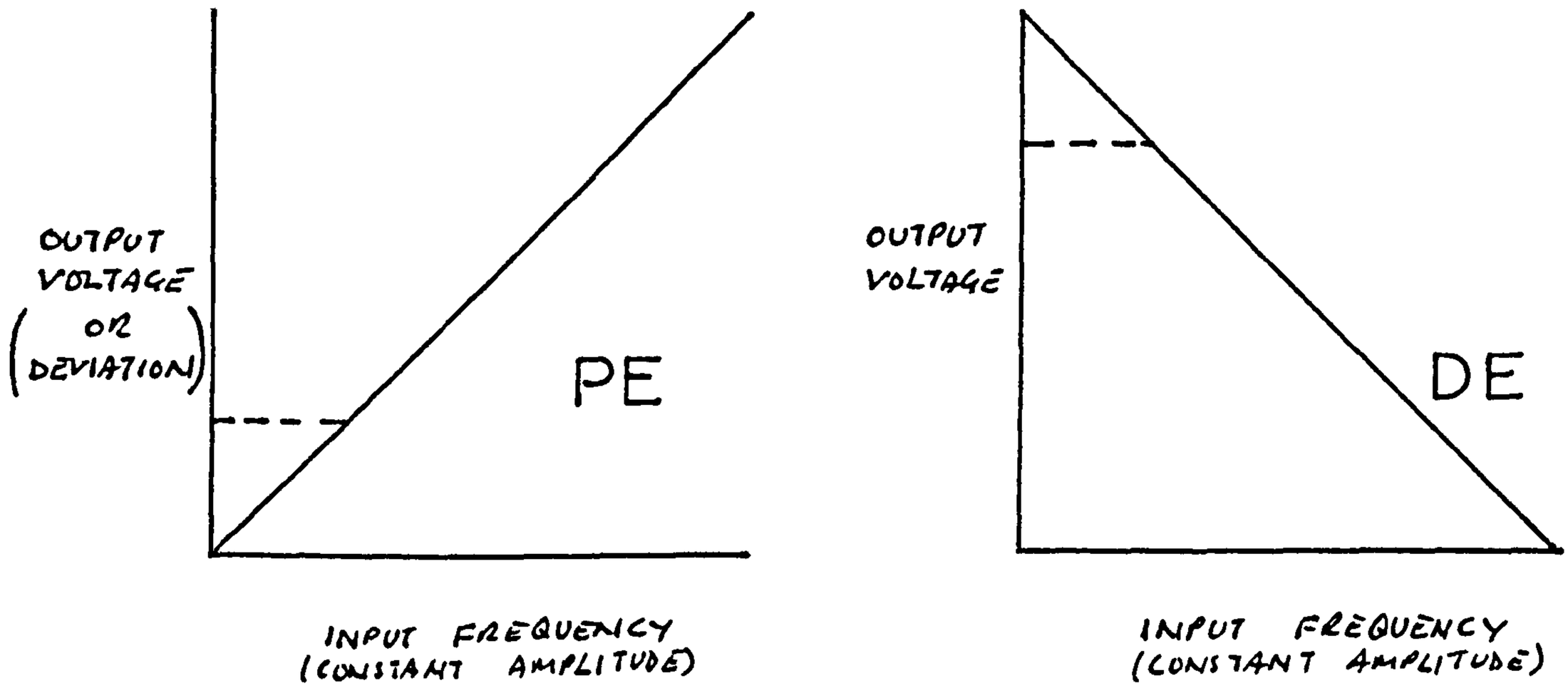

Fig. E.1 Pre- and De-Emphasis Caracteristics

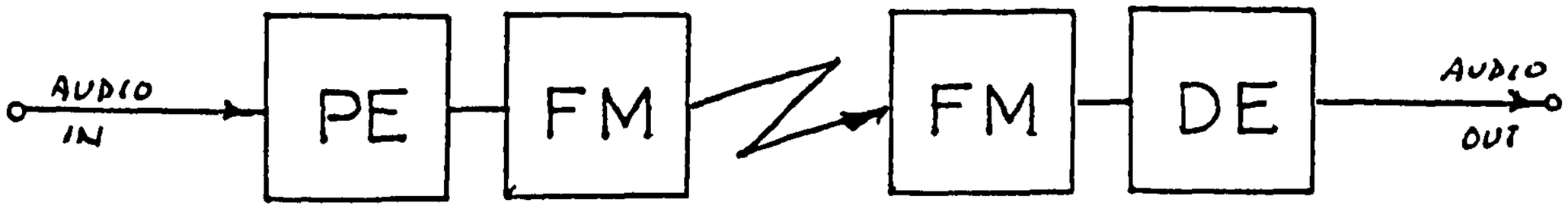

Fig. E.2 PE and DE Concept I

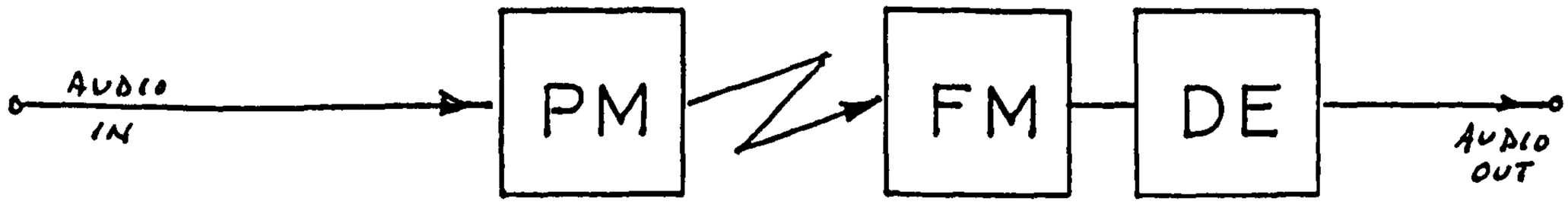

Fig. E.3 PE and DE Concept II

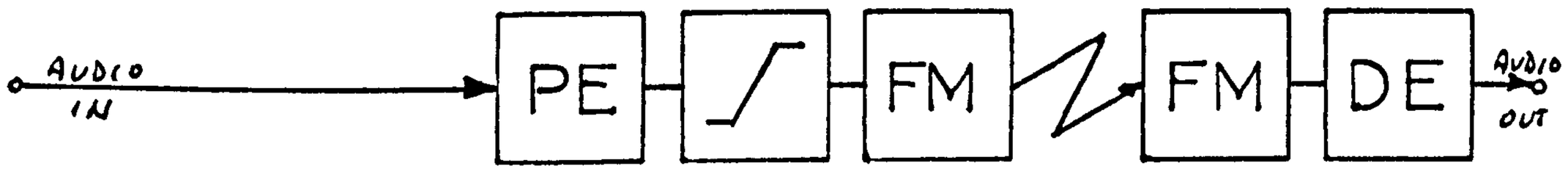

Fig. E.4 PE and DE Concept III

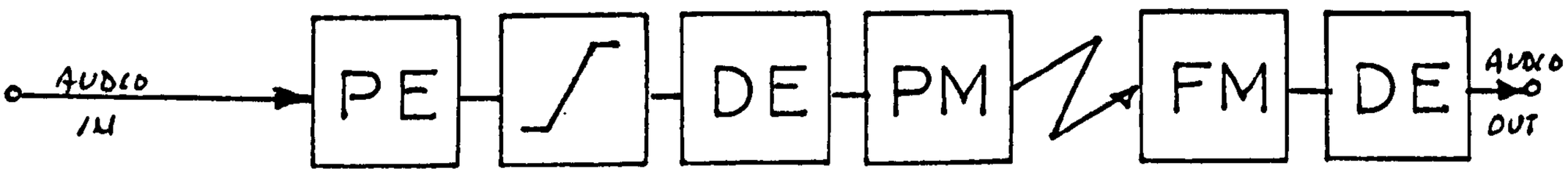

Fig. E.5 PE and DE Concept IV

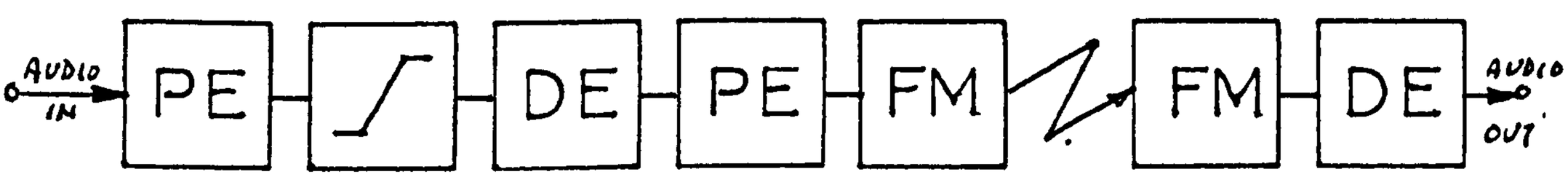

Fig. E.6 PE and DE Concept V

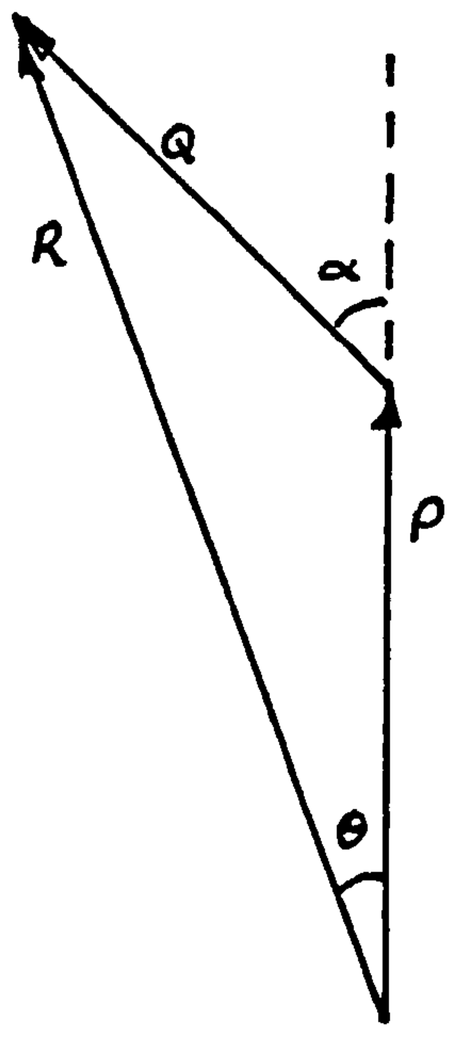

Fig. F.1 Phasor Diagram of Two QS Carriers and their Resultant

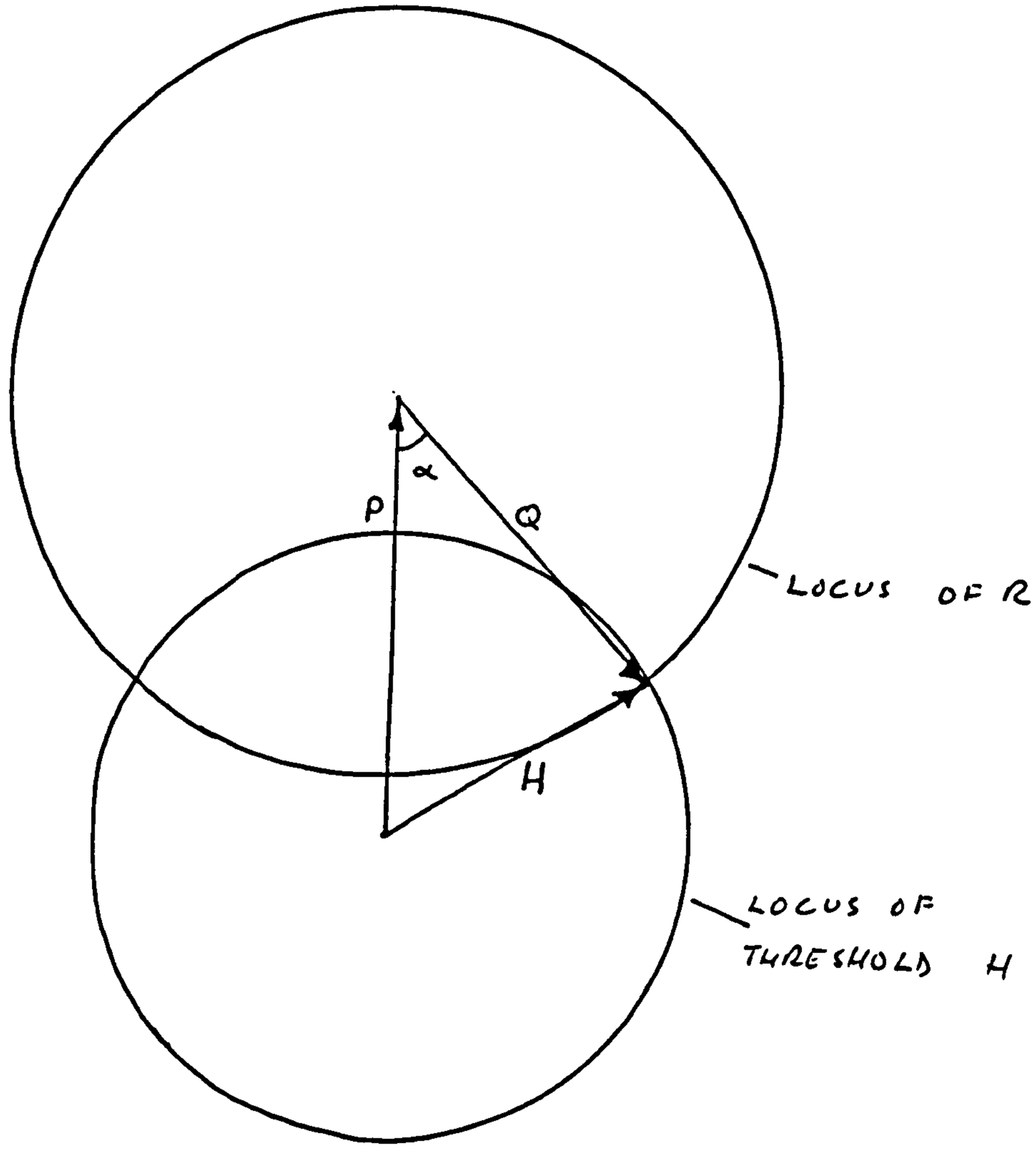

Fig. G.1 Two Carrier QS Phasor Diagram Showing Threshold Levels

Fig. G.2 Three Carrier QS Phasor Diagram Showing Threshold Levels

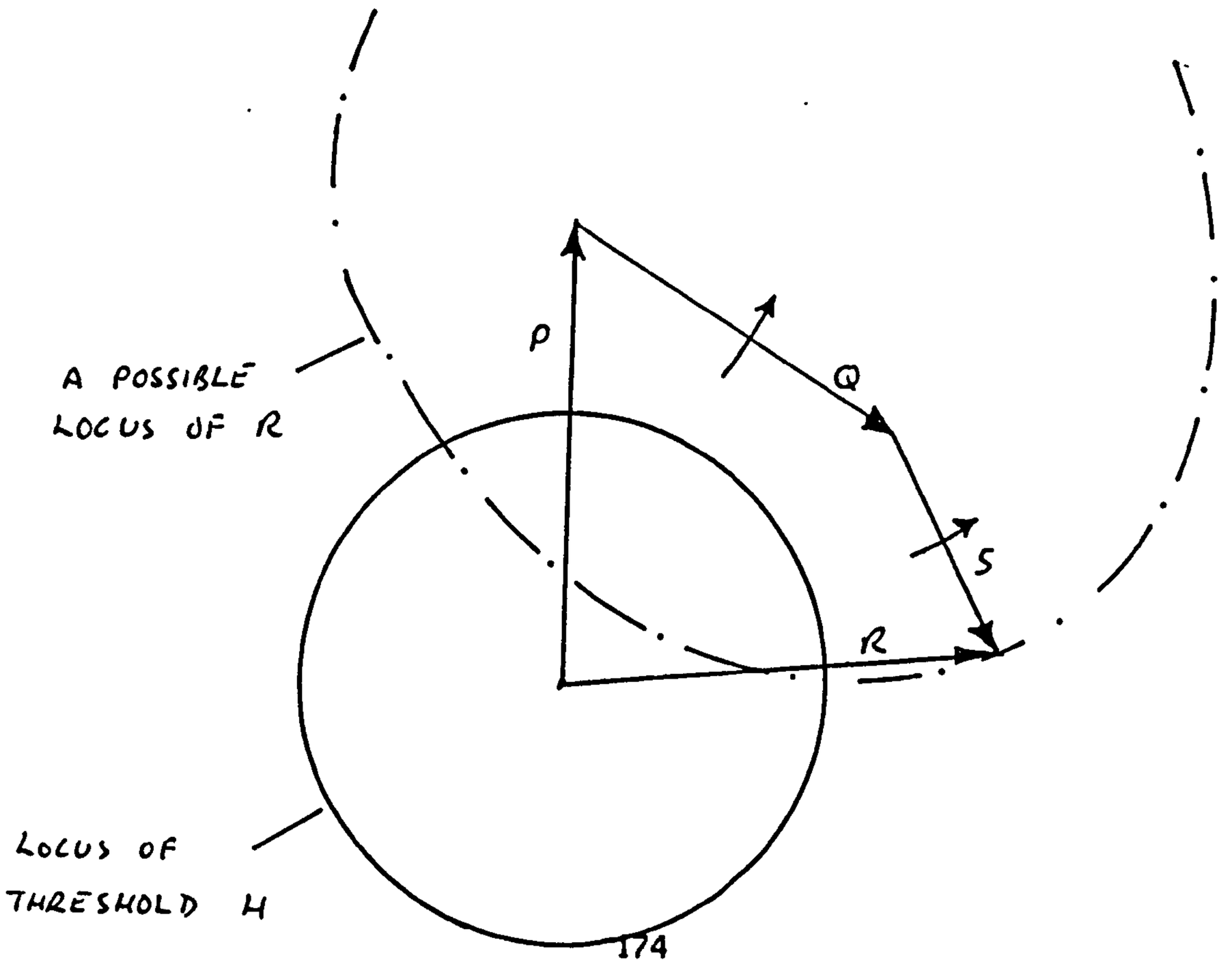

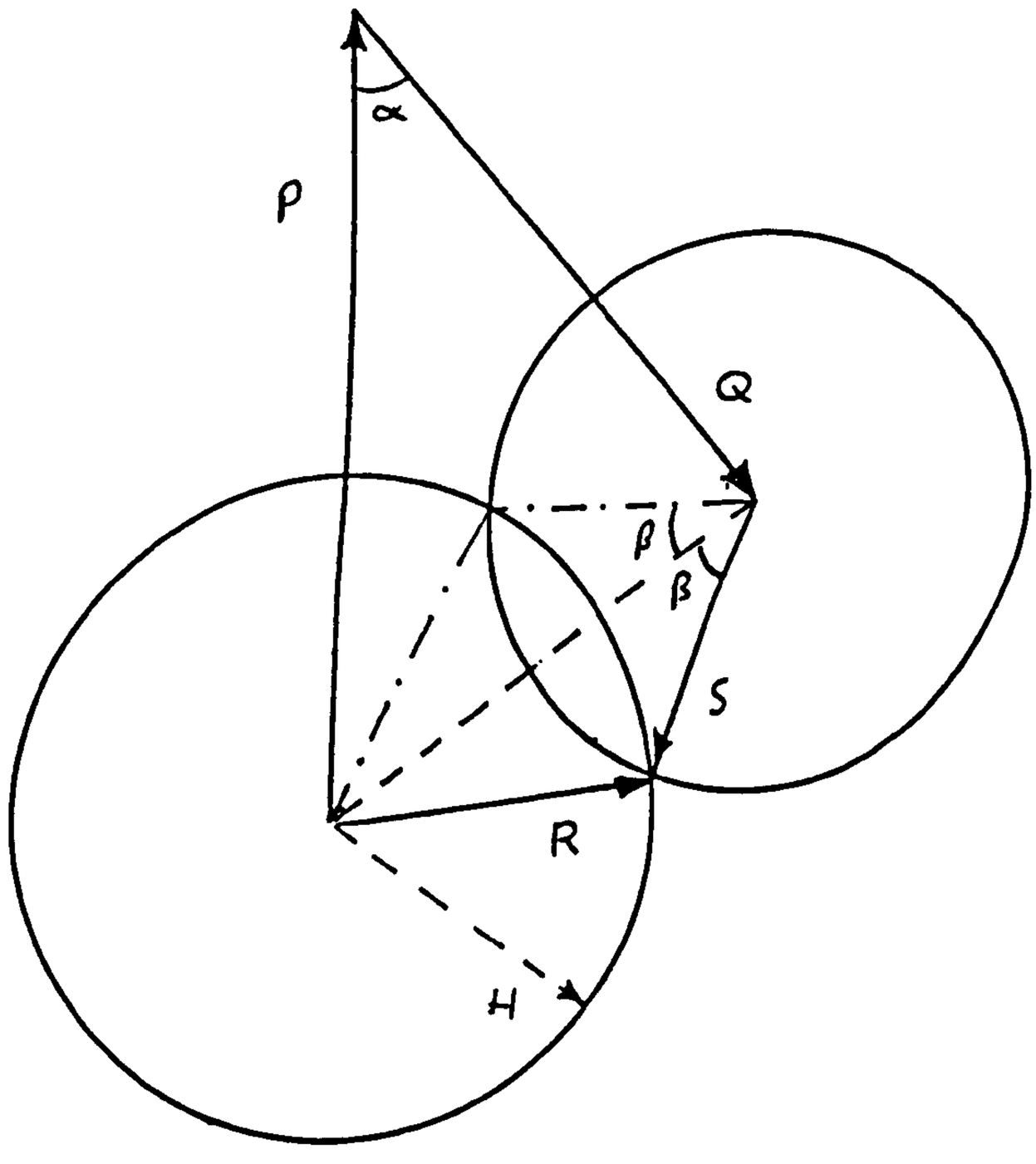

Fig. G.3 Derivation of Probabilities

Fig. G.4(a,b) Derivation of Integration Limits

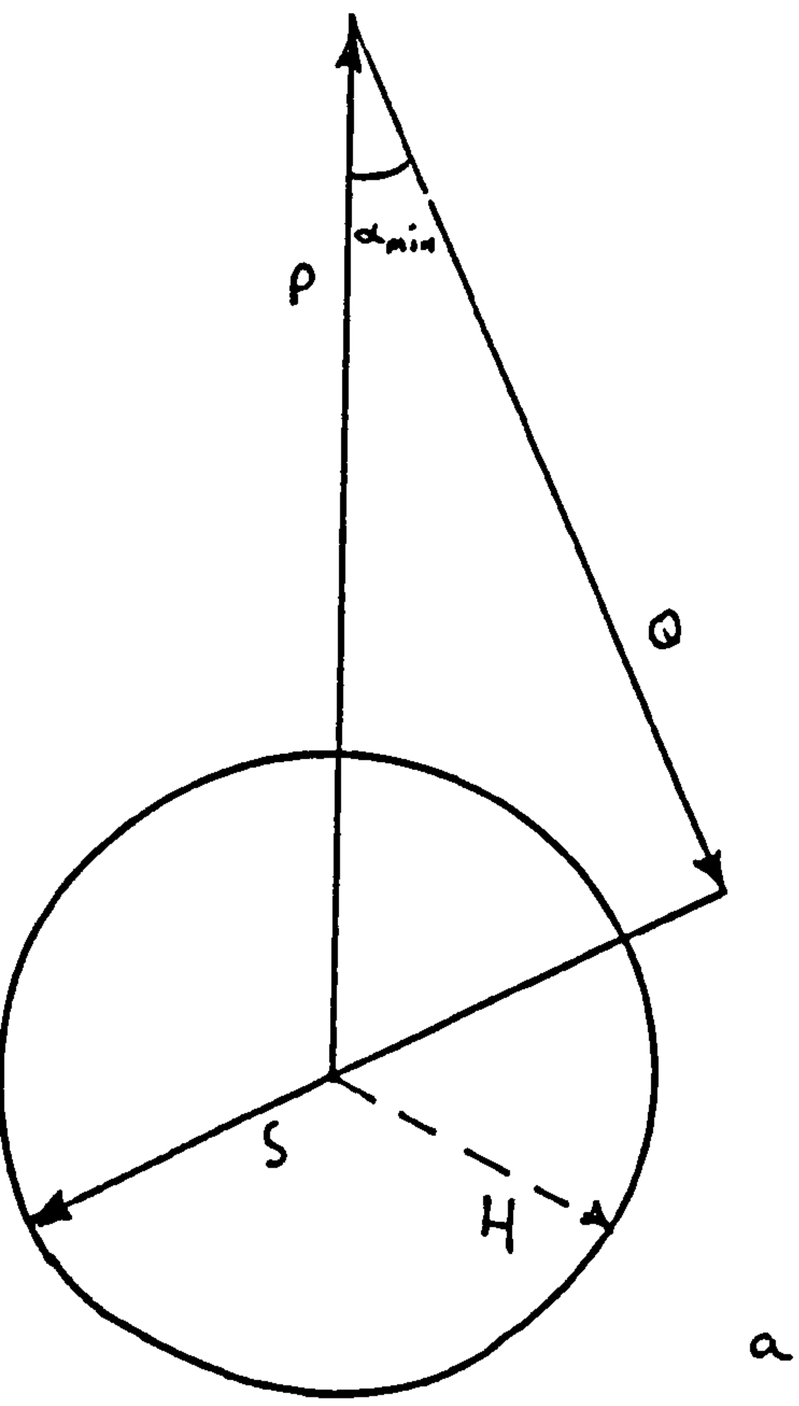

a

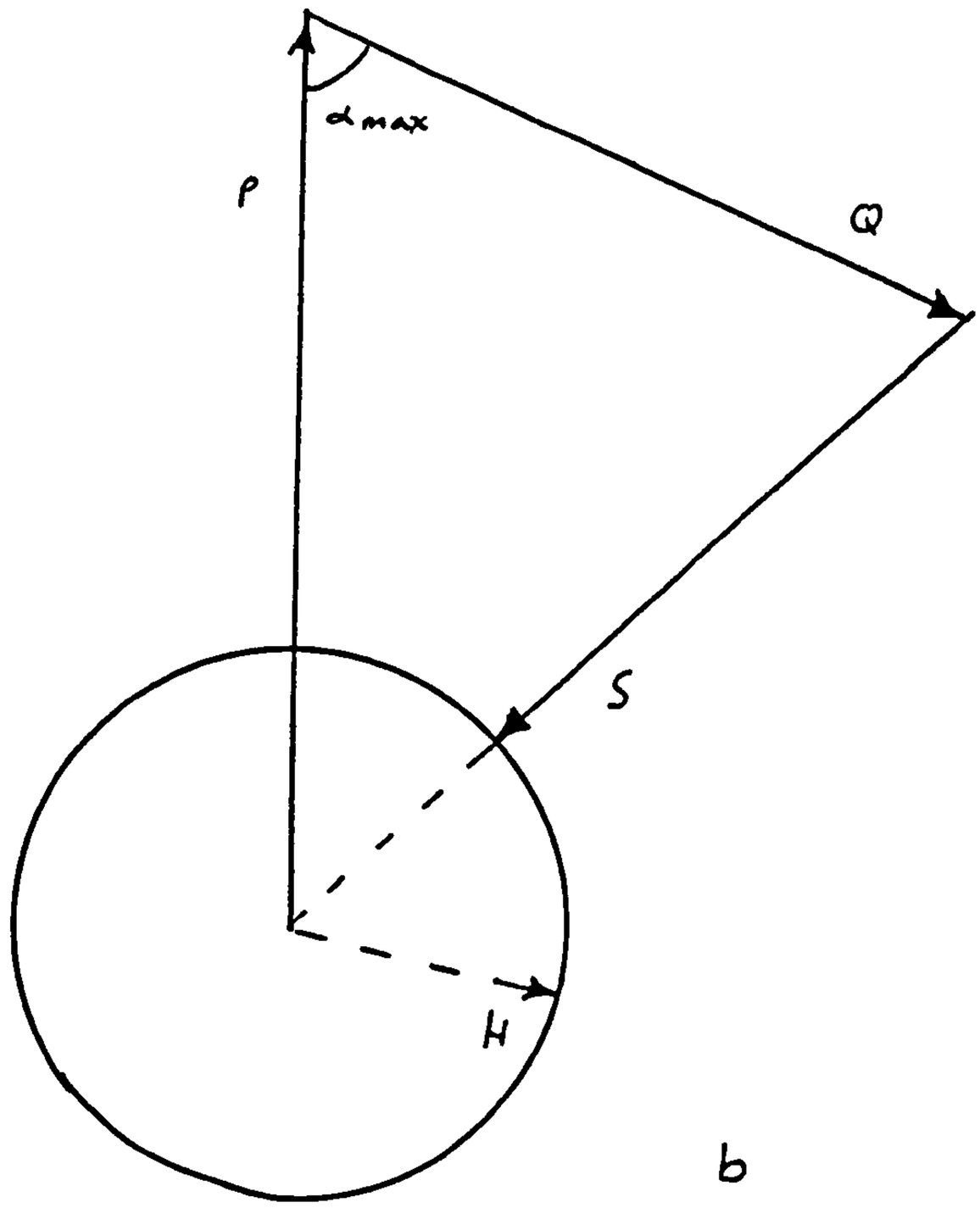

b

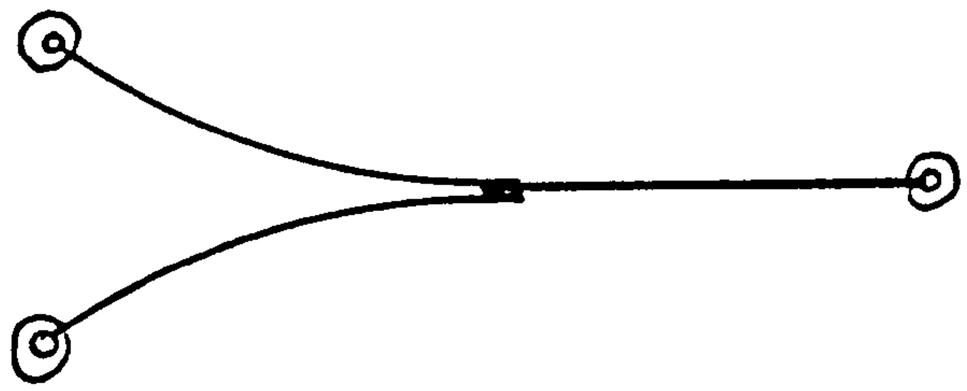

Fig. H.1 Cable Coupling Harness

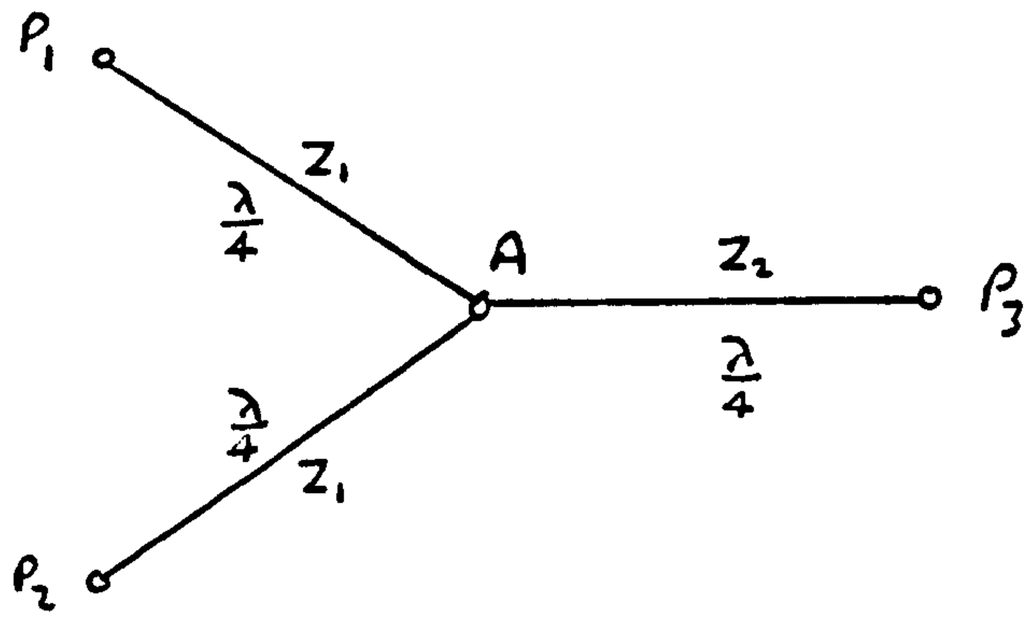

Fig. H.2 Structure of Harness

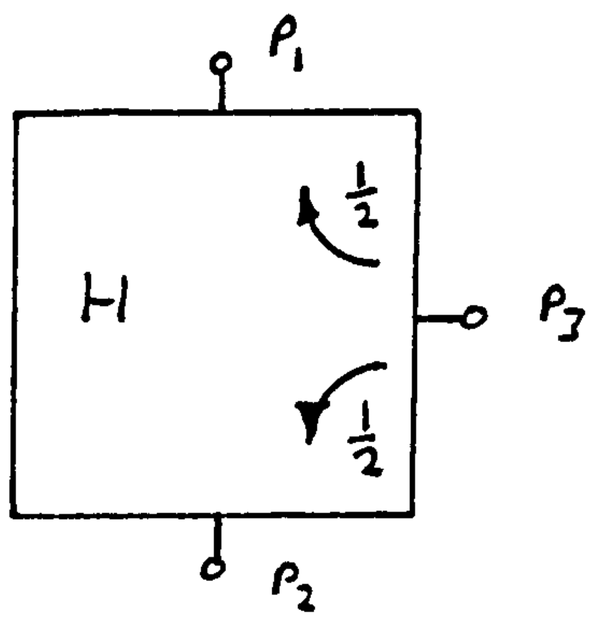

Fig. H.3 Power Flow in Harness I

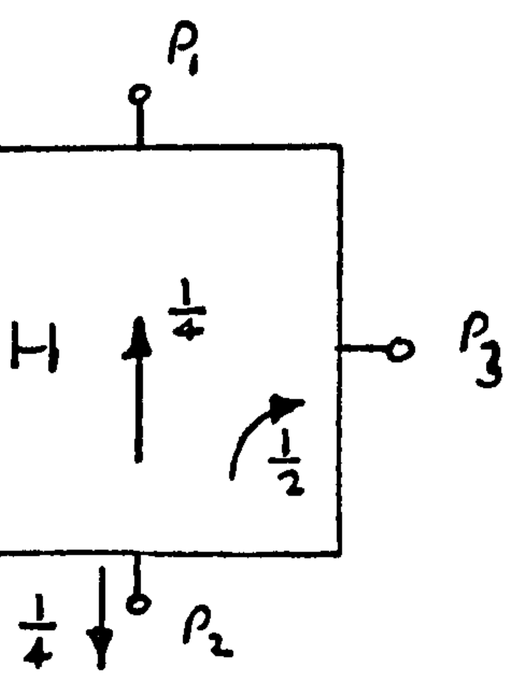

Fig. H.4 Power Flow in Harness II

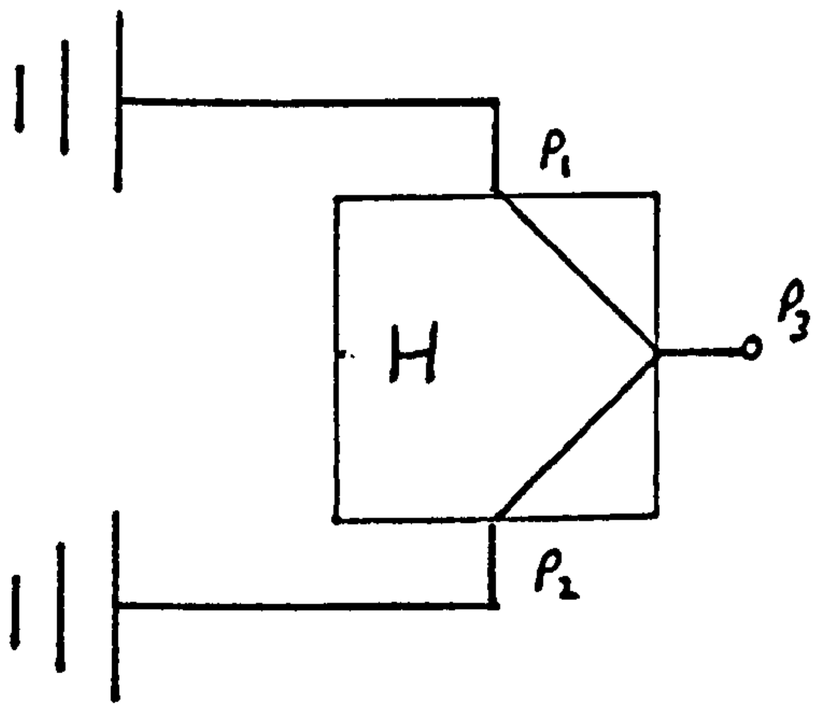

Fig. H.5
Connection of Harness to Aerials

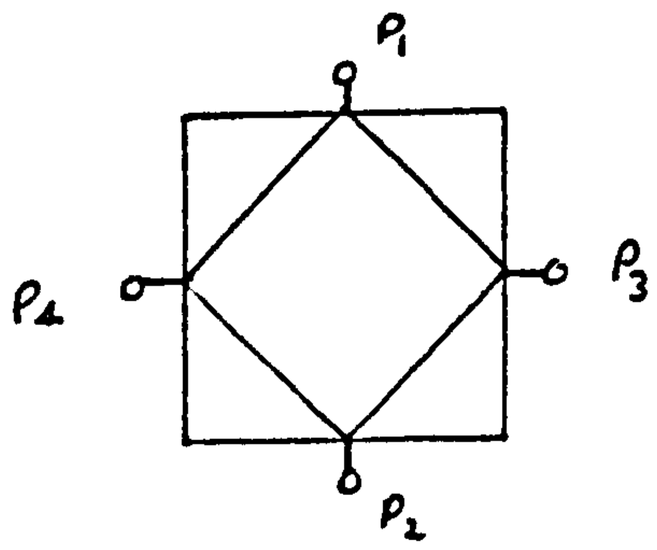

Fig. H.6
Alternative Form - The Hybrid

Fig. H.7
Couplings Required to Simulate Aerials

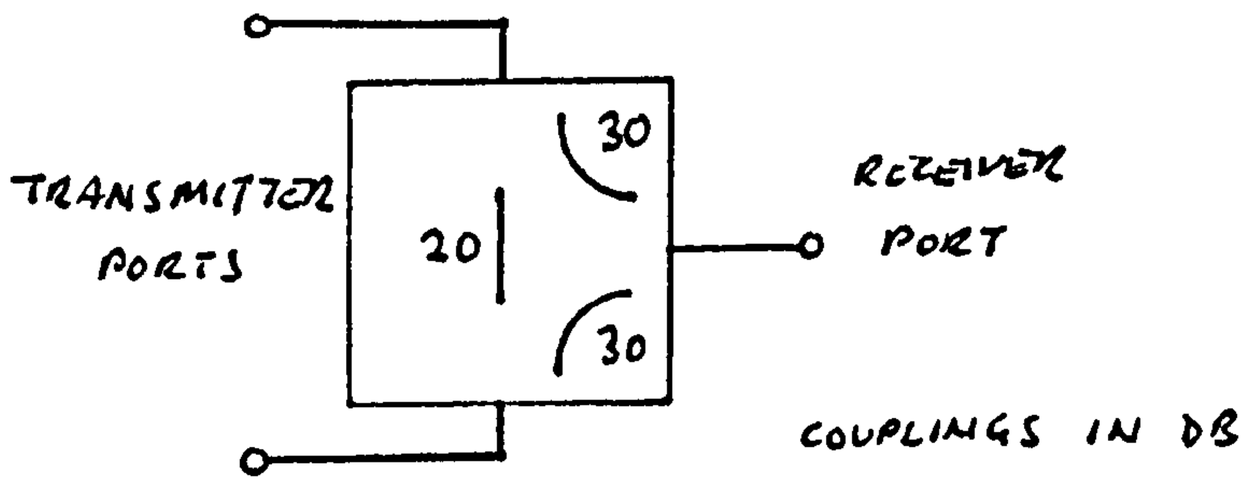

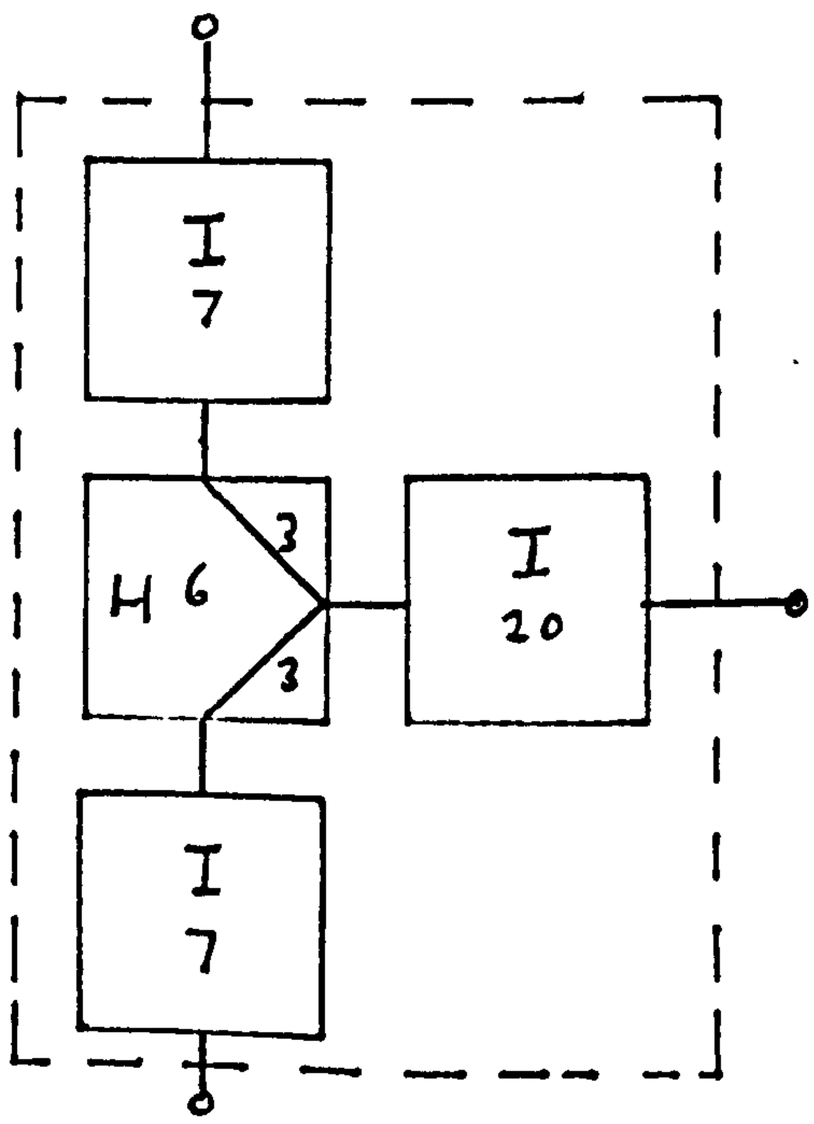

Fig. H.8
Achievement of Required Couplings

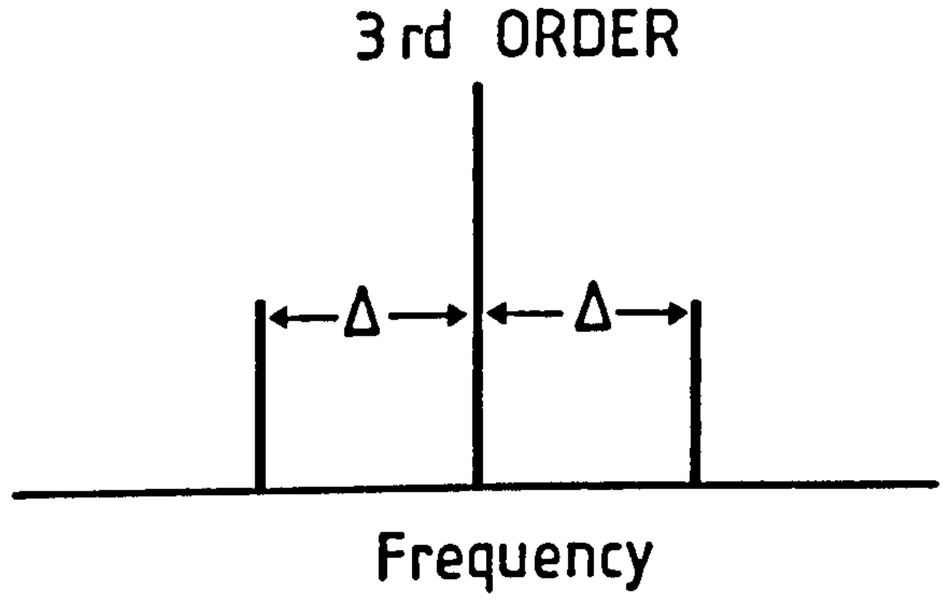

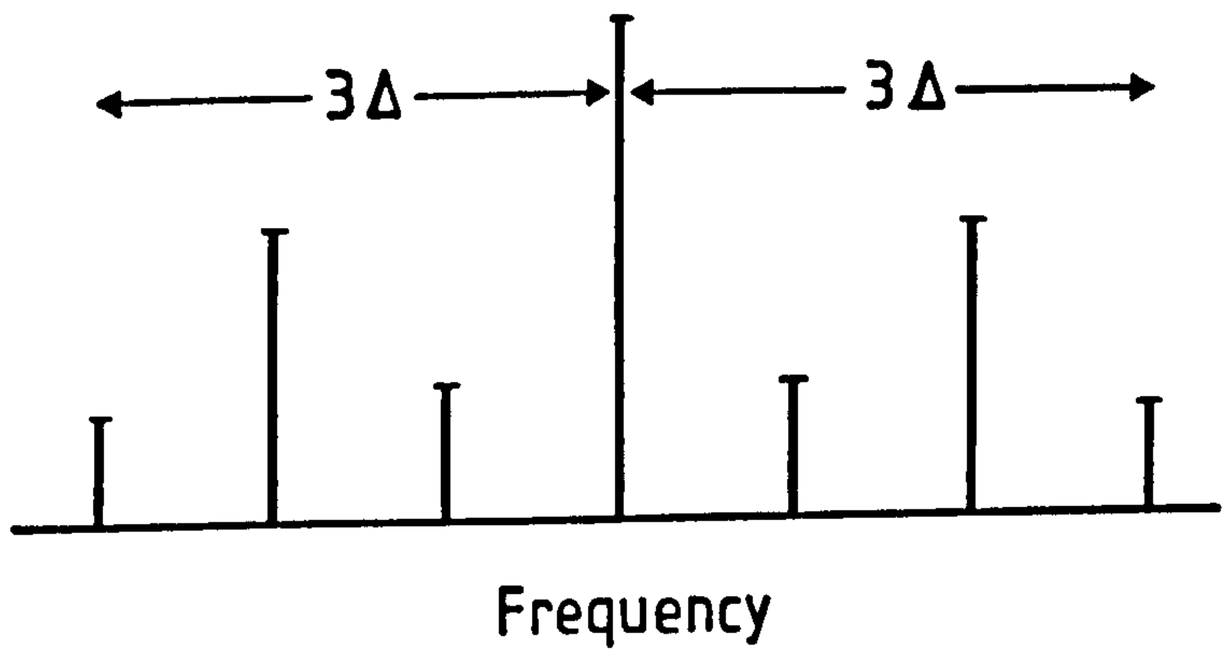

Fig. J.1 Intermodulation Spectrum with Modulation

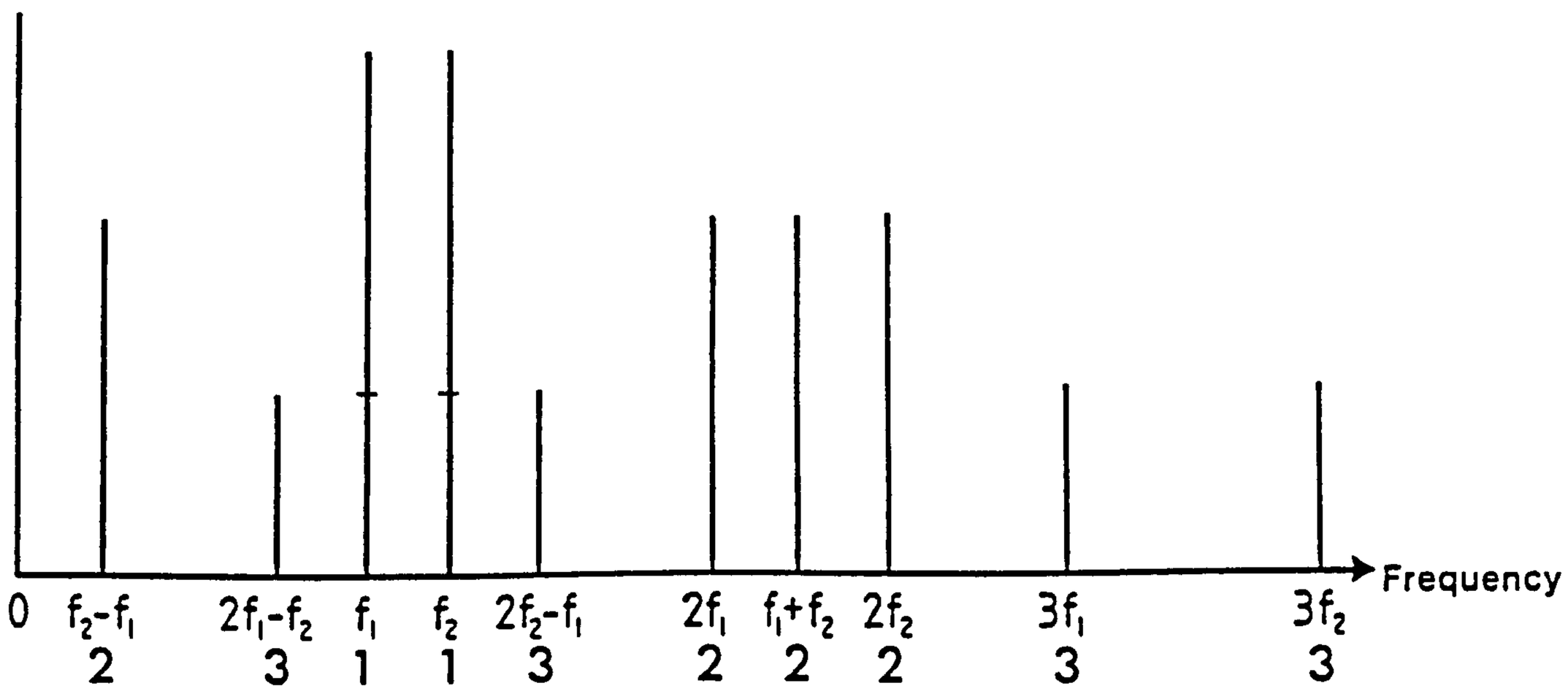

Fig. J.2 Intermodulation Spectrum for Low Orders

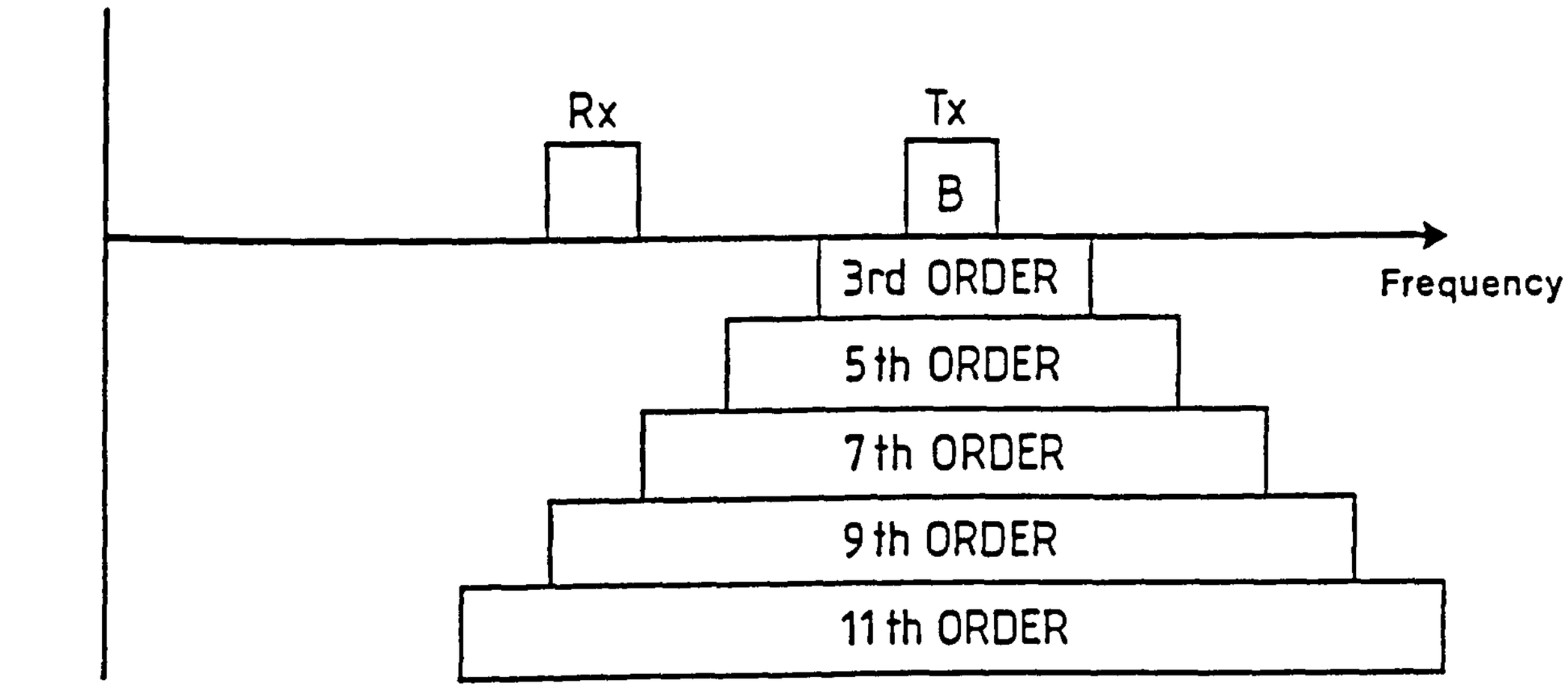

Fig. J.3 Intermodulation Bands

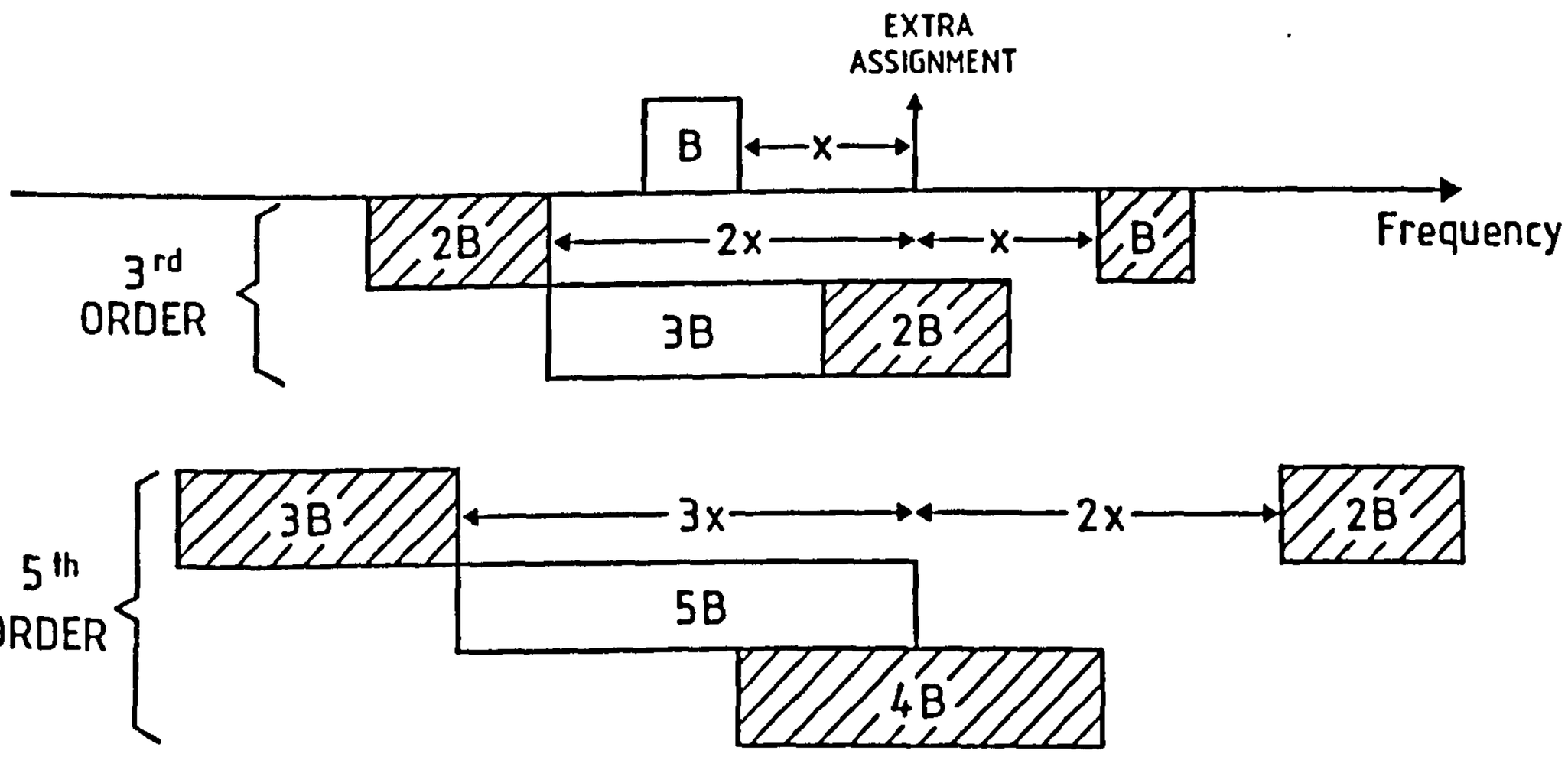

Fig. J.4 Intermodulation Bands for an Extra Assignment

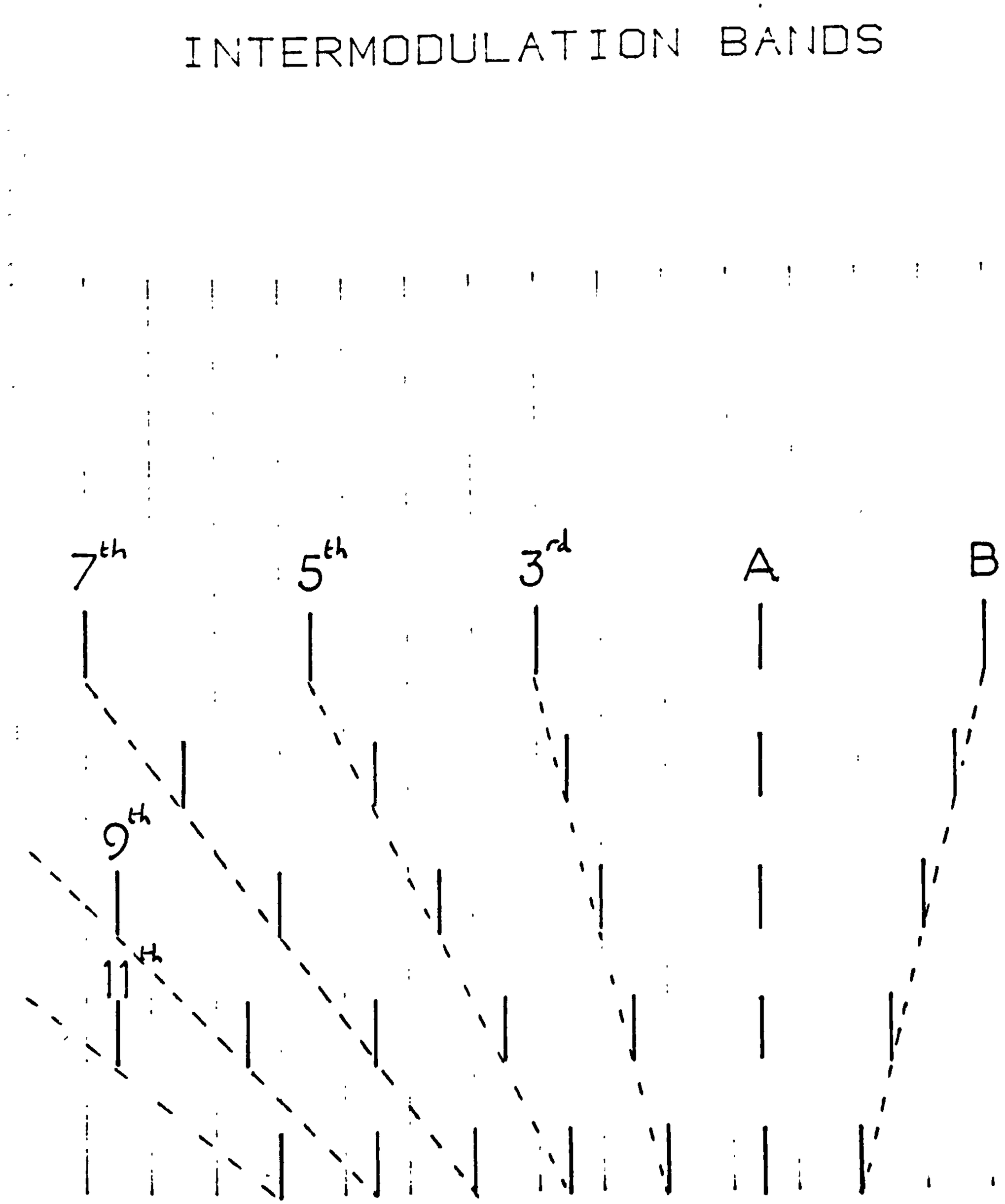

Fig. W.1 Intermodulation Distrbution for Two Fixed Emissions A and B

INTERMODULATION BANDS

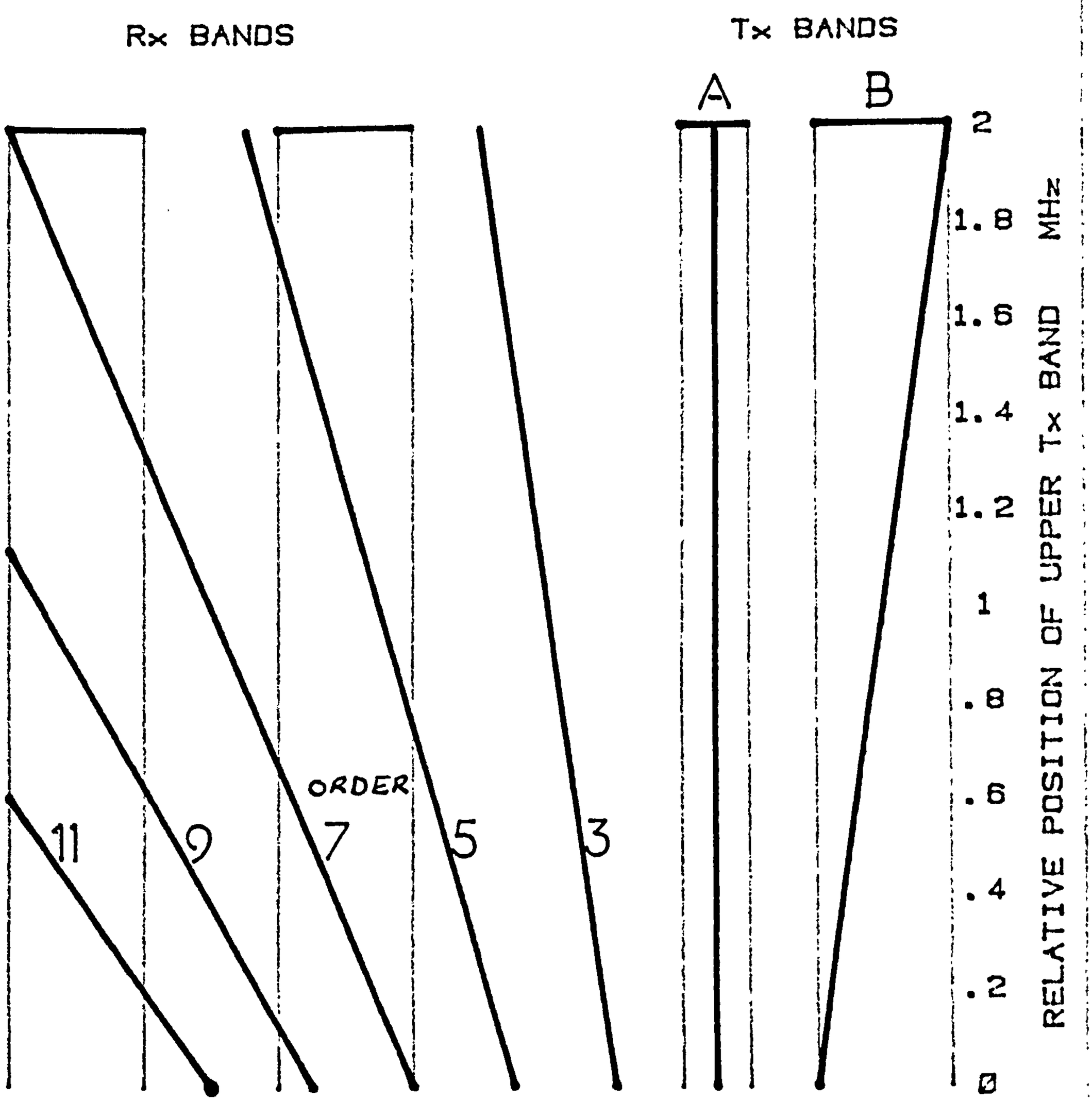

Fig. W.2 Intermodulation Distrbution for Two General Emissions

INTERMODULATION BANDS

Fig. W.3 Intermodulation Distrbution for Two Bands of Emissions

```
  190 MODE7
  195 ON ERROR GOTO 2500
  200REM COPYRIGHT CrowCraft-R E Fudge 16 NOV 1983
  210REM THIS CALCULATES THE INTERMODS UP TO 11TH ORDER FROM THE TRANSMIT BANDS
WHICH FALL INTO THE RECEIVE BANDS.
  220REM THE Tx BANDS ARE 152-153(LINK) AND 154-156(MAIN)MHz. EACH IS CHANNELED
FROM THE BOTTOM-80Ch/MHz.
  230REM THE RxBANDS ARE 142-144 AND146-148MHz.THEY ARE CHANNELED FROM 142
240REM THE RESULTS ARE STORED AND THEN PRINTED ON NEC PRINTER
250 CLS
300 DIM L%(10):DIM U%(10):DIM P%(320):DIM Q%(320):DIM R%(320):DIM S%(320)
310L%=0:U%=0
320PRINT''"GIVE THE LOW TxBAND CHANNEL NUMBERS      ENDING WITH 999"
330L%=L%+1
340INPUTL%(L%)
350IF L%(L%)=999 THEN L%=L%-1:GOTO 365
360GOTO 330
365 VDU2
370PRINT"LOW BAND CHANNELS ARE:-"
380FORN%=1 TOL%:PRINTL%(N%),;:NEXT
383 PRINT
385 VDU3
390PRINT''"GIVE THE UPPER TxBAND CHANNEL NUMBERS    ENDING WITH 999"
400U%=U%+1:INPUT U%(U%)
410IF U%(U%)=999 THEN U%=U%-1:GOTO425
420GOTO400
425 VDU2
430PRINT"UPPER BAND CHANNELS ARE:-"
440FORN%=1 TOU%:PRINTU%(N%),;:NEXT
445 VDU3
450 PRINT'"PRESS 'ESCAPE' TO EXIT AND PRINT RESULTS SO FAR"
500PRINT'"WORKING ON 5TH ORDER AT FRACTION";
510FOR C%=1 TO L%:PRINT TAB(35);C%;"/"L%;:VDU8,8,8,8,8,8
520FORD%=C% TO L%:FORE%=D% TO L%
530Z%=L%(C%)+L%(D%)+L%(E%)+480
540FORG%=1 TO U%:FORH%=G% TO U%
550Y%=Z%-U%(G%)-U%(H%)
560IF Y%>0 ANDY%<161 THENP%(Y%)=P%(Y%)+1
570IF Y%>320 ANDY%<481THENP%(Y%-160)=P%(Y%-160)+1
580NEXT:NEXT:NEXT
590NEXT:NEXT
600PRINT'"FINISHED 5TH ORDERS"
700PRINT"WORKING ON 7TH ORDER AT FRACTION";
710 FORC%=1 TO L%:PRINTTAB(35);C%;"/"L%;:VDU8,8,8,8,8,
730FORD%=C% TO L%:FORE%=D% TO L%:FORF%=E% TO L%
740Z%=L%(C%)+L%(D%)+L%(E%)+L%(F%)+320
750FORG%=1 TO U%:FORH%=G% TO U%:FORI%=H% TO U%
760Y%=Z%-U%(G%)-U%(H%)-U%(I%)
770IF Y%>0 ANDY%<161 THENQ%(Y%)=Q%(Y%)+1
780IF Y%>320 ANDY%<481THENQ%(Y%-160)=Q%(Y%-160)+1
790NEXT:NEXT:NEXT:NEXT
800NEXT:NEXT:NEXT
810PRINT'"FINISHED 7TH ORDERS"
900B%=0
905PRINT"WORKING ON 9TH ORDER AT FRACTION";
910REPEAT
920B%=B%+1:PRINTTAB(35);B%;"/"L%;:VDU8,8,8,8,8,8
930FORC%=B% TO L%:FORD%=C% TO L%:FORE%=D% TO L%:FORF%=E% TO L%
```

Fig. X.1a Computer Program for Calculation of Intermodulation Channels

```
 940Z%=L%(B%)+L%(C%)+L%(D%)+L%(E%)+L%(F%)+160
 950FORG%=1 TO U%:FORH%=G% TO U%:FORI%=H% TO U%:FORJ%=I% TO U%
 960Y%=Z%-U%(G%)-U%(H%)-U%(I%)-U%(J%)
 970IF Y%>0 ANDY%<161 THENR%(Y%)=R%(Y%)+1
 980IF Y%>320 ANDY%<481THENR%(Y%-160)=R%(Y%-160)+1
 990NEXT:NEXT:NEXT:NEXT
1000NEXT:NEXT:NEXT:NEXT
1010UNTIL B%=L%
1020PRINT'"FINISHED 9TH ORDERS"
1100A%=0
1105 PRINT"WORKING ON 11TH ORDER AT FRACTION";
1110REPEAT
1120A%=A%+1:PRINTTAB(35);A%;"/"L%;:VDU8,8,8,8,8,8
1125 B%=A%-1
1130REPEAT
1140B%=B%+1
 1150FORC%=B% TO L%:FORD%=C% TO L%:FORE%=D% TO L%:FORF%=E% TO L%
 1160Z%=L%(A%)+L%(B%)+L%(C%)+L%(D%)+L%(E%)+L%(F%)
 1170FORG%=1 TO U%:FORH%=G% TO U%:FORI%=H% TO U%:FORJ%=I% TO U%:FORK%=J% TO U%
 1180Y%=Z%-U%(G%)-U%(H%)-U%(I%)-U%(J%)-U%(K%)
 1185 REM
 1190IF Y%>0 ANDY%<161 THENS%(Y%)=S%(Y%)+1
 1200IF Y%>320 ANDY%<481THENS%(Y%-160)=S%(Y%-160)+1
 1210NEXT:NEXT:NEXT:NEXT:NEXT
 1220NEXT:NEXT:NEXT:NEXT
 1230UNTIL B%=L%
 1240UNTIL A%=L%
 1250PRINT'"FINISHED 11TH ORDERS"
 1500 REM IF ERROR =27 THEN GOTO 'OUTPUT ROUTINE'
 2000REM OUTPUT ROUTINE
 2005 VDU2
 2010PRINT'''"THIS TABLE SHOWS, FOR EACH ORDER No, THE NUMBER OF INTERMODS. FALL
ING ON THE       RECEIVE CHANNELS"
 2015 PRINT'
 2020PRINT"    CHANNEL","    FREE!","      ORDER","      ORDER","      ORDER","      C
RDER"
 2030PRINT"        No.","    ","           5","           7","           9","          11"
 2035PRINT''
 2040VDU1,&1B,1,&54,1,&31,1,&38 :REM CONDENSED LINES PITCH 18
 2050FOR J% =1 TO 160
 2060A$=" ":IF P%(J%)+Q%(J%)+R%(J%)+S%(J%)=0 A$="     ¥"
 2070PRINTJ%,A$,P%(J%),Q%(J%),R%(J%),S%(J%)
 2080NEXT
 2090 PRINT'''
 2100FOR J% =161 TO 320
 2110A$=" ":IF P%(J%)+Q%(J%)+R%(J%)+S%(J%)=0 A$="     ¥"
 2120PRINTJ%+160,A$,P%(J%),Q%(J%),R%(J%),S%(J%)
 2130NEXT
 2150VDU1,&1B,1,&41
 2160PRINT''''''
 2170VDU3
 2180VDU7
 2190PRINT "      ALL DONE"
 2200END
 2500 IF ERR =17 THEN GOTO 2600
 2510 REPORT:PRINT"AT LINE No. ";ERL
 2520 END
 2600 PRINT"CURRENTLY WORKING ON ";W%;" ORDER"
 2610 PRINT"FOR A PRINTOUT OF RESULTS PRESS  P  ":PRINT"ALTERNATELY CONTINUATIO
MIGHT BE       POSSIBLE  -PRESS   C  "
 2620 V$=GET$
 2630 IF V$="C" GOTO ERL
>
```

Fig. X.1b Computer Program for Calculation of Intermodulation Channels

LOW BAND CHANNELS ARE:-

1 3 6 10 23 31 42

UPPER BAND CHANNELS ARE:-

1 16 34 58 68 74

THIS TABLE SHOWS, FOR EACH ORDER No, THE NUMBER OF INTERMODS. FALLING ON THE RECEIVE CHANNELS

CHANNEL No.	FREE!	ORDER 5	ORDER 7	ORDER 9	ORDER 11
1		0	0	208	486
2		0	0	206	477
3		0	0	216	474
4		0	0	215	467
5		0	0	219	459
6		0	0	216	452
7		0	0	223	445
8		0	0	219	441
9		0	0	229	432
10		0	0	226	432
11		0	0	232	418
12		0	0	228	419
13		0	0	234	411
14		0	0	233	406
15		0	0	241	397
16		0	0	237	394
17		0	0	244	386
18		0	0	241	390
19		0	0	248	382
20		0	0	243	374
21		0	0	249	369
22		0	0	244	359
23		0	0	252	353
24		0	0	252	351
25		0	0	258	348
26		0	0	253	338
27		0	0	258	336
28		0	0	252	331
29		0	0	262	322
30		0	0	259	318
31		0	0	272	314
32		0	0	264	307
33		0	0	267	304
34		0	0	265	300
35		0	0	273	296
36		0	0	271	294
37		0	0	274	285
38		0	0	275	279
39		0	0	277	275
40		0	0	273	275
41		0	0	280	262
42		0	0	277	261
43		0	0	278	258
44		0	0	277	249
45		0	0	284	246
46		0	0	277	247
47		0	0	284	235
48		0	0	282	230
49		0	0	288	228
50		0	0	281	226
51		0	0	294	223
52		0	0	283	215
53		0	0	286	215
54		0	0	286	209
55		0	0	289	203
56		0	0	287	199
57		0	0	293	199
58		0	0	292	193
59		0	0	289	189
60		0	0	288	189
61		0	0	289	185
62		0	0	286	178
63		0	0	289	171
64		0	0	288	172
65		0	0	294	167
66		0	0	289	163
67		0	0	294	160
68		0	0	287	159

Fig. X.2a Distribution of Intermod Products in the Receive Bands I

69	0	0	290	152
70	0	0	292	153
71	0	0	294	146
72	0	0	289	146
73	0	0	294	140
74	0	0	289	134
75	0	0	293	137
76	0	0	291	135
77	0	0	291	127
78	0	0	287	128
79	0	0	290	124
80	0	0	287	116
81	0	0	290	119
82	0	0	285	115
83	0	0	290	112
84	0	0	284	106
85	0	0	281	109
86	0	0	282	104
87	0	0	284	100
88	0	0	282	97
89	0	0	283	94
90	0	0	282	95
91	0	0	285	93
92	0	0	279	92
93	0	0	279	88
94	0	0	275	87
95	0	0	275	81
96	0	0	273	81
97	0	0	279	79
98	0	0	272	78
99	0	0	275	73
100	0	0	270	76
101	0	0	266	71
102	0	1	269	69
103	0	0	266	71
104	0	1	263	64
105	0	0	267	61
106	0	1	262	62
107	0	1	262	62
108	0	2	263	59
109	0	1	260	57
110	0	2	257	54
111	0	2	259	55
112	0	2	256	51
113	0	3	255	51
114	0	3	251	49
115	0	2	255	48
116	0	4	250	45
117	0	4	247	45
118	0	4	248	47
119	0	4	242	41
120	0	6	240	41
121	0	3	242	39
122	0	7	238	39
123	0	6	237	37
124	0	7	237	38
125	0	6	233	34
126	0	8	228	34
127	0	6	229	33
128	0	8	225	32
129	0	10	225	31
130	0	9	223	29
131	0	8	224	29
132	0	10	222	29
133	0	9	223	29
134	0	12	213	24
135	0	10	215	27
136	0	12	209	26
137	0	9	211	24
138	0	14	211	22
139	0	12	206	23
140	0	13	203	22
141	0	11	202	20
142	0	16	200	21
143	0	13	197	21
144	0	16	196	18
145	0	15	191	17
146	0	15	191	17
147	0	15	190	15
148	0	19	190	18
149	0	17	187	15
150	0	20	185	15
151	0	18	183	16
152	0	21	180	13
153	0	18	178	12
154	0	23	179	14
155	0	20	176	11
156	0	24	169	11
157	0	21	171	12
158	0	23	166	11
159	0	25	166	12
160	0	24	161	10

Fig. X.2b Distribution of Intermod Products in the Receive Bands I

321	0	46	2	0
322	0	46	2	0
323	0	45	1	0
324	0	45	0	0
325	0	43	3	0
326	0	44	0	0
327	0	41	1	0
328	0	43	1	0
329	0	42	1	0
330	0	45	1	0
331	0	34	0	0
332	0	39	1	0
333	0	37	2	0
334	0	35	1	0
335	1	38	0	0
336	0	37	2	0
337	1	34	0	0
338	0	37	0	0
339	1	36	0	0
340	1	35	1	0
341	2	37	0	0
342	1	31	0	0
343	1	33	0	0
344	2	33	1	0
345	2	34	0	0
346	2	32	0	0
347	3	32	1	0
348	2	28	0	0
349	3	28	0	0
350	4	29	0	0
351	2	28	1	0
352	4	27	0	0
353	3	25	0	0
354	4	27	0	0
355	3	25	1	0
356	4	25	0	0
357	5	23	0	0
358	3	24	0	0
359	4	23	0	0
360	4	25	0	0
361	5	23	0	0
362	4	25	0	0
363	5	22	0	0
364	4	20	0	0
365	4	21	0	0
366	5	21	1	0
367	7	19	0	0
368	4	19	0	0
369	5	19	0	0
370	5	18	0	0
371	6	19	0	0
372	4	16	0	0
373	6	15	0	0
374	6	16	0	0
375	6	17	0	0
376	7	16	0	0
377	6	16	0	0
378	6	15	0	0
379	7	15	0	0
380	7	17	0	0
381	10	14	0	0
382	6	14	0	0
383	8	13	0	0
384	8	12	0	0
385	7	11	0	0
386	8	13	0	0
387	11	12	0	0
388	7	11	0	0
389	7	10	0	0
390	9	10	0	0
391	10	9	0	0
392	7	10	0	0
393	10	9	0	0
394	8	8	0	0
395	10	10	0	0
396	8	9	0	0
397	11	10	0	0
398	9	8	0	0
399	10	8	0	0

Fig. X.2c Distribution of Intermod Products in the Receive Bands I

400	11	7	0	0
401	11	8	0	0
402	10	7	0	0
403	11	8	0	0
404	10	6	0	0
405	8	6	0	0
406	11	5	0	0
407	11	5	0	0
408	13	6	0	0
409	10	4	0	0
410	10	5	0	0
411	11	6	0	0
412	11	6	0	0
413	12	5	0	0
414	10	5	0	0
415	14	3	0	0
416	11	5	0	0
417	13	4	0	0
418	12	5	0	0
419	14	5	0	0
420	14	3	0	0
421	13	4	0	0
422	13	3	0	0
423	15	3	0	0
424	12	3	0	0
425	14	3	0	0
426	14	2	0	0
427	13	3	0	0
428	13	2	0	0
429	13	3	0	0
430	11	2	0	0
431	13	2	0	0
432	13	1	0	0
433	15	2	0	0
434	12	2	0	0
435	13	1	0	0
436	12	2	0	0
437	12	2	0	0
438	13	2	0	0
439	15	2	0	0
440	14	2	0	0
441	14	2	0	0
442	14	1	0	0
443	13	0	0	0
444	13	1	0	0
445	11	0	0	0
446	11	1	0	0
447	14	1	0	0
448	14	1	0	0
449	12	1	0	0
450	11	0	0	0
451	13	1	0	0
452	12	2	0	0
453	13	1	0	0
454	13	0	0	0
455	14	2	0	0
456	12	0	0	0
457	14	0	0	0
458	14	0	0	0
459	13	1	0	0
460	16	0	0	0
461	12	0	0	0
462	11	0	0	0
463	13	1	0	0
464	13	0	0	0
465	13	0	0	0
466	11	1	0	0
467	11	0	0	0
468	13	0	0	0
469	9	0	0	0
470	11	1	0	0
471	10	0	0	0
472	9	0	0	0
473	12	0	0	0
474	12	1	0	0
475	13	0	0	0
476	9	0	0	0
477	11	0	0	0
478	10	0	0	0
479	11	0	0	0
480	11	0	0	0

Fig. X.2d Distribution of Intermod Products in the Receive Bands I

LOW BAND CHANNELS ARE:-

1	2	3	4	5	6

UPPER BAND CHANNELS ARE:-

20	28	38	47	58

THIS TABLE SHOWS, FOR EACH ORDER No, THE NUMBER OF INTERMODS. FALLING ON THE RECEIVE CHANNELS

CHANNEL No.	FREE!	ORDER 5	ORDER 7	ORDER 9	ORDER 11
1		0	0	157	0
2		0	0	161	0
3		0	0	165	0
4		0	0	169	0
5		0	0	172	0
6		0	0	175	0
7		0	0	176	0
8		0	0	179	0
9		0	0	181	0
10		0	0	182	0
11		0	0	182	0
12		0	0	184	0
13		0	0	188	0
14		0	0	189	0
15		0	0	190	0
16		0	0	193	0
17		0	0	196	0
18		0	0	199	0
19		0	0	200	0
20		0	0	201	0
21		0	0	204	0
22		0	0	202	0
23		0	0	204	0
24		0	0	203	0
25		0	0	202	0
26		0	0	200	0
27		0	0	198	0
28		0	0	198	0
29		0	0	197	0
30		0	0	193	0
31		0	0	193	0
32		0	0	192	0
33		0	0	192	0
34		0	0	191	0
35		0	0	190	0
36		0	0	191	0
37		0	0	190	0
38		0	0	190	0
39		0	0	190	0
40		0	0	189	0
41		0	0	187	0
42		0	0	185	0
43		0	0	184	0
44		0	0	181	0
45		0	0	176	0
46		0	0	173	0
47		0	0	169	0
48		0	0	166	0
49		0	0	160	0
50		0	0	156	0
51		0	0	154	0
52		0	0	150	0
53		0	0	147	0
54		0	0	145	0
55		0	0	143	0
56		0	0	142	0
57		0	0	139	0
58		0	0	138	0
59		0	0	137	0
60		0	0	133	0
61		0	0	131	0
62		0	0	128	0
63		0	0	125	0
64		0	0	121	0
65		0	0	116	0
66		0	0	113	0
67		0	0	109	0
68		0	0	104	0

Fig. X.3a Distribution of Intermod Products in the Receive Bands II

69		0	100	0
70		0	96	0
71		0	92	0
72		0	88	0
73		0	84	0
74		0	81	0
75		0	77	0
76		0	73	0
77		0	70	0
78		0	67	0
79		0	63	0
80		0	59	0
81		0	56	0
82		0	53	0
83		0	49	0
84		0	46	0
85		0	43	0
86		0	41	0
87		0	38	0
88		0	36	0
89		0	35	0
90		0	34	0
91		0	32	0
92		0	31	0
93		0	31	0
94		0	29	0
95		0	28	0
96		0	27	0
97		0	25	0
98		0	24	0
99		0	22	0
100		0	20	0
101		0	17	0
102		0	15	0
103		0	11	0
104		0	9	0
105		0	7	0
106		0	5	0
107		0	3	0
108		0	2	0
109		0	1	0
110		0	1	0
111	*	0	0	0
112	*	0	0	0
113	*	0	0	0
114	*	0	0	0
115	*	0	0	0
116	*	0	0	0
117	*	0	0	0
118	*	0	0	0
119	*	0	0	0
120	*	0	0	0
121	*	0	0	0
122	*	0	0	0
123	*	0	0	0
124	*	0	0	0
125	*	0	0	0
126	*	0	0	0
127	*	0	0	0
128	*	0	0	0
129	*	0	0	0
130	*	0	0	0
131	*	0	0	0
132	*	0	0	0
133	*	0	0	0
134	*	0	0	0
135	*	0	0	0
136	*	0	0	0
137	*	0	0	0
138	*	0	0	0
139	*	0	0	0
140	*	0	0	0
141	*	0	0	0
142	*	0	0	0
143	*	0	0	0
144	*	0	0	0
145	*	0	0	0
146	*	0	0	0
147	*	0	0	0
148	*	0	0	0
149	*	0	0	0
150		0	1	0
151		0	1	0
152		0	2	0
153		0	3	0
154		0	5	0
155		0	6	0
156		0	8	0
157		0	9	0
158		0	11	0
159		0	11	0
160		0	12	0

Fig. X.3b Distribution of Intermod Products in the Receive Bands II

321	*	0	0	0	0
322	*	0	0	0	0
323	*	0	0	0	0
324	*	0	0	0	0
325	*	0	0	0	0
326	*	0	0	0	0
327	*	0	0	0	0
328	*	0	0	0	0
329	*	0	0	0	0
330	*	0	0	0	0
331	*	0	0	0	0
332	*	0	0	0	0
333	*	0	0	0	0
334	*	0	0	0	0
335	*	0	0	0	0
336	*	0	0	0	0
337	*	0	0	0	0
338	*	0	0	0	0
339	*	0	0	0	0
340	*	0	0	0	0
341	*	0	0	0	0
342	*	0	0	0	0
343	*	0	0	0	0
344	*	0	0	0	0
345	*	0	0	0	0
346	*	0	0	0	0
347	*	0	0	0	0
348	*	0	0	0	0
349	*	0	0	0	0
350	*	0	0	0	0
351	*	0	0	0	0
352	*	0	0	0	0
353	*	0	0	0	0
354	*	0	0	0	0
355	*	0	0	0	0
356	*	0	0	0	0
357	*	0	0	0	0
358	*	0	0	0	0
359	*	0	0	0	0
360	*	0	0	0	0
361	*	0	0	0	0
362	*	0	0	0	0
363	*	0	0	0	0
364	*	0	0	0	0
365	*	0	0	0	0
366	*	0	0	0	0
367	*	1	0	0	0
368	*	1	0	0	0
369	*	2	0	0	0
370	*	3	0	0	0
371	*	4	0	0	0
372	*	5	0	0	0
373	*	6	0	0	0
374	*	6	0	0	0
375	*	6	0	0	0
376	*	5	0	0	0
377	*	5	0	0	0
378	*	4	0	0	0
379	*	4	0	0	0
380	*	4	0	0	0
381	*	5	0	0	0
382	*	5	0	0	0
383	*	6	0	0	0
384	*	6	0	0	0
385	*	6	0	0	0
386	*	6	0	0	0
387	*	7	0	0	0
388	*	6	0	0	0
389	*	7	0	0	0
390	*	7	0	0	0
391	*	8	0	0	0
392	*	9	0	0	0
393	*	11	0	0	0
394	*	11	0	0	0
395	*	12	0	0	0
396	*	12	0	0	0
397	*	12	0	0	0
398	*	12	0	0	0
399	*	11	0	0	0

Fig. X.3c Distribution of Intermod Products in the Receive Bands II

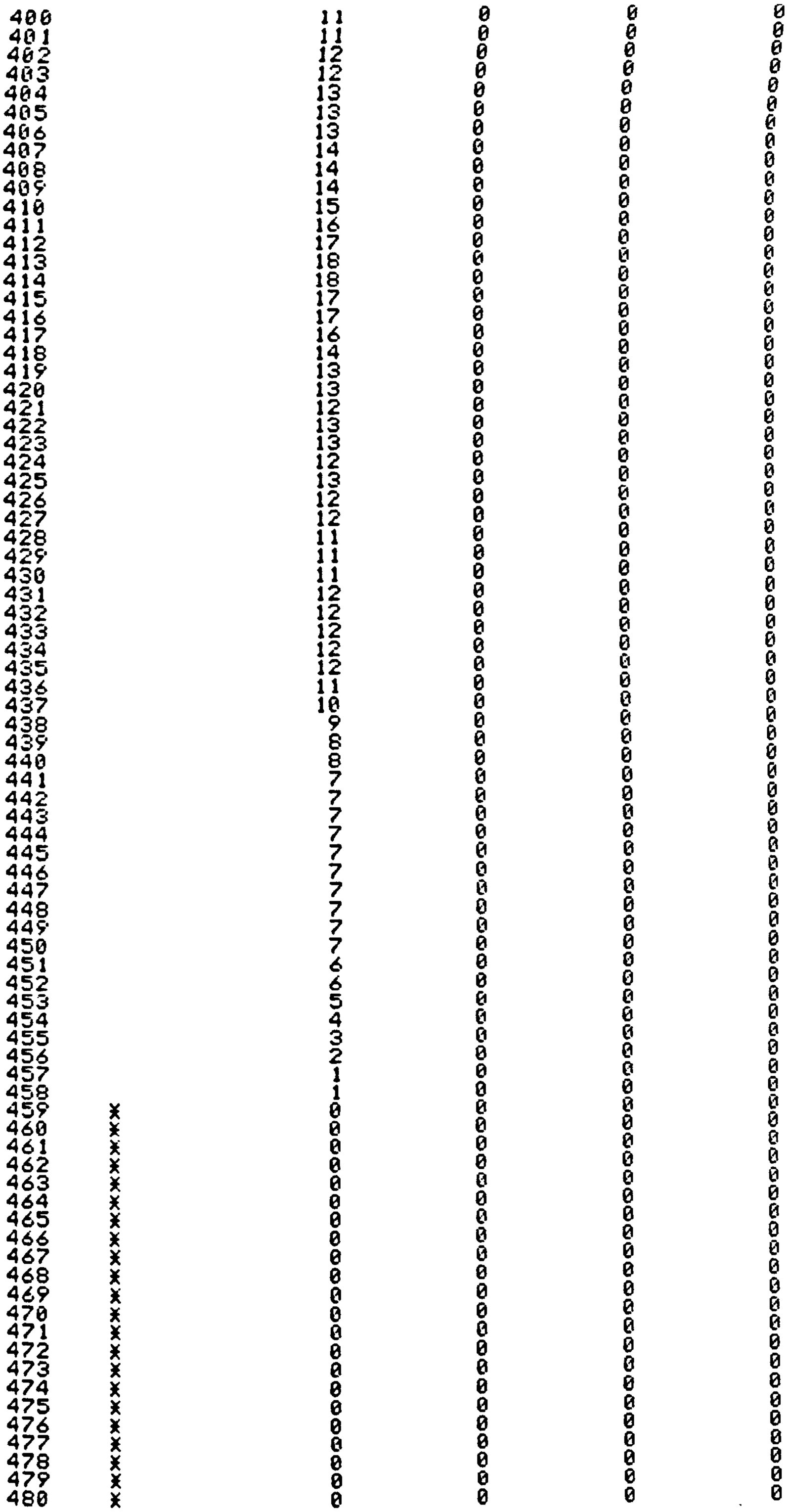

Fig. X.3d Distribution of Intermod Products in the Receive Bands II

LOW BAND CHANNELS ARE:-

71	72	73	74	75	76	77

UPPER BAND CHANNELS ARE:-

70	71	72	73	74	75

THIS TABLE SHOWS, FOR EACH ORDER No, THE NUMBER OF INTERMODS. FALLING ON THE RECEIVE CHANNELS

CHANNEL No.	FREE!	ORDER 5	ORDER 7	ORDER 9	ORDER 11
1	*	0	0	0	0
2	*	0	0	0	0
3	*	0	0	0	0
4	*	0	0	0	0
5	*	0	0	0	0
6	*	0	0	0	0
7	*	0	0	0	0
8	*	0	0	0	0
9	*	0	0	0	0
10	*	0	0	0	0
11	*	0	0	0	0
12	*	0	0	0	0
13	*	0	0	0	0
14	*	0	0	0	0
15	*	0	0	0	0
16	*	0	0	0	0
17	*	0	0	0	0
18	*	0	0	0	0
19	*	0	0	0	0
20	*	0	0	0	0
21	*	0	0	0	0
22	*	0	0	0	0
23	*	0	0	0	0
24	*	0	0	0	0
25	*	0	0	0	0
26	*	0	0	0	0
27	*	0	0	0	0
28	*	0	0	0	0
29	*	0	0	0	0
30	*	0	0	0	0
31	*	0	0	0	0
32	*	0	0	0	0
33	*	0	0	0	0
34	*	0	0	0	0
35	*	0	0	0	0
36	*	0	0	0	0
37	*	0	0	0	0
38	*	0	0	0	0
39	*	0	0	0	0
40	*	0	0	0	0
41	*	0	0	0	0
42	*	0	0	0	0
43	*	0	0	0	0
44	*	0	0	0	0
45	*	0	0	0	0
46	*	0	0	0	0
47	*	0	0	0	0
48	*	0	0	0	0
49	*	0	0	0	0
50	*	0	0	0	0
51		0	0	0	1
52		0	0	0	2
53		0	0	0	5
54		0	0	0	10
55		0	0	0	20
56		0	0	0	36
57		0	0	0	63
58		0	0	0	102
59		0	0	0	163
60		0	0	0	248
61		0	0	0	369
62		0	0	0	529
63		0	0	0	743
64		0	0	0	1013
65		0	0	0	1355
66		0	0	0	1768
67		0	0	0	2264
68		0	0	0	2857

Fig. X.4a Distribution of Intermod Products in the Receive Bands III

Fig. X.4b Distribution of Intermod Products in the Receive Bands III

400		0	767	0	0
401		0	726	0	0
402		0	670	0	0
403		0	601	0	0
404		0	524	0	0
405		0	443	0	0
406		0	365	0	0
407		0	289	0	0
408		0	223	0	0
409		0	165	0	0
410		0	118	0	0
411		0	80	0	0
412		0	53	0	0
413		0	32	0	0
414		0	19	0	0
415		0	10	0	0
416		0	5	0	0
417		0	2	0	0
418		0	1	0	0
419		0	0	0	0
420		0	0	0	0
421		0	0	0	0
422		0	0	0	0
423		0	0	0	0
424		0	0	0	0
425		0	0	0	0
426		0	0	0	0
427		0	0	0	0
428		0	0	0	0
429		0	0	0	0
430		0	0	0	0
431		0	0	0	0
432		0	0	0	0
433		0	0	0	0
434		0	0	0	0
435		0	0	0	0
436		0	0	0	0
437		0	0	0	0
438		0	0	0	0
439		0	0	0	0
440		0	0	0	0
441		0	0	0	0
442		0	0	0	0
443		0	0	0	0
444		0	0	0	0
445		0	0	0	0
446		0	0	0	0
447		0	0	0	0
448		0	0	0	0
449		0	0	0	0
450		0	0	0	0
451		0	0	0	0
452		0	0	0	0
453		0	0	0	0
454		0	0	0	0
455		0	0	0	0
456		0	0	0	0
457		0	0	0	0
458		0	0	0	0
459		0	0	0	0
460		0	0	0	0
461		0	0	0	0
462		0	0	0	0
463		0	0	0	0
464		0	0	0	0
465		0	0	0	0
466		0	0	0	0
467		0	0	0	0
468		0	0	0	0
469		0	0	0	0
470		0	0	0	0
471		0	0	0	0
472		0	0	0	0
473		0	0	0	0
474		0	0	0	0
475		0	0	0	0
476		0	0	0	0
477		0	0	0	0
478		0	0	0	0
479		0	0	0	0
480	*	0	0	0	0

Fig. X.4c Distribution of Intermod Products in the Receive Bands III

303	**********	0	0	0	0
304	**********	0	0	0	0
305	**********	0	0	0	0
306	**********	0	0	0	0
307	**********	0	0	0	0
308	**********	0	0	0	0
309	**********	0	0	0	0
310	**********	0	0	0	0
311	**********	0	0	0	0
312	**********	0	0	0	0
313	**********	0	0	0	0
314	**********	0	0	0	0
315	**********	0	0	0	0
316	**********	0	0	0	0
317	**********	0	0	0	0
318	**********	0	0	0	0
319	**********	0	0	0	0
320	**********	0	0	0	0
321	**********	0	0	0	0
322	**********	0	0	0	0
323	**********	0	0	0	0
324	**********	0	0	0	0
325	**********	0	0	0	0
326	**********	0	0	0	0
327	**********	0	0	0	0
328	**********	0	0	0	0
329	**********	0	0	0	0
330	**********	0	0	0	0
331	**********	0	0	0	0
332	**********	0	0	0	0
333	**********	0	0	0	0
334	**********	0	0	0	0
335	**********	0	0	0	0
336	**********	0	0	0	0
337	**********	0	0	0	0
338	**********	0	0	0	0
339	**********	0	0	0	0
340	**********	0	0	0	0
341	**********	0	0	0	0
342	**********	0	0	0	0
343	**********	0	0	0	0
344	**********	0	0	0	0
345	**********	0	0	0	0
346	**********	0	0	0	0
347	**********	0	0	0	0
348	**********	0	0	0	0
349	**********	0	0	0	0
350	**********	0	0	0	0
351	**********	0	0	0	0
352	**********	0	0	0	0
353	**********	0	0	0	0
354	**********	0	0	0	0
355	**********	0	0	0	0
356	**********	0	0	0	0
357	**********	0	0	0	0
358	**********	0	0	0	0
359	**********	0	0	0	0
360	**********	0	0	0	0
361	**********	0	0	0	0
362	**********	0	0	0	0
363	**********	0	0	0	0
364	**********	0	0	0	0
365	**********	0	0	0	0
366	**********	0	0	0	0
367	**********	0	0	0	0
368	**********	0	0	0	0
369	**********	0	0	0	0
370	**********	0	0	0	0
371	**********	0	0	0	0
372	**********	0	0	0	0
373	**********	0	0	0	0
374	**********	0	0	0	0
375	**********	0	0	0	0
376	**********	0	0	0	0
377	**********	0	0	0	0
378	**********	0	0	0	0
379	**********	0	0	0	0
380	**********	0	0	0	0
381	**********	0	0	0	0
382	**********	0	0	0	0
383	**********	0	0	0	0
384	**********	0	0	0	0
385	**********	0	0	0	0
386	**********	0	0	0	0
387	**********	0	0	0	0
388	**********	0	0	0	0
389	**********	0	0	0	0
390	**********	0	0	0	0
391	**********	0	0	0	0
392	**********	0	0	0	0
393	**********	0	0	0	0
394	**********	0	0	0	0
395	**********	0	0	0	0
396	**********	0	0	0	0
397	**********	0	0	0	0
398	**********	0	0	0	0
399	**********	0	0	0	0
400	**********	0	0	0	0
401	**********	0	0	0	0
402	**********	0	0	0	0
403	**********	0	0	0	0
404	**********	0	0	0	0
405	**********	0	0	0	0
406	**********	0	0	0	0
407	**********	0	0	0	0
408	**********	0	0	0	0
409	**********	0	0	0	0
410	**********	0	0	0	0
411	**********	0	0	0	0
412	**********	0	0	0	0
413	**********	0	0	0	0
414	**********	0	0	0	0
415	**********	0	0	0	0
416	**********	0	0	0	0
417	**********	0	0	0	0
418	**********	0	0	0	0
419	**********	0	0	0	0
420	**********	0	0	0	0
421	**********	0	0	0	0
422	**********	0	0	0	0
423	**********	0	0	0	0
424	**********	0	0	0	0
425	**********	0	0	0	0
426	**********	0	0	0	0
427	**********	0	0	0	0
428	**********	0	0	0	0
429	**********	0	0	0	0
430	**********	0	0	0	0
431	**********	0	0	0	0
432	**********	0	0	0	0
433	**********	0	0	0	0
434	**********	0	0	0	0
435	**********	0	0	0	0
436	**********	0	0	0	0
437	**********	0	0	0	0
438	**********	0	0	0	0
439	**********	0	0	0	0
440	**********	0	0	0	0
441	**********	0	0	0	0
442	**********	0	0	0	0
443	**********	0	0	0	0
444	**********	0	0	0	0
445	**********	0	0	0	0
446	**********	0	0	0	0
447	**********	0	0	0	0
448	**********	0	0	0	0
449	**********	0	0	0	0
450	**********	0	0	0	0
451	**********	0	0	0	0
452	**********	0	0	0	0
453	**********	0	0	0	0
454	**********	0	0	0	0
455	**********	0	0	0	0
456	**********	0	0	0	0
457	**********	0	0	0	0
458	**********	0	0	0	0
459	**********	0	0	0	0
460	**********	0	0	0	0
461	**********	0	0	0	0
462	**********	0	0	0	0
463	**********	0	0	0	0
464	**********	0	0	0	0
465	**********	0	0	0	0
466	**********	0	0	0	0
467	**********	0	0	0	0
468	**********	0	0	0	0
469	**********	0	0	0	0
470	**********	0	0	0	0
471	**********	0	0	0	0
472	**********	0	0	0	0
473	**********	0	0	0	0
474	**********	0	0	0	0
475	**********	0	0	0	0
476	**********	0	0	0	0
477	**********	0	0	0	0
478	**********	0	0	0	0
479	**********	0	0	0	0
480	**********	0	0	0	0
481	**********	0	0	0	0
482	**********	0	0	0	0
483	**********	0	0	0	0
484	**********	0	0	0	0
485	**********	0	0	0	0
486	**********	0	0	0	0
487	**********	0	0	0	0
488	**********	0	0	0	0
489	**********	0	0	0	0
490	**********	0	0	0	0
491	**********	0	0	0	0
492	**********	0	0	0	0
493	**********	0	0	0	0
494	**********	0	0	0	0
495	**********	0	0	0	0
496	**********	0	0	0	0
497	**********	0	0	0	0
498	**********	0	0	0	0
499	**********	0	0	0	0

Fig. X.4d Distribution of Intermod Products in the Receive Bands III

REFERENCES

ALLSEBROOK, K., and PARSONS, J. D. (1977). Mobile radio propogation in British cities at frequencies in the VHF and UHF bands. Proc. IEE. 124(2) 95-102.

AL-NUAIMI, M. O. (1978). Response of an AM receiver to a quasisynchronous multi-am-transmitter field. Proc IEE 125(3) 190-194.

AL-NUAIMI, M. O. (1981). Analysis of response of FM mobile receiver in quasisynchronous field. Proc IEE. 128 Part F (5) 317-322

ASQUE, V. (1982). Subjective assessment of tolerances for quasi-synchronous amplitude modulation. IEE. Conf. Publ. 209 (April) 98-102

BAILEY, G. C. et al (1980). Studies on the Reduction of Intermodulation Generation in Communications Systems. Naval Research Laboratory memorandum Report 4233. Washington D.C. USA (July 7)

BAJWA, A. S. and PARSONS, J. D. (1982). Small area characterisation of UHF urban and suburban mobile radio propagation. Proc IEE Part F (129) 102-109

BURBERRY, R.A. and SMITH R. W. (1974). Mobile Arial Research and Development Study. Report to Home Office under contract DT/74/96/3

BUTLER, J. and LOWE, R (1961). Beam forming matrix simplities design of electronically scanned antennas. Electronics Design (April) 170-173

COLIN, R. E. (1966). Foundations for Microwave Engineering (New York McGraw-Hill)

CCIR (1978a). Recommendation 562. Vol. X. Kyoto 167-170

CCIR (1978b). Report 567-1. Vol. X. Kyoto 163-172

CLARKE, R. H. (1968). A Statistical Theory of Mobile Radio Reception. Bell Syst. Techn. J. 47 (July): 957-1000

DEBNEY, C. W. and STEWART. R. D. (1983). Interference Analysis and Modelling of Multiple Basestation Sites for Mobile Radio Services. 5th and 6th Quarterly Reports from University of Southampton to Home Office. Contract FP3056

EDWARDS, K. J., KERSLEY, L. and SHRUBSOLE, L. F. (1982). Sporadic - E Propagation at VHF (iv) Comparative Studies. Final Report by University College of Wales, Aberystwyth to Home Office. Agreement RT/JA/3

EDWARDS, R., DURKIN, J. and GREEN, D. H. (1969). Selection of interference-free frequencies for multiple channel mobile radio systems. Proc IEE 116 (8)

FAGOT and MAGNE (1961). Frequency Modulation Theory. (London, Pergamon Press)

FRENCH, R. C. (1976). Radio propagation in London at 462 MHz. Radio and Electronic Eng. 46 (July) 333-336

FRENCH, R. C. (1979). The Effect of Fading and Shadowing on Channel Reuse in Mobile Radio. IEE Trans. VT-28 (3) 171-181

FUDGE, R. E. (1978). A commutating aerial diversity system. IEE Conf. Publ. 162 (April) 207-209

FUDGE, R. E. (1984a). An analysis of quasi-synchronous AM mobile radio operation and recommended design parameter values. Proc IEE Part F (to be publised).

FUDGE, R. E. (1984b?). Mobile Radio in the Radio Receiver: LF-UHF (GOSLING, W. Ed.) (London Peter Peregrinus) to be published

GARDINER, J. G. and FUDGE, R. E. (1984?). Aerials and Base Station Design in Land Mobile Radio Systems (HOLBECHE, R. Ed.) (London Peter Peregrinus) to be published

GOSLING, W. (1978). A simple mathetmatical model of co-channel and adjacent channel interface in land mobile radio. Radio and Electronic Eng. 48 (Dec) 619-622

HOME OFFICE (1981). Directorate of Radio Technology - Report on Comparative Tests of Modulation Methods for Private Mobile Radio

KEEBLE, R. S. 1983. Personal Communication

KENT, A. N. (1979). Quasi-synchronous operations in UHF FM personal mobile radio system. Home Office, Directorate of Telecommunications, R&D technical memorandum, 36.

JAKES, W. C. (Ed.) (1974). Microwave Mobile Communications. (New York: Wiley Interscience)

LORENZ, R. W. (1980). Field strength prediction method for a mobile telephone system using a topographical data bank. IEE Conf. Publ. 188, 6-11

MACDONALD, V. H. (1979). The Cellular Concept. Bell Syst. Tech. J. 58 (January)

MATTHEWS, P. A. (1965). Radio Wave Propagation VHF and Above (London Chapman and Hall Ltd.)

MATTHEWS, P. A., and DRURY, D. A. (1980). Direct sequence spread spectrum system analysis for land mobile radio communication. IEE. Conf. Publ. 184. 187-191

McGEEHAN, J. P., LIGHTFOOT, G., LYMER, A., and GOSLING, W. (1981). Optimisation of the Wolfson SSB Receiver. IERE Cont. Publ. 50 (July) 417-429

MERRIMAN, J. H. H. (1983). Independent review of the Radio Spectrum (30-960 MHz) (London: Her Majesty's Stationery Office CMND.8666)

MURASZKO, J. T. (1978). Quasi-synchromous transmission. Communications International (June)

OKUMURA, Y. et al. (1968). Field Strength and its variability in VHF and UHF Land Mobile Service, Rev. Elec. Comm. Lab. 16 (Sept.) 825-873

PANNELL, W. M. (1979). Frequency engineering in mobile radio bands (Cambridge Granta Technical Editions in association with Pye Telecommunications Ltd.)

PARSONS, J. D., IBRAHIM, M. F., and SAMUEL, R. J. (1980). Median signal strength prediction for mobile radio propagation in London. Electron. Lett. 16(5) 172-173

PARSONS, J. D., and IBRAHIM, M. F. (1983). Signal strength predictions in built-up areas. Part 2: Signal Variability. Proc. IEE 130 Part (5) 385-391

PETROVIC, V. (1983). Reduction of spurious emission from radio transmitters by means of modulation feedback. IEE Conf. Publ. 224 (Sept.) 44-49

PEARCE, J. N. (1983). Personal Communication

QUARRELL, P. J. (1983). Personal Communication

SUZUKI, H. (1977). A statistical model for urban radio propagation. IEEE Trans. Com-25 673-680

WOOD, A. (1962). The physics of music. (London: Methuen, 6th Edition)

ZAID, M. A. M. A., and LOCKART, G. B. (1982). Envelope detectable single side-band signals in mobile radio. IEE Conf. Publ 209 103-108